THE HYDRODYNAMIC BEHAVIOUR AND MASS TRANSFER CHARACTERISTICS OF SINGLE DROPLETS IN A PULSED SIEVE PLATE COLUMN

by

ADEL SHAYE AL-JIMAZ MSc

Doctor of Philosophy

THE UNIVERSITY OF ASTON IN BIRMINGHAM

February 1992

The University of Aston in Birmingham

THE HYDRODYNAMIC BEHAVIOUR AND MASS TRANSFER CHARACTERISTICS OF SINGLE DROPLETS IN A PULSED SIEVE PLATE COLUMN

ADEL SHAYE AL-JIMAZ
Doctor of Philosophy
1992

Summary

The literature relating to the performance of pulsed sieve plate liquid-liquid extraction columns and the relevant hydrodynamic phenomena have been surveyed. Hydrodynamic behaviour and mass transfer characteristics of droplets in turbulent and non-turbulent conditions have also been reviewed.

Hydrodynamic behaviour, i.e terminal and characteristic velocity of droplets, droplet size and droplet breakup processes, and mass transfer characteristics of single droplets ($d_e \leq 0.6$ cm) were investigated under pulsed (mixer-settler & transitional regimes) and non-pulsed conditions in a 5.0 cm diameter, 100 cm high, pulsed sieve plate column with three different sieve plate types and variable plate spacing. The system used was toluene (dispersed) - acetone - distilled water.

Existing photographic techniques for following and recording the droplet behaviour, and for observing the parameters of the pulse and the pulse shape were further developed and improved. A unique illumination technique was developed by which a moving droplet could be photographed using cine or video photography with good contrast without using any dye.

Droplet size from a given nozzle and droplet velocity for a given droplet diameter are reduced under pulsing condition, and it was noted that this effect is enhanced in the presence of sieve plate. The droplet breakup processes are well explained by reference to an impact-breakup mechanism. New correlations to predict droplet diameter based on this mechanism are given below.

$$\frac{d_{crit} V_{crit}^2 \rho_d}{\sigma} + 1.79 \frac{d_{crit}^2 g \Delta\rho}{\sigma} = 3.12$$

or in dimensionless groups as follows:-

$$(We)_{crit} = 3.12 - 1.79 (Eo)_{crit}$$

A correlation based on the isotropic turbulence theory was developed to calculate droplet diameter in the emulsion regime.

$$d_{32} = K_8 \left(\frac{\sigma}{\rho_c}\right)^{0.6} \psi^{-0.4}$$

Experimental results show that in the mixer-settler and transitional regimes, pulsing parameters had little effect on the overall dispersed phase mass transfer coefficient during the droplet formation and unhindered travel periods.

Key words:- Mass Transfer, Liquid-Liquid Extraction, Pulsed Sieve Plate Column, Single Droplet.

ACKNOWLEDGEMENTS

The author is greatly indebted to and expresses his gratitude to Dr. M.P. Wilson for his supervision encouragement, motivation and constructive criticism and to Dr. C.J. Mumford for his help, suggestions and supervision.

The author also wishes to thank Mr. N. Roberts and the entire staff of the Chemical Engineering Department's workshop, analytical laboratory and stores.

Finally, thanks are due to The Public Authority of Applied Education and Training, The State of Kuwait for their encouragement and financial support.

CONTENTS

LIST OF FIGURES

Figure No.

Page No.

LIST OF TABLES

PART I

LITERATURE REVIEW

CHAPTER 1

CHAPTER 2

CHAPTER 3

CHAPTER 4

CHAPTER ONE

INTRODUCTION

1.1 Introduction

In the chemical process industries, the separation of the constituents of an homogeneous liquid mixture is a problem frequently encountered. Solvent extraction, or more precisely, liquid-liquid extraction, is a possible separation technique widely used both on the industrial scale and in the laboratory. Liquid -liquid extraction may be used in preference to other methods of separation, for instance distillation, evaporation, crystallisation, etc, when these methods prove to be impracticable or uneconomical through one or more of the following considerations:-

1. The components have low volatility.
2. The components in the mixture have essentially the same volatility.
3. The components are sensitive to the high temperature that would be required for separation.
4. The solute in the feed solution is present in a relatively small amount.

Liquid-liquid extraction can be defined as the selective removal of one or more components from an homogeneous liquid mixture using a second liquid "solvent", which is partially or wholly immiscible with the original solution and which is chosen such that the desired component of the mixture preferentially transfers or is extracted into the second liquid.

In contrast to distillation, knowledge regarding the design and performance of extraction columns is still far from satisfactory. The reason for this lies mainly in the complex behaviour of poly-dispersity of the droplet size distribution, resulting from formation, breakup and coalescence of the droplets as well as the influence of these parameters on mass transfer and axial mixing. Up to now, the results of extraction research show that a safe design of extraction columns based on fundamentals is impossible unless these factors have been taken into account.

Liquid-liquid extraction is an important mass transfer operation which has a wide range of application in industry, such as the pharmaceutical, chemical, petrochemical, petroleum and nuclear industries.

1.2 Liquid-Liquid Extraction Equipment

The main requirements for efficient liquid-liquid extraction are as follows:-

1. Efficient contact between phases.
2. Efficient separation of phases after contact.

1.2.1 Classification of Equipment

There are a number of ways in which liquid-liquid extraction equipment may be classified. One scheme divides contactors into two groups, stagewise (discrete-stage) and differential (continuous). A further sub-classification can be made according to whether the counter-current flow is produced by the action of gravity via the density difference between the phases or by an applied force.

In the first group the components are mixed, extracted and then separated in discrete

stages. In the second group the immiscible phases are contacted counter-currently and the equivalent stages are accommodated in one container. In a differential contactor, mass transfer take place throughout the unit under the influence of a continuous concentration gradient and the phases are only separated at the two exits. Differential contactors can provide a degree of separation equivalent to more than one theoretical stage, the key parameter determining the degree of separation being the length. Figure 1.1 shows a typical classification of solvent extraction contactors.

1.2.2 Selection of Equipment

Only a general guide to contactor selection is possible since a great many variables are involved. Although each contactor has advantages and disadvantages, the choice for any particular extraction depends largely upon experience. The most important considerations in selecting a contactor for a specific duty are:-

1. The number of stages or transfer units required.
2. The volumetric throughput.
3. The residence time.
4. The economic factors.

Differential contactors are preferable to stage-wise contactors when large throughputs are needed since they offer economies in agitation power cost, floor space and solvent inventory. They can operate with relatively low phase ratio, and their flexibility of operation also enables extraction to be performed with systems likely to form fine dispersions (67), by operation with low rates of agitation. Figure 1.2 shows a schematic diagram which may be used as a general guide for selection.

1.3 The Pulsed Sieve Plate Column

1.3.1 Introduction

The efficiency of a simple sieve-plate column can be appreciably increased by the application of an oscillating pulse to the contents of the column as originally proposed by Van Dijck (170). This has the effect of increasing both turbulence and interfacial areas. The mass transfer efficiency is thus greatly improved over that of an unpulsed column, and there is a substantial reduction in HETS or HTU values. Because of the high efficiency of pulsed-plate columns and because the hydraulic pulsation can be activated from a safe area, pulsed perforated-plate columns have been widely used in the nuclear industry. In the UK, pulsed plate columns are the preferred liquid-liquid extraction contactor for the proposed European Demonstration Reprocessing Plant (EDRP) handling irradiated fast fuels, and also for the new Thermal Oxide Reprocessing Plant (THORP) at British Nuclear Fuels (159). The original diagram is illustrated in Figures 1.3 & 1.4. The features and fields of industrial application of pulsed columns are given in Table 1.1.

The pulsing action is supplied by leading a pulse leg from the bottom of the column to the pulse generator. A reciprocating plunger or piston pump is a common mechanical pulsing device. However, the unit has the following disadvantages:-

1. Corrosive liquid may contact the piston.
2. High speed pulsing may cause cavitation.

Bellows or diaphrams, constructed with stainless steel, Teflon, or other material, actuated by a reciprocating mechanism, are also used as pulse generators. Several workers (10, 128, 160) have reported an alternative arrangement using air pulses

controlled by a solenoid valve and timer. The pneumatic pulse developed by DSM is another unique design (22).

1.3.2 Operational Characteristics

Several workers (111, 104, 139, 160, 161, 164) investigated the operational characteristics of pulsed sieve-plate columns; unfortunately design equations are not reliable. Sege and Woodfield (139) described the operating characteristics of the pulsed perforated-plate column. Several distinct regions of operation can be distinguished depending on the flow rate and degree of pulsation. As illustrated in Figure 1.5 there are five regimes; mixer-settler, emulsion, unstable and two flooding regimes.

As shown in Figure 1.6, the mixture-settler regime occurs at low throughput rates and frequencies. It is characterised by the separation of the light and heavy phases into discrete, clear layers in the interplate space during the quiescent portions of the pulse cycle. Usually, this layer is not sufficient to provide enough buoyancy force to overcome the interfacial tension force and push the liquid through the perforations. During the upward portion of the pulse cycle the light phase is forced up through the perforations, dispersing it as droplets through the heavy phase layer. Similarly the heavy phase descends during the downward portion of the pulse cycle. In many cases complete coalescence does not occur but the droplets are densely packed at a plate.

The emulsion " dispersion " regime, as shown in Figure 1.6, is characterised by small droplet size (typically about 0.16 cm. or less in diameter) and uniform dispersion of one phase into the other at all times, which provides the most efficient regime due to high interfacial contact area per unit volume.

The unstable regime, as shown in Figure 1.6, is characterised by a wide distribution in

the size of dispersed phase droplets in different sections of the column due to irregular coalescence and reversals of the continuous phase in short sections of the column. At this regime, the efficiency of the column is generally poorer than in the emulsion regime, and often fluctuates widely.

Complete flooding occurs due to the increase in the throughput or the frequency beyond the unstable regime. Complete flooding is defined as the exit of one of the entering streams through the effluent line intended for the other phase.

It should be noted that the above mentioned regimes are difficult to identify and the limiting flow due to insufficient pulsing is not determined only by pulse frequency or even by the pulse product " $f * A_p$ ". The flow ratio also affects this flooding limit (106).

1.4 Mass Transfer

Mass transfer between the phases is increased by dispersion of one phase in the form of droplets in order to establish conditions for a high mass transfer rate. The rate of diffusion of a solute within a single phase depends on the concentration gradient of solute existing within that phase.

For a given concentration gradient, a high mass transfer rate is achieved by; large interfacial area per unit volume and high overall mass transfer coefficient and may be represented by the following equation:-

$$N_A = K\ A\ \Delta C \qquad 1.1$$

where:-

N_A is the rate of solute transfer in moles per unit time.

K is the overall mass transfer coefficient which is dependent on the series resistance to diffusion inside the droplet, outside the droplet and possibly at the interface and can be written in the following form:-

$$\frac{1}{K_d} = \frac{1}{k_d} + \frac{m}{k_c} \qquad 1.2$$

and

$$\frac{1}{K_c} = \frac{1}{k_c} + \frac{1}{\dot{m} k_d} \qquad 1.3$$

where m & $\dot{m}$ are the distribution cofficients

The total interfacial area depends upon the droplet size distribution and the dispersed phase hold-up since the interfacial area per unit volume is given by:-

$$a = \frac{6x}{d_{32}} \qquad 1.4$$

where x is the hold-up and d_{32} the specific surface diameter. The total interfacial area is given by :-

$$A = a V \qquad 1.5$$

where V is the contactor volume.

In pulsed columns which are the subject of this study, the application of pulse energy increases turbulence and aids breakup of dispersed phase droplets to compensate for any coalescence at the perforated plate, thereby greatly improving the mass transfer efficiency as compared to an unpulsed column.

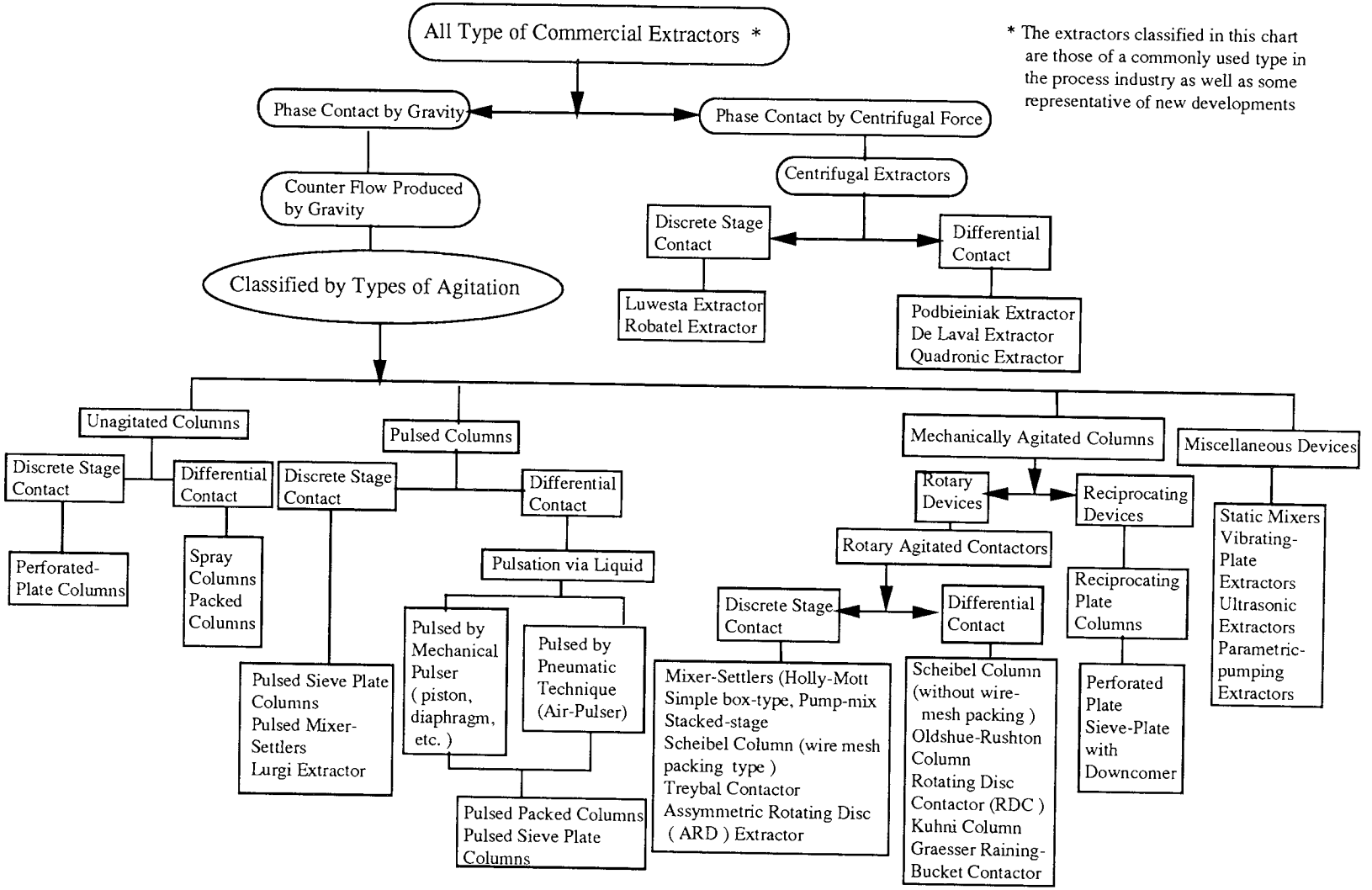

Figure 1.1 Classification of Commercial Extractors

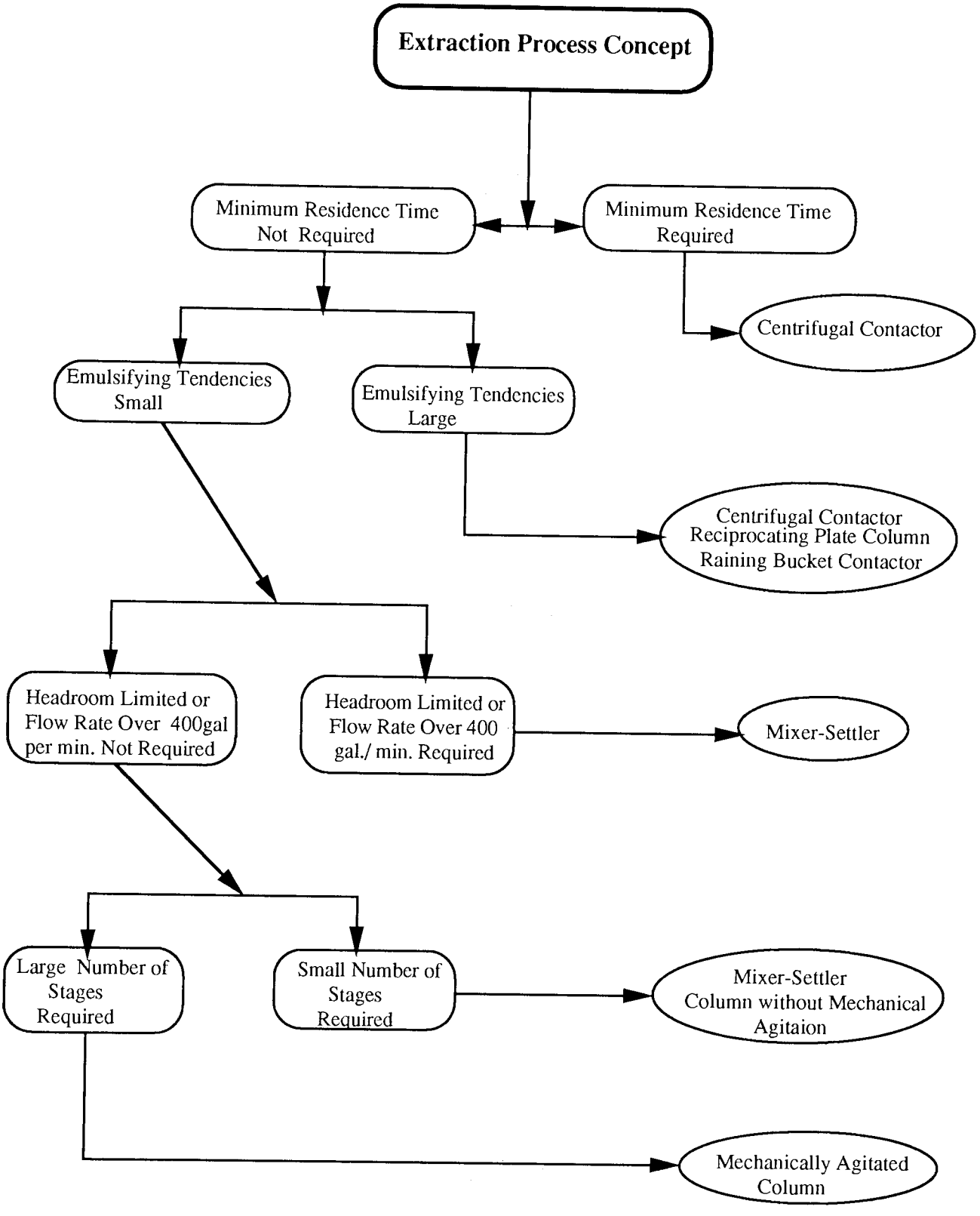

Figure 1.2 Decision Network for Extraction Equipment Selection.

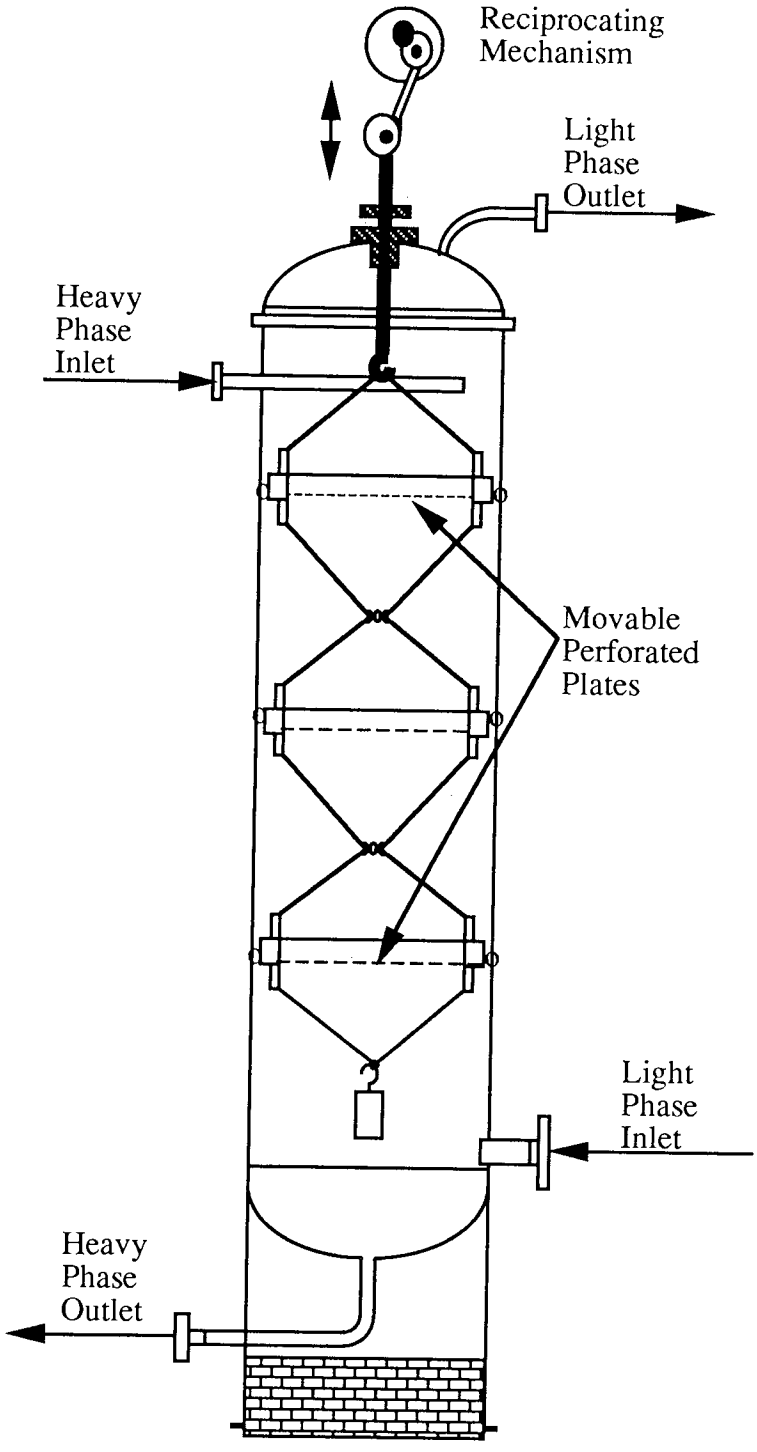

Figure 1.3 Original Diagram of the Reciprocating Sieve Plate Column. (170)

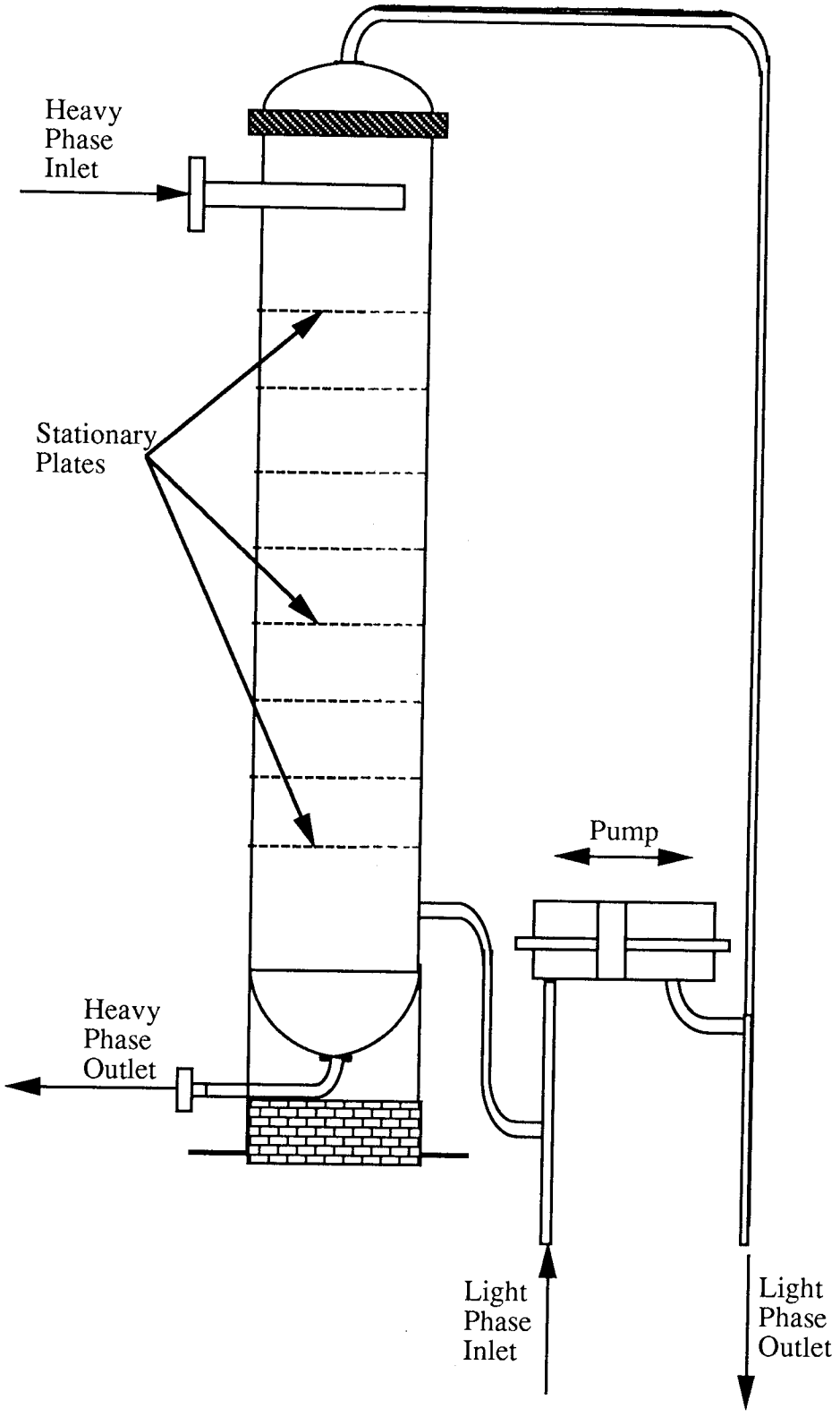

Figure 1.4 Original Diagram of the Pulsed Sieve-plate Column. (170)

Table 1.1 Summary of Features and Industrial Application of Commercial Extractors

Types of Extractor	General Features	Fields of Industrial Application
Unagitated columns	Low capital cost Low operating & maintenance cost Simplicity in construction Handles corrosive material	Petrochemical Chemical
Mixer-settler	High-stage efficiency Handles wide solvent ratios High capacity Good flexibility Reliable scale-up Handles liquids with high viscosity	Petrochemical Nuclear Fertilizer Metallurgical
Pulsed column	Low HETS No internal moving parts Many stages possible	Nuclear Petrochemical Metallurgical
Rotary-agitation columns	Reasonable capacity Reasonable HETS Many stages possible Reasonable construction cost Low operating & maintance cost	Petrochemical Metallurgical Pharmaceutical Fertilizer
Reciprocating-plate columns	High throughput Low HETS Great versatility & flexibility Simplicity in construction Handles liquids containing suspended solids Handles mixtures with emulsifying tendencies	Pharmaceutical Petrochemical Metallurgical Chemical
Centrifugal extractors	Short contacting time for unstable material Limited space required Handles systems with little liquid density difference. Handles easily emulsified material	Pharmaceutical Nuclear Petrochemical

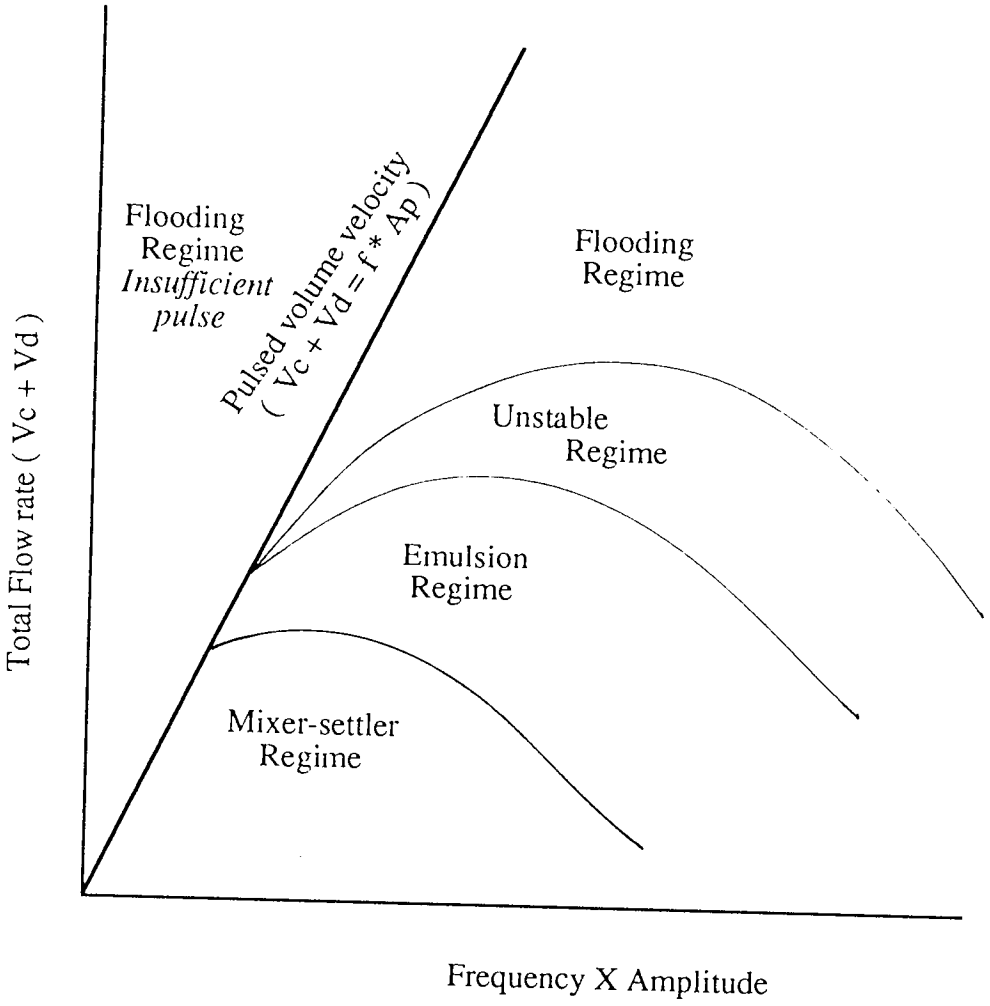

Figure 1.5 Regimes of Pulsed Sieve Plate Column Operation (149)

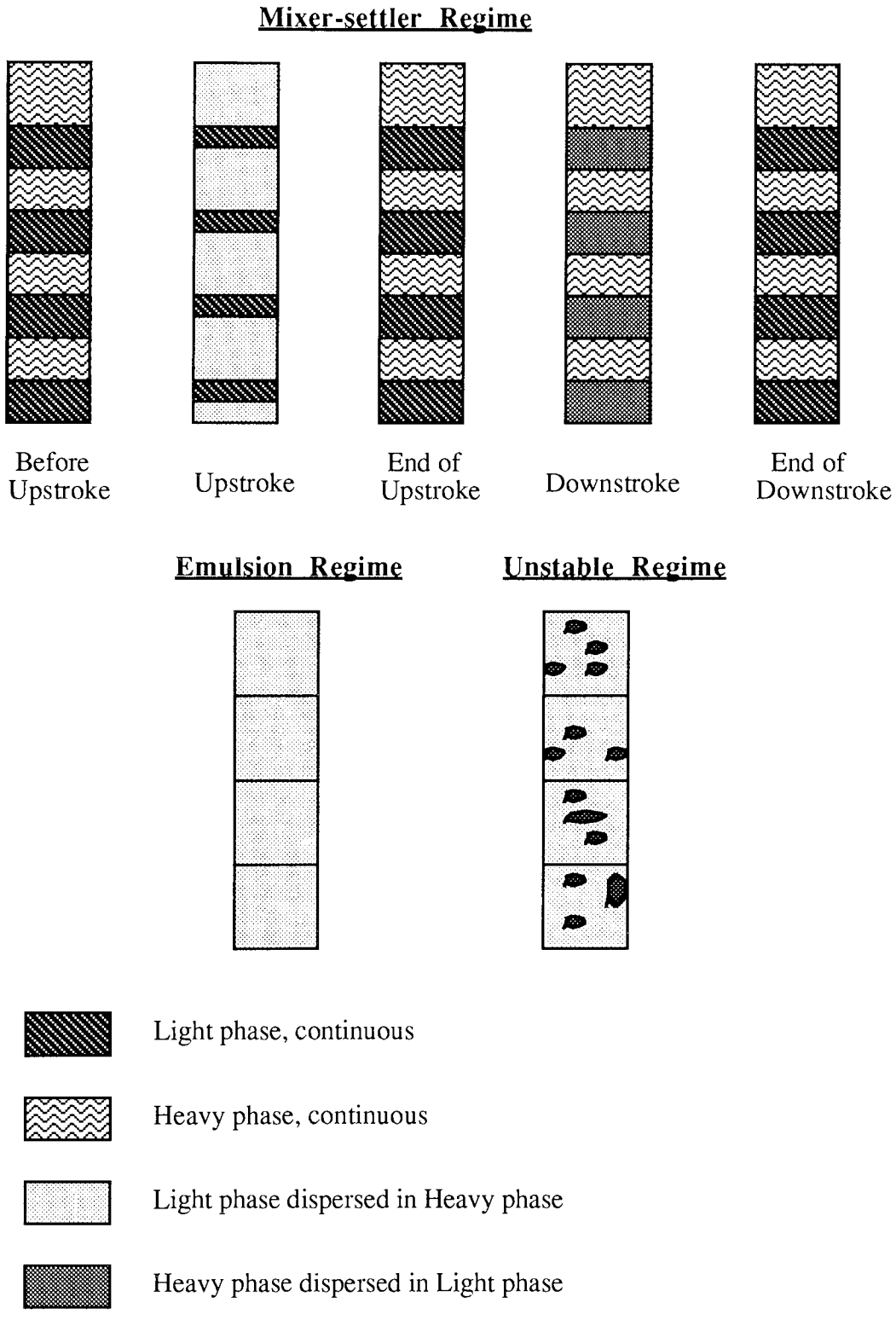

Figure 1.6 The Operating Regimes of Pulsed Sieve-plate Column

The mass transfer studies on liquid-liquid systems in pulsed columns have been mostly restricted to the estimation of the height equivalent of a theoretical stage HETS, or height of a transfer unit HTU and not the mass transfer coefficient. The apparent transfer unit height will sometimes show a minimum value in the emulsion (dispersion) regime because at high pulse velocities increasing axial mixing may be more important than decreasing droplet size, increasing interfacial area and increasing mass transfer coefficient (139, 161,149).

Droplets rising, or falling, show several interesting phenomena as they travel freely through the continuous phase. They may be stagnant, or possess internal circulation, or deform and oscillate. The terminal velocity and mass transfer rate are both related to these phenomena, and they are also affected by pulsing parameters and the presence of sieve-plates.

1.5 The Purpose of this Study

The purpose of this study is to examine the behaviour of single droplets in;

1. Pulsed spray column.
2. Pulsed sieve-plate column.

and in particular:-

1. To study and investigate the motion of single droplets under various operating conditions and a wide range of operating conditions, so a better understanding of the behaviour of a swarm of droplets inside the column may be achieved.

2. To examine and investigate the droplet breakup mechanisms in pulsed sieve-plate columns, and to try to establish a better understanding of a relationship of the parameters which have an effect upon the droplet breakup process.

3. To study and examine the effect of pulsing parameters and sieve-plate characteristics on the mass transfer coefficient of single droplets.

CHAPTER TWO

DROPLET HYDRODYNAMICS

The complex situation involving a swarm of droplets moving in a highly mobile liquid field does not lend itself easily to fundamental investigation. Simplifications necessary to set up a model upon which to base mathematical analyses are numerous and often unrealistic. To gain knowledge that will lead to a better model, many investigators have invested considerable effort in examining the phenomena pertinent to single moving droplets. It is not immediately obvious that the knowledge gained from observation of the performance of individual droplets can be directly applied to complex extraction operations. However, if even a little progress can be made by way of this approach, the extensive research into it will have been worthwhile.

It is in this light that the present study will examine the phenomena exhibited by single moving droplets in pulsed columns. Mass transfer is always dependent upon the hydrodynamics prevailing, and therefore both the fluid mechanics and the mass transfer characteristics are discussed.

Previous workers have found the Reynolds number alone is insufficient to classify the different behaviours of drops during their travel in the continuous phase. Therefore Weber, Strouhal, Schmidt and Sherwood numbers, or other groups of physical properties -Table 2.1- may also be included to characterise the behaviour of the droplet. The effect of different values of these dimensionless groups on the behaviour of a drop is explained in Chapter 4. However droplet Reynolds number has been used as a rough guide to the hydrodynamic state of droplets as follows:-

1.	Stagnant, or rigid droplets	$Re < 1.0$
2.	Circulating droplets	$1.0 < Re < 200$
3.	Oscillating droplets	$Re > 200$

2.1 Stagnant Droplets

This is a limiting case which will hold for small droplets, usually < 1.0 mm. in diameter, or when the ratio of dispersed to continuous phase viscosity is high, or if droplet circulation is eliminated by the presence of a surfactant.

To a first approximation, the terminal velocity for smaller droplets can be calculated by established correlations for solid spheres (81). In most cases, liquid droplets of small diameter move faster than solid spheres of the same size and density, because of;

1. The lower drag coefficient for a liquid droplet than for a rigid sphere.
2. The mobility of the liquid droplet surface.

Any hydrodynamic consideration of a drop moving in a liquid field starts with the Navier-Stokes equations, as given in many representative books on fluid mechanics (90, 155).

Bird (15) solved the equation of motion for a single droplet, and obtained the following expression for the form drag

$$F_p = 2 \pi \mu_c R V \qquad 2.1$$

Addition of the shear force over the surface of the sphere, and from the equations of motion the following expression for the viscous drag is obtained

$$F_\mu = 4 \pi \mu_c R V \qquad 2.2$$

Table 2.1 Dimensionless groups related to droplet behaviour

Dimensionless Groups	Definition
Reynolds Number	$Re = \frac{V d_e \rho}{\mu_c}$
Modified Reynolds Number	$Re = \frac{\rho_c \omega d_e^2}{\mu_c}$
Schmidt Number	$Sc = \frac{\mu}{\rho D}$
Sherwood Number	$Sh = \frac{K d_e}{D}$
Strouhal Number	$Sr = \frac{\omega d_e}{V}$
Weber Number	$We = \frac{d_e V^2 \rho}{\sigma}$
Galileo Number	$Ga = \frac{d_e^3 \rho^2 g}{\mu^2}$
Peclet Number	$Pe = \frac{d_e V}{D}$
Eotvos Number	$Eo = \frac{g \Delta\rho d_e^2}{\sigma}$
Morton Number	$M = \frac{g \mu^4 \Delta\rho}{\rho^2 \sigma^3}$
Ohnesorge Number	$Oh = \left(\frac{\mu_d}{\rho_d \sigma d_e} \right)^{0.5}$

Then the total drag is :-

$$F_T = F_\mu + F_p = 6 \pi \mu_c R V \qquad 2.3$$

Note that the total drag is composed of two-thirds shear stress and one-third form drag (86).

For a spherical liquid droplet moving in a liquid field, the boundary is not rigid. Instead, it moves over the surface of the sphere in axial symmetry from a front stagnation point to a rear stagnation point. New area is being continuously created in the forward regions and equivalent area is being destroyed in the rear portion of the droplet. Hadamard (57), and independently Rybezynski (131), carried out similar analyses. Carrying the solution only to the first approximation, one arrives at a Stokes-law correction factor

$$F = 6 \pi \mu_c R V \left(\frac{3\mu_d + 2\mu_c}{3\mu_d + 3\mu_c} \right) \qquad 2.4$$

which simply states that the terminal velocity of the droplet whose interface is mobile, V, is given by :-

$$V = \left(\frac{3 \mu_d + 2 \mu_c}{3 \mu_d + 3 \mu_c} \right) V_{stokes} \qquad 2.5$$

Therefore the velocity depends upon the viscosity of both phases. For a very viscous droplet in a low viscosity field the correction factor reduces to unity. For a very low viscosity droplet moving in a viscous liquid field the correction factor approaches 1.5. If the viscosities of the two fluids are equal, the correction factor is equal to 1.2.

The derivations of Hadamard and Boussinesq are based on a model involving laminar flow of both drop and field fluids. Inertial forces are deemed negligible, and viscous forces dominant. The upper limit for the application of such equations is generally thought of as Re < 1.0.

2.2 Circulating Droplets

Internal circulation and the mobility of the interface are associated with the fluid sphere only, and not with the rigid sphere. For this reason the total interfacial area for the mass transfer from a rigid sphere to the other fluid phase remains constant except for a small change due to dissolution or sublimation. On the other hand, interfacial area of a circulating fluid sphere is continuously destroyed on the downstream hemisphere. The presence of very small traces of impurities which are surface active may inhibit internal circulation, but this effect can be partially overcome by the presence of diffusing solute being miscible in both phases (86, 88, 61). Linton and Sutherland (102) proposed that all solvents resulted in circulating drops if the solvent and water were carefully purified, but the purification required depended on the size of the drop. The smaller the drop the greater the purification required. They (102) also confirmed the observation of Garner et al (48) that the higher the interfacial tension the more rapidly the drops circulate. Direct observation by motion picture has established the circulation patterns (87). Reynolds number has great effect on the circulation inside the drop, depending upon, the physical properties for the two phases, and the drop diameter.

Terminal velocity for a circulating drop is more than that for an equivalent sphere (100, 131). Kintner et al (87), using a tapered tube, were able to match the velocity of fall of the drop with the velocity of the rising field. They (87) found that internal circulation was slowly damped out as the interface changed its character and became more contaminated.

It has been found that circulation velocity increases with the diameter of the drop, and with the ratio of external to internal viscosity, and that droplets of a given system do not circulate below a certain size. Bond et al (17) presented a relationship for the critical size at which circulation begins, while Garner et al (45) developed a correlation for Reynolds number that must be exceeded in order that circulation is present, for limited droplet viscosities and interfacial tension ranges.

2.3 Oscillating Droplets

Drop oscillations are expected when the drop size in a low viscosity field liquid is increased above the laminar flow region. At a critical size, generally at a drop diameter of about 0.3 cm. and when Reynolds number exceeds 200, the droplet flattens and generally assumes an oblate ellipsoidal shape showing a tendency to oscillate and the drop then undergoes symmetric periodic change from an oblate ellipsoid to a prolate one and back to oblate again. All oscillatory movements cause an alternate creation and destruction of interfacial area.

A generic graphical correlation of the possible shapes of a moving drop in infinite media using the Reynolds number, the Eotvos number, and the Morton number was proposed by Grace (52) and is shown in Figure 2.1. This correlation does not apply to systems with a large value of density and viscosity ratio. The effect of the walls of the container on the droplet hydrodynamics will be briefly discussed in section 2.6.

As expected, in the region of low Re and Eo the drop is spherical. At higher Re and intermediate Eo the drop shape is ellipsoidal, while the spherical or ellipsoidal cap shape require large values of both Re and Eo.

Oscillation may be started by the tearing-away from the droplet forming device, or by

intermittent shedding of vortices from the droplet wake (40, 69). The former mechanism would conflict with the Winnikow et al (185) observation that droplet oscillation started at some distance from the nozzle, and this distance decreased as the droplet diameter increased.

Various workers have proposed different correlations and models to describe and predict the frequency and the amplitude of oscillation. A valuable review of these models and correlations has been presented by Al-Faize (3) and Al-Hassan (4).

2.4 Velocities of moving Droplets

The study of the movement of a swarm of drops through a continuous phase medium is an important aspect of liquid extraction since the velocities of the drop phase determine the extractor capacity and the relative motion between drop and bulk fluid affects the convective mass transfer between phases. The hydrodynamics of this aspect is so complex that one seeks to analyse first the more simple cases such as the movement of single liquid droplets through another liquid medium without mass transfer between phases.

Various workers have reported that the liquid drop attains its terminal velocity only after a rise of about 5.5 to 15.0 cm. above the nozzle after an initial acceleration period.

Terminal velocity measurements have been reported by a number of investigators for drops in a wide variety of liquid-liquid systems. The agreement in the reported data was not good.

Starting with the Navier-Stokes equations of motion, for a rigid liquid sphere the equations reduced to:-

$$V_{stokes} = \frac{d^2}{18\,\mu_c}\left(\rho_d - \rho_c\right) g \qquad 2.6$$

The relationship for a spherical droplet moving in a liquid field where the boundary is not rigid is represented by equation 2.5.

Various correlations (89) have been proposed to relate terminal velocity, drop peak velocity and maximum drop size to the physical properties of the system by adopting dimensional analysis methods and later verification by comparing with experimental results. One such attempt (89) involved a theoretical approach to the mechanics of droplet motion by considering the force balance on a moving drop which can be mathematically given as :-

$$\rho_d \pi d_e^3 \frac{dV_d}{dt} = \frac{\pi}{6} d_e^3 g\left(\rho_d - \rho_c\right) - C_D \frac{\pi}{4} d_e^2 \rho_c \frac{V_d^2}{2} \qquad 2.7$$

At steady state terminal velocity the acceleration term may be considered zero and by equating the gravity forces to the sum of buoyancy and drag forces,the above equation becomes :-

$$\frac{\pi}{6} d_e^3 g\left(\rho_d - \rho_c\right) = C_D \frac{\pi}{8} d_e^2 \rho_c V_d^2 \qquad 2.8$$

and

$$V_d = \sqrt{\frac{4\,g\,d_e\left(\rho_d - \rho_c\right)}{3\,C_D \rho_c}} \qquad 2.9$$

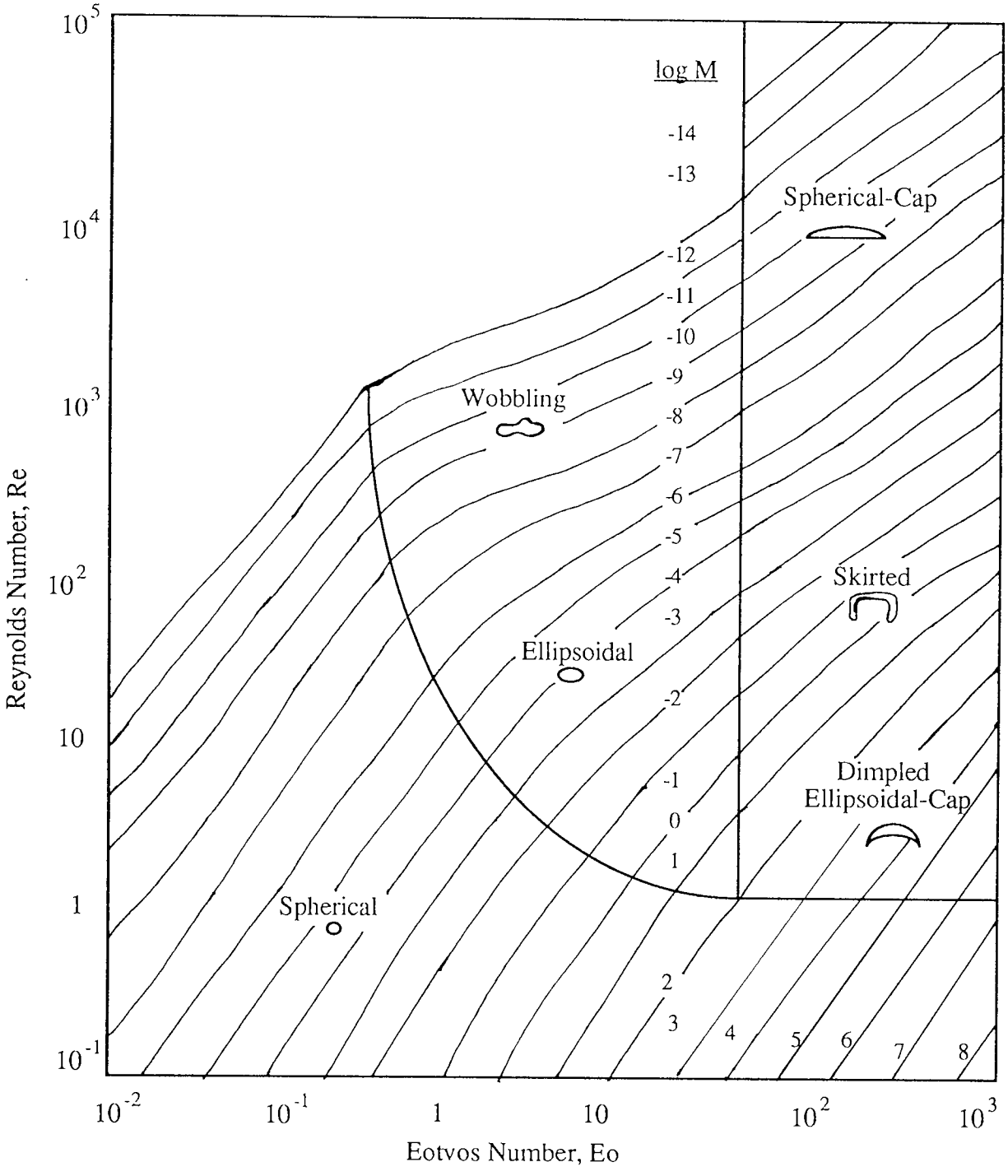

Figure 2.1 Shape Regimes for Bubbles & Droplets in unhindered Gravitational Motion through Liquids (52)

The drag coefficient can be defined as :-

$$C_D = \frac{4}{3} \frac{(\rho_d - \rho_c)}{\rho_c} \frac{g\,d}{V_d^2} \qquad 2.10$$

Hu and Kintner (71) examined the movement of droplets, of ten different organic liquids, through water and presented a relationship for their experimental data involving the Weber number, the Reynolds number " $10 < Re < 2200$ ", and a physical property group. They introduced the curve shown in Figure 2.2, from which the entire relationship could be predicted for a liquid droplet rising, or falling, through a liquid field of reasonable viscosity (up to 5.0 cp). The kind of motion the droplet experiences critically affects the rates of heat and mass transfer between the phases. However there is little mention in the literature of droplet hydrodynamics when mass transfer is taking place.

A typical plot of terminal velocity of rise, or fall, of a drop of oil in water is shown in Figure 2.3. For very pure systems, the relevant curve is ABCD, where at region "A" the droplet is very small with poor internal circulation. At region (B) freely internal circulation in the droplet starts, and it is eliminated at region (C). At these regions (B&C) the droplet moves considerably faster than a rigid sphere, because of the mobility of the droplet phase. After region (C) the oscillation and deformation starts, and the droplet velocity decreases. Thorson et al (166) proposed an equation to calculate the terminal velocities for a high interfacial tension system and for Reynolds number from 40 to 900 as follows :-

$$V_t = \left(\frac{6.5}{1.65 - \left(\frac{\Delta\rho}{\rho_d} \right)} \sqrt{\frac{\sigma}{(3\rho_d + 2\rho_c)}} \right) \Big/ \sqrt{d} \qquad 2.11$$

Vignes (175) proposed the following correlation

$$V_t = \frac{d}{4.2}\left(\frac{g\,\Delta\rho}{\rho_c}\right)^{2/3}\left(\frac{\rho_c}{\mu_c}\right)^{1/3}\left(1-\frac{Eo}{6}\right) \qquad 2.12$$

The above correlation was best fitted by the results of Mekasut et al (114) for terminal velocity. This correlation also gave a better prediction of droplet velocity than obtained from Hu and Kintner's correlation (71).

Grace et al (52) examined data from 25 sources and proposed correlations for partially contaminated droplets. The criteria which the data have to meet to be included here were as follows :-

$Eo < 40.0, M < 10^{-3}$, for $Re > 0.2$

and $d_e / D < 0.12$ for $Re > 100.0$

where the restrictions on d_e / D ratio assure that wall effects are negligible.The resulting correlation is:-

$$J = 0.94\,H^{0.757} \quad \text{for} \quad 2.0 < H < 59.3 \qquad 2.13$$

$$J = 3.42\,H^{0.441} \quad \text{for} \quad H > 59.3 \qquad 2.14$$

where:-

$$H = \frac{4}{3}\,Eo\,M^{-0.149}\left(\frac{\mu_c}{\mu_w}\right)^{-0.14}$$

$$J = Re\,M^{0.149} + 0.857$$

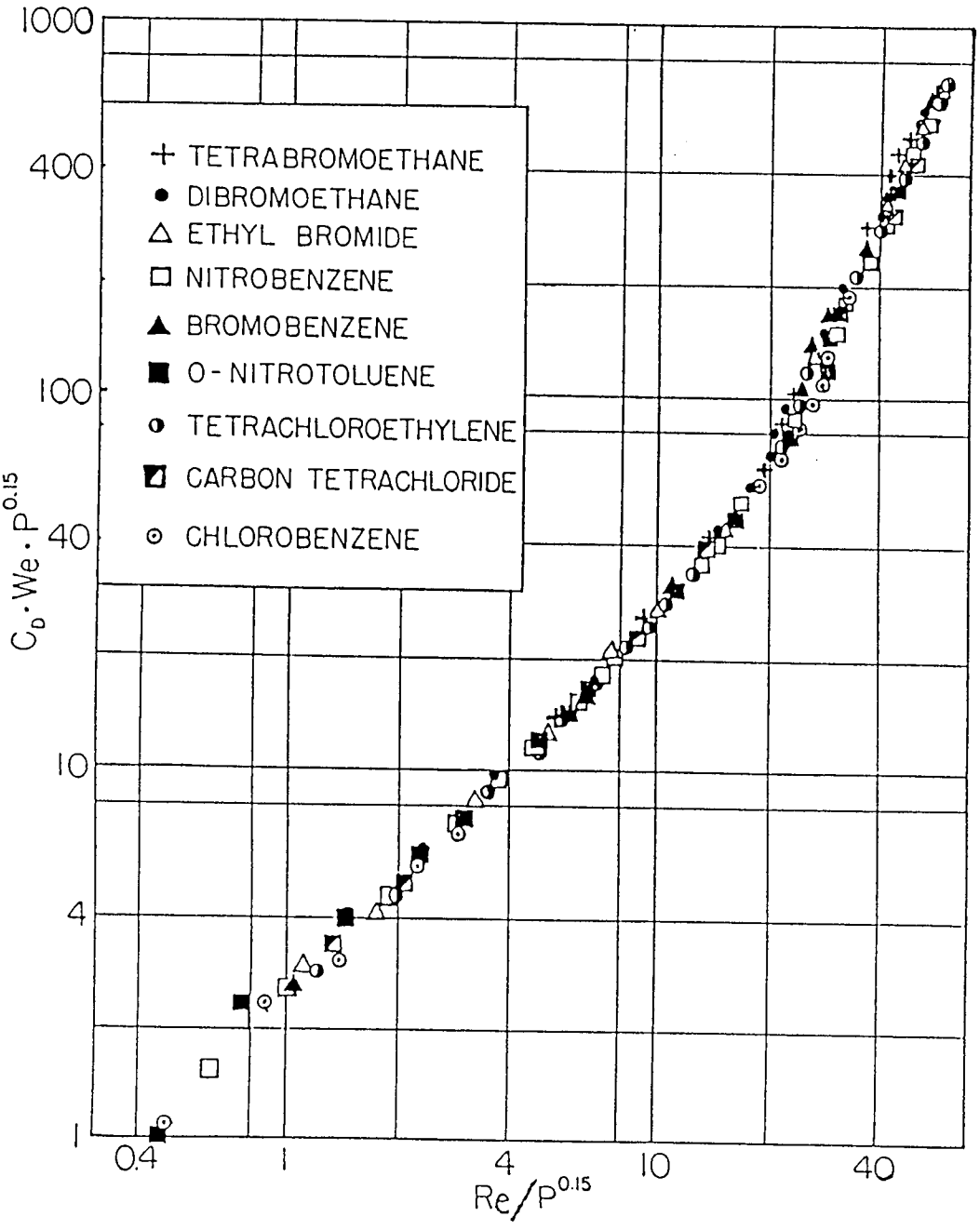

Figure 2.2 General Correlation

The value of the parameters H&J can be calculated using the above equations; then the terminal velocity is calculated using the following equation :-

$$V_t = \frac{\mu_c}{\rho_c d_e} M^{-0.149} (J - 0.857) \qquad 2.15$$

Misek (116) proposed the following equation to predict terminal velocity for droplet sizes in the range 0.05-0.5 cm.

$$V_t = 0.249\, d_e \left(\frac{g^2 \Delta\rho^2}{\rho_c \mu_c} \right)^{0.333} \qquad 2.16$$

2.4.1 Effect of Drag

In liquid liquid extraction the hydrodynamics of the drop are far beyond the limits of application of the preceding equations (16, 86). A drop moving through a liquid at such a velocity that the viscous forces could be termed negligible cannot exist. In real situations, both viscous and inertial terms have to be considered, and the Navier-Stokes equations cannot then be solved. For a droplet moving through an infinite medium with constant velocity, a global force balance leads to the following definition of the drag coefficient.

$$C_D = \frac{4}{3} \frac{(\rho_d - \rho_c)}{\rho_c} \frac{g\, d}{V_d^2} \qquad 2.10$$

in which "d" is the diameter of the sphere.

In the case of oblate or prolate ellipsoidal droplets the axis parallel to the line of motion would replace "d". Figure 2.4 represents the relationship between Reynolds number

and the drag coefficient. The drag coefficient is less for a rigid sphere than for that of a liquid droplet of the same size and density. This is a result of the mobility of the droplet surface , that is carried from the forward stagnation point to the rear by shear, and also to the droplet contents that are circulating internally. The result of the Hu and Kintner (71) correlation was a plot of log "$C_D We P^{0.15}$" against log "$Re P^{0.15}$" where "P" is a dimensionless physical property group.

$$P = \frac{\rho_c \sigma^3}{g \mu^4} \frac{\rho_c}{\Delta\rho} = \frac{4}{3} \frac{Re^4}{C_D We^3}$$

Johnson et al (78) extended the above equation to continuous phase viscosities of 20 Cp by using an additional parameter $\left(\frac{\mu_c}{\mu_w}\right)^{0.14}$ in the ordinate. It was reported that the effect of density on fall velocity is greater than the effect of surface tension (78).

2.4.2 Wake Formation and Hydrodynamics

To study mass transfer from a droplet it is essential to know the characteristics of the boundary layer around it. An invisible wake which exists at the rear of a moving droplet has been studied by many investigators for non-oscillating and oscillating liquid drops with, and without mass transfer (61, 189). The wake may be made visible by placing a dye in the droplet and allowing it to be transferred to the continuous phase, or by using a shadow technique. A boundary separation will be observed as a ring on the rear surface of the droplet.

The mass transfer mainly occurs into the boundary layer forward of the separation ring and travels in this layer around the wake to the trailing filament. Mass transfer of solute

from the droplet to the wake, and then to the continuous phase, depends upon solute concentration.

Yeheskel et al (189) grouped modes of wake shedding into three ranges of Re and C_D of the droplets. In range (A) for droplets Re < 150, the only shedding of elements of the wake is from the straight or wavy tail of the wake. In range (B)for droplet Re between 150 and 800 wake shedding was cyclic, from alternate sides of an oscillating wake, without oscillation of the droplets themselves. The drag coefficient was lower than that for a solid sphere, and decreased with increasing Reynolds number. In range (C) for droplet Re > 800 random wake shedding occurred with oscillation of the droplets and drag coefficient increased sharply with increasing Reynolds number.

The ratio of wake volume to droplet volume was found to be independent of droplet size and interfacial tension, and to be a linear function of " $\Delta \rho / \rho_c$ " ratio (189). It was also found that the relative wake volume, was about one third of that of a single droplet for a vertical assemblage, and about twice for horizontal assemblages (190).

Wakes were classified into two types; one for non-oscillating droplets, which was characterised by the vortex threads and the other for oscillating droplets, which was characterised by the periodic discharge of vorticity.

Later,Wilson (184) studied the characteristics of the vortex region and wake at the rear of a moving droplet in the range 20 < Re < 700. A critical Reynolds number was indicated below which the vortex volume increases with the increasing of Reynolds number.

Considerably less work has been described for open turbulent wakes, although some excellent photographs have been published (178, 112). Wake shedding appears to be

responsible for the wobbling motion often exhibited by spherical-cap bubbles with Reynolds number less than 150.

2.5 Shape of Moving Droplets

The study of the shape of moving droplets is useful in understanding their dynamics since the drag depends on the shape of the moving droplet. Namely, the shape of the moving droplet is defined by the balancing of interfacial tension, viscous forces,and inertial forces at the interface (179).

As shown in Figure 2.1 the fluid particle shapes can be classified as follows:-

1. Spherical, this shape is attained when inertial forces are negligible with respect to interfacial tension and viscous forces.

2. Ellipsoidal, indicates the shape obtained by rotating an ellipse about one of its principal axes. If this is the minor one, the ellipsoid is said to be oblate, other wise it is prolate.

3. Spherical-cap or ellipsoidal-cap, this shape is quite similar to the upper segment cut from a sphere or an ellipsoid, with a flat and sometimes indented base. This shape is peculiar to large drops. Kintner (86) reported that drop distortion can be classified according to the viscosity of the continuous phase.

Garner et al (47) estimated the area of non-oscillating oblate drops using the eccentricity "E" of an ellipsoidal drop. They (47) explained this type of distortion of mobile drops on the basis of a relative change in the outside hydrodynamic pressure and the inside

pressure due to internal circulation.Drop deformation occurs mostly in the region near the peak point of terminal velocity vs drop diameter plot shown in Figure 2.1. In this region, as the drop size increases, deformation, vibration and oscillation, wobbling and changes in wake pattern become important phenomena.

2.6 Wall Effects

The movement of fluid particles usually takes place in limited containers, whose walls may affect the field motion. Fluid particles moving in small vessels maintain a spherical shape up to Reynolds number lower than those characteristic of fluid particles moving in an infinite medium. In fact, drops moving through infinite media tend to be flattened in the vertical direction, while the container wall tends to cause elongation (178). A wall correction factor is necessary in order to interpret the experimental data in terms of a drop moving in an infinite medium. This correction factor is a function of the diameter ratio "DR" which is the ratio between the diameter of the volume equivalent sphere and the diameter of the container. Grace et al (52) represented some useful general criteria for wall effects to be negligible as follows :-

$DR < 0.6$	for	$Re < 0.1$	2.16.a
$DR < 0.08+0.02 \log_{10} Re$	for	$0.1 < Re < 100$	2.16.b
$DR < 0.12$	for	$Re > 100$	2.16.c

If the wall effects are present, they can be estimated using the above correlations. In the range $Eo < 40$ and $Re > 200$ the terminal velocity correlation factor becomes independent of Re, and can be estimated using the following relationship (49) :-

$$\frac{V_K}{V_t} = \left(1 - (DR)^2 \right)^{\frac{3}{2}} \qquad 2.17$$

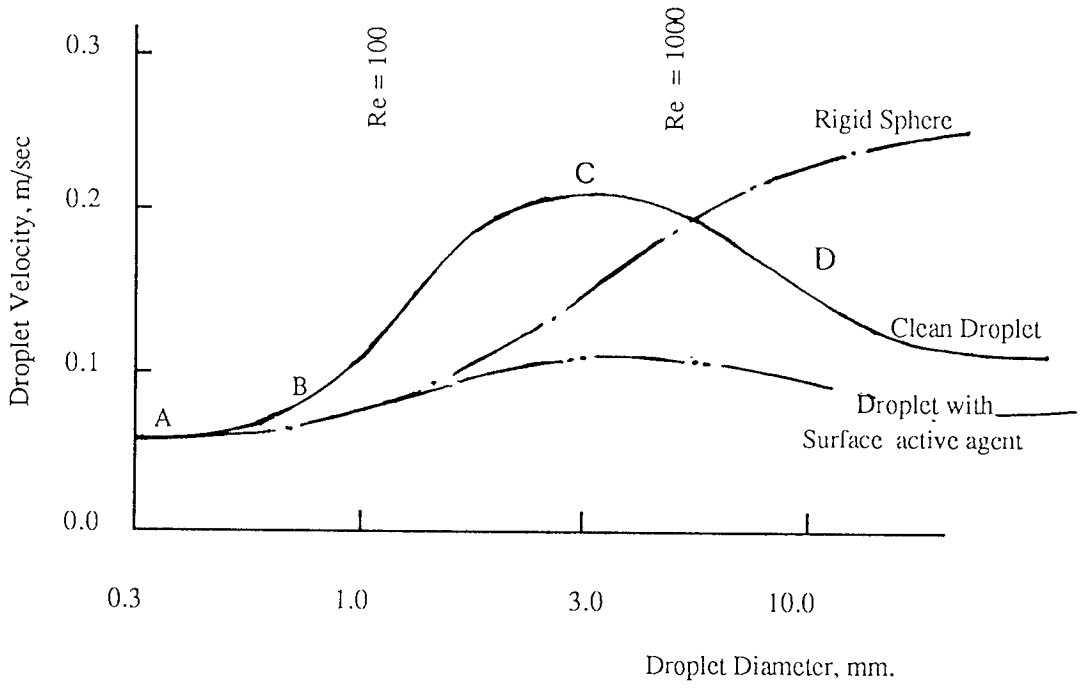

Figure 2.3 Terminal Velocity of Rise, or Fall of Droplet of Oil in Water

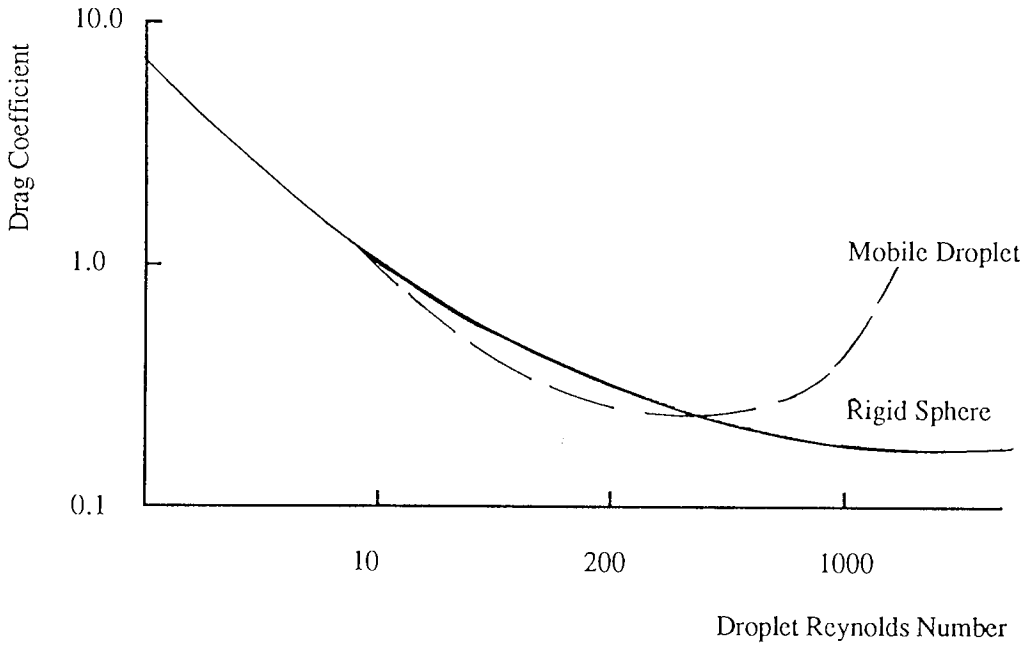

Figure 2.4 Correlation of drag coefficient & Reynolds number for rigid sphere & mobile droplet

For the case of large drops, Eo > 40 & for 0.125 < Re < 0.6, the relationship proposed by Wallis (177) can be used;

$$\frac{V_K}{V_t} = 1.13 \ \exp\ (-DR) \qquad 2.18$$

All previous investigators were in agreement that the Reynolds number of the droplet and the presence of adjacent droplets have an effect on droplet hydrodynamics.

2.7 Effect of Surfactants

It has been observed by many investigators (56, 78) that surface-active agents when present even as a minute trace, affect drop dynamics by way of damping the oscillations, reducing the internal circulation and then increasing the drag on the droplet. The experimental data reported in the literature has limited value, due to the absence of complete specification regarding the purity of, and correct physical constants for, the chemicals used. Chemicals of dubious purity such as tap water must be avoided, and much of the data in the literature must be used with caution because of the suspected presence of surface-active agents (86). The data of several authors on the rate of fall of carbon tetrachloride drops through water showed wide differences for the intermediate size of drops, even though some good agreement among the data for very small and for very large drops was seen (96). This difference was attributed to the presence of surface-active agents of a type that can segregate near the interface.

It has been shown (94) that drop-soluble surfactants lower the interfacial tension and cause small drops to be formed, which behave like rigid spheres. Davies (35) indicated that for clean interfaces circulation should occur in any drop irrespective of the size and that small drops showed more sensitivity to damping of internal circulation

than large ones. The presence of impurities reduced the mass transfer by reducing the frequency and amplitude of oscillation. The influence of impurities decreases with increasing viscosity of the continuous phase (105).

Based on the above, the materials of construction of some of the recirculating apparatus described in the literature " including aluminium tanks or piping, or packed pumps and gaskets " could introduce enough impurities to affect the experimental results.

CHAPTER THREE

THE EFFECT OF APPLIED TURBULENCE UPON DROPLET BEHAVIOUR

3.1 Introduction

Turbulence may be induced in a fluid through an electrostatic field, sonic or ultra-sonic vibration and through mechanical agitation. Many workers have studied the effects of applied turbulence upon droplet behaviour, e.g; droplet diameter, droplet velocity, droplet shape, and the mass transfer from or / and to droplets.

For example applied turbulence has been shown to have a significant effect on the droplet diameter. The droplets produced in an electrostatic field are smaller than droplets produced in a non-turbulent field, which will of course also affect the interfacial area (9, 28, 153, 154, 157, 158, 188). Thornton and his coworker (9, 153, 154) studied the behaviour of single droplets in an electrostatic field; they found that the presence of a field caused the interface to behave as if its interfacial tension was very low. In mechanically agitated equipment, the applied turbulence also has a significant effect on the droplet diameter. Shinnar and Church (142) demonstrated the effects of agitation in a mixer on a particle and the conditions around it. Breakup and coalescence of droplets has been reported to be caused by viscous shear forces or by turbulent pressure fluctuations, both produced by turbulent agitation (110, 126, 174).

In mixer-settler equipment, as in other mechanically agitated equipment, the droplet diameter is inversely proportional to the agitation energy (18, 19, 113).

Turbulence also has an effect on the shape of the droplet. In electrostatic fields, circulation and oscillation have been seen to be suppressed in very small droplets (153, 154). Clark (31) studied the shape of droplets in a mixer-settler. Away from the impeller, not one single droplet appeared to significantly distort from the spherical shape. However, several deformed droplets appeared in the region close to the impeller. A recent model of Logsdail et al (107) assumed that the droplet deformation in a mixer is caused by the external inertial stress arising out of the turbulent pressure fluctuations. They reported that the deformation most probably starts through the formation of a depression on the droplet interface and this depression propagates resulting in distortion and possibly subsequent breakage (107).

Recently, Kumar et al (94) introduced alternative mechanisms of droplet breakage in stirred vessels. They proposed, apart from the breakage due to turbulent stresses in the region just surrounding the impeller, two other mechanisms which operate in the flow of the impeller itself. These mechanisms, i.e. breakage through plane hyperbolic flow near the impeller and the shear flow in the boundary layer on the impeller, yield different values of maximum stable droplet sizes.

Koshy et al (89) studied the effect of surfactants on droplet breakage in turbulent liquid dispersions. They concluded that the breakage of droplets in stirred dispersions is influenced by the presence of surfactant not only through the reduction of interfacial tension, but also by the generation of an interfacial tension gradient across the droplet.

Applied turbulence has an effect on droplet velocity. The droplets having detached from their formation nozzles were found to move at higher velocities in an electric field than when they moved in an uncharged field (154). In mechanically agitated equipment, droplet velocity reduced under the effect of turbulence, especially in pulsed columns.

Several workers (16, 62, 63, 92) have studied the formation and breakage of bubbles, both experimentally and theoretically. Most of these studies were based on the isotropic

turbulence theory, therefore comparison between them and the droplet studies is useful.

The effect of applied turbulence on the mass transfer rate is discussed in this paragraph. Thornton et al (164) found that the mass transfer coefficient in the organic (dispersed) phase was enhanced in an electrostatic field. The enhancement of mass transfer efficiency was reported to be due to the increase of effective interfacial area of the droplets and the intensive circulating motion inside the droplet. Also it was generally recognised (42) that sonic and ultra-sonic vibrations increased the mass transfer coefficient in mechanically agitated equipment as was demonstrated by several workers.

The effect of applied turbulence, in pulsed columns, on the droplet behaviour are discussed in more detail in the next sections, while its effect on the mass transfer rates is discussed in subsection 4.4 of Chapter 4.

3.2 Droplet Size in Pulsed Columns

Knowledge of droplet size is very important in the design and understanding of liquid-liquid extraction pulsed columns, since droplet size influences all the other hydrodynamic parameters. The mass transfer efficiency is also influenced because the interfacial area is a function of droplet size. The dispersed phase residence time distribution also depends on droplet size distribution.

3.2.1 Energy Dissipation

Most of the equations for the calculation of the droplet size in mechanically agitated columns are based on the theory of isotropic turbulence of Kolmogoroff. On a stability analysis of a droplet in a turbulent flow field the dependence of droplet size on the supplied energy and the physical properties of the system is given according to the following relationship:-

$$d_{max}\,\alpha\left(\frac{\sigma}{\rho_c}\right)^{0.6}\psi^{-0.4} \qquad 3.1$$

where ψ is the energy dissipation in cm^2/sec^3

The calculation of the energy dissipation in the presence of a sieve plate in a pulsed column has been carried out in various ways. Jealous and Johnson (75) considered the power input necessary to operate a pulsed perforated-plate column by dividing the power into the three categories of static head, inertia of liquid, and friction loss. They (75) calculated the friction loss, assuming a perforation as an orifice and neglecting the pressure recovery after passing through the orifice. They (75) proposed the following equation:-

$$\psi = \frac{2\pi^2}{3}\left(\frac{1-\phi^2}{2C_o^2\phi^2 h_c}\right)\left(A_p * f\right)^3 \qquad cm^2/sec^3 \qquad 3.2$$

where:-

C_o :- is the discharge coefficient, and equal 0.6

ϕ :- is the free area of the sieve plate .

h_c :- axial height of one compartment.

On the other hand, Miyauchi and Oya (119) corrected the pressure recovery as follows to calculate the rate of energy dissipation in pulsed perforated plate columns. The pressure loss across an orifice is given approximately by:-

$$\Delta P = \frac{(1-\phi)(1-\phi^2)}{2C_o^2}\rho_c U_o^2 \qquad 3.3$$

The mean rate of energy dissipation (ψ) per unit mass of column fluid is expressed as follows:-

$$\psi = \frac{\left(\frac{H}{h_c} + 1\right) \Delta P \, \phi \, \frac{\pi}{4} D_T^2 U_o}{\rho_c \frac{\pi}{4} D_T^2 H} \qquad 3.4$$

substituting 3.3 into 3.4, one can get

$$\psi = \left(\frac{1}{h_c} + \frac{1}{H}\right) \frac{\phi\left(1-\phi\right)\left(1-\phi^2\right)}{2\,C_o^2} U_o^3 \qquad 3.5$$

For sinusoidal pulsing, U_o^3 is expressed as follows:

$$U_o^3 = \frac{5}{3\sqrt{2}} \pi^2 \left(\frac{A_p * f}{\phi}\right)^3 \qquad 3.6$$

substituting 3.6 into 3.5, one can get:-

$$\psi = \frac{5\,\pi^2}{3\sqrt{2}} \left(\frac{h_c}{H} + 1\right) \frac{\left(1-\phi\right)\left(1-\phi^2\right)}{2\,C_o^2 \phi^2 h_c} \left(A_p * f\right)^3 \qquad 3.7$$

when hc/H<< 1 , the above equation becomes :-

$$\psi = \frac{5\,\pi^2}{3\sqrt{2}} \frac{\left(1-\phi\right)\left(1-\phi^2\right)}{2\,C_o^2 \phi^2 h_c} \left(A_p * f\right)^3 \qquad 3.8$$

Thornton (162) approached the evaluation of energy dissipation from the equation of the standard orifice velocity as follows :-

$$U_o^2 = \frac{2\,\Delta P\, C_o^2}{\left(1-\phi^2\right)\rho_c} \qquad 3.9$$

This velocity is also related to the instantaneous pulse velocity and the fractional free area by the following equation:-

$$U_o = \frac{1}{\phi}\frac{dy}{dt} \qquad 3.10$$

from 3.9 and 3.10 the frictional pressure drop is given by:-

$$\Delta P = \frac{\rho_c\left(1-\phi^2\right)}{2\,\phi^2\, C_o^2}\left(\frac{dy}{dt}\right)^2 \qquad 3.11$$

The energy dissipation per unit mass of fluid is given by:-

$$\psi = \left(\frac{\rho_c\left(1-\phi^2\right)N}{2\,\phi^2\, C_o^2 H}\left(\frac{dy}{dt}\right)^2\right)\left(\frac{dy}{dt}\right) \qquad 3.12$$

where N is number of plates. For a sinusoidal wave pulse,

$$y = \frac{A_P}{2}\sin 2\pi t f \qquad 3.13$$

and

$$\frac{dy}{dt} = \frac{A_P}{2}2\pi f \cos 2\pi t f \qquad 3.14$$

for one complete cycle of pulsing and by substituting 3.14 into 3.12, one can get:

$$\psi = \frac{\pi^2 N\left(1-\phi^2\right)}{2\phi^2 C_o^2 H}\left(A_p f\right)^3 \qquad 3.15$$

and since $H/N = h_c$; equation 3.15 becomes as follows:-

$$\psi = \frac{\pi^2\left(1-\phi^2\right)}{2 C_o^2 \phi^2 h_c}\left(A_p * f\right)^3 \qquad 3.16$$

Recently Godfrey et al (51) applied Bernoulli's equation to a flow through a single hole, assuming no flow interactions, and putting the required area ratio equal to the free area fraction, ϕ.

The pressure drop over a plate is given by:-

$$\Delta P = \frac{\rho_c\left(1-\phi^2\right)}{2\phi^2 C_o^2} V_p^2 \qquad 3.17$$

where V_p is superficial velocity.

The energy dissipation was evaluated by the same method as used by Thornton (162). By replacing the superficial velocity, V_p, by an average pulse velocity, f*Ap, the energy dissipation is represented as follows :-

$$\psi = \frac{\left(1-\phi^2\right)}{2 C_o^2 \phi^2 h_c}\left(A_p * f\right)^3 \qquad 3.18$$

From the previous equations it is clear that there was no agreement about a general formula for the energy dissipation; this subject is discussed in more detail in Chapter 7, where a new correlation for energy dissipation is introduced. Boyadziev and Spassov (21) introduced a definition for the lowest limit of the maximum local kinetic energy dissipated into the dispersion passing through the plate per unit plate area as follows:-

$$e_m = \frac{\rho_c (A_p * f)^3}{2\phi^2} \qquad kg/sec^3 \qquad 3.19$$

In section 2.3, equation 3.19 is verified in more detail. It was mentioned (118) that the local energy dissipation cannot be easily determined, at sufficiently high Reynolds numbers, so e_m may be replaced by the average dissipation rate per unit mass, which is just the power input per unit mass.

Recent work by Godfrey et al (51) has shown that the discharge coefficient C_o is not constant at 0. 6 for the pulse conditions. They (51) introduced a correlation to calculate C_o for pulsing conditions.

3.2.2 Droplet Breakup

Rational design requires a knowledge of the distribution of droplet sizes in a column. In the general case the poorly understood phenomena of breakage and coalescence have a strong influence on the characteristics of the dispersed phase. The problem can be simplified and meaningful results obtained by first analysing only the breakage process, since coalescence is often reduced to a negligible level in many systems. This is particularly true in dilute-dispersed phase systems or when surface-active agents are present to increase the resistance to coalescence or when a solute is present, mass

transfer may reduce the coalescence frequency substantially (54, 138, 148).

The droplet breakup process increases with intensity of agitation as well as with increase in residence time of droplets in the column. The forces controlling deformation and breakup comprise two dimensionless groups; a Weber number (We) and a viscosity group (Nvi). Breakup occurs when (We) exceeds a critical value (We)crit (65). For the simplest case, namely an isotropic homogeneous turbulence, the main contribution to the kinetic energy is made by the fluctuations in the continuous phase where the Kolmogoroff energy distribution law is valid (65).

Clay (27) proposed that droplets could breakup in a turbulent field by three possible mechanisms; laminar shear, turbulent shear, and turbulent pressure fluctuations. Sleicher (147) observed that droplets breakup only very close to the wall where the turbulence is least homogeneous and least isotropic. All the above studies were carried out for droplet breakup in turbulent pipe flow.

Miyanami et al (118) presented a mechanism of droplet breakup in a multistage vibrating disc column. They (118) observed that the breakup of the drops in the column at low frequency vibration was associated with two recognisable loci these being at the lip of the hole of the vibrating disk and within the hole itself, but at higher vibrating speeds, the droplet breakup within the hole becomes dominant. The droplet breakup by disk vibration is thought to be dominated by the instantaneous maximum speed of disk vibration.

In the evaluation of droplet size in axially agitated plate columns, Sovova and Prochazka (150) mentioned that the effect of agitation on the droplet breakage depends not only on the frequency and amplitude of the vibration but also on the shape of periodic wave motion. Through experimental observation, Shou and Zheng (143) saw that droplet breakup occurred mainly in the field near the holes in the vibrating plates. They (143) assumed that turbulent shear forces near the holes in the plate control the

breakage processes.

Recently, Eid et al (38) studied experimentally the droplet breakage probability and daughter drop size distribution in a pulsed sieve plate column. From their (38) experimental observations, two particular breakage mechanisms were exhibited:-

1. Droplet breaks after one or more passages through the sieve plate.
2. Droplet breaks without having passed through the sieve plate.

The second mechanism is mainly observed when the droplet is located just below the plate at the upstroke dead-point of pulsation; at this time shear stresses are so strong that the droplet is stretched until it breaks. The probability of breakage is affected by the following factors:-

1. The intensity of pulsation.
2. The ratio of droplet diameter to plate hole diameter " d_e / d_h ".
3. The distance between the droplet formation device and the sieve plate.

3.2.3 Droplet Diameter Correlations

Many workers have studied droplet size under pulsed conditions. Most of the correlations which have been developed to predict the droplet size are based on the energy dissipation concept which is mentioned in section 3.2.2. The correlations which are used to calculate the droplet diameter are listed below :-

Assenov and Penchev (8) proposed a correlation for predicting the droplet diameter in well agitated conditions as follows:-

$$d_{32} = 0.01 \left(\frac{\sigma}{\Delta\rho\, g} \right)^{0.5} \left(\frac{A_p * f \mu_c}{\sigma} \right)^{-0.5} N^{-0.1} \qquad 3.20$$

Kagan et al (80) developed the following correlation in a pulsed sieve plate column, 5.6 cm in diameter :-

$$d_{32} = 0.92 \left(\frac{\sigma}{\rho_c g} \right)^{0.5} \left(\frac{\rho_c}{g \mu_c} \right)^{-0.5} \left(A_p^* f \right)^{-0.3} N^{-0.11} \qquad 3.21$$

Khemangkorn et al (83) proposed a correlation for the Sauter mean diameter in a column 5. 0 cm in diameter as follows :-

$$d_{32} = 0.173 \left(\frac{\sigma}{\rho_c} \right)^{0.6} \left(\frac{\gamma_c}{h_c \beta_c} \right)^{-0.4} \left(A_p^* f \right)^{-1.2} \qquad 3.22$$

where:-

$$\gamma_c = \frac{5\pi^2}{6\sqrt{2}} \frac{1 + h_c/H}{C_o} \qquad \text{and} \qquad \beta_c = \frac{\phi^2}{(1-\phi)\left(1-\phi^2\right)}$$

Boyadzhiev and Spassov (21) presented the following correlation for droplet size at highly turbulent regimes and based on the maximum local kinetic energy dissipation concept mentioned in section 2.2.

$$d_{32} = 0.57 \left(\frac{\sigma}{\rho_c} \right)^{0.6} \left(\frac{\left(A_p^* f \right)^3}{d_h \phi^2} \right)^{-0.4} \qquad 3.23$$

Equation 3.23 is not correct, the correct equation -3.24- is shown below and the derivation in detail is shown in appendix C.1.

$$d_{32} = k_4 \left(\frac{\sigma}{\rho_c} \right)^{0.6} \left(\frac{(A_p * f)^3}{d_h \phi^3} \right)^{-0.4} \qquad 3.24$$

and the definition of the maximum local kinetic energy dissipation should be;

$$e_m = \frac{(A_p * f)^3}{d_h \phi^3} \qquad cm^2/sec^3 \qquad 3.25$$

and not

$$e_m = \frac{\rho_c (A_p * f)^3}{2 \phi^2} \qquad kg/sec^3 \qquad 3.19$$

Misek (117) proposed the following correlation;

$$d_{32} = 0.439\, d_h \left(\frac{\sigma \phi^{0.5}}{d_h \rho_c} \right)^{0.6} \left(\pi A_p * f + V_c \right)^{-1.2} \qquad 3.26$$

Schmidt (137) proposed a correlation to determine the droplet diameter as follows:-

$$d_{32} = 1.70 \left(\frac{\sigma^{0.5} \mu_c^{0.1}}{\rho_c^{0.6} g^{0.4}} \right) (A_p * f)^{-0.3} N^{-0.11} \qquad 3.27$$

Shenlin et al (136) presented the following correlation;

$$d_{32}=0.048\left(\frac{\sigma}{\rho_c}\right)^{0.544}\left(A_p^{0.8} * f^{-1.12}\right) \qquad 3.28$$

Kubica and Zdunkiewicz (91) developed a correlation for droplet size in a pulsed column, 6.1 cm in diameter. Based on five systems and d_h = 0. 3 cm only.

$$d_{32}= 0.0135\, d_T \left(\frac{(A_p * f)^2 \rho_c d_h}{\sigma}\right)^{-0.225}\left(\frac{\mu_c}{\mu_d}\right)^{0.0163} \qquad 3.29$$

Pietzch and Pilhofer (124) developed an equation for predicting droplet size based on the motion of droplets in the vicinity of the plates as follows :-

$$d_{32}=\sqrt{\frac{6\,\sigma}{\Delta\rho\, g + b\,\rho_d}+\frac{9}{64}\left(\frac{C'_D V_k^2 \rho_c}{\Delta\rho\, g + b\,\rho_d}\right)} - \frac{3}{8}\left(\frac{C'_D V_k^2}{\Delta\rho\, g + b\,\rho_d}\right) \qquad 3.30$$

where:-

$$V_K = V_t + \frac{f\, A_P}{\phi}$$

and

$$b = \frac{V_K^2}{\sqrt{0.905^{\,d_h/\phi}}}$$

the drag cofficient is defined as $C'_D = \frac{4}{3}\frac{Ar}{Re}$

Vassallo et al (171) proposed a correlation to predict the droplet diameter, as a function of hold- up and pulse intensity as follows:-

$$d_{32} = 8.36 * 10^{-5}\left[\left(A_p * f \right)^{-0.87} - \left| 1 - x \right|^{-0.36} \right]^{-0.60} \qquad 3.31$$

The above correlation is the only one which shows the droplet diameter as a function of hold-up but the subtraction of different dimensions is unreasonable.

3.3 Droplet Velocity in a Pulsed Field

There are several different representative velocities for a droplet depending upon the condition in which the droplet is moving. Under non-pulsed conditions and without the existence of sieve-plates or packing elements in the column, i.e. "empty column", the droplet velocity is simply the free moving terminal velocity. The representative velocity under pulsed conditions and at very low hold-up x --> 0 is termed the characteristic velocity "V_k". For moderate hold-up " $0 < x < 0.3$ " the representative velocity is called the slip velocity "V_s". These two velocities and their relationship to the free moving terminal velocity are illustrated in the following sections.

3.3.1 Droplet Velocity in a Pulsed Spray Column

The general behaviour of free particles in a sinusoidal velocity field can be represented by a non-linear Langevin equation. The non-linear relation in which the drag is proportional to the square of the relative velocity leads to the Mathieu equation. Stability criteria based on the Mathieu equation are applied to bubble-liquid systems in the sonic and ultrasonic region, to liquid droplet systems in pulse columns to solid-liquid systems by using drag coefficients obtained from measurements of terminal velocities (68). In a conventional pulsed extraction column, in which pulse frequencies are typically 0.5 to 2.5 Hz and amplitudes from 5 to 50 mm (68), the drop can have a

velocity lower than the terminal velocity because of the nature of the forces involved. Houghton (68) demonstrated that it was theoretically possible to arrest the directional motion of particles by applying a sinusoidal velocity to the continuous phase in which they were suspended. These theoretical predictions have been found on lumped parameter models for particle fluid systems involving a balance of forces.

Houghton et al (68, 169), Baird and Ritcey (11), Chonowski and Anglino (30), Brush et al (25) and Wallis et al (177) have confirmed these demonstrations experimentally. Special consideration must be given to the situation in pulsed columns, because of the low frequency and high amplitude compared with the conditions applying in the above equations.

a. Houghton et al Study

Houghton et al (68, 169) studied the behaviour, whilst falling under gravity, of four sizes of precision sapphire spheres (0.0794-0.4764 cm in diameter) and six sizes of glass spheres (0.0208-0.505 cm. in diameter) in a vertically oscillating water column (utilising electrodynamic shaking) at frequencies and amplitude ranges of 5-50 Hz and 0-1.0 cm. respectively. Houghton et al (68) pointed out that an apparent increase in the drag force for oscillating particle-fluid systems may only be symptomatic of other more complicated phenomena. In addition to drag coefficient increase there can be a change in the drag law exponent, phase lag in the external fluid acceleration and influence of an acceleration history force, often called the Basset force, although their overall influence could be empirically equivalent to a phase lag in fluid acceleration.

A vertical resolution of forces on a free particle in a sinusoidal velocity field are; particle-fluid drag, buoyancy, inertia of particle, and inertia of displaced fluid forces. A n'th power drag law has been used to generalise the flow regimes since $n = 1$ corresponds to Stokes or creeping flow while $n = 2$ implies Newtonian or inertial behaviour, fractional drag exponent $1 < n < 2$ representing intermediate flow regimes.

The numerically computed velocities were compared with the following analytic prediction due to Houghton (68) for the relative particle-fluid velocity and a drag law of square form (n =2).

$$\frac{V_k}{V_t} = \left\{ \frac{1}{2} + \frac{1}{2a} + \frac{1}{2a}\sqrt{\left(1 - 2a - 4a\left(\frac{q^2}{2a} - 1\right)\right)} \right\}^{0.5} \qquad 3.32$$

where:-

$$a = \frac{3\,\rho_c \left| \rho_p - \rho_c \right| C_D}{2\left(\rho_p + 0.5\,\rho_c\right)^2 R\,\omega^2}$$

$$q = \frac{3\,\rho_c \left| \rho_p - \rho_c \right| C_D A_P}{4\left(\rho_p + 0.5\,\rho_c\right)^2 R}$$

and

$$\omega = 2\,\pi\,f$$

The above equation is in good agreement with numerically calculated velocities (Vk\Vt) when (q^2/ 2a) < 0.5 (73).

b. Baird et al Study

Baird and Ritcey (11) studied the effect of vertical oscillation on the average terminal velocities of plastic spheres in water. The sphere diameters ranged from 0.32 to 1.27 cm and oscillation frequencies were from 0.88 to 2.37 Hz with amplitudes from 2.8 to 10.0 cm. They (11) solved equation 2.7 numerically subject to the assumptions that B(t) = 0 and that the virtual mass coefficient (x) is constant at 0.5 and the velocity distribution around the particle is assumed to be the same during oscillation as at steady state, for the same relative particle-fluid velocity (quasi-steady-state).

Rearrangement of equation 2.7 gives the particle acceleration as :-

$$\frac{dV_d}{dt} = \frac{\left[1.5 \frac{dV_c}{dt} + (1 - \xi) g - \frac{3 C_D}{8 r} (V_d - V_d) | V_d - V_c | \right]}{(\xi + 0.5)} \qquad 3.33$$

where:-

$$\xi = \frac{\rho_d}{\rho_c}$$

For sinusoidal liquid pulsations

$$V_c = A_p \omega \cos \omega t \qquad 3.34$$

and

$$\frac{dV_c}{dt} = A_p \omega^2 \sin \omega t \qquad 3.35$$

Equation 3.33 was solved to obtain the velocity compared to the terminal value.

$$\frac{V_k}{V_t} = \left\{ 1 - 2 \left(\frac{\xi - 1}{2\xi - 1} \right)^2 + \left(\frac{A_p \omega}{V_t} \right)^2 \right\}^{0.5} \qquad 3.36$$

Equation 3.36 give a greater retardation than the numerical solution given by Houghton (68), particularly in the case of the small diameter sphere (0.3 cm).

An interesting feature of equation 3.36 is that it appears to predict that the mean velocity

can be reduced to zero at sufficiently large values of the amplitude and frequency. Values of $A_p w/V_c$ required to give this condition are greatly in excess of those used in pulsed extraction columns.

c. Chonowski Study

Chonowski and Anglino (30) studied the behaviour of falling single drops of chlorobenzene in oscillating water. At frequencies of pulse of f > 2.5 Hz , and amplitude A_p >1.5 cm. the drop velocity was reduced by more than 30%; such conditions might be used in pulsed columns. They (30) made a theoretical analysis of the motion of a drop in a pulsed medium. The drag coefficient was modified to take into account the dynamic effects; the equation was solved for two cases.

Grace et al (32) mentioned that the general applicability of the results of the Chonowski and Anglino (30) equation is untested and that the equation might not be valid. Hussain (72) found that it was difficult to run the Chonowski equation reliably on the computer to compare the predicted and experimental Vk/Vt values, possibly because of an error in the equation.

d. Brush Study

Brush et al (25) studied the motion of quartz spheres, 0.12 cm in diameter, in a vertically oscillating water column at 3.5-6.7 Hz and a range half-amplitude of fluid oscillation from 1.17 to 5.08 cm. The following equation is the motion of a sphere settling in an oscillating fluid.

$$\rho_d \frac{\pi d^3}{6}\frac{dV_d}{dt} = \frac{\rho \pi d^3}{6}\frac{dV_c}{dt} + K\frac{d^3}{6}\left(\frac{dV_c}{dt} - \frac{dV_d}{dt}\right) + A\left(V_c - V_d\right) + \frac{\pi d^3}{6}\left(\rho_d - \rho_c\right) g \qquad 3.37$$

where:-

$$K = \frac{1}{2} + \frac{9}{4} N$$

$$A = 3 \mu \pi d \left(1 + {}^{1}/_{N} \right)$$

$$N = \frac{\sqrt{8 \nu}}{d \sqrt{\omega}}$$

and ν is the kinematic viscosity of the fluid,

The integration of equation 3.37 gives:

$$\frac{V_k}{V_t} = \frac{N}{1 + N} \qquad 3.38$$

Equation 3.38 is valid for small values of N which is inturn indicative of large particles or high frequencies of oscillation. It should be noted that the mathematical solution is restricted to small amplitude oscillation, and the fluid amplitude is the same order of magnitude as the diameter of the sphere.

Mukundan (120) presented a relationship for the characteristic velocity "Vk", in a pulsed spray column as follows:-

$$V_k = 0.32 \left(\frac{g \Delta\rho \sigma}{\rho_c^2} \right)^{1/4} \left(\frac{(A_P f)^2}{2 g d_T} \right)^{-1/12} \qquad 3.39$$

where d_T is the diameter of the column.

In the above equation the droplet diameter has been ignored; that means for a given system the characteristic velocity is constant for any droplet diameter. This is an unexpected result.

3.3.2 Droplet Velocity in a Pulsed Sieve Plate Column

Gayler et al (50) showed that, in the absence of droplet coalescence, the superficial velocities of the dispersed and continuous phases can be related to the dispersed phase hold-up (x) and the characteristic velocity (Vk) by the following equation:-

$$\frac{V_d}{x} + \frac{V_c}{1 - x} = V_k (1 - x) \qquad 3.40$$

Misek (117) proposed another correlation to calculate the characteristic velocity as follows:-

$$\frac{V_d}{x} + \frac{V_c}{1 - x} = V_k (1 - x) \exp [(z - 4.1) x] \qquad 3.41$$

where z is a coefficient of coalescence. The above expression can be approximated by a power function of $(1- x)^n$. Thornton (162) presented a relationship between the slip velocity and the characteristic velocity based on experimental data with no coalescence between droplets as follows :-

$$V_S = V_k (1 - x) \qquad 3.42$$

Kiating et al (84) modified the above equation , so that

$$V_S = V_k (1 - x)^n \qquad 3.43$$

Shenlin et al (136) , using four types of liquid-liquid system, showed that the parameter " n " could be correlated in terms of physical properties and operation variables by:-

$$n = \frac{1 + m' M'}{2 - m'} \qquad 3.44$$

where:-

$m' = 1$ for $Re < 1.0$

$m' = 0.5$ for $20 < Re < 500$

$$Re = \frac{V_t d \rho_c}{\mu_c}$$

$$M' = 0.084 \left(\frac{\mu_c}{\mu_d} \right)^{0.26} P^{0.17}$$

$$P = \frac{\rho_c^2 \sigma^3}{\mu_c^4 \Delta\rho g}$$

Thornton (161) proposed a correlation to calculate the characteristic velocity in a pulsed sieve-plate column as follows :-

$$\left[\frac{V_k \mu_c}{\sigma} \right] = 0.6 \left[\frac{\psi_f \mu_c^5}{\rho_c \sigma^4} \right]^{-0.24} \left[\frac{\rho_c \sigma d_h}{\mu_c^2} \right]^{0.9} \left[\frac{\mu_c^4 g}{\sigma^3 \Delta\rho} \right]^{1.01} \left[\frac{\Delta\rho}{\rho_c} \right]^{1.8} \left[\frac{\mu_d}{\mu_c} \right]^{0.3} \qquad 3.45$$

where:-

$$\psi_f = \frac{\pi^2 N \left(1 - \phi^2 \right) \left(A_p f \right)^3}{2 \phi^2 C_o^2 H}$$

The results obtained in an investigation of pulsed columns carried out by Misek (117)

do not confirm the validity of the above equation. The main reason is that equation 3.45 was not verified experimentally for the full range of values of the variables. This concerns especially the size of the plate holes, which were practically not varied, as most experiments were carried out with plates of a free area 0.25 and holes of 0.317 cm diameter. C_o is assumed constant at 0.6 but in fact it varies with agitation as has been shown before.

Shenlin et al (136) developed another correlation to calculate characteristic velocity as follows:-

$$V_k = 9.63 \left(\frac{3\mu_d + 3\mu_c}{3\mu_d + 2\mu_c} \right)^{2.75} \left(\frac{\Delta\rho}{\mu_c} \right)^{0.666} \left(\frac{\rho_c}{\mu_c} \right)^{0.333} \qquad 3.46$$

The dimensions of (ρ_c / ρ_d) are not sec^{-3} and it is suspected that the above equation is in error. Also the geometrical and operation parameters have been ignored in the Shenlin equation. In the Thornton and Shenlin equations, the droplet diameter is absent.

Batey et al (13) presented a correlation to calculate the characteristic velocity in a pulsed sieve-plate column as follows:-

$$V_k = \frac{(1+I)^{-1} \left[0.12\, d_{32}^{1.29} (\Delta\rho\, g)^{0.79} \right]}{\left(\rho_c^{0.24}\, \mu_c^{0.53} \right)} \qquad 3.47$$

Vassallo et al (171) have shown that in a particular case.

$$V_s = 6.19 * 10^{-4} (A_p * f)^{-0.87} (1 - x)^{0.64} \qquad 3.48$$

Batey et al (12) proposed nearly the same correlation as follows:-

$$V_s = \text{const.} \left(A_p * f \right)^{-1.33} \left(1 - x \right) \qquad 3.49$$

Hussain et al (73) proposed an empirical correlation to calculate the ratio of the characteristic velocity to the terminal velocity of single droplets in a pulsed sieve-plate column as follows:-

$$\frac{V_k}{V_t} = 1 - \left[\frac{d_{32}}{\left(1 + \beta h_c \right) d_h} \right] - \left[\frac{A_p f}{1 + 0.95 h_c} - \frac{\left(A_p f \right)^2}{1 + 28.3 h_c} \right] \qquad 3.50$$

where:-

$$\beta = 0.0268 + 0.0365 \phi$$

The droplet diameter (d_{32}) ,which was used to evaluate the above equation, was always less than the sieve-plate hole diameter (d_h), which is not true in the experimental situations.

Kumar and Hartland (93) presented a correlation to calculate the slip velocity in the pulsed column as follows :-

$$V_s = K_1 \exp\left[K_2 \left| A_p f - \left| A_p f \right|_m \right| \right] \Delta\rho^{0.29} \rho_d^{0.67} \mu_d^{-0.66} \phi^{0.44} h_c^{0.43} \qquad 3.51$$

where:-

$$\left(A_p f \right)_m = 9.69 * 10^{-3} \left(\frac{\sigma \Delta\rho^{0.25} \phi}{\mu_d^{0.75}} \right)^{0.33}$$

and

$K_1 = 6.84 * 10^{-6}$

and

$K_2 = - 36.8$

Recently, Vohradsky and Sovova (176) studied the motion of single droplets in the countercurrent Karr column with vibrating plates. They concluded that the ratio of the characteristic velocity to the terminal velocity is lower than one and diminishes with increasing intensity of vibration, velocity of the continuous phase and droplet size.

CHAPTER FOUR

MASS TRANSFER CHARACTERISTICS

4.1 Introduction

In liquid-liquid extraction processes, there are three factors which influence the mass transfer rate during the different stages of the droplet's life (formation, free travel, and coalescence), viz, the area of contact, effective driving force, and the mass transfer coefficient. These factors are not easily evaluated even for the simple case, i.e. the spray column, because there is no simple relationship between the area of contact and variables of design and as mentioned above there are three stages in which mass transfer takes place.

Furthermore the dispersed phase tends to present a wide distribution of drop sizes, which results in different characteristics of droplet behaviour during the free travel period (i.e. for stagnant, circulating, and oscillating droplet). For each type of droplet behaviour there will be a particular mass transfer mechanism. It is thought better to consider the three factors separately for the three different stages in the life of each droplet.

4.2 Mass Transfer During Droplets Formation

The droplet size is of primary importance because if determines the surface area over which mass transfer will take place. Therefore it is important to know :-

1. The volume of the droplet as a function of the time of formation.
2. The surface area of the droplet as a function of the volume.

Numerous correlations have been proposed to determine mass transfer rates or mass transfer coefficients during droplet formation; the most important ones are summarised in Table 4.1. Data for droplet formation in the absence of mass transfer is of limited value since uncertainty exists regarding the influence of concentration, density, viscosity, and interfacial tension.

Scheele and Meister (135) proposed a correlation which is widely-used in calculating the droplet volume at low velocities of dispersed phase into a stationary continuous phase with average deviation of experimental results of about 11.0%. Values of overall mass transfer efficiency during droplet formation ranging from 10% to 50% have been reported by several investigators (99, 135, 141). Other investigators (59, 125, 133) reported that the amount of mass transfer during droplet formation was approximately 10% of the total. However, Sherwood (141) found that 40% of the over all mass transfer occurred during the droplet formation stage. Much of the published experimental studies have lacked a good technique for direct measurement of mass transfer during droplet formation and have been confined to very large formation times (2 sec to 50 sec). Brounshtein et al (23) reported that a good prediction of mass transfer rate during droplet formation could be obtained by sampling close to the nozzle. The best fit of the experimental data was provided by a correlation 4.9 proposed by Johnson and Hamielec (79). The equations in Table 4.1 (from equation 4.1 to equation 4. 8) are all similar with merely a different value of the constant.

4.3 Mass Transfer During Droplet Travel Through Continuous Phase

The hydrodynamic state of the droplet, i.e. Stagnant, circulating, or oscillating, has a significant effect upon the mass transfer during droplet travel through the continuous phase. A stagnant or rigid droplet will possess a low mass transfer rate because there is

Table 4.1 Correlations of Mass Transfer During Droplet Formation

Author & Reference	Correlation	Remarks	Eq. No.
Licht and Pensing (101)	$K_{df}=\frac{6}{7}\left(\frac{D_d}{\pi t_f}\right)^{0.5}$	The whole area ages to the penetration theory. Only area variation with time is considered.	4.1
Heertjes et al (59)	$K_{df}=\frac{24}{7}\left(\frac{D_d}{\pi t_f}\right)^{0.5}$	Velocity of diffusion is small compared with velocity of drop growth.	4.2
Groothuis et al (53)	$K_{df}=\frac{4}{3}\left(\frac{D_d}{\pi t_f}\right)^{0.5}$	With droplet diameter between 0.35-8.5 mm. the rate of absorption increases at Re >750.	4.3
Coulson et al (34)	$K_{df}=2\sqrt{3/5}\left(\frac{D_d}{\pi t_f}\right)^{0.5}$	Average time of exposure and average exposed surface elements of different ages.	
Heertjes and Nie (60)	$K_{df}=2\left\{\frac{r_o}{a_d}+\frac{2}{3}\right\}\left(\frac{D_d}{\pi t_f}\right)^{0.5}$	At slow formation rates the fresh surface model was very successful.	4.5
Ilkovic (74)	$K_{df}=1.31\left(\frac{D_d}{\pi t_f}\right)^{0.5}$	Based on the surface stretch mechanism, proved by many workers and used successfully.	

continued/....

Table 4.1 continued

Author and Reference	Correlation	Remarks	Eq. No.
Angelo et al (7)	$K_{df} = \frac{2}{\sqrt{t}} \left(\frac{D_d}{\pi t_f} \right)^{0.5}$	For the more restricted situation of Ilkovic	4.7
Sawistowski (133)	$K_{df} = \frac{40}{7} \left(\frac{D_d}{\pi t_f} \right)^{0.5}$	For a sphere, whose volume is linearly related to time.	4.8
Johnson et al (79)	$E_m = \frac{C_1 - C_2}{C_1 - C^*} = \frac{20.6}{d_e} \left(\frac{D_d}{\pi t_f} \right)^{0.5}$	Most practical because, " the end effect criteria" still exist.	4.9

no internal mixing. On the other hand a circulating or oscillating drop will exhibit higher mass transfer rate because of the vigorous mixing inside the droplet. The presence of a wake behind the moving droplet influences the overall mass transfer rate (43, 70, 85). In the next sections, the mass transfer coefficients of both phases will be discussed separately according to the hydrodynamic states of the droplet.

4.3.1 The Dispersed Phase Mass Transfer Coefficient

When the resistance to mass transfer is in the dispersed phase,the overall transfer rate is controlled by the transfer mechanism inside the droplet, which is influenced by the hydrodynamics of the system. The degree of internal circulation and oscillation affects the mass transfer coefficient inside the droplet. Hadamard (57) postulated that circulation inside a droplet will occur above a droplet Reynolds number of 1.0 and Levich (98) demonstrated that circulation would take place between Reynolds numbers of 1.0 and 150. Levich (98) and Garner and Skelland (45) considered that the surface tension of the dispersed phase would affect the circulation rate.

In many cases the experimental mass transfer rate has been seen to be greater than predicted by the model (49, 79, 90, 144). The dispersed phase mass transfer models have been presented in the form of mass transfer coefficient " k_d " or as an extraction efficiency "E_m". The common assumptions for all models are that the droplet is spherical and of constant volume and that the solute concentration is sufficiently dilute for the physical properties to be considered constant. The fluids are assumed to be Newtonian and incompressible.

4.3.1.1 Stagnant Droplets

For very small droplets, usually < 1mm in diameter, with no internal circulation, the dominant mechanism of mass transfer is molecular diffusion. Newman (121) developed a correlation for the drying of porous solids with negligible resistance to mass transfer in the continuous phase; the correlation is as follows:-

$$E_m = 1 - \frac{6}{\pi^2} \sum_{n=1}^{\infty} \frac{1}{n^2} \exp\left[\frac{-n^2 \pi^2 D_d t_e}{r^2} \right] \qquad 4.10$$

Vermeulen (173) found that equation 4.10 could be reduced to an empirical expression by taking the first term and neglecting the ratio ($6/\pi^2$). So for n =1

$$E_m = 1 - \exp\left[\frac{-\pi^2 D_d t_e}{r^2} \right]^{0.5} \qquad 4.11$$

which for values of Em < 0.5 reduces by a series expansion neglecting higher order terms to:-

$$E_m = \pi \left[\frac{D_d t_e}{r^2} \right]^{0.5} \qquad 4.12$$

Treybal (168) proposed a correlation for mass transfer coefficient based on a linear concentration-difference driving force:-

$$k_d = \frac{2 \pi^2 D_d}{3 d} \qquad 4.13$$

Equation 4.13 has been considered to be applicable to rigid spheres (168).

4.3.1.2 Circulating Droplets

At a given Reynolds number and droplet size the solute inside the droplet tends to circulate. Experimental studies indicate that the rate of mass transfer is enhanced when circulation take place in comparison with a rigid sphere. As a result of circulation the fluid inside the droplets is completely mixed by either laminar or turbulent circulation.

a. Laminar Circulation.

Internal circulation is laminar for Re > 1.0. Kronig and Brink (90) used the Hadamard-Rybezynski (57, 131) flow patterns to derive a relationship for droplet internal circulation. They (90) assumed that the time of circulation is small compared to the time of solute diffusion, the solute diffusion is in a direction perpendicular to the internal streamlines, and that the continuous phase resistance is negligible. They proposed the following equation: -

$$E_m = 1 - \frac{3}{8} \sum_{n=1}^{\infty} A_n^2 \exp\left[-\lambda_n \frac{16 D_d t_e}{r^2} \right] \qquad 4.14$$

A_n and λn are Eigen values and have been presented by Heertjes et al (127) for values of n from 1 to 7 and have been summarised in Table 4.2. Calderbank and Korchinski (26) introduced a constant effective diffusivity (R) equal to 2.25 to equation 4.11; they obtained :-

$$E_m = 1 - \exp\left[\frac{-\pi^2 R D_d t_e}{r^2} \right]^{0.5} \qquad 4.15$$

where R is usually defined as the ratio of the effective diffusivity to the molecular diffusivity.

Table 4.2. Values of A_n and λ_n for n =1 to n =7

n	A_n	λ_n
1	1.33	1.70
2	0.60	8.50
3	0.36	21.1
4	0.35	38.5
5	0.28	63.0
6	0.22	89.0
7	0.16	123.8

For Em < 0.5 equation 4.15 is written as:-

$$E_m = \pi \left[\frac{R\, D_d\, t_e}{r^2} \right]^{0.5} \qquad 4.16$$

b. Turbulent Circulation.

The turbulent circulation situation is characteristic of fluid particles in the high Reynolds number region. When circulation is present the interior of the droplet may be considered perfectly mixed at any time. Handlos and Baron (58) proposed a particular model of the turbulent internal motion, which takes into account the vibration of the

considered perfectly mixed at any time. Handlos and Baron (58) proposed a particular model of the turbulent internal motion, which takes into account the vibration of the

droplet as well as the circulation patterns within it. Later Wellek et al (179) reported that the Handlos and Baron model (58) describes the unsteady state mass transfer mechanism for a droplet possessing a special type of turbulent internal circulation. The proposed model is :-

$$k_d = \frac{3.75 * 10^{-3} V_t}{\left(1 + \left[\frac{\mu_d}{\mu_c}\right]\right)} \qquad 4.17$$

or in dimensionless group form;

$$Sh_d = 3.73 * 10^{-3} \frac{Pe_d}{\left(1 + \left[\frac{\mu_d}{\mu_c}\right]\right)} \qquad 4.18$$

The conditions for application of this model are not easily defined but Re>150 and We>3.3 are suggested. Handlos and Baron (58) recommended that when resistance to mass transfer exists in the continuous phase, the Higbie (64) relation should be assumed for k_c.

$$k_c = \sqrt{\frac{4}{\pi}\frac{D_c}{t_e}} \qquad 4.19$$

The overall mass transfer coefficient is obtained by means of the two film resistance theory.

$$\frac{1}{K_d} = \frac{m}{(k_c)_{HG}} + \frac{1}{(k_d)_{HB}} \qquad 4.20$$

Skelland and Wellek (146) studied the resistance to mass transfer inside droplets and extended the Handlos and Baron (58) model with a continuous phase resistance. They (146) presented their results in the following dimensionless correlation.

$$Sh_d = 31.4\, T_m^{-.338}\, Sc_d^{-1.25}\, We^{.371} \qquad 4.21$$

Olander (123) considered short times of contact, but assumed only mass transfer resistance in the continuous phase. He proposed the following equation:-

$$k_d = 0.972\, k_{HB} + 0.075\, \frac{d}{t} \qquad 4.22$$

Based on penetration theory the mass transfer coefficient (k_d) may be estimated as follows:-

$$k_d = 2 \left[\frac{D_d}{\pi\, t_e} \right]^{0.5} \qquad 4.23$$

where t_e is the time of exposure. Assuming t_e as the time taken by the droplet to travel a distance equal to the diameter of the droplet under its terminal velocity, the above equation may be written as:-

$$k_d = 2 \left[\frac{D_d V_t}{\pi d_p} \right]^{0.5} \qquad 4.24$$

4.3.1.3 Oscillating Droplets

Oscillation takes place, at low continuous phase velocity, at approximately Reynolds numbers greater than 150-200. Mass transfer coefficient for an oscillating droplet is

20 times higher than for the rigid droplet (143, 125). Several single droplet models and correlations have been proposed depending upon the different concepts of droplet physical phenomena. Hydrodynamic factors which affect any of the three variables in equation 1.1 will be reflected in the transfer rate. For an oscillating droplet, dispersed phase mass transfer coefficient can be predicted approximately by the Handlos and Baron model equation 4.25. However Rose and Kintner (127) proposed equation 4.26, by assuming a constant value of the mass transfer zone , to account for changes in area resulting from the oscillation, and that the local mass transfer coefficient varied in proportion to the thickness of the zone.

A good review of the different theoretical models according to their importance and the techniques used and empirical correlations for the oscillating droplet has been presented by Al-Faize (3) and Al-Hassan (4). A summary of the most important correlations are shown in Table 4.3.

4.3.2 The Continuous Phase Mass Transfer Coefficient

The continuous phase mass transfer coefficient may be evaluated in terms of the resistance in the film surrounding the droplet through which the transfer takes place by molecular diffusion.

Many correlations for the continuous phase mass transfer have been proposed in the literature; the most important ones will be discussed in this section. An assumption as to the interfacial area is implicit in all the expressions, the usual choice for the area of a nonspherical droplet being that of a sphere of equivalent volume. The droplet size and internal solute hydrodynamic state, ie. droplet Reynolds number and droplet shape, lead to enormous changes in droplet characteristics depending on the droplet state ie. stagnant, circulating, or deformed and oscillating.

4.3.2.1 Stagnant Droplet

For a rigid droplet, some workers (46, 48) have proposed a general correlation based on the boundary layer theory for the rate of mass transfer from, or to, a solid sphere as follows:-

$$Sh_c = A + B\, Re^m Sc^n \qquad 4.30$$

where:-

m is an index of the effect of convective velocity on mass transfer

and

n is an index of the effect of the ratio of momentum and diffusion boundary layer thickness on mass transfer.

Examples of values of these constants are given in Table 4.4.

Linton and Sutherland (103) proposed a model for mass transfer coefficients of stagnant droplets of benzoic acid measured in uniform flow in a water tunnel, the correlation is as follows:-

$$Sh_c = 5.82 * 10^{-1} Re^{0.5} Sc^{0.33} \qquad 4.31$$

Rowe et al (129) proposed a correlation which included a term accounting for the diffusion process as follows:-

$$Sh_c = 2 + 7.6 * 10^{-1} Re^{0.5} Sc^{0.33} \qquad 4.32$$

In the above two equations, the effect of the wake on the mass transfer coefficient is ignored, Later, Kinard et al (85) proposed a correlation which includes the effect of

the wake as follows:-

$$Sh_c = 2 + (Sh)_n + 4.5 * 10^{-1} Re^{0.5} Sc^{0.33} \qquad 4.33$$

Garner and Tayeban (49), proposed a modified correlation for mass transfer from stagnant, non-circulating spherical droplets as follows:-

$$Sh_c = 2 + 0.55\ Re^{0.5} Sc^{0.5} \qquad 4.34$$

4.2.2.2 Circulating Droplets

Many workers (49, 45, 79, 90) have mentioned that the continuous phase mass transfer coefficient is increased when circulation takes place inside a droplet and this has been explained by the associated reduction in the boundary layer thickness.

By using the velocity distribution for potential flow, Boussinesq (20) and Ruckenstein (130) found the following expression for the average Sherwood number:-

$$Sh_c = \frac{2}{\sqrt{\pi}} Re^{0.5} Sc^{0.5} \qquad 4.35$$

which assumes that there is no boundary layer separation.

Later, West et al (180) introduced a correlation factor (f_c) which depends upon the dispersed phase properties.

$$Sh_c = \frac{2 * f_c}{\sqrt{\pi}} Re^{0.5} Sc^{0.5} \qquad 4.36$$

Table 4.3 Dispersed Phase Mass Transfer Correlations During Droplet Travel

Author and Reference	Correlation	State of Droplets	Remarks	Eqn No.
Newman (121)	$E_m = \frac{C_1 - C_2}{C_1 - C^*} = \pi \left(\frac{D_d t_e}{r^2} \right)^{0.5}$	Stagnant	For small drop size	4.12
Kronig and Brink (90)	$E_m = 1 - \frac{3}{8} \sum_{n=1}^{\infty} A_n^2 \left(\frac{-16 \lambda_n D_d t_e}{r^2} \right)$	Laminar Circulation	No continuous phase resistance Re > 1	4.14
Calderbank et al (26)	$E_m = \frac{C_1 - C_2}{C_1 - C^*} = \pi \left(\frac{R D_d t_e}{r^2} \right)^{0.5}$	Laminar Circulation	R is the ratio of effective diffusivity to molecular diffusivity	4.16
Handlos and Baron (58)	$Sh_d = \frac{3.75 * 10^{-3} Pe_d}{1 + \left(\frac{\mu_d}{\mu_c} \right)}$	Turbulent Circulation	No continuous phase resistance Re ≥ 1000	4.18
Skelland and Wellek (146)	$Sh_d = 3.14 T_m^{-1.338} Sc_d^{-0.125} We^{0.371}$	Circulating	Drops falling in a stationary continuous phase	4.21
Olander (149)	$k_d = 0.972 k_{HB} + 0.075 \frac{d}{t}$	Circulating	No continuous phase resistance short contact time Re > 1, R=2.25	4.22
Rose and Kintner (127)	$k_d = 0.45 \left(D_d \omega \right)^{0.5}$	Oscillating	For symmetrical spherical drops	4.25
Angelo et al (7)	$k_d = \left[\frac{4 D_d \omega \left(1 - \varepsilon + \frac{3}{8} \varepsilon^2 \right)}{\pi} \right]^{0.5}$	Oscillating	For integral number of completed oscillations	4.26

continued/...

Table 4.3 *continued*

Author & Reference	Correlation	State of drop	Remarks	Eqn. No.
Brunson & et al (24)	$Sh_d = \frac{2}{\pi}\left[\frac{d^2\omega}{2D}\left(1+0.687\,\varepsilon^{\frac{1}{2}}\right)\right]^{0.5}$	Oscillating	With 26% absolute deviation	4.27
Yamagauchi (187)	$Sh_d = 1.14\,(Re)^{0.56}\,(Sc_d)^{0.5}$	Oscillating	For transfer of low solute concentration from aqueous drop to organic continuous phase	4.28
Al-Hassan (4)	$k_d = 4.3\,\varepsilon^{2.692}\,E_o^{1.672}\,(D_d\omega_{exp})^{0.5}$	Oscillating		4.29

Garner and Skelland (45) concluded that, internal circulation occurs only above a certain value of the local Reynolds number of the droplet (Re > 70). The rate of mass transfer was studied as a function of the Reynolds number, and it was found that the time taken for a given mass transfer was much longer below a Reynolds number of 70, at which value circulation commences.

Garner and Tayeban (49) developed a correlation from their experimental data taking into account the influence of the wake;

$$Sh_c = 0.6 * Re^{0.5} Sc^{0.5} \qquad 4.37$$

Heertjes et al (59) introduced a function (h) instead of the constant in the above equation;

$$Sh_c = h * Re^{0.5} Sc^{0.5} \qquad 4.38$$

where h is a function of $\{ \mu_c / (\mu_c + \mu_d) \}$ and varies from 0.1 to 0.95 while $\{\mu_c / (\mu_c + \mu_d)\}$ varies from zero to ten.

By using partially-miscible, binary liquid-liquid systems of low interfacial tension, Garner et al (47) observed that the exponent of the Schmidt group in equation 4.28 is 1/2 for fully-circulating potential flow, and 1/3 for stagnant droplets. They (47) concluded that the exponent of the Schmidt number for a circulating droplet should be between 1/2 and 1/3. They (47) proposed the following correlation;

$$Sh_c = - 126 + 1.80 Re^{0.5} Sc^{0.42} \qquad 4.39$$

Mekasut et al (114) studied the transfer of iodine from an aqueous continuous phase to carbon tetrachloride droplets; the resistance to mass transfer was assumed to be solely

in the continuous phase. Sherwood number was correlated to the Galileo number for droplets less than 0.26 cm in diameter by;

$$Sh_c = 1.04 * Ga^{0.4} \qquad 4.40$$

At droplet Reynolds number less than 4.0 (109, 151) a boundary layer separation takes place giving rise to a wake which travels behind the droplet. Initially an unsteady build-up of solute in the wake occurs due to the transfer from the rear of the droplet and from the boundary layer surrounding the outside of the wake. At steady state conditions, solute transfer takes place from the wake to the boundary layer surrounding the wake and then into the continuous phase. The high initial mass transfer rates were attributed to the presence of the wake.

Working with heat transfer rather than mass transfer, Elizinga and Banchero (39) proposed the following correlation:-

$$Sh_c = 5.52 \left\{ \frac{\mu_c + \mu_d}{2\mu_c + 3\mu_d} \right\}^{3.47} \left\{ \frac{d\sigma\rho_c}{\mu_c^2} \right\}^{0.056} Pe_c^{0.5} \qquad 4.41$$

Treybal (168) reported that droplet oscillation and interfacial turbulence produced higher coefficients than for stagnant and circulating droplets.

Thorsen et al (165) proposed a correlation which is applicable to circulating and non-circulating droplets. This indicates that internal circulation does not affect the specific mechanisms of mass transfer in pure liquid-liquid systems;

$$Sh_c = -178 + 3.62\ Re^{0.5} Sc^{0.33} \qquad 4.42$$

They (165) stated that the rapid increase in the continuous phase mass transfer coefficient with increasing Reynolds number was due to the combined effect of an increased disturbance intensity around the separation point.

4.2.2.3 Oscillating Droplets

For the majority of correlations for the continuous phase mass transfer coefficient, a sphere or equivalent sphere, is used to represent the liquid droplet geometry. When distortion from a sphere takes place the significance of this distortion is primarily that the surface area increases rapidly with any increase in distortion, and this may be accounted for in any mass transfer calculation.

Many workers (79, 146, 186) have used correlations to estimate the rates of mass transfer for oscillating droplets with turbulent internal circulation, but the effect of oscillation causes higher rates of mass transfer than does circulation (49, 127).

A good review of the different theoretical models and empirical correlations for oscillating droplets have been presented by Al-Faize (3) and Al-Hassan (4). A summary of the most important correlations are listed in Table 4.4.

4.4 MASS TRANSFER IN PULSED COLUMN.

4.4.1 Mass Transfer In Pulsed Spray Column

Mass transfer studies reported in the literature have either concentrated on the single droplet in non agitated systems or upon mass transfer from swarms of droplets in agitated systems. The study of mass transfer for single droplets in agitated systems has been largely neglected.

The study of mass transfer to and/or from a single droplet in a pulsed spray column is very rare. There are, however, a few publications covering mass transfer to and/or from a swarm of droplets in a pulsed spray column (14, 108, 122). Lurie and Shaver for instance (108) indicated that pulsing had little effect on the efficiency of a spray column. Whereas other workers (14, 168) in their investigations, with a frequency range from 3.33 to 8.33 Hz, noted that for a constant throughput the mass transfer efficiency of a pulsed spray column increased at high pulse frequency (above 6.67 Hz). They (108) did not study the effect of the pulse at low frequency (below 3.33 Hz).

From the above review, it is clear that there is no agreement between the various experimental investigations with regard to the effect of pulsing upon the mass transfer in pulsed spray column.

As mentioned in Chapter 1, one of the aims which the present work placed emphasis upon was the study of the pulsing effect on mass transfer from large droplets in pulsed spray columns. Experimental investigation, data evaluation and the discussion of the results of the pulsing effect on mass transfer from such droplets is illustrated in Chapters 5, 7 & 8 respectively.

4.4.2 Mass Transfer in Pulsed Sieve Plate Column

In pulsed sieve plate columns, the application of pulse energy increases turbulence and aids breakup and coalescence of dispersed phase droplets at the perforated plates, there by greatly improving the mass transfer efficiency as compared to unpulsed sieve plate columns.

Several workers studied the mass transfer of swarms of droplets in pulsed sieve plate columns. In the past, extraction equipment was designed for a given duty by

assessing the number of theoretical stages or transfer units, then translating these units into a column height via the height equivalent to a theoretical stage (HETS) or height of the transfer unit (HTU) concept. This procedure was uncertain and was probably based on empirical correlations, and in some cases was applied to situations remote from the experimental conditions under which they were established (76).

As mentioned in Chapter 1, the mass transfer studies have been restricted to the estimation of HETS or HTU. The HETS showed a steep decrease in value with pulse velocity ($f*A_p$) up to a critical value, then attained almost a constant value. Khemangkorn et al (82) reported that the mass transfer direction has very little effect on HTU.

As shown in Figures 4.1 & 4.2, the mass transfer coefficients evaluated from concentration profile for all types of extraction columns are widely scattered and cannot be correlated easily (152).

Several workers (73, 31, 41, 82, 152) studied the effect of pulsing upon the mass transfer rate. Hussain et al (73) concluded that, at constant droplet size, the pulsing parameters have little effect on the value of mass transfer coefficient up to the point at which droplets breakup, as shown in Figure 4.3. Other workers (33, 41) reported that agitation affects drop size and hence interfacial area but not the mass transfer coefficient to a marked extent. Khemangkarn et al (82) also concluded that, for both mass transfer directions, the effect of pulsing parameters upon the mass transfer coefficient is limited and scattered, as shown in Figure 4.4.

Wiezhi et al (182) concluded from their experimental study that the wave shape of pulsing has an effect upon the mass transfer rate. In pulsed sieve plate columns, the

efficiency of the mass transfer rate increases if such a column is operated with a trapezoidal wave (182).

In the present study, an attempt is made to evaluate the mass transfer rate of single droplets moving through a pulsed sieve plate column by applying the general mass transfer equation 1.1.

$$N_A = K\ A\ \Delta C \qquad 1.1$$

In order to apply the above equation, it is necessary to be able to evaluate each term on the right side of the equation reasonably accurately in order to estimate N_A. The mass transfer coefficient and the driving force are dependent on the physical chemistry of the system to be studied. The interfacial area is dependent on the physical properties of the system and the environment within which the system exists, i.e. the equipment geometry and mechanical energy input.

Table 4.4 Continuous Phase Mass Transfer Correlations During Droplet Travel

Author and Reference	Correlation	State of Droplets	Remarks	Eqn No.
Linton et al (103)	$Sh_c = 0.582 (Re)^{0.5} (Sc)^{0.33}$	Stagnant	Ignores diffusion and wake effects	4.31
Rowe et al (129)	$Sh_c = 2 + 0.76 (Re)^{0.5} (Sc)^{0.33}$	Stagnant	Accounts for diffusion process	4.32
Kinard et al (85)	$Sh_c = 2 + (Sh_c)_n + 0.45 (Re)^{0.5} (Sc)^{0.33}$	Stagnant	Includes diffusion process and wake effects	4.33
Boussinesq et al (20)	$Sh_c = 1.13 (Re)^{0.5} (Sc)^{0.5}$	Circulating	Assumes no boundary layer separation	4.35
Garner and Tayeban (49)	$Sh_c = 0.6 (Re)^{0.5} (Sc)^{0.5}$	Circulating	Not valid for Re > 450	4.37
Garner et al (47)	$Sh_c = -126 + 1.8 (Re)^{0.5} (Sc)^{0.42}$	Circulating	For partially miscible binary system of low σ	4.39
Mekasut et al (114)	$Sh_c = 1.04 (Ga)^{0.49}$	Circulating	$Ga = d_e^3 \rho_c^2 g / \mu_c^2$	4.40
Thorsen et al (166)	$Sh_c = -178 + 3.62 (Re)^{0.5} (Sc)^{0.33}$	Circulating	Applicable for circulating & non-circulating droplets	4.42
Garner and Tayeban (49)	$Sh_c = 50 + 8.5 \times 10^{-3} (Re)(Sc)^{0.7}$	Oscillating	Successfully used by other workers (129)	4.43
Yamaguchi et al (187)	$Sh_c = 1.4 (Re')^{0.5} (Sc)^{05}$	Oscillating	$Re' = \rho_c \omega d^2 / \mu_c$	4.44
Mekasut et al (114)	$Sh_c = 6.74 (Ga)^{0.34}$	Oscillating	Ignores the effect of ferquency of oscillation	4.45

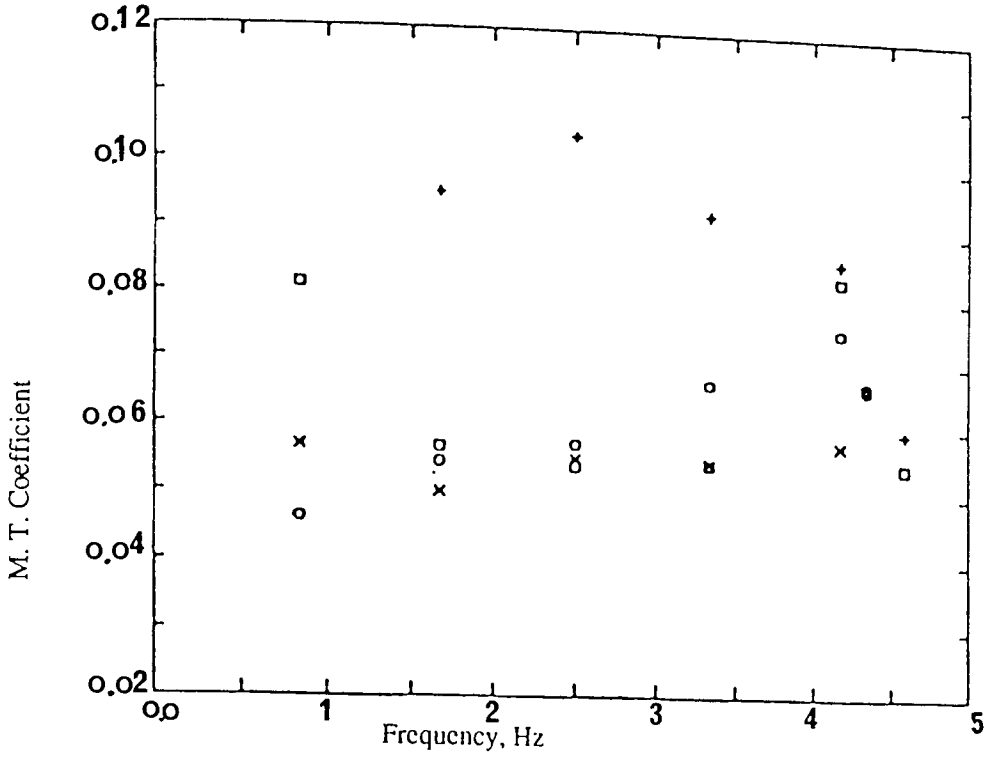

Figure 4.1 Effect of Frequency of Pulsing on M.T.Coefficient (152)

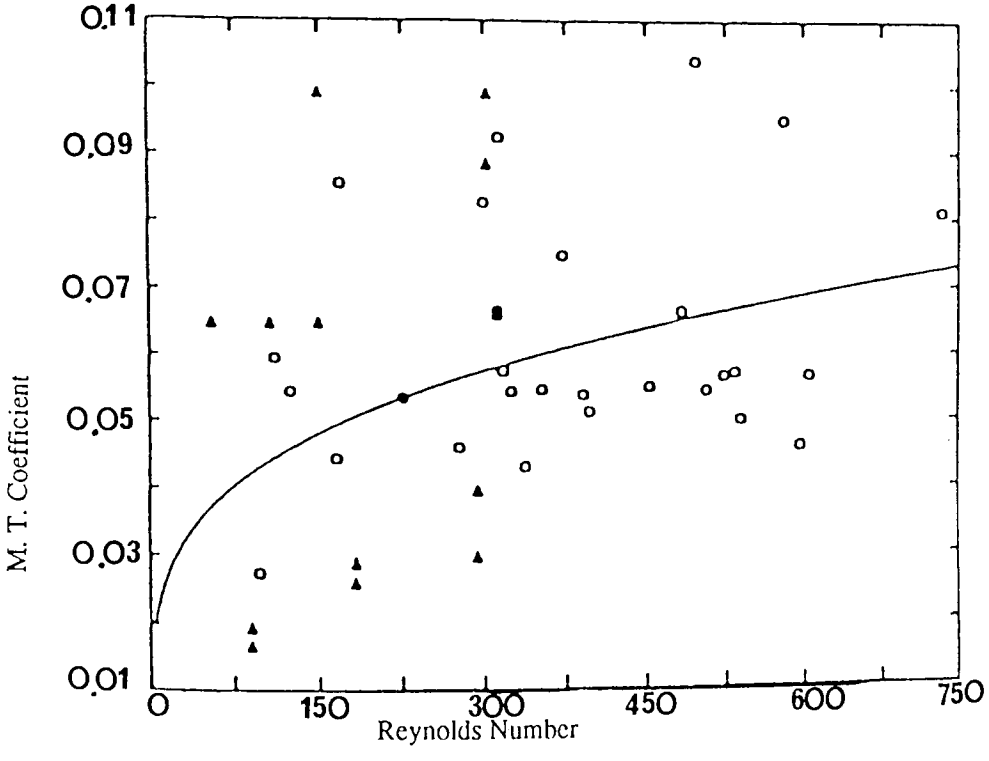

Figure 4.2 Variation of M.T.Coefficient with Re (152)

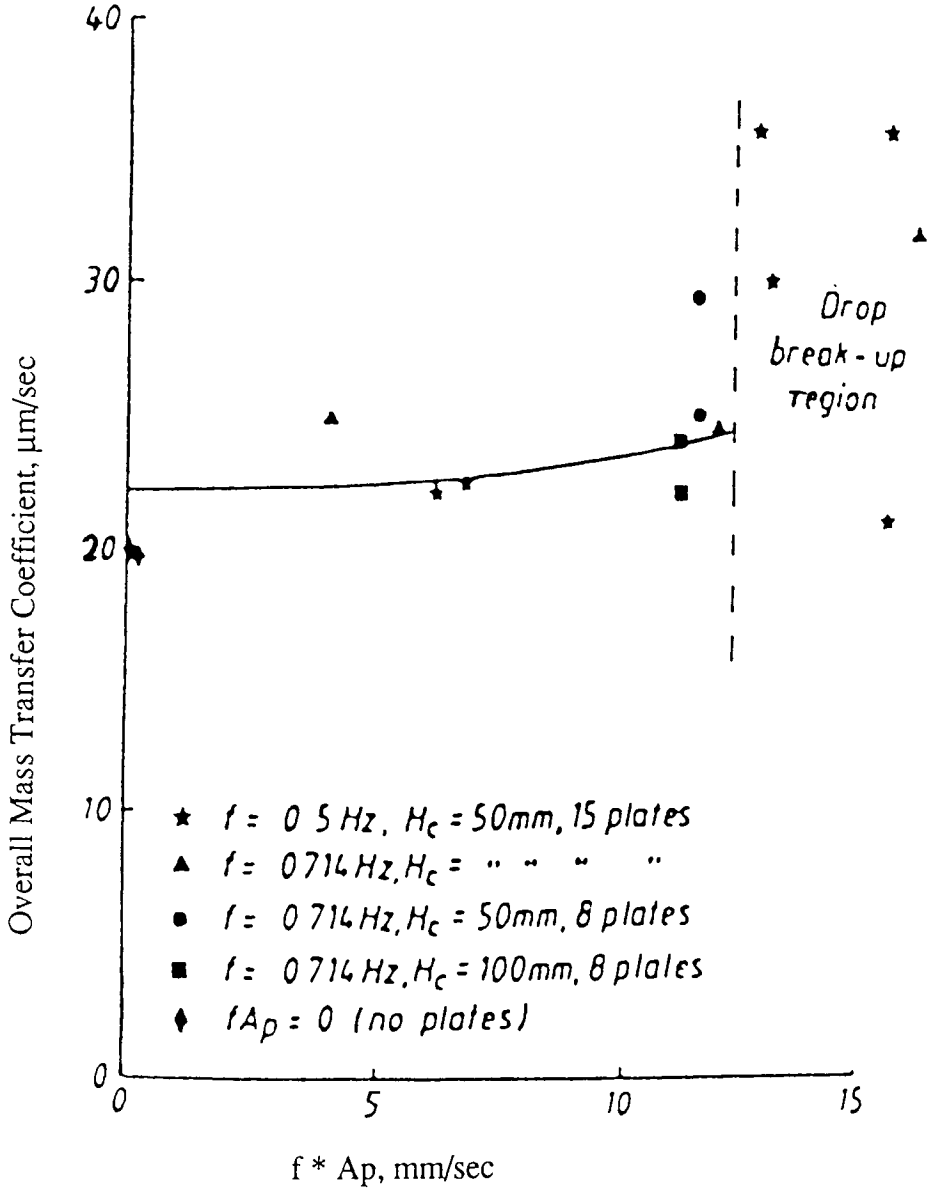

Figure 4.3 Effect of Pulsing Intensity on Overall Mass Transfer Coefficients (73)

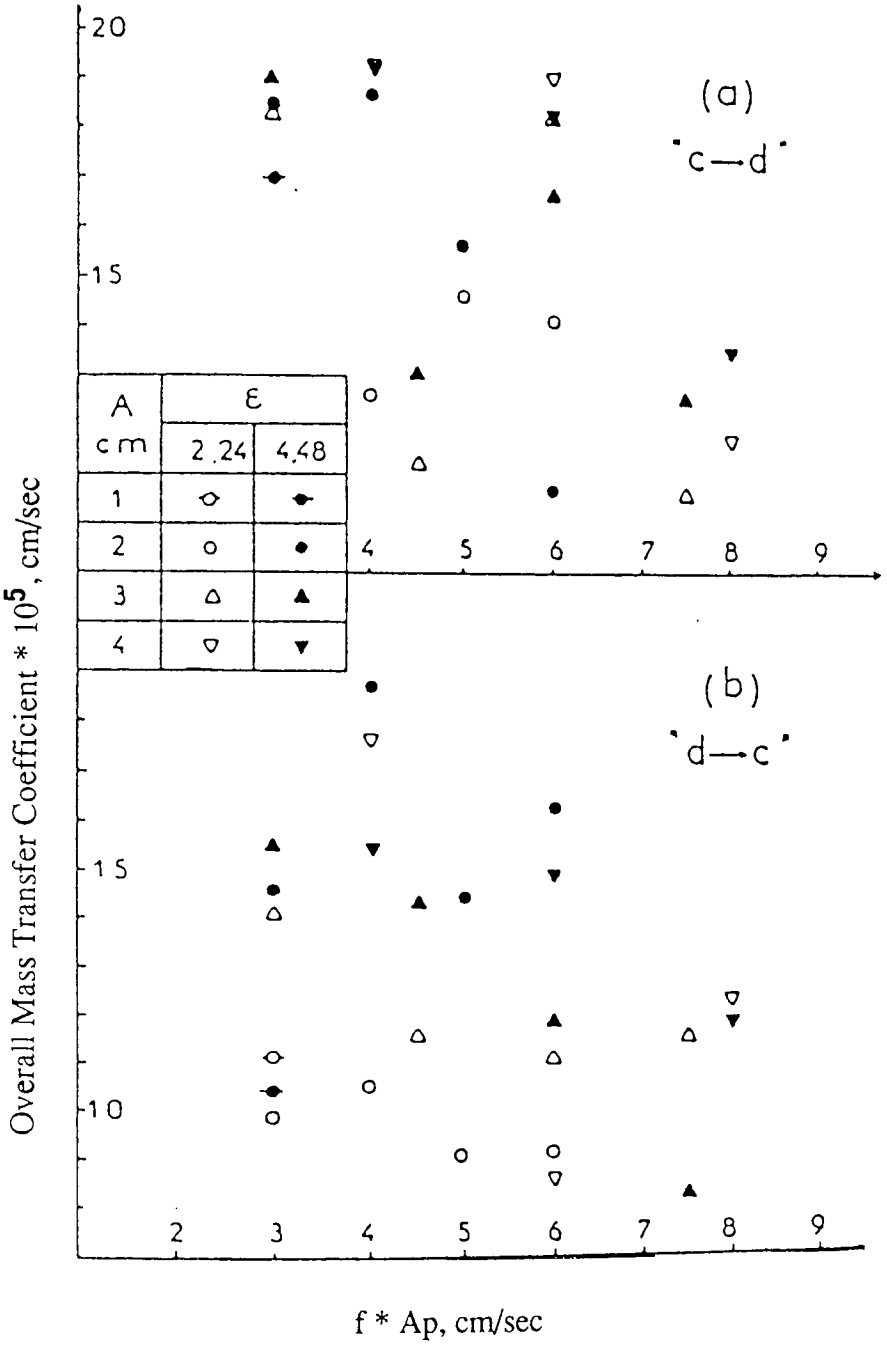

Figure 4.4 Variation of Overall Mass Transfer Coefficients with Pulsing Intensity (82)

PART II

EXPERIMENTAL INVESTIGATION AND MEASUREMENT TECHNIQUES

CHAPTER 5

CHAPTER 6

CHAPTER FIVE

EXPERIMENTAL INVESTIGATION

The aims of the experimental investigation were to study the hydrodynamic characteristics and the mass transfer rates of single droplets in a countercurrent column for both :-

a. A spray column (with and without pulsing), or

b. A pulsed sieve plate column.

The apparatus was designed to disperse a uniform stream of droplets in a continuous liquid phase, and to study the mass transfer rates from single droplets during formation and the free travel periods at various droplet velocities, and during droplet breakup.

The system chosen for study was toluene-acetone-distilled water; the dispersed phase was the toluene in which the solute (acetone) concentration varied up to 10% wt/wt. This system was selected because it was amongst the systems recommended by the European Federation of Chemical Engineers (EFCE) for testing the performance of liquid-liquid extraction columns (181), and was adopted because all the constituents were available to the required high purity , and physical property data were known for comparison with experimentally - determined values.

The essential operating requirements were:-

1. That investigation could be made of the effect of pulsation parameters (frequency & amplitude) and the sieve plate characteristics on the

hydrodynamic behaviour and mass transfer rates of single droplets.

2. That a range of significant parameters could be investigated; i.e. drop size, solute concentration, flow rate, pulsing parameters, sieve-plate characteristics, and temperature.

3. That the droplet characteristics could be recorded using photographic techniques and the dispersed phase samples could be withdrawn reproducibly from different positions within the column.

5.1 Equipment Description

A flow diagram of the apparatus is shown in Figure 5.1. and a general arrangement in Figure 5.2. The process lines, the feed and effluent tanks were arranged for counter-current contact of the two phases in a column of 5.0 cm. diameter and 100.0 cm. height.

The apparatus incorporated some improvements upon that designed by Al-Hassan (4) by introducing a sieve-plate cartridge assembly and an air pulsing system. A new illumination technique was developed, by which the photographic record could be achieved without adding dye to the materials. To measure the concentration of the solute in the droplet after formation and during the travelling periods, a novel collecting device was used.

The apparatus consisted of a Stuart- Turner stainless steel centrifugal pump, type no. 12 which was used to transfer the continuous phase from the reservoir (A) to the top vessel (B) or to saturate the continuous phase with the toluene by

recirculating the liquid. The continuous phase reservoir was made up of two vessels of 60 litres capacity together with an intermediate vessel of 10 litres capacity located immediately before the test section to provide a constant delivery head. A glass wool filter was placed before the test section in the continuous phase line to separate any micro droplets that might be present. All the continuous phase vessels were connected together with an overflow system to ensure no spillage of liquid. The dispersed phase was gravity fed from a 5.0 litres constant head (Mariotte) vessel to the test section.

5.1.1 Controls

The flow of the continuous phase was supplied from the constant head device and regulated by a p.t.f.e. valve (1.75 mm., QVF). The continuous phase flow rate was monitored by a small Rotameter (type metric 7F with stainless steel float) and controlled via a balance leg. The flow rate of the continuous phase was held constant during the experiment. The balance leg was used also to control the level of the continuous phase in the test section. The flow rate of the continuous phase was measured by collecting the output (extract) over a fixed time (60 sec).

The dispersed phase flow rate was required to be low in order to produce single discrete droplets of reproducible size. This was achieved by using a Mariotte bottle to supply the dispersed phase through a Rotoflow p.t.f.e. valve. The flow was determined by measuring the volume of the output (raffinate) over a fixed time period (20 min.).

The temperature of both phases was controlled by circulating water through an external electric heater. The heating liquid reservoir was a 20 litre vessel made from

300 mm. QVF pipe with stainless steel backed flanges.

A Churchill Chiller Thermocirculator "05 CTC/V " with the following operating parameters was chosen to control the temperature; working temperature range -15o to 60^{o} C, pump circulating rate 680 litre /hour with zero head; maximum pump head for no restriction 4.75 m., heater rating upto 1.5 KW; nominal HP of refrigeration 0.5. The heater was fitted with an overall temperature safety cut-out device. The thermocirculator was chosen for its fine control within $\pm 0.05^{o}$ C, simplicity of operation and safety. The control was obtained by setting the required temperature on the controller dial.

Chilling was necessary since the illumination required to photograph the droplet heated the liquids. Comark thermocouples (K76P) were used to measure the temperature at different points in the test section and in the transfer lines (especially near the output and input of the two phases and in such positions that did not disturb the flow). The temperatures were indicated on a Comark electronic thermometer (type 1601) which incorporated a Comark thermocouple selector unit (type 1694F).

The test section temperature was controlled by passing the heating liquid (distilled water) through the jacket. The temperature for all the experiments was set at 22^{o}C. This was just above the highest temperature reached in the room. Stainless steel coils maintained the temperature in the continuous phase as shown in Figures 5.1. and 5.2. A shell and tube glass heat exchanger was fitted in the dispersed phase lines immediately before the test section. In addition an electric heater (air convector of 1KW capacity) was fitted inside the cabinet enclosing the equipment to control its temperature.

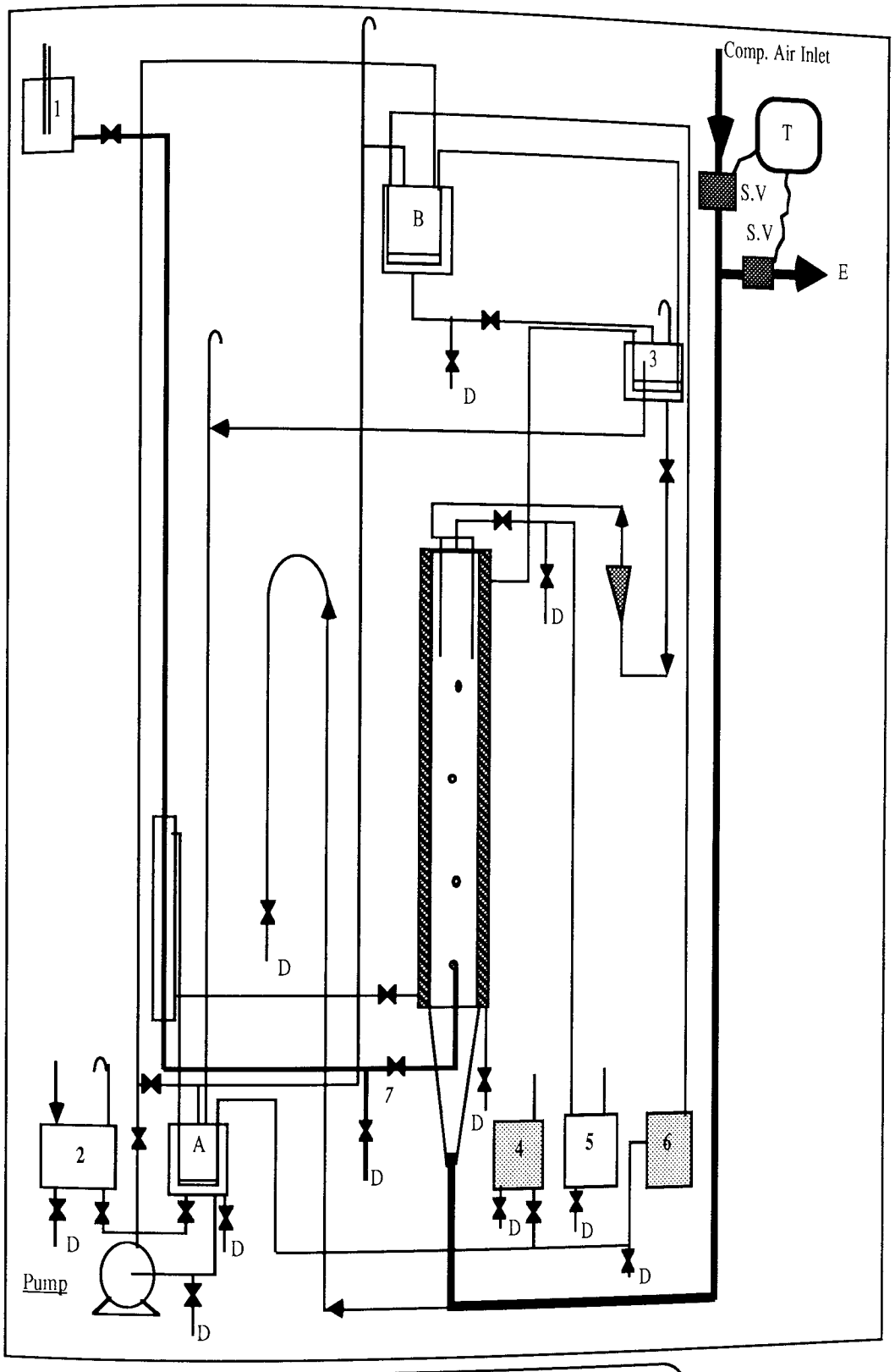

1 Dispered phase reservoir
2 Continuous phase reservoir
3 Constant head vessel
4 Heating liquid resevoir
5 Raffinate vessel
6 Churchill heater
7 Needle valve
D Drain
E Exhaust
SV Solenoid valve
T Timer

Figure 5.1 Diagram of Experiment Apparatus

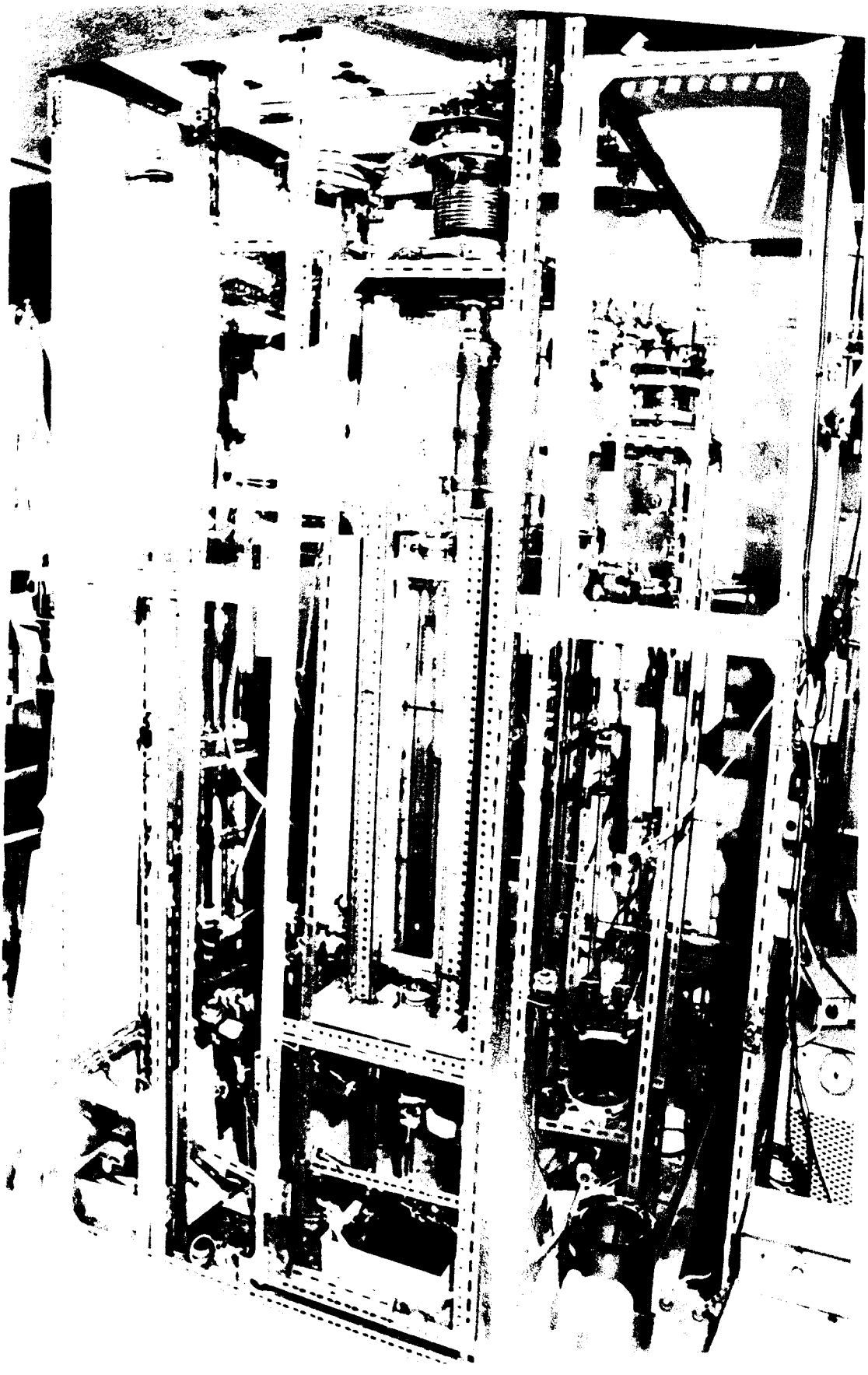

Figure 5.2 General Arrangement of Experimental Apparatus

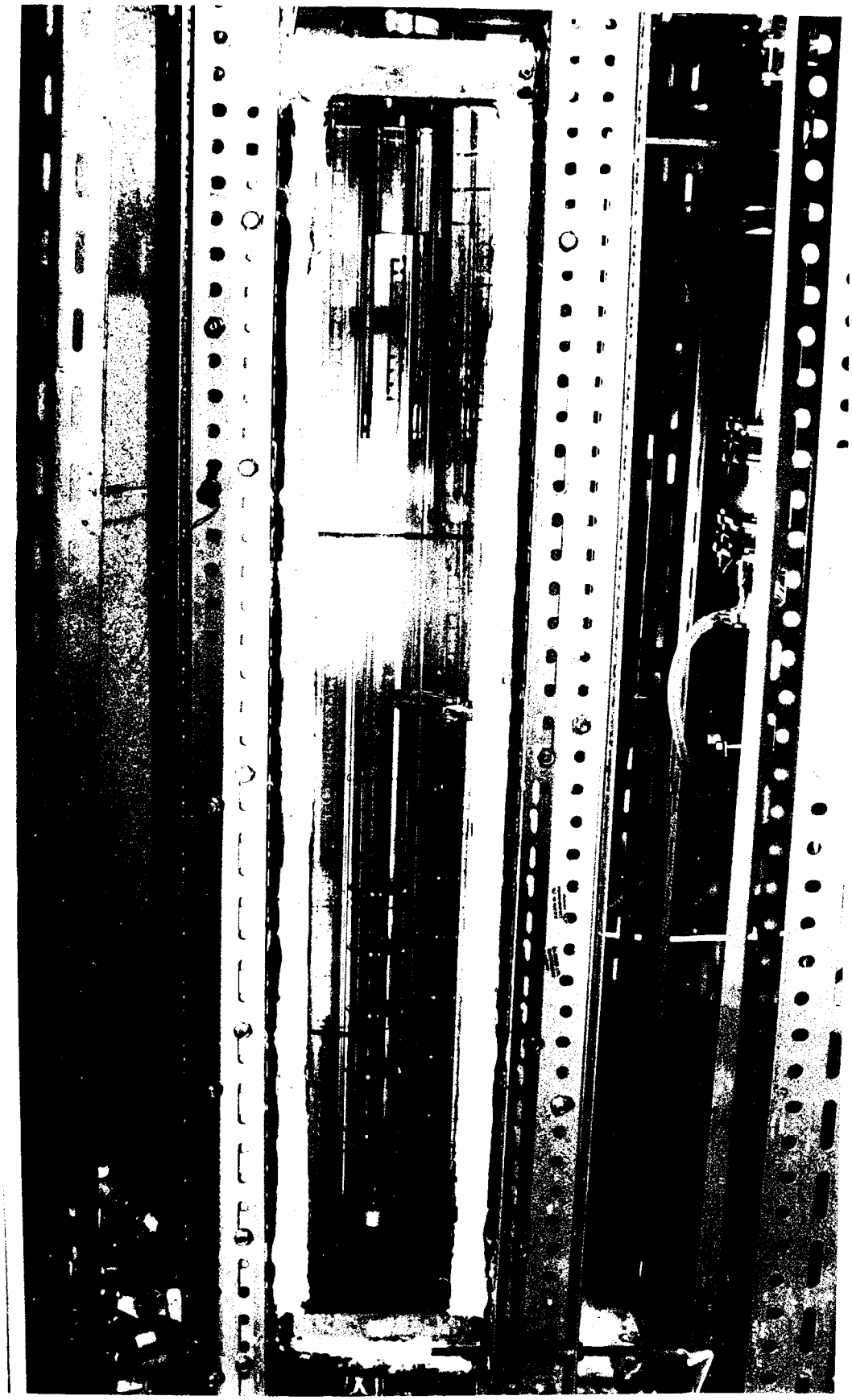

Figure 5.3 Test Section

5.1.2 Design of Test Section

The test section consisted of a 5.0 cm. internal diameter and 100. cm. long QVF glass tube, as shown in Figure 5.3. It was enclosed in a square jacket with its front and back made of 6.0 mm. thick high quality glass sheet, and the other two sides of polypropylene 6.0 mm. thick backed by mild steel sheets 9.0 mm. thick. This arrangement allowed droplets to be photographed without any appreciable distortion when the square section was filled with the continuous phase. The top end of the jacket was constructed of polypropylene (6.0 mm. thick) supported by stainless steel sheet of 6.0 mm thickness. The seal at the corners of the four walls of the jacket was obtained by securing them to the base and bottom, and with steel straps as shown in Figure 5.3. Thus the glass sheets were placed in grooves of the polypropylene, and p.t.f.e. sealant was inserted inside the grooves. In addition Dow Corning Silica (733RTV) was used as a seal on the outside of the column and inside the jacket, and Silastic (733RTV) and Silastic (732RTV) were used on the outside of the jacket. The lower end of the column was constructed from glass as shown in Figure 5.4 with provision for inserting and holding the nozzles to provide a single stream of droplets of the dispersed phase.

The heavy phase (continuous phase) was introduced into the column through two stainless steel distributors, which were connected to the column by a p.t.f.e. paste and a Viton gasket.

Six dispersed phase sampling points were built into the column to allow the droplets to be withdrawn, immediately after detachment from the nozzle or at 10.0, 20.0, 30.0, 40.0, and 50.0 cm. respectively from the tip of the nozzles by means of hypodermic needles. This followed the technique developed by Jeffreys and Bonnet

(77). The sampling probe incorporated a drop filter, a small hollow cylinder made from materials wetted by the dispersed phase, which accommodated successive layers of dispersed phase wetted micromesh cloth. The materials used were p.t.f.e. and nylon micromesh (1 μ width of opening). One end of the cylinder was welded to a 22 gauge hypodermic needle with its open tip protruding into the cylinder chamber, as shown in Figure 5.5 and Figure 5 .6.

Mirrors were installed in the jacket in order to observe and measure the third dimension of any drop. These mirrors were supported on a stainless steel shaft on the right side of the column as shown in Figure 5.3. They were secured in the vertical plane by a shaft that could be rotated. These mirrors were adjusted to enable the shape of a droplet to be photographed from the side.

5.1.3 Nozzles

Nozzles constructed of glass with internal diameter ranging from 0.02 cm. to 0.30 cm were used in this study as shown in Figure 5.4 and Table 5.1. The minimum length of the outlet section of the nozzle was 9.0 cm to smooth the flow of dispersed phase prior to droplet formation. The tips of the glass nozzles were ground so that the plane of the tip was at a right angle to the axis of the nozzle so that undesirable wetting of the outside of the nozzle by the dispersed phase could be easily detected. The nozzles were provided with two hooks to fix them as shown in Figure 5.4.

5.1.4 Plate Cartridges

As shown in Figure 5.7; three types of plates were used, 49.5 mm. ±0.5 mm. in

Table 5.1 Nozzle Diameter

Nozzle	G1	G2	G3	G4	G5	G6	G7	G8	G9	G10	G11	G12
Diameter mm	0.2	0.3	0.5	0.7	1.0	1.2	1.5	1.7	2.0	2.2	2.5	3.0

diameter and 2.0 mm. thickness, all of them made of stainless steel (University made),the holes were drilled. The specifications are listed below in Table 5.2.

The holes are arranged on a triangular pattern. The plates were connected by three stainless steel screw rods of 2.0 mm. diameter. Three holes of 2.2 mm. were drilled in each plate at 120 ^{o} interval for the tie rods. The tie rods were fixed at the bottom to a stainless steel base as shown in Figure 5.8.

5.1.5 Generation of The Pulse

The pulse was generated using two electrically timed two way solenoid valves connected to a compressed air line and exhausting to the atmosphere. A University-made timer was used to obtain pulse frequencies up to 2.0 Hz. The desired amplitude was achieved by adjusting the pressure and the amount of the compressed air passing through to the test section, using a valve operated by hand. The amplitude used in this work is the average distance between maximum and minimum displacement of 10 cycles. The amplitude and frequency were measured by recording the motion of the liquid surface in the column as a function of the time, for frequencies; 0.54, 0.62, 0.71, 0.85, 1.03, 1.35 Hz. The recorded

video film was used also to check the pulse shape (sinusoidal) as shown in Figures 5.9, 5.10 & 5.11.

5.2 Selection of Liquid - Liquid System

Important factors in the study of extraction of solute from the organic phase were the physical properties e.g. viscosity, density, surface and interfacial tension of the dispersed phase all of which influenced the droplet behaviour. Therefore great care was taken with purity. The system toluene-acetone-distilled water was chosen for this investigation for the following reasons:-

1. The solubility data was available for the system (140, 176) as shown in Figures A5, Appendix A.
2. The system was selected in order to allow comparison with previous work.
3. The solvent could be easily recovered and purified.
4. The concentration of solute has a significant effect on interfacial tension of the system.
5. The Acetone solution could be expected to reach equilibrium at all points along the interface very rapidly (133).

5.2.1 Materials Used

Toluene and acetone of Analar grade were used without further purification. The specifications of these materials are given in Appendix A. Surface and interfacial tensions were checked repeatedly . The raffinate, and any unused feed were mixed together, the concentration was measured and then the actual amount of solute needed was added for the next experiment.

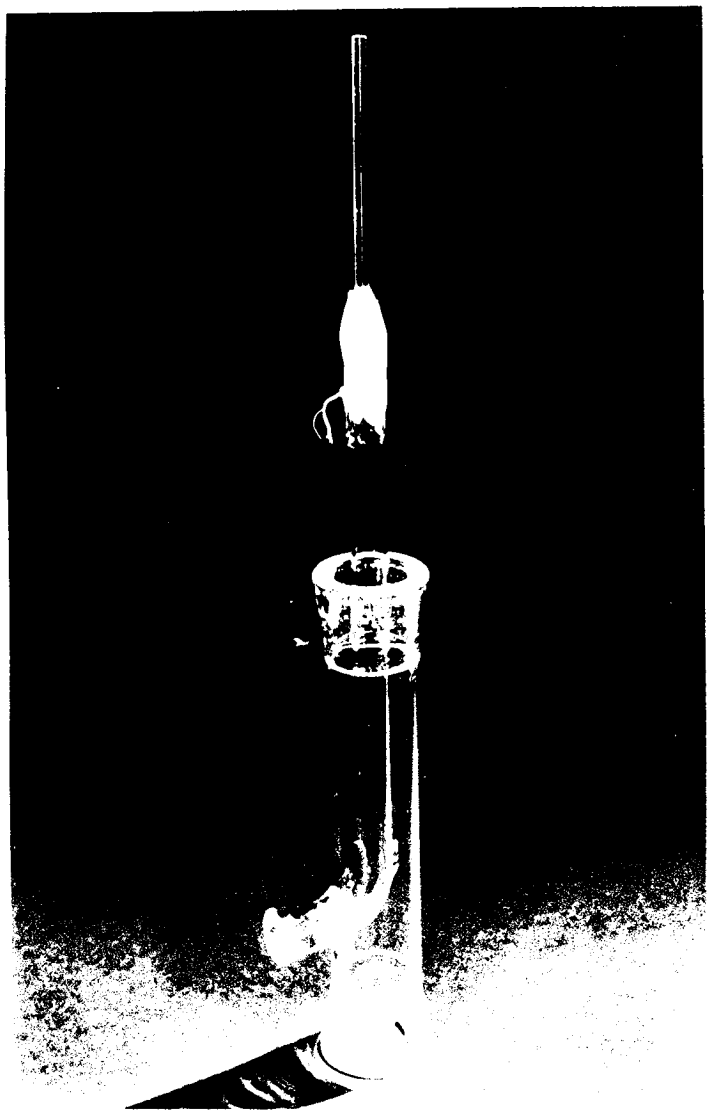

Figure 5.4 The Connection of Nozzle

Figure 5.5 Dispersed Phase Sampling Assembly
a. Sample Bottle and Syringe Assembly

Figure 5.5 Dispersed Phase Sampling Assembly
b. Assembly Sampling Head Inside Column

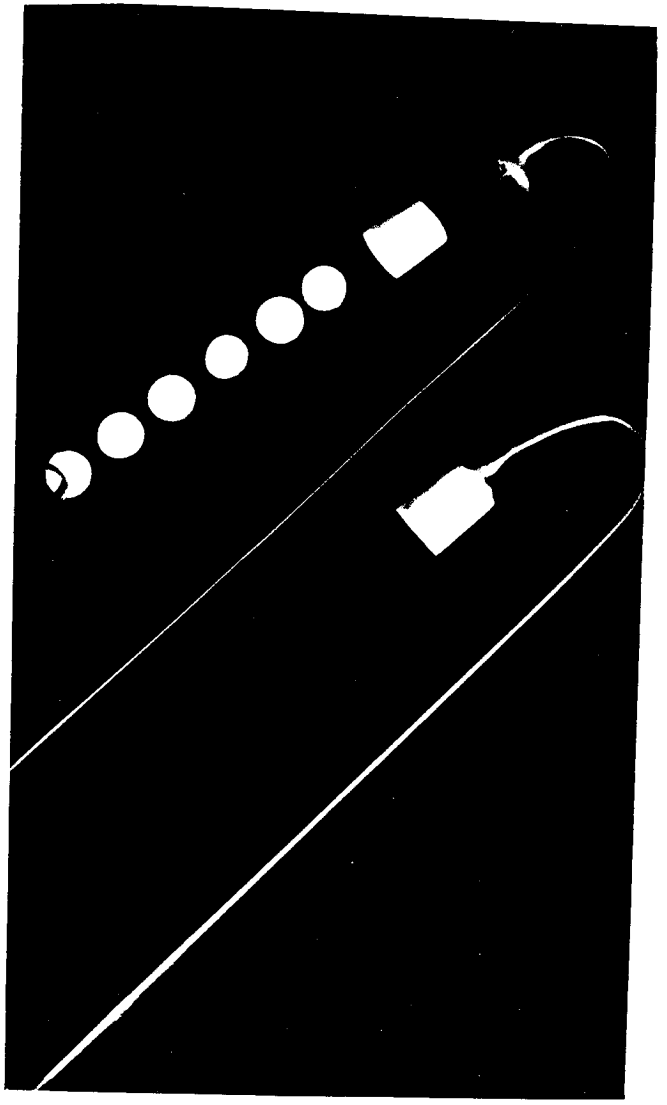

Figure 5.6 The Sampling Head
(Dismantled for Illustration Purposes)

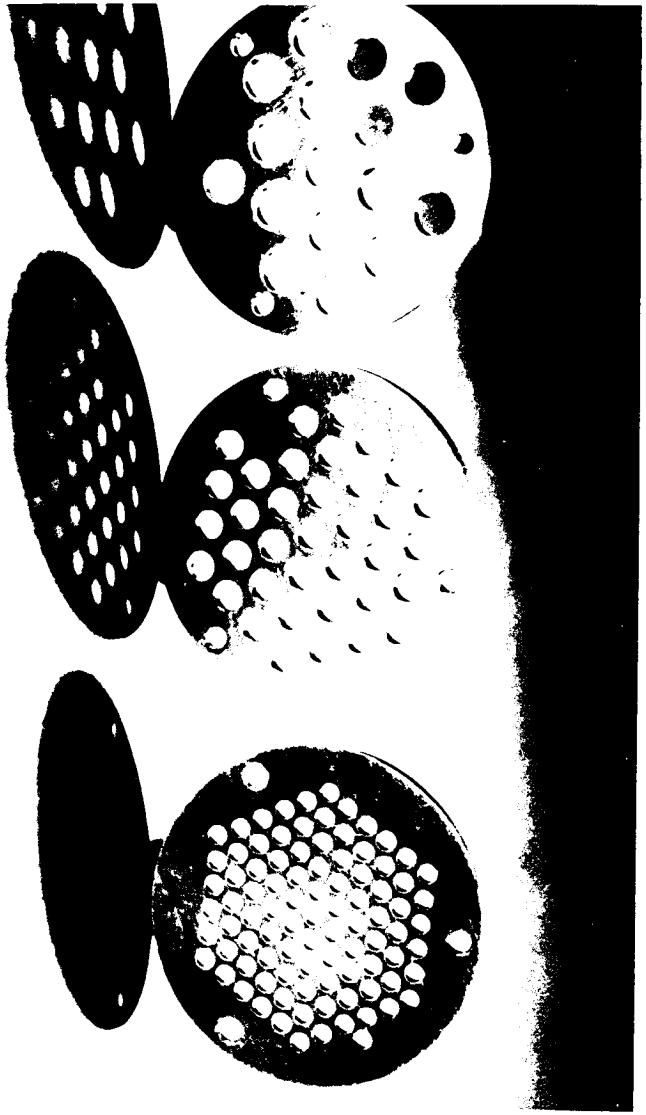

Figure 5.7 Sieve Plate with Different Characteristics

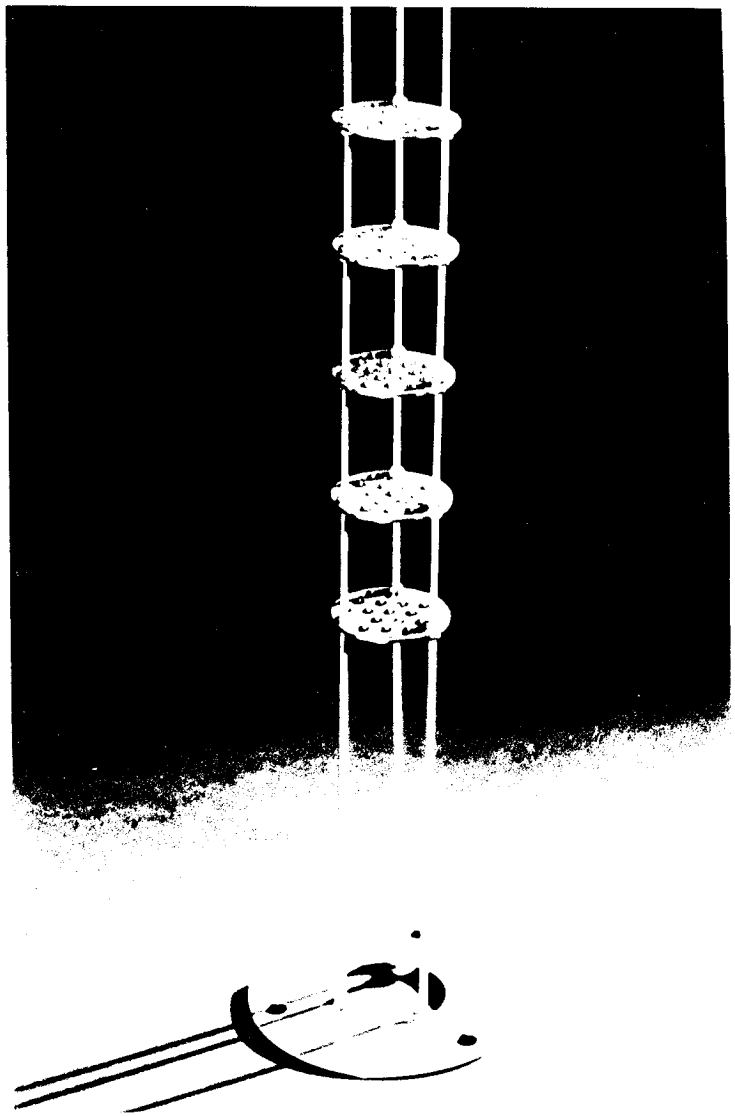

Figure 5.8 Sieve Plate Cartridge

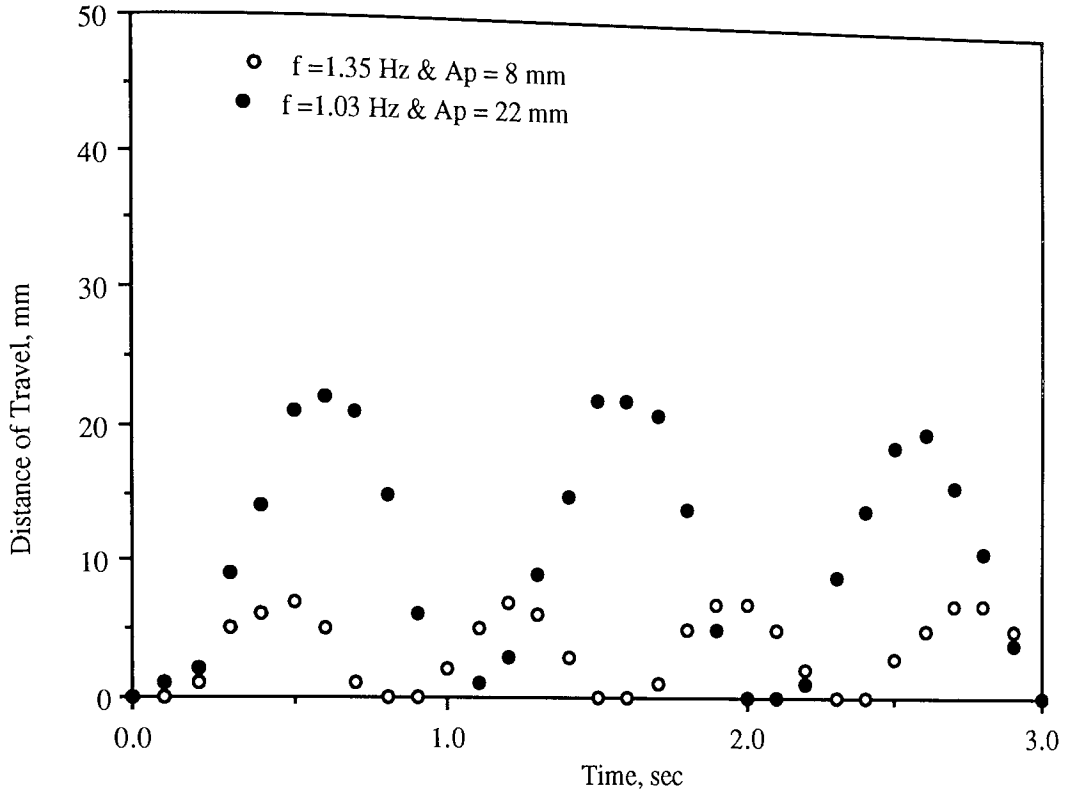

Figure 5.9 The Liquid Pulsed Motion in the Column

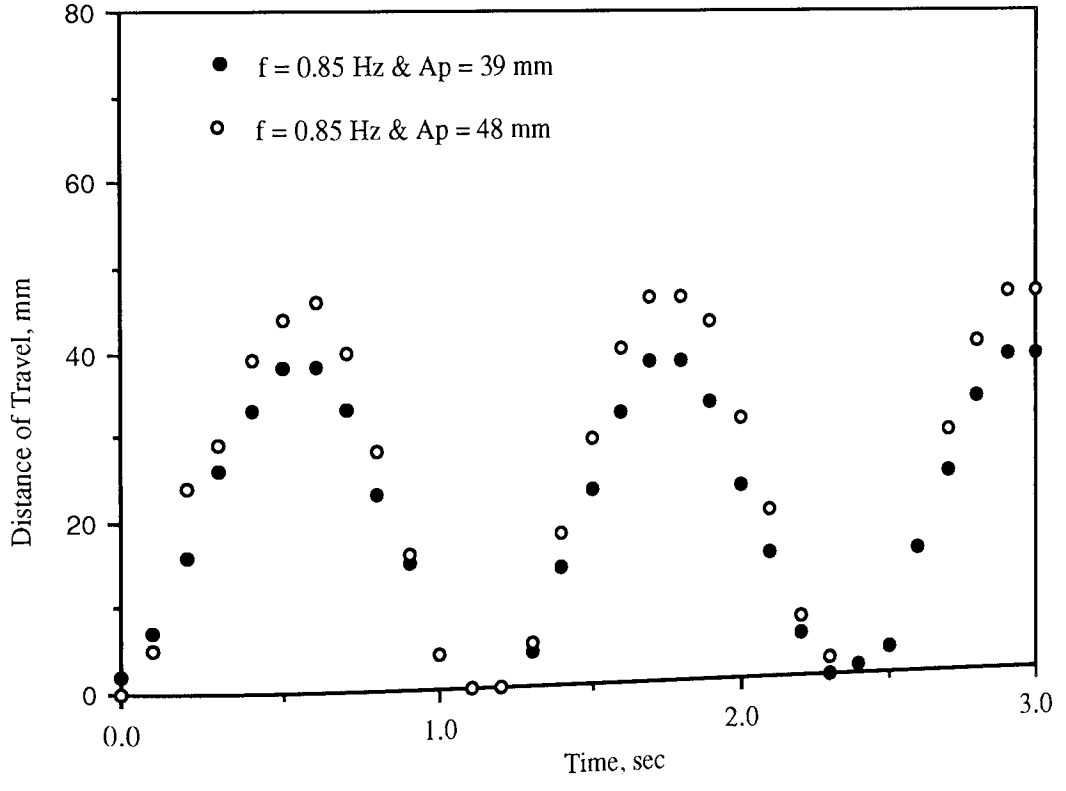

Figure 5.10 The Liquid Pulsed Motion in the Column

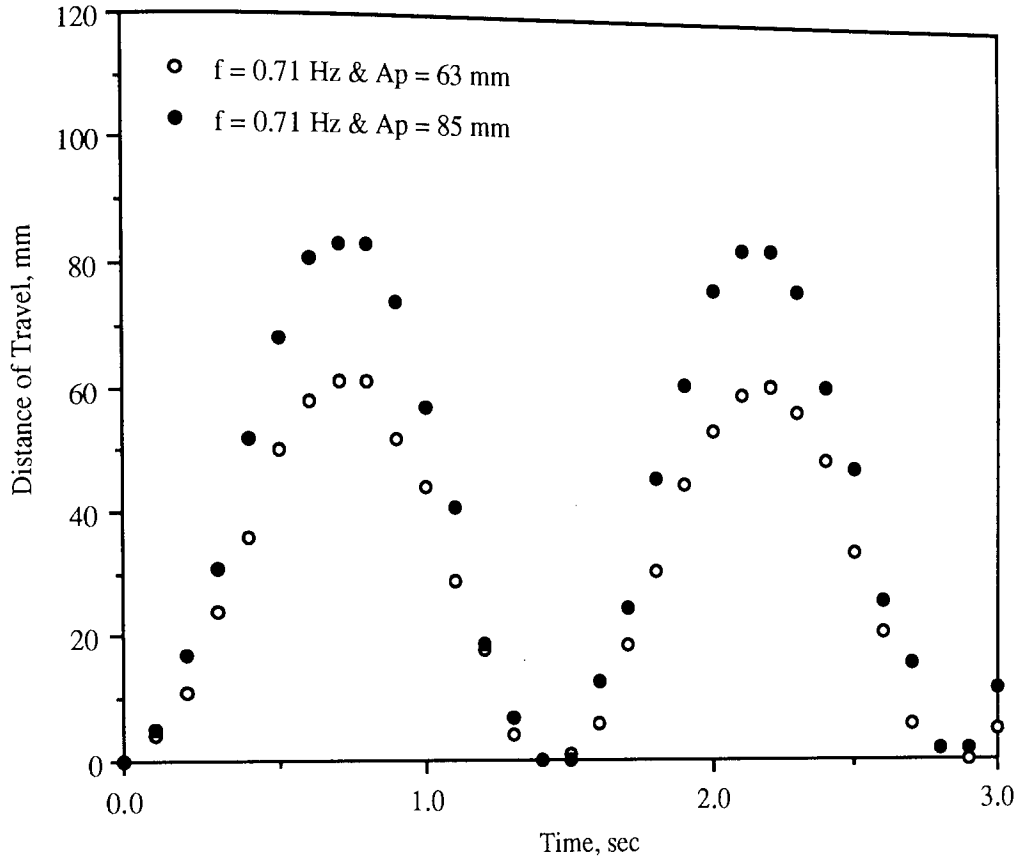

Figure 5.11 The Liquid Pulsed Motion in the Column

Table 5.2. Plate Specifications

hole diameter, mm.	free area, %	no. of the holes/plate
2.5	23.00	92
4.0	23.04	36
6.0	23.04	16

5.3 Physical Properties

The physical properties of the system, for different concentrations, were measured. The samples with different concentrations of acetone were prepared and then saturated with water. Several determinations were made and the mean values were reported.

5.3.1 Densities

Water density at 20.5 ^{o}C was quoted from the Handbook of Chemistry and Physics (180).The densities of solutions were measured using a specific gravity bottle at 20.5 $\pm$ 0.1^{o}C, allowing the absorbed air to be released. These were corrected to the density of water quoted, relative to that of distilled water used. The results are shown in Figure A.2, Appendix A.

5.3.2 Viscosities

Viscosities were determined by timing the passage of the fluid through a capillary viscometer immersed in a constant temperature bath (20.5 $\pm$ 0.1 ^{o}C). A Cannon-Fenske Viscometer (type 35/IP/CF) was always used. The measurements were corrected to that of water at 22 ^{o}C (180) and the results are shown in Figure A.3, Appendix A.

5.3.3 Interfacial and Surface Tensions

Interfacial and surface tensions were measured with a ring tensiometer (torsion

balance) at 20.5 $\pm$ 0.1 ^{o}C. The measurement of the interfacial tension was made with water saturated with the solvent " toluene", and the recorded measurements were those taken within 60 seconds of the contact of the two phases. The results are shown in Figure A.4, Appendix A.

5.3.4 Diffusivities

The diffusivities were determined using the Wilke and Chang correlation (183) for acetone diffusion in both phases at 22.0^{o} C, as follows:-

$$D=7.4*10^{-8}\frac{(x\,M)^{0.5}\,T}{\mu * V^{0.6}} \qquad 5.1$$

where:-

x	Association parameter, usually (1.0) for non-polar solvent and (2.6) for water
M	Molecular weight, gm.
T	Temperature, ^{o}K.
μ	Viscosity of the solvent
V	Molal volume of solute at normal boiling point, cm^3 / gmmole.

The physical properties of the system (toluene-acetone-distilled water) are summarised in Table 5.3.

5.4 Cleaning Procedures

In any study of the hydrodynamics and mass transfer characteristics from single

droplets, great care must be taken to ensure purity of the system and the cleanliness of the apparatus, in order to obtain reproducible results (98, 44, 168, 67, 3, 4). Consequently, an aqueous solution of 2.% Decon-90 decontaminant was used to clean the apparatus. The whole apparatus was filled with the solution which was circulated through the system for an hour, at a temperature of about 40° C, and then left for 24 hours to soak, after which the solution was pumped through all parts of the apparatus again and then drained. Following this, hot filtered water was pumped through the whole apparatus for half an hour and then drained through different drain points. This was repeated until the apparatus was shown to be free of the surface active agent, by checking the surface tension. The apparatus was next filled with distilled water heated to 60° C and kept at this temperature whilst recirculating for an hour. The contents were then drained. Finally, the apparatus was rinsed with distilled water, and it was ensured that all sampling and drain points were flushed.

Great care was taken in this cleaning procedure which was repeated during each series of experiments, and repeated whenever it was thought necessary. Between the tests the continuous phase side was rinsed with distilled water, while the dispersed side was rinsed with pure solvent. Surface and interfacial tensions were checked regularly. Special attention was paid to cleaning the nozzles. They were cleaned with chromic acid and then rinsed thoroughly with distilled water.

Table 5.3 Physical Properties of the System; Toluene-Acetone-Water

Concentration g mole/ lit	Concentration % wt / wt	Density gm/cm^3	Viscosity Cp	Interfacial Tension dyne / cm
0.00	0.00	0.866	0.756	29.2
0.40	2.69	0.864	0.743	24.3
0.66	4.45	0.863	0.736	22.4
1.45	9.94	0.859	0.707	17.5
2.51	16.93	0.857	0.692	13.9
2.63	17.81	0.855	0.678	13.1
3.50	24.46	0.849	0.669	11.8
3.79	25.68	0.847	0.668	11.5

Continuous Phase

Diffusivity of Acetone at $22^{\circ}C = 1.178*10^{-5}$ cm^2/sec & Density at $20.5^{\circ}C = 0.997$ gm/cm^3

Viscosity at $22^{\circ}C = 0.961$ Cp and Surface Tension at 20.5° C = 70.4 dyne/cm

CHAPTER SIX

MEASUREMENT TECHNIQUES AND EXPERIMENTAL PROCEDURES

6.1 Measurement Techniques

6.1.1 Photographic Techniques

The droplet sizes, in the spray column, were measured using a still camera. A Chinon GM-3 (Macrolens) camera was used with special long focal length lens; f 1/14 and it was mounted on a stand at a distance of 1.3 m. A black and white Kodak film (SAS400) was used. A stainless steel solid sphere of known diameter (6.0 mm.),to serve as a standard, was kept suspended in the liquid (continuous phase) and photographed along with the droplets. The droplet sizes were measured in relation to this sphere. The time required for a single droplet to travel up the column between two marked points was measured using a Casio electronic stop watch which measures to 1/100 second. The lower marked point was 15 cm. above the tip of the nozzle to avoid the zone of acceleration and the higher marked point was 70 to 80 cm further up the column. A video camera was also used in measuring the droplet sizes in the spray column and in the pulsed sieve plate column. It is discussed in more detail in the following paragraphs.

One of the most important parts of this study was the improvement of the photographic techniques for following the droplet behaviour during travel in the test section. A JVC, NewVicon colour video camera with 1:1.4 /9.8-80.0 zoom lens with a maximum aperture of f 1.3 - 1.5 m was used to record on Scotch VHS

tapes. The data was displayed using a Video, Panasonic NV-G45HQ Super 4 head Double Super Fine Slow, and a Panasonic colour T.V.which was used as a monitor. The data required from the tapes included:-

1. Sizes and velocities of moving droplet.
2. Droplet residence time and time delay.
3. Droplet breakup and droplet inerfacial area.
4. Frequencies and amplitudes of pulsing.

It was difficult to use the photographic technique because of the small difference in densities and refractive indices between the dispersed phase and the continuous phase (7, 49, 120, 145, 151). A dye could be used to improve the contrast. It was found (4) that the most suitable dye was iodine, which had no effect on the interfacial and surface tensions or the other physical properties if its concentration was held in the range of 20 - 30 ppm.(4). However, acetone affects the iodine only by changing its colour from violet-brown to brown, and then to yellow depending on the concentration of each substance. The fresh solution changed colour after two hours, therefore the iodine was added prior to the start of an experiment.

Tests with a light meter showed that a greater intensity of light was emitted from the column than from the mirrors, because of the position of the mirrors; therefore a neutral density filter in the form of an acetate sheet was positioned on the bright side of the column on the front side of the test section to reduce the light intensity to equal that from the mirrors (4). A diffuser with 1.56 mm. thick polypropylene sheet was used as shown in Figure 6.1. The lighting was provided by four Jupiter 650 watt quartz iodine, sealed beam flood lights with RR Beard 1000 watt quartz flood lights as " fill in ".

Most of the dyes mentioned in the literature, when examined (4), were found to affect the interfacial tension. Thus an effort was made to solve this problem by eliminating the need for dye addition in the photographic technique. A new illumination technique was developed in which a moving droplet could be photographed by motion pictures or video camera with good contrast without using any dye. This was done by replacing the above mentioned lighting system with a tube lighting system positioned in the middle line of the test section and by repositioning the neutral density filter, as shown in Figure 6.1. The droplet outline was made obvious by a refraction of the dark/light boundary at the droplet circumference.

Four transparent plastic millimetre scales were fixed at the rear of the square jacket over its full length, another two scales were fixed on the front of the jacket, one at each side. In each run 3 to 5 droplets were followed by the video camera from their formation at the tip of the nozzle to the top of the column. The video camera was mounted on a purpose built stand in order to record the rising droplet from the same plane (at 0.1 second intervals), i.e. by arranging the camera and the droplet at the same horizontal line. The continuous phase movement, in pulsing operation conditions, was represented by recording its position in the column at intervals of 0.1 second.

6.1.2 Concentration Determination

There are a number of different methods for measuring the concentration of acetone in the dispersed and continuous phase. Comparison of the these methods was done by testing known concentrations of acetone solutions, so that the most suitable method could be chosen.

A Pye Unicam Ultra-Violet Spectrophotometer (SP1800) was used to determine the acetone concentration by measuring the relative absorbance of ultra-violet radiation. Calibration charts of relative absorbance against the acetone concentration were prepared by measuring the relative absorbance of solutions of known acetone concentration, as shown in Figures A.6 and A.7, Appendix A.

The sample to be measured was placed in 10 mm. path-length quartz cells. The instrument was first zeroed by inserting a liquid blank in both cells. The wave length at which maximum absorption of acetone was obtained was found to be 286 nm. for the toluene phase solution and 276 nm. for the aqueous solution. The cells and the samples (in sealed bottles) were maintained at a constant temperature of $20.5 \pm 0.1^{o}C$ in a thermostatically-controlled water bath for about one hour before the readings were taken.

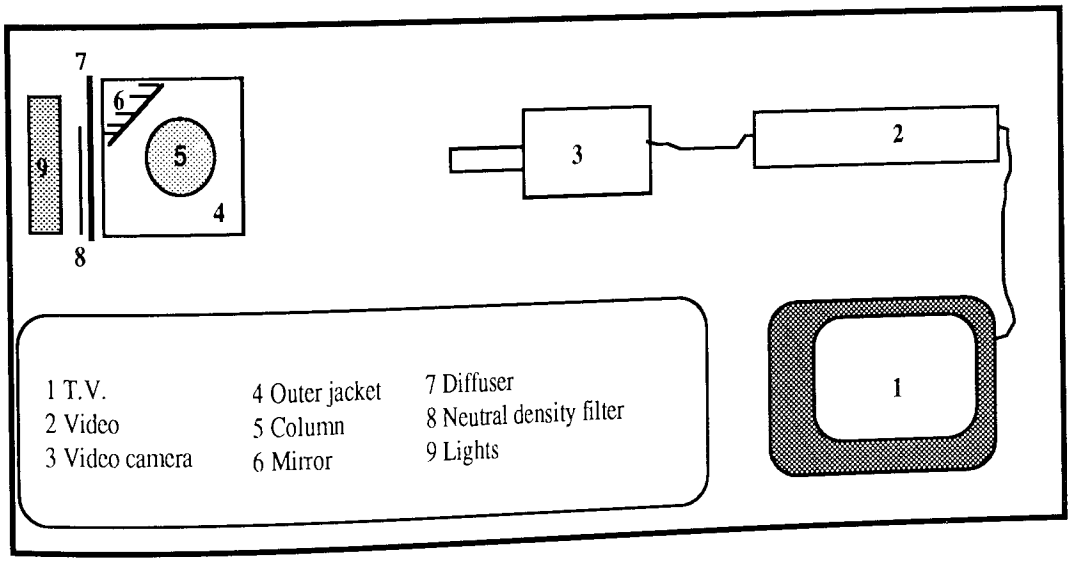

Figure 6.1. Arrangement for Droplet Photography

There are two other methods which were previously used to determine acetone concentration (4, 5,132). The two methods were the Messinger iodoform and the refractive index method (55). The initial experiments involving the measurement of refractive index did not give reproducible result and it was observed that one sample gave scattered readings when checked over a period of time. This could be due to the fact that the layer of sample used introduced the possibility of solute evaporation from the refractometer cell.This problem is eliminated by using a large sample as in the Ultra-Violet Spectrophotometer.

The Messinger iodoform method, which measured the acetone concentration depending on the reaction between an alkaline solution of acetone with an excess of iodine to form iodoform (55), did not yield satisfactory results (3).This was probably due to the sensitivity of the chemicals used, iodine and sodium thiosulphate, to light, temperature and time. The method of relative absorbance was found to be very convenient and gave more accurate, reproducible results than the other methods described.

6.2 Preparation of Phases

The two phases were prepared 20 hours prior to the experiment. The dispersed phase was prepared in a 10 litres QVF aspirator, which was sufficient for four experiments. By calculating the solute volume required to make 10 litres of the dispersed phase according to the data reported by Seidell (140), then water was added until its quantity was just over that required for saturation. The solution was mixed with a Gallenkamp stirrer (SS530) for one hour, and then left over night. The exact concentration obtained was determined just prior to an experiment by Ultra-Violet spectrophotometery.

The continuous phase was mixed with an excess of toluene (20-30 ml) by circulating of the liquid through the apparatus using a Stuart Turner centrifugal pump. The liquids were circulated for an hour to ensure complete saturation.

6.3 Operation Procedures

6.3.1 Hydrodynamics

The cabin heater was switched on an hour before the start of an experiment. The Churchill heater was turned on, after the valves on the heating liquid circulation were opened, with a setting of 22 ^{o}C. Following this the required volume of the dispersed phase (toluene saturated with water) was transferred to the reservoir. Then the dispersed phase input line to the test section was filled to the tip of the nozzle to avoid any continuous phase creeping into the line of dispersed phase.

The test section was filled with the continuous phase, and the desired flow rate was set via the constant head line in the leg balance and manual control valve, to maintain a constant level of liquid at the top of the column,and such that no continuous phase flowed via the raffinate outlet. Thus, when the droplet reached the top of the column, it flowed side ways and was separated from the continuous phase.

To avoid the effect of coalescence, the continuous phase was introduced 30 cm below the coalescence zone. For the pulsing conditions the desired frequency and amplitude were set by adjusting the pressure of the compressed air and the timer. At this stage the flow of dispersed phase was turned on and set by adjusting the needle valve; this marked the start of the experiment.

The flow rate of the dispersed phase was controlled by regular adjustments, by measuring the time required for 10 droplets discharged from the nozzle using a stop watch of ± 0.01 second accuracy. The flow rate could be adjusted to within ± 0.5 second of the required value. The continuous phase flow rate was measured with an accuracy of ± 2 ml. per minute, by collecting the output flowing to drain in a measuring cylinder for one minute. Some of the experiments were carried out with no flow of the continuous phase.

As mentioned in section 6.1.1.,the video camera was used to record the droplet behaviour during the formation and travelling periods. For each experiment 3 to 5 individual droplets were filmed; the rate at which 10 droplets left the nozzle was recorded. The motion of the surface of the continuous phase was filmed, at the beginning of each experiment, to allow determination of the frequency and amplitude of the pulsing and to check the wave form of the pulse. Whilst the experiment was in progress the flow rates, the temperature at various points, and the level of continuous phase in the top vessel, were checked regularly.

The observations of the hydrodynamics of droplets were carried out under four different operating modes; i.e. spray column, sieve-plate column, pulsed spray column, and pulsed sieve plate column. The characteristics of a single droplet; i.e. droplet diameter, droplet velocity, droplet breakup, droplet residence time, and the time of droplet retention through mechanical obstruction were observed for the various operating modes. The results of observations of the hydrodynamics are presented and evaluated in Chapter 7.

6.3.2 Mass Transfer

Experiments were carried out following the same procedure as detailed in section

6.3.1, but with the addition of mass transfer occurring between the droplet and the continuous phase. Initial runs were carried out to determine the time taken for the column to reach steady state conditions with regard to concentration of the transfer component. This was found to require 20 minutes. In subsequent experiments after steady state conditions had been attained, 5 ml samples were withdrawn from the dispersed phase sample ports which were placed at a point immediately above the formation nozzle and up the column at distances of 10, 20, 30, 40, and 60 cm above the tip of nozzles, as mentioned in Chapter 5 and as shown in Figure 6.2. The samples were put in sealed bottles and analysed by Ultra-Violet Spectrophotometry as discussed earlier. Results of mass transfer experiments were evaluated and the overall mass transfer coefficients were calculated as discussed in Chapter 7.

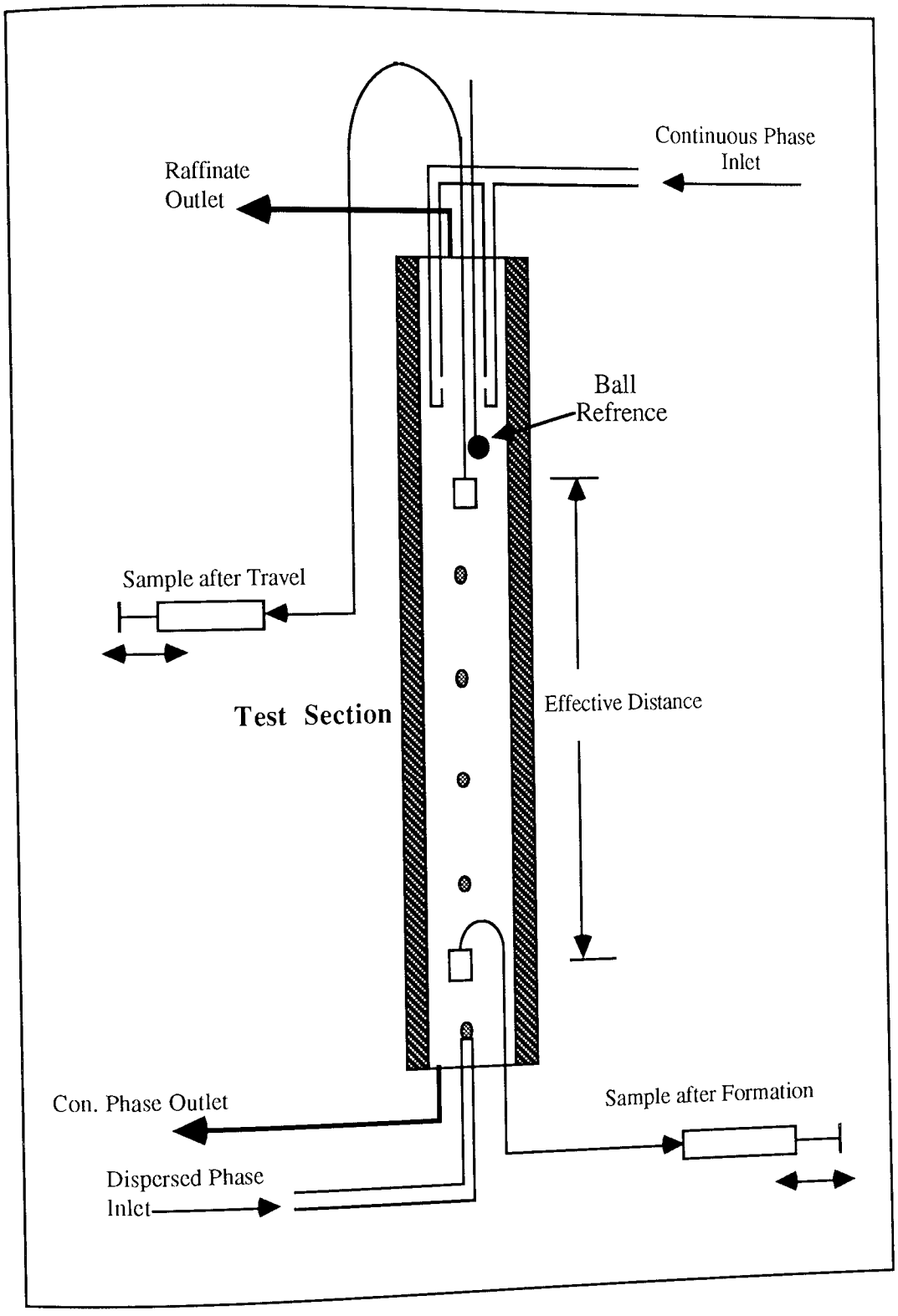

Figure 6.2 Diagram Representing the Droplet Sampling Technique

PART III

TREATMENT AND DISCUSSION OF RESULTS AND CONCLUSIONS & RECOMMENDATIONS

CHAPTER 7

CHAPTER 8

CHAPTER 9

CHAPTER SEVEN

TREATMENT OF RESULTS

7.1 Hydrodynamics

7.1.1 Terminal velocity

Terminal velocity is defined in Chapter 3 as the distance travelled by a free moving droplet in unit time under non-pulsing conditions and without plate or packing elements in the column. The terminal velocity of the studied system was measured experimentally for a range of droplet diameter 0.25-0.60 cm. Figures 7.1,7.2 ,7.3 and 7.4 represent this relationship for different droplet diameters .The procedure for measurement of terminal velocity is presented in Chapter 5. Figure 7.5 represents the experimental terminal velocity data for the system under study. The experimental terminal velocity was compared with values predicted for mobile droplets using equations 2-13 to 2-20. Figure 7.6 shows the comparison between the experimental and the predicted values. Table 7.1 contains experimental and predicted data.

7.1.2 Characteristic Velocity

The characteristic velocity is defined in Chapter 3 as the distance travelled by a droplet in unit time under pulsing conditions and/or the presence of a sieve plate. The experimental procedure for measuring the characteristic velocity using a photographic technique is presented in Chapter 5. The pulsing conditions cover the mixer-settler and transitional regions over the frequency range from 0.50 to 1.05 Hz and amplitude up to 9.0 cm. The effects of the pulsing parameters, the presence and characteristics of sieve plates, and the combined effects of both on the

Table 7.1 Experimental and Predicted Terminal Velocity Data

Droplet Diameter mm.	Predicted Droplet Terminal Velocity, mm/sec				Exp. de,mm	Exp. Drop Ter. Vel. mm/sec
	Eq. 2.11	Eq. 2.12	Eq 2.15	Eq. 2.16		
2	245.3	55.7	63.64	59.79	3.9	112
2.25	231.2	62.2	70.16	67.26	4	113.9
2.5	219.4	68.5	75.87	74.74	4.6	121.5
2.75	209.2	74.5	81.31	82.21	4.6	123.6
3	200.2	80.4	86.48	89.68	4.7	122.9
3.25	192.4	86	91.23	97.16	4.8	125.4
3.5	185.4	91.4	95.67	104.63	4.7	122.5
3.75	179.1	96.5	99.96	112.1	4.9	125.5
4	173.4	101.3	104.12	119.58	4.9	123.3
4.25	168.2	105.8	108.05	127.05	5	121.1
4.5	163.5	109.9	111.89	134.52	5.1	122.5
4.75	159.1	113.7	115.54	142	5.2	122.5
5	155.1	117.1	119.03	149.47	5.2	124
5.25	151.4	120.1	127.6	156.95	5.3	122.8
5.5	147.9	122.7	123.5	164.42	5.3	122.5
5.75	144.6	124.9	123	171.89	5.4	124
6	141.6	126.6	122.6	179.37	4.5	116.7
					5.5	122.5
					5.8	122
					5.8	120.7
					5.9	122
					5.9	120.7

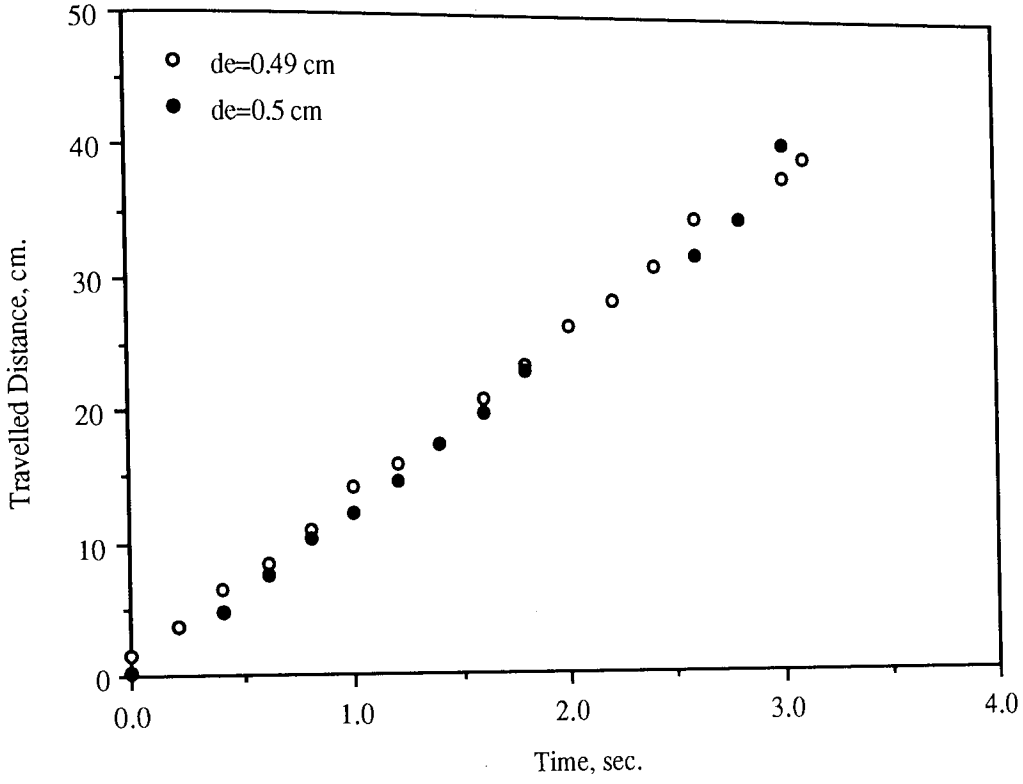

Figure 7.1 Relationship between Travelled Distance & Measured Time

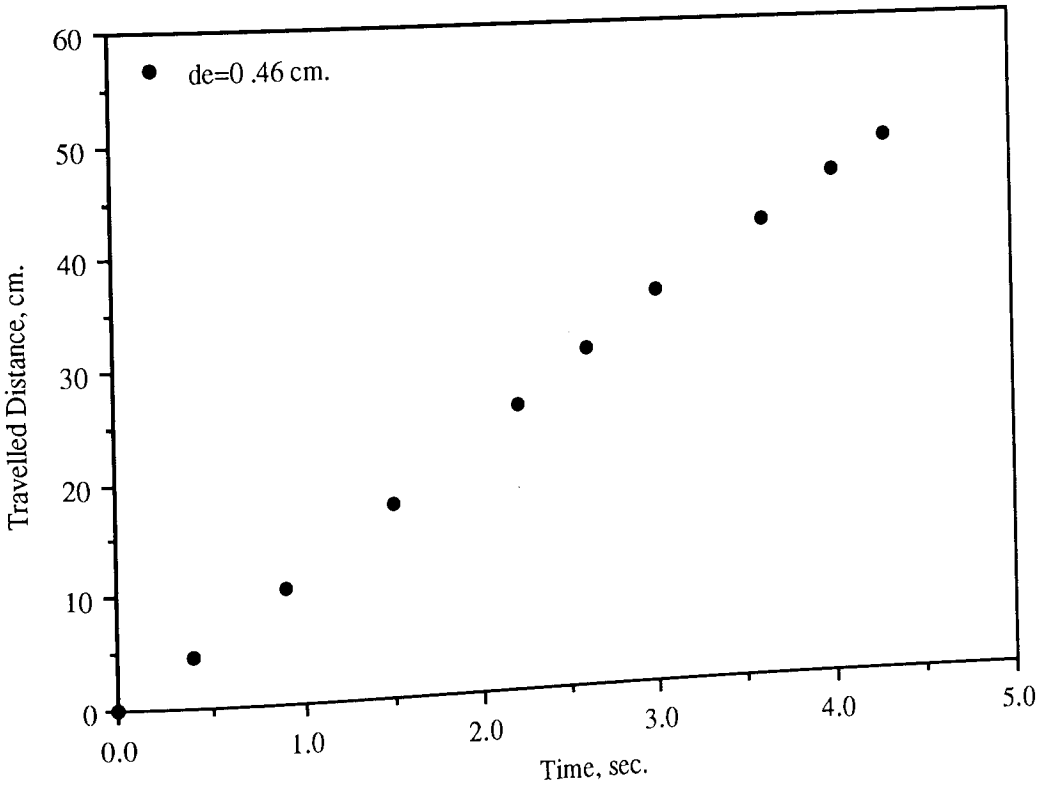

Figure 7.2 Relationship between Travelled Distance &Measured Time

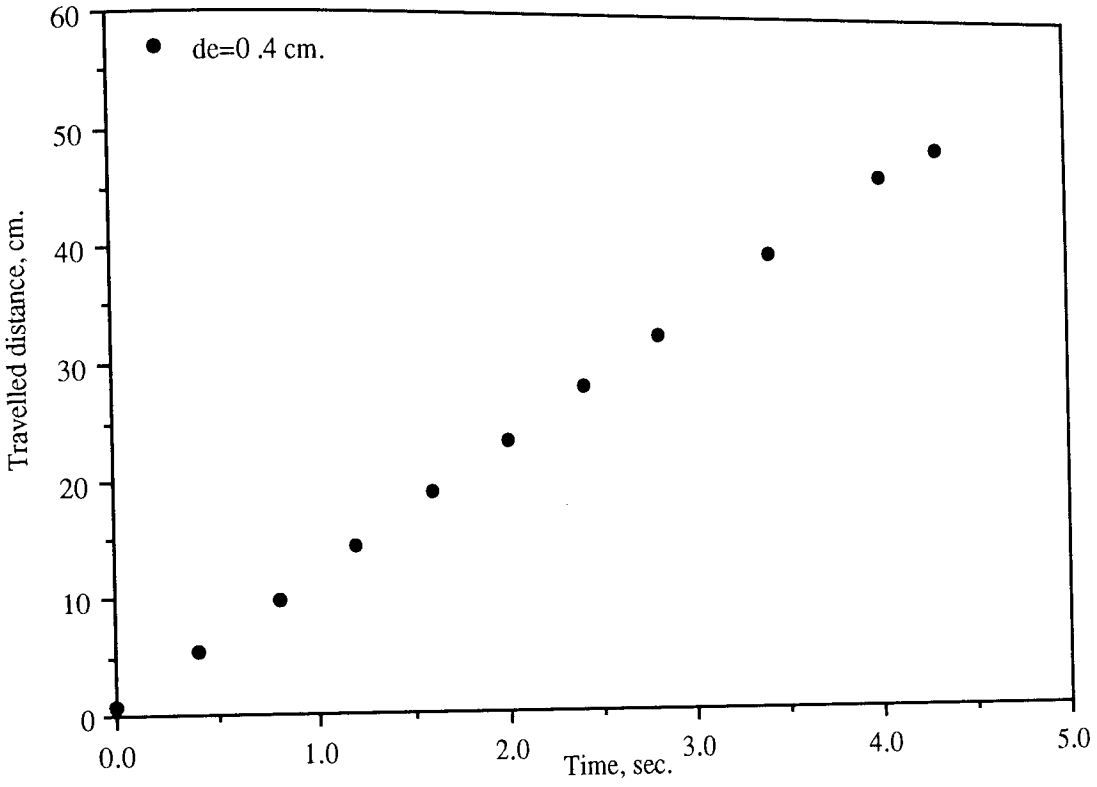

Figure 7.3 Relationship between Travelled Distance & Measured Time

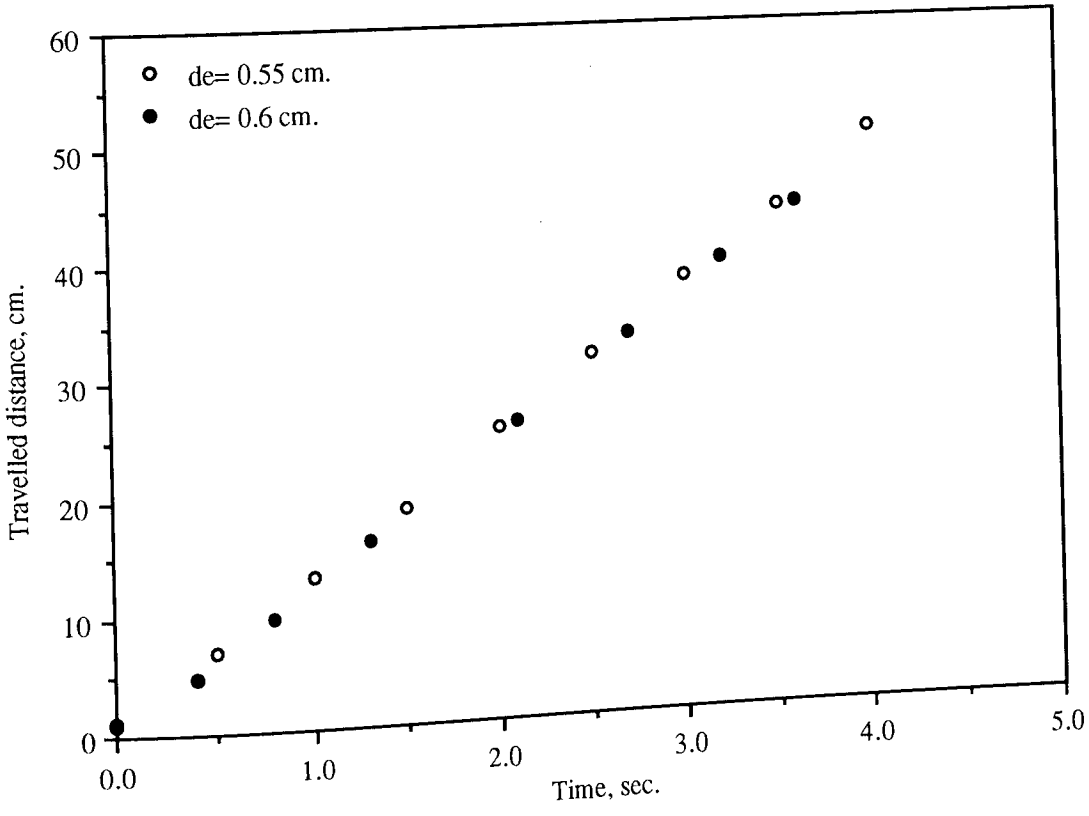

Figure 7.4 Relationship between Travelled Distance & Measured Time

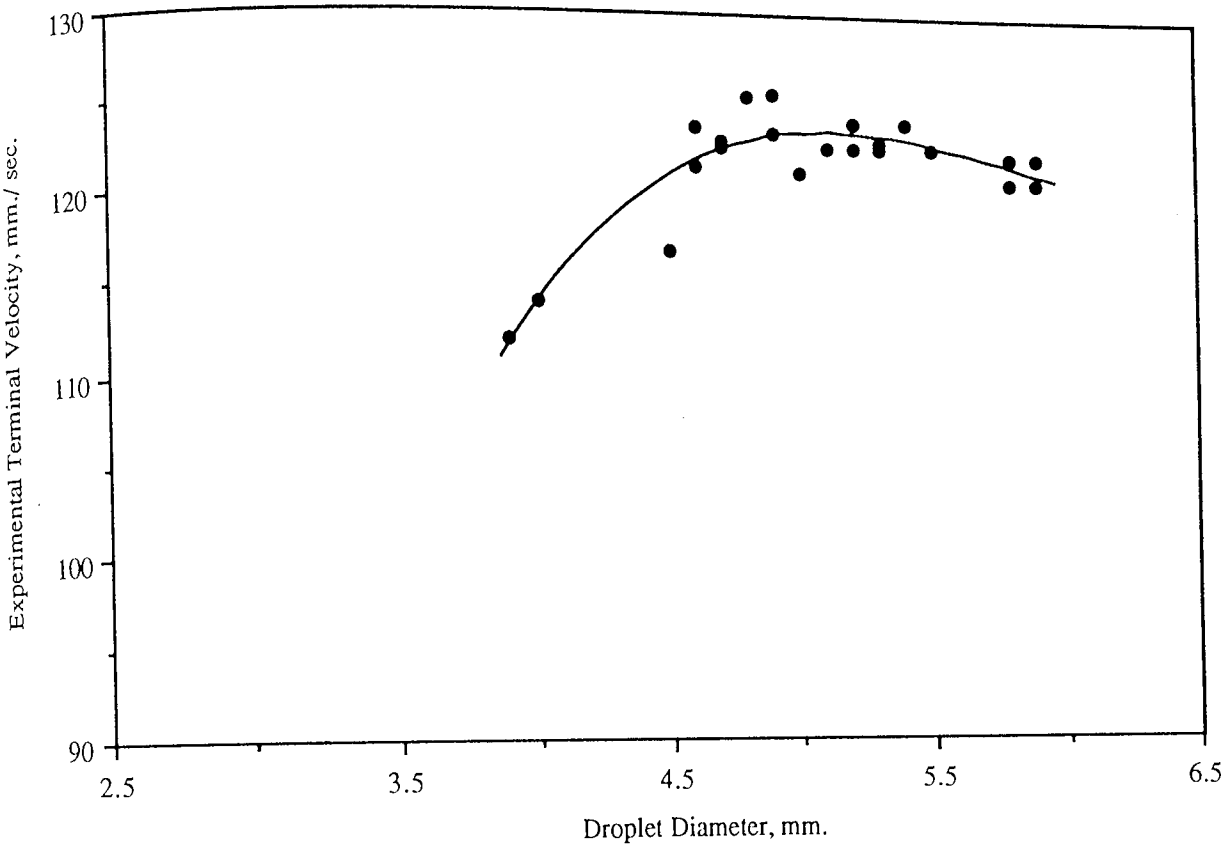

Figure 7.5 Experimental Terminal Velocity as Function of Droplet Diameter

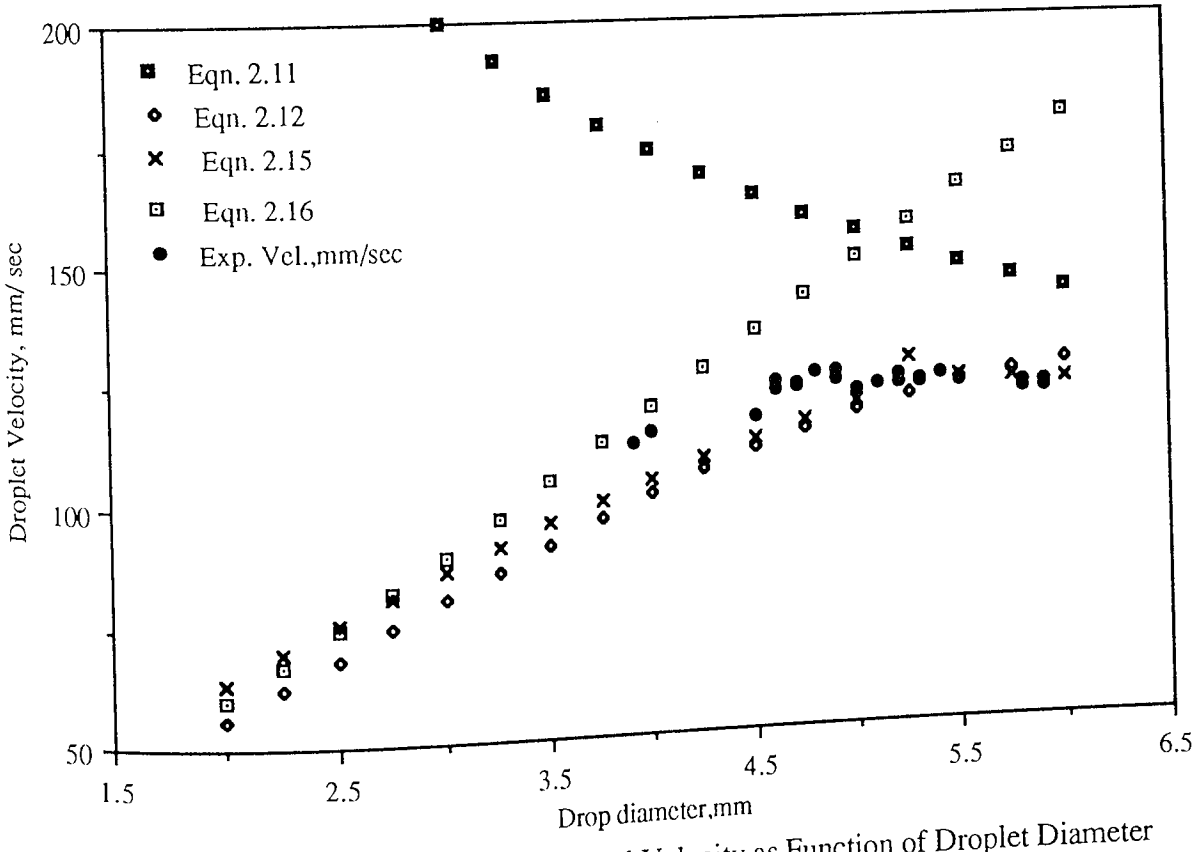

Figure 7.6 Predicted & Experimental Terminal Velocity as Function of Droplet Diameter

characteristic velocity are presented in paragraphs 7.1.2.1, 7.1.2.2, and 7.1.2.3 respectively. A complete set of data is listed in Appendices B.1.1 & B.1.2.

7.1.2.1 Effect of Pulsing

The effect of pulsing parameters on droplet motion, in the absence of sieve plates, was studied at frequencies of 0.54, 0.62, 0.71, 0.83 and 1.02 Hz with amplitudes in the range 0.5-9.0 cm. When the droplet is subjected to pulsing its absolute instantaneous velocity relative to a fixed datum point in the column will change as a result of the pulsing. The droplet moves with a velocity higher than its terminal velocity during the up-stroke of pulsing and lower than its terminal velocity during the down-stroke of pulsing. However, this study was interested in the change in the velocity of a droplet relative to its continuous phase. Thus to eliminate the apparent acceleration and deceleration of the droplet caused by the bulk movement of the continuous phase, the characteristic velocity (V_k) was determined as the distance moved by the droplet during a full cycle of the pulse divided by the time for this complete cycle (1/f). In practice, the distance moved over several cycles was measured in order to increase the experimental accuracy. Parameters which may have an effect on droplet motion are the frequency and the amplitude of the pulsing, and the droplet diameter.

a. Effect of Amplitude

At constant frequency i.e. 0.54 Hz as in Figures 7.7 & 7.8 the velocity during the up-stroke of the pulsing is higher than the terminal velocity and this effect increases as the amplitude of pulsing increases.This velocity becomes lower than the terminal velocity on the down-stroke of pulsing and as the amplitude of pulsing increases the droplet velocity decreases. The droplet motion may be momentarily reduced to zero or moved in the opposite direction as shown in Figures 7.7, 7.8, 7.9 & 7.10 for

"f= 0.54 Hz, Ap= 7.09 cm" & "f= 0.54 Hz, Ap=9.61 cm" & "f = 0.62 Hz, Ap=8.67 cm" respectively. In this case the droplet velocity suffered reduced velocity and then stopped for about 0.5 second then moved upwards with a velocity lower than its terminal velocity until the beginning of the up-stroke of the pulse cycle.

b. Effect of frequency of pulsing

The experimental data for amplitudes in the narrow range of about 0.2 cm with frequencies of 0.54, 0.62, 0.83, and 1.02 Hz and almost the same droplet diameter are presented in Figures 7.11, 7.12, 7.13 & 7.14. As is shown in these Figures it was found that the fluctuations in droplet velocity increased as the frequency of pulsing increased.

7.1.2.2 Effect of droplet Diameter

The experimental data for constant frequency, and a narrow range of amplitude and different droplet diameters are presented in Figures 7.15, 7.16, 7.17, 7.18 & 7.19. The experiments were carried out to examine the effect of droplet diameter on the motion of droplets in pulsed conditions.

7.1.2.3 Effect of the Plates Characteristics

Experiments were carried out using sieve-plates with hole diameters of 2.5, 4.0 and 6.0 mm and with constant free area of 23% to test the effect of (d/d_h) using the system toluene-water . The experiments were carried out at plate spacings of 25, 50 75, and 100 mm. The experiments showed a reduction in Vk/Vt as a function of (d/dh), Figures 7.27 & 7.28 show the effect of the sieve-plates on the motion of the droplet.

7.1.2.3 Combined Effect of the Pulsing Parameters & Plate Characteristics

Experiments were carried out to study the combined effect of the pulsing parameters and the presence of plates on the droplet characteristic velocity. The operating conditions were the same as in subsections 7.1.2.2 & 7.1.2.3. Figures 7.20-7.30 show the combined effect of both on the droplet behaviour.

7.1.3 Droplet Breakup

In this study three different mechanisms are considered to illustrate the droplet breakup in the pulsed sieve plate column under mixer-settler and transitional pulsing conditions. For a given system, the droplet diameter correlations depend mainly on the type of droplet breakup mechanism. The first droplet breakup mechanism to be considered is based on the formation of the droplet at a nozzle. Droplet formation at a nozzle may be characterised by the kind of formation mechanism i.e., either jetting or non-jetting droplet formation. The second droplet breakup mechanism to be considered is based on the theory of isotropic turbulence developed by Kolmogoroff. The third mechanism under consideration is that of impact breakup. The three droplet breakup mechanisms are considered in the following sub-sections.

7.1.3.1 Jetting and Non-Jetting Breakup Mechanism

In the absence of any reliable information for application of this mechanism to plate orifices, the correlations based on studies of liquid jets forming at the nozzle tip have been considered. Based on the maximum jet length at which breakup into droplets occurs, the relationship between the physical properties, hole diameter, and the jet velocity may be presented by a correlation proposed by Vedaiyan (172) , originally for a spray column. This may be used for a pulsed sieve-plate column after some modification. The modified correlation is as follows:-

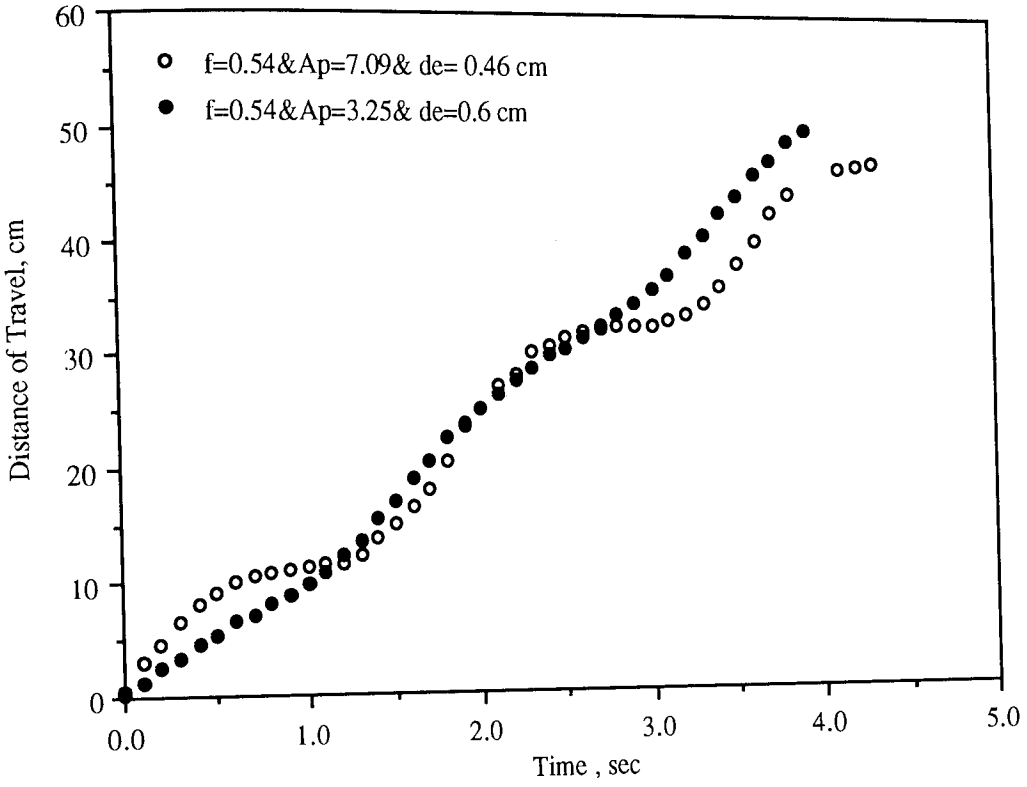

Figure 7.7 Effect of Amplitude of Pulsing on Droplet Movement

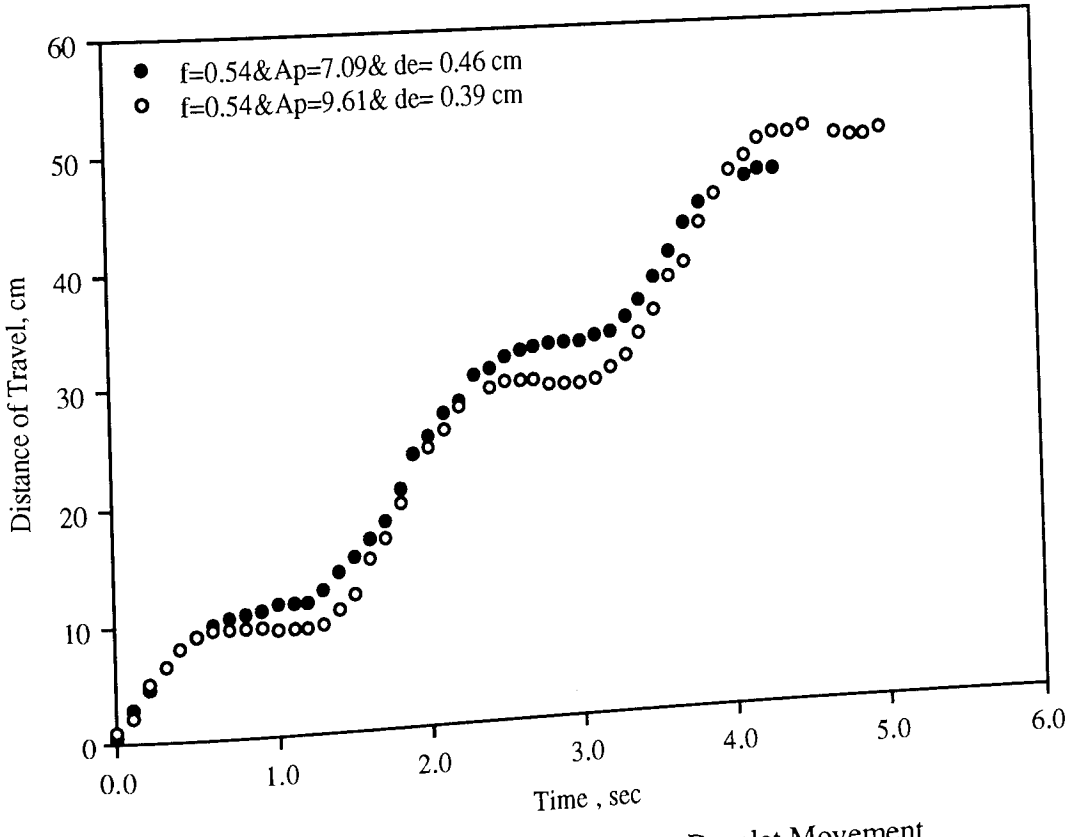

Figure 7.8 Effect of Amplitude of Pulsing on Droplet Movement

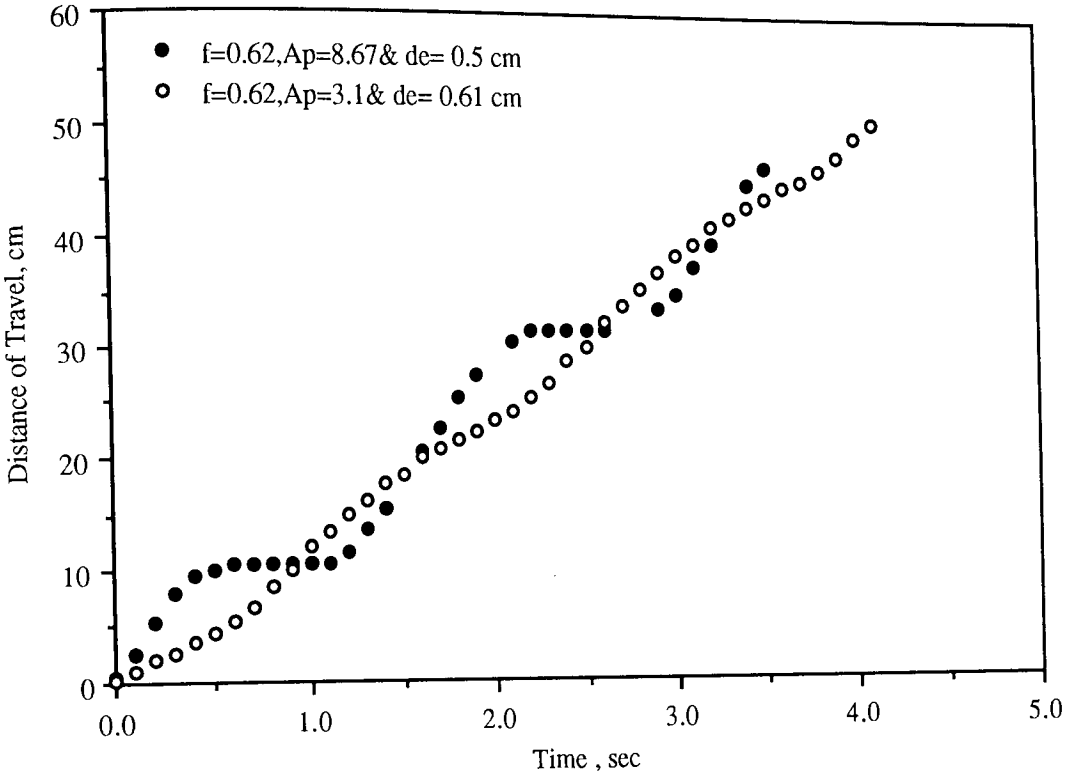

Figure 7.9 Effect of Amplitude of Pulsing on Droplet Movement

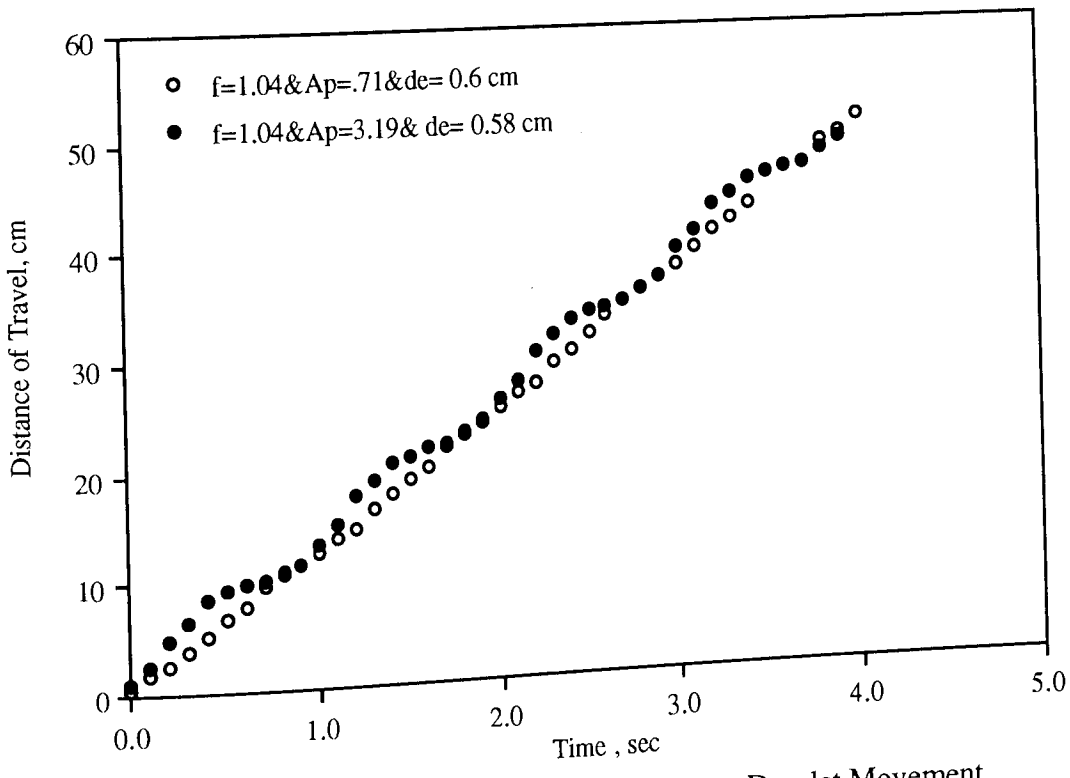

Figure 7.10 Effect of Amplitude of Pulsing on Droplet Movement

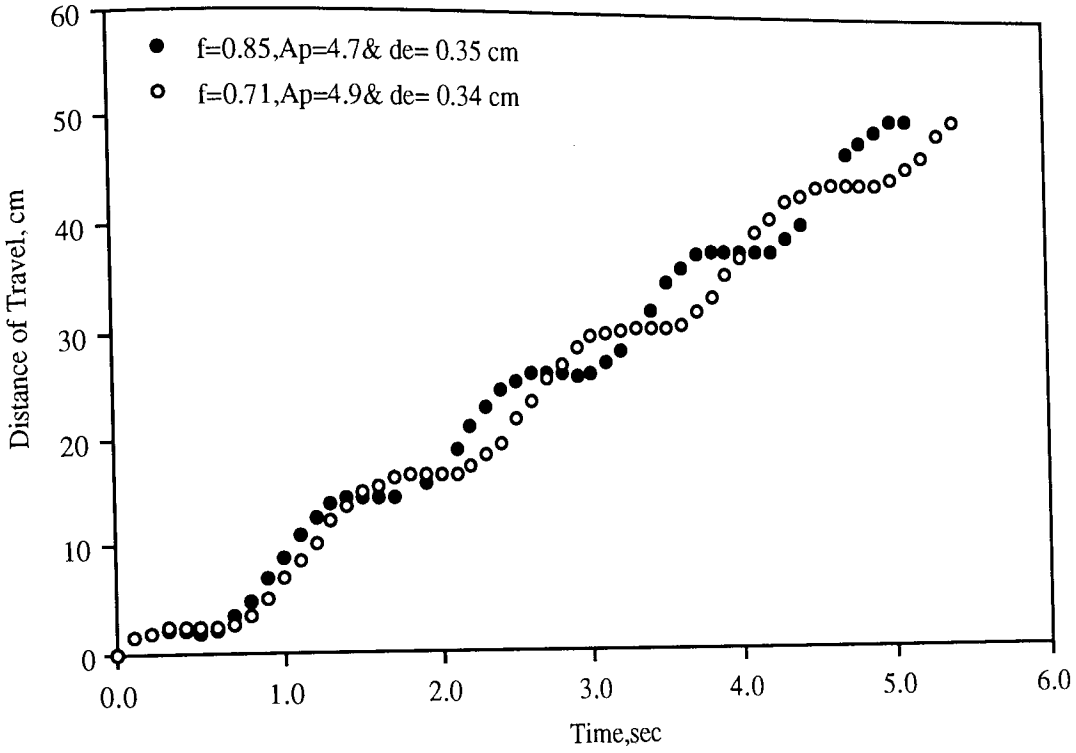

Figure 7.11 Effect of Frequency of Pulsing on Droplet Movement

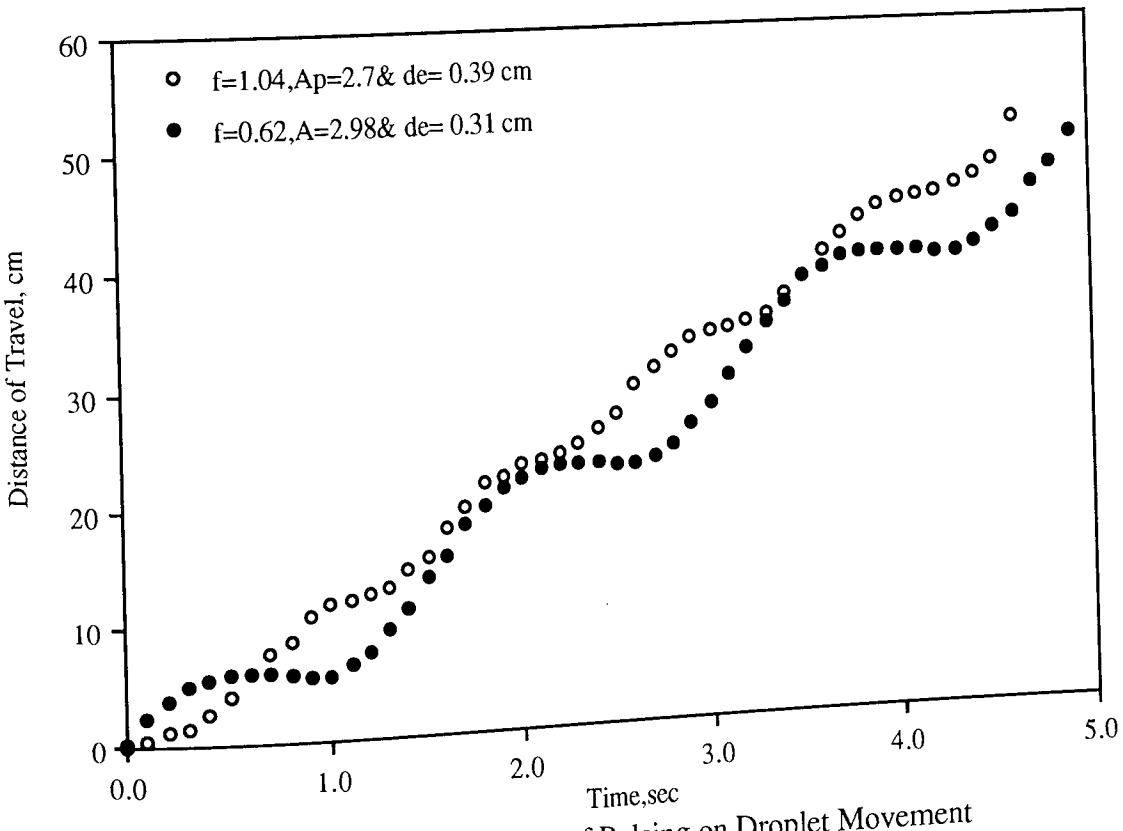

Figure 7.12 Effect of Frequency of Pulsing on Droplet Movement

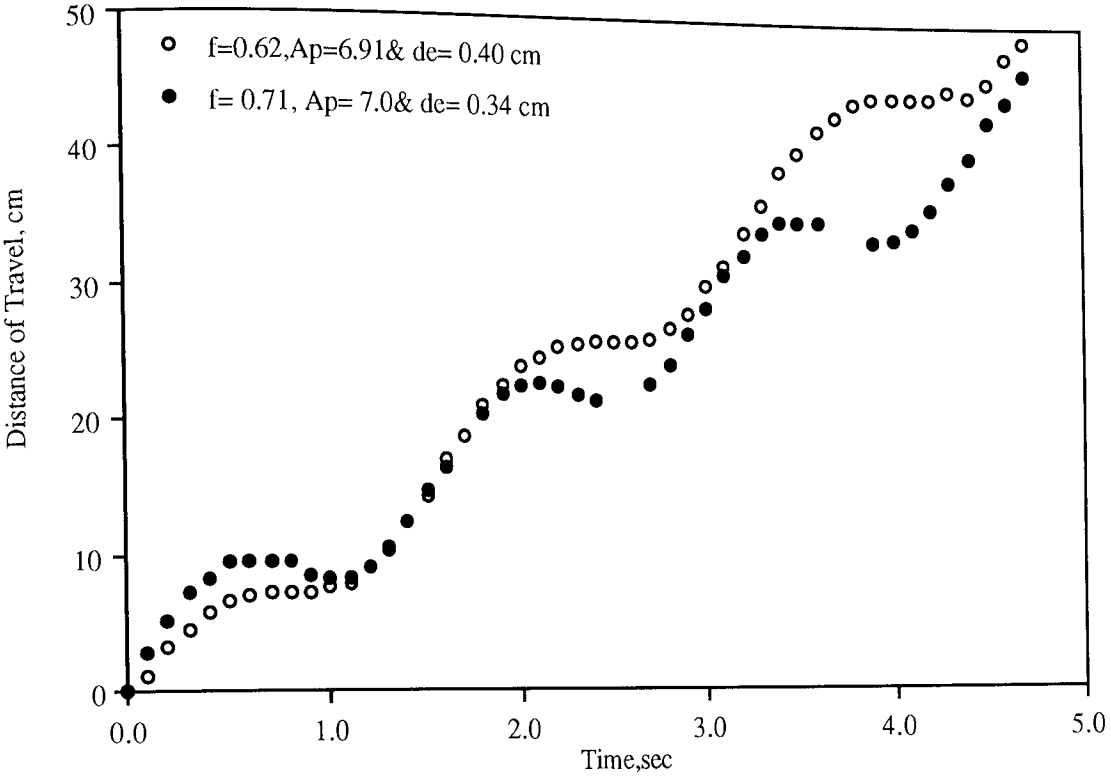

Figure 7.13 Effect of Frequency of Pulsing on Droplet Movement

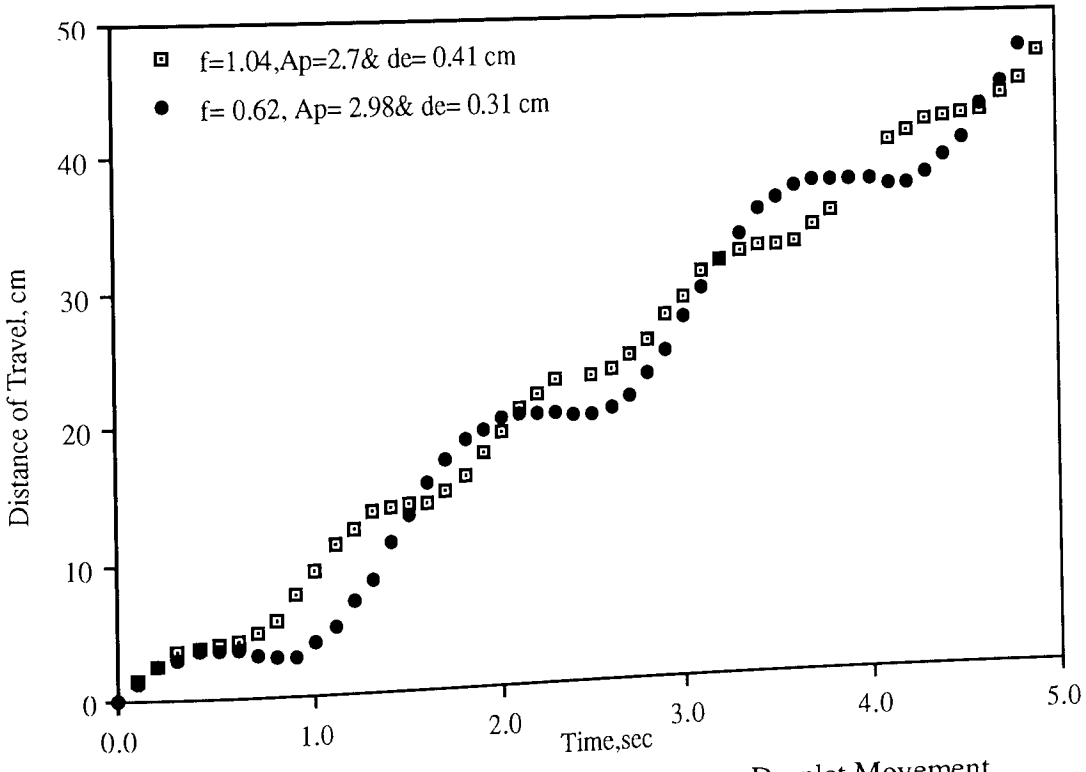

Figure 7.14 Effect of Frequency of Pulsing on Droplet Movement

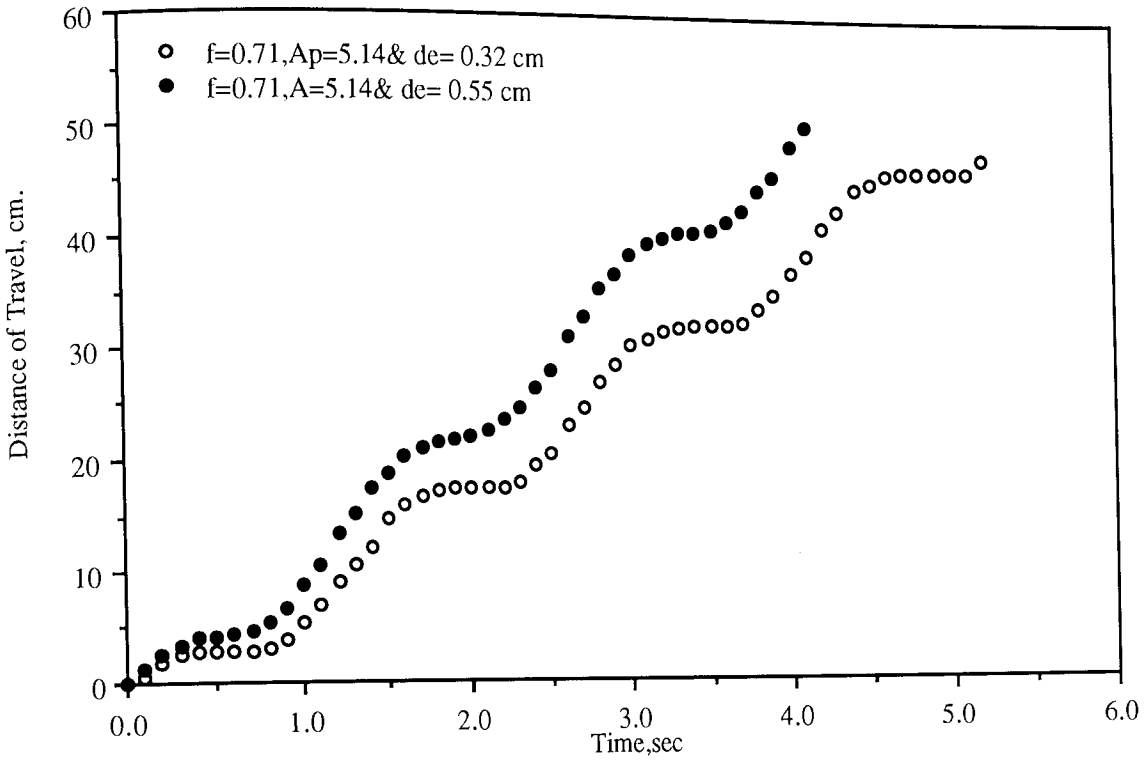

Figure 7.15 Effect of Droplet Diameter on Droplet Movement in Pulsing Condition

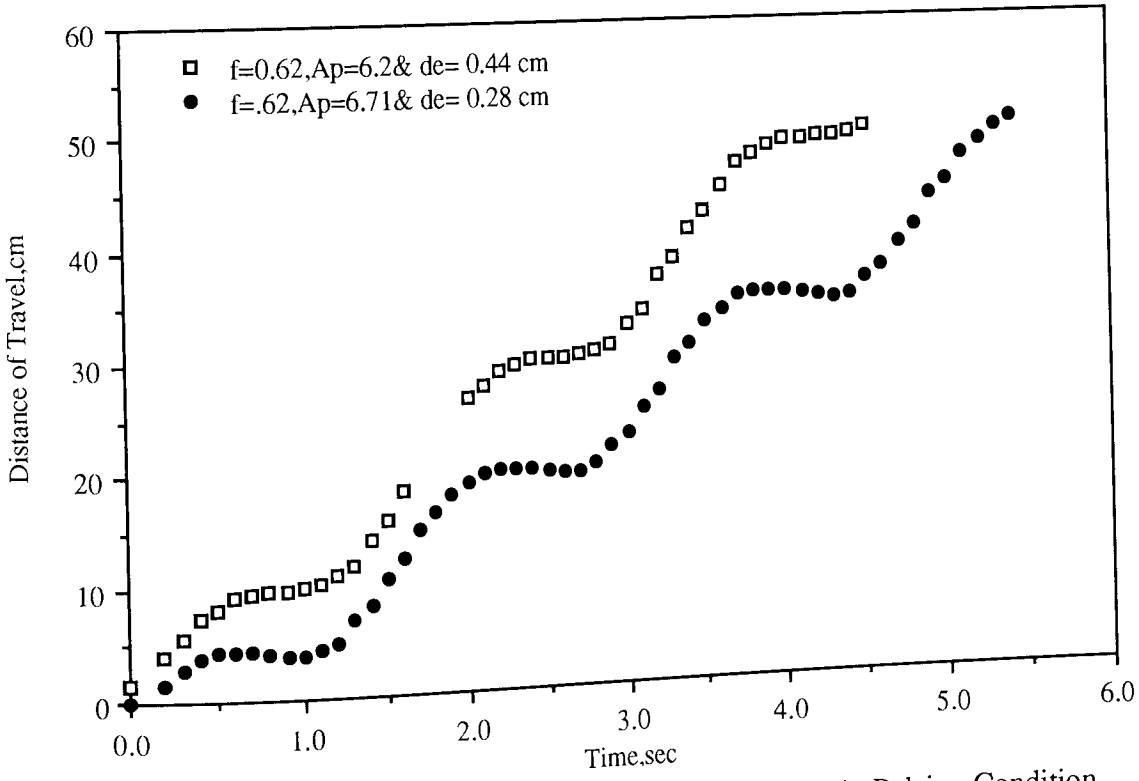

Figure 7.16 Effect of Droplet Diameter on Droplet Movement in Pulsing Condition

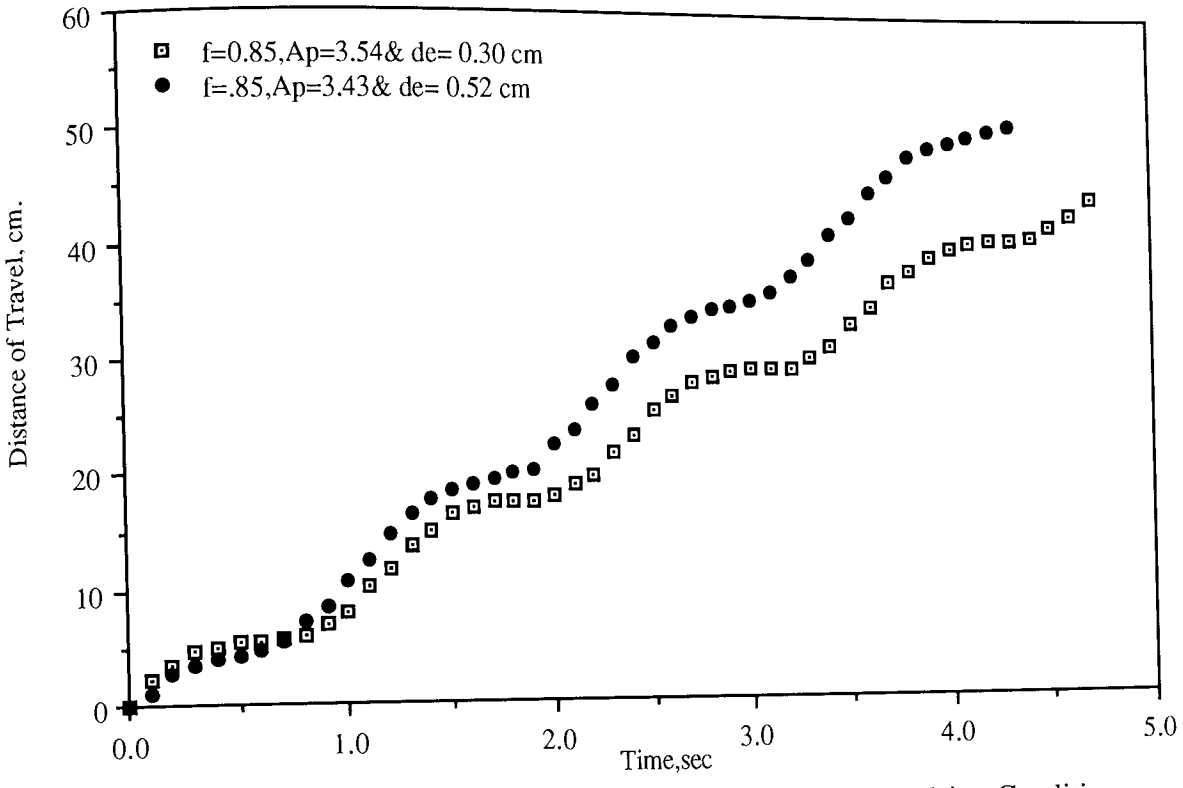

Figure 7.17 Effect of Droplet Diameter on Droplet Movement in Pulsing Condition

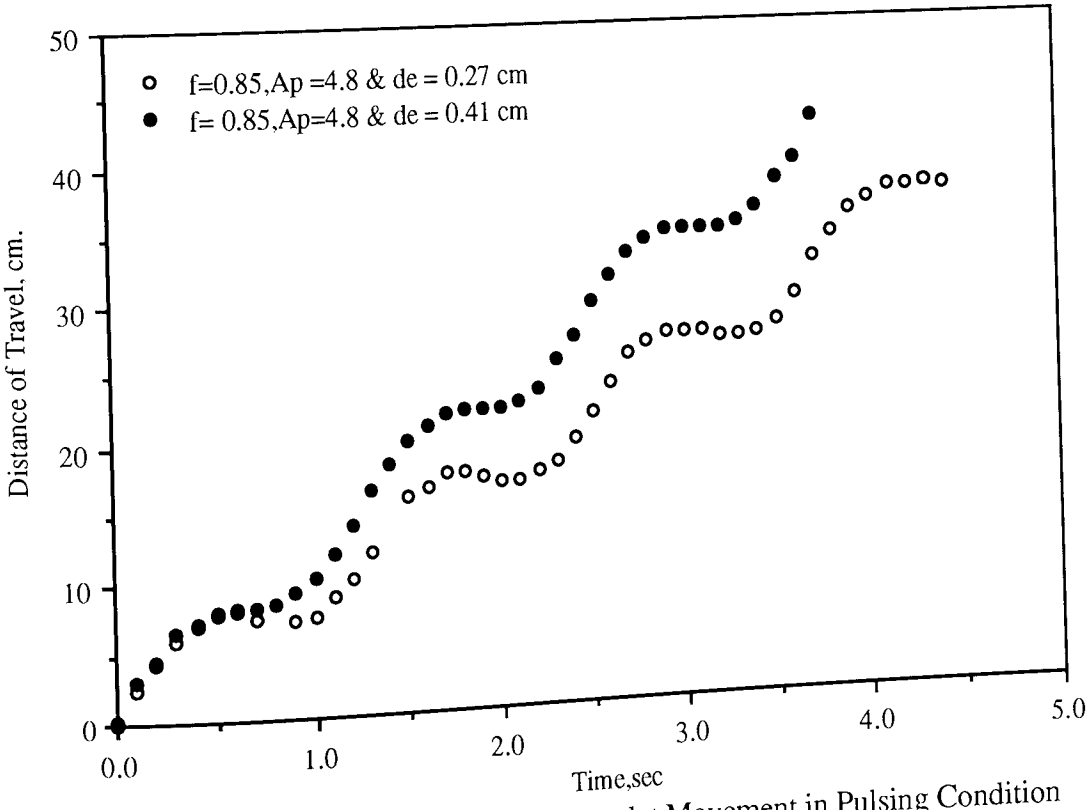

Figure 7.18 Effect of Droplet Diameter on Droplet Movement in Pulsing Condition

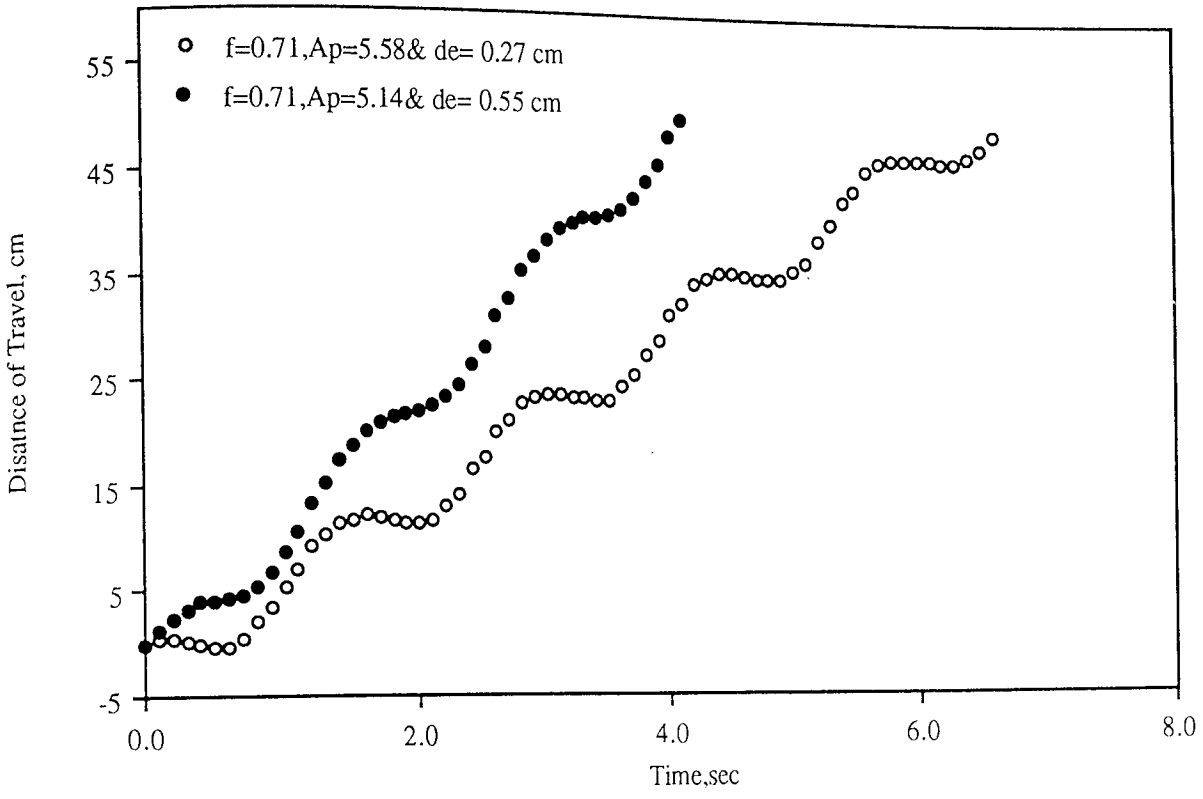

Figure 7.19 Effect of Droplet Diameter on Droplet Movement

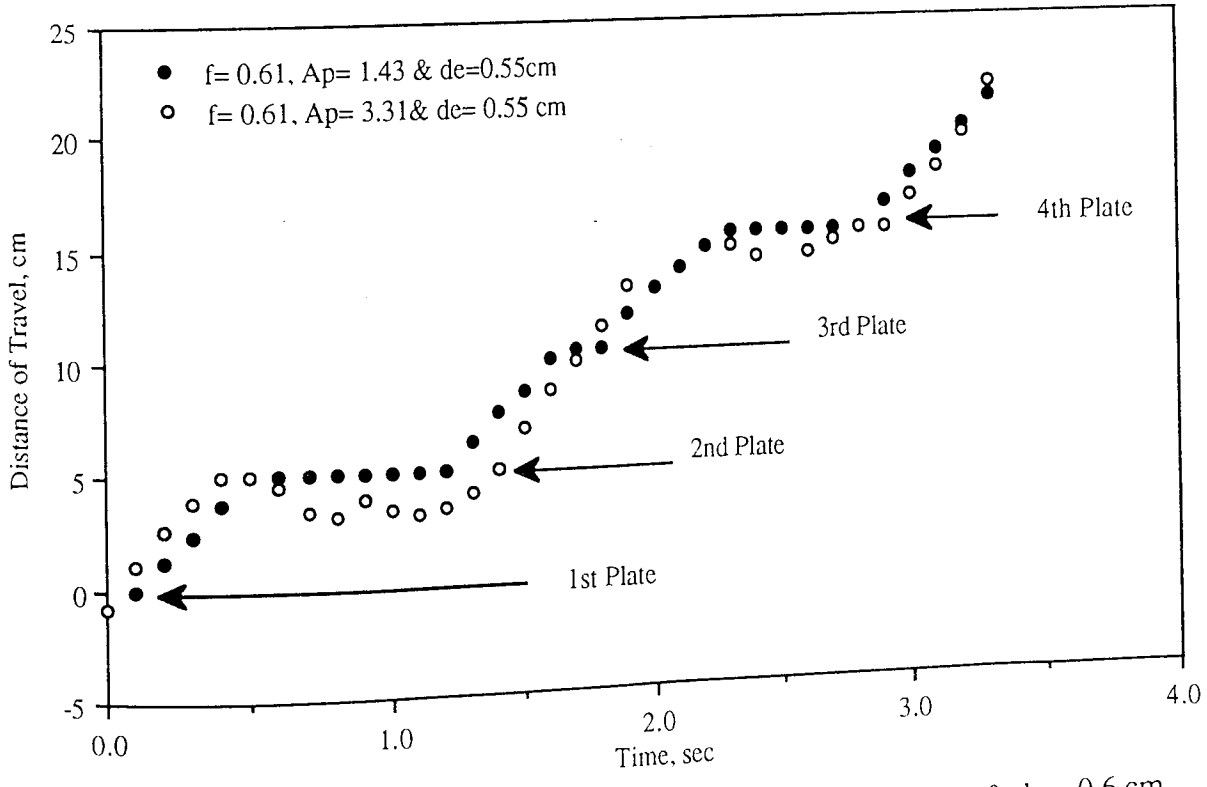

Figure 7.20 Effect of Sieve-Plate on Droplet Movement for, h_c = 5.0 cm & d_h = 0.6 cm

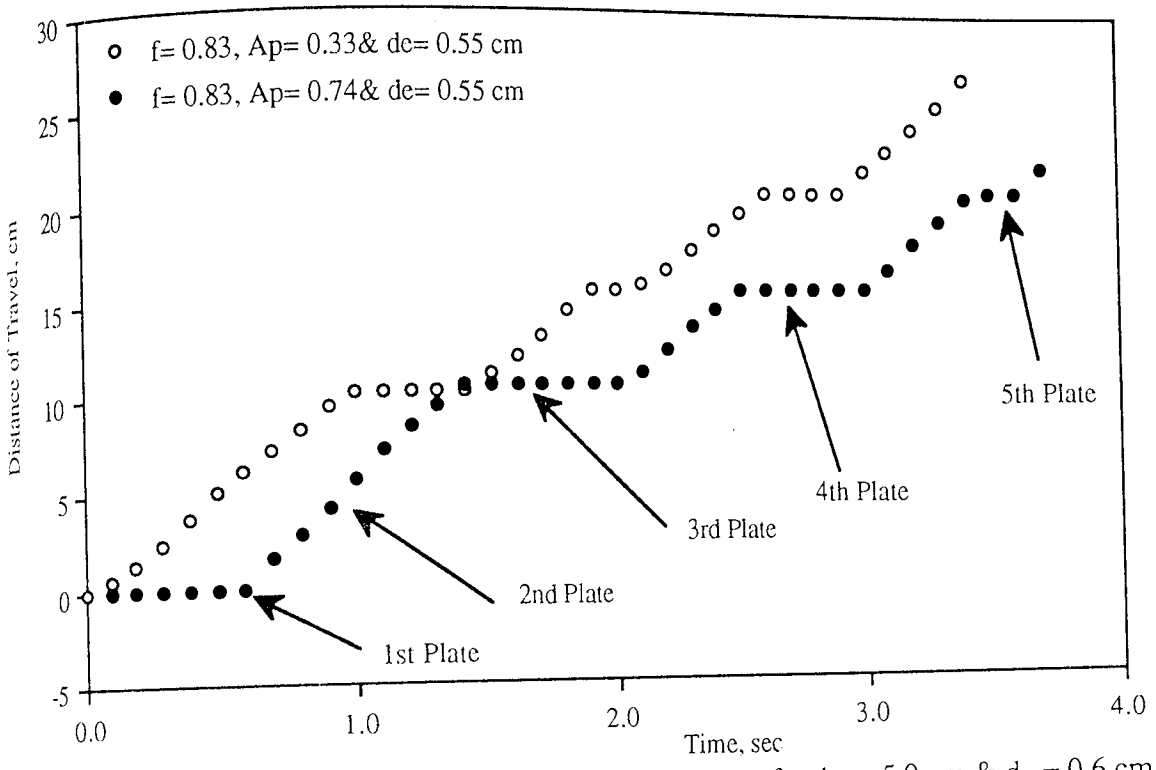

Figure 7.21 Effect of Sieve-Plate on Droplet Movement for, h_c = 5.0 cm & d_h = 0.6 cm

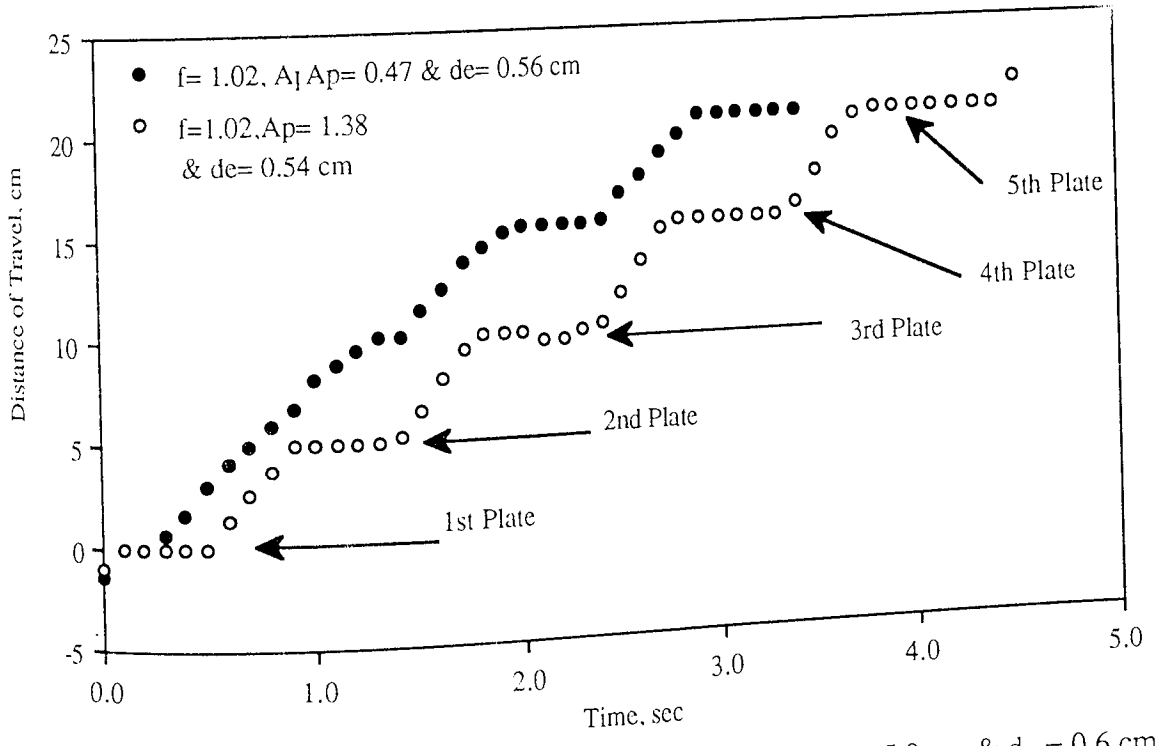

Figure 7.22 Effect of Sieve-Plate on Droplet Movement for, h_c = 5.0 cm & d_h = 0.6 cm

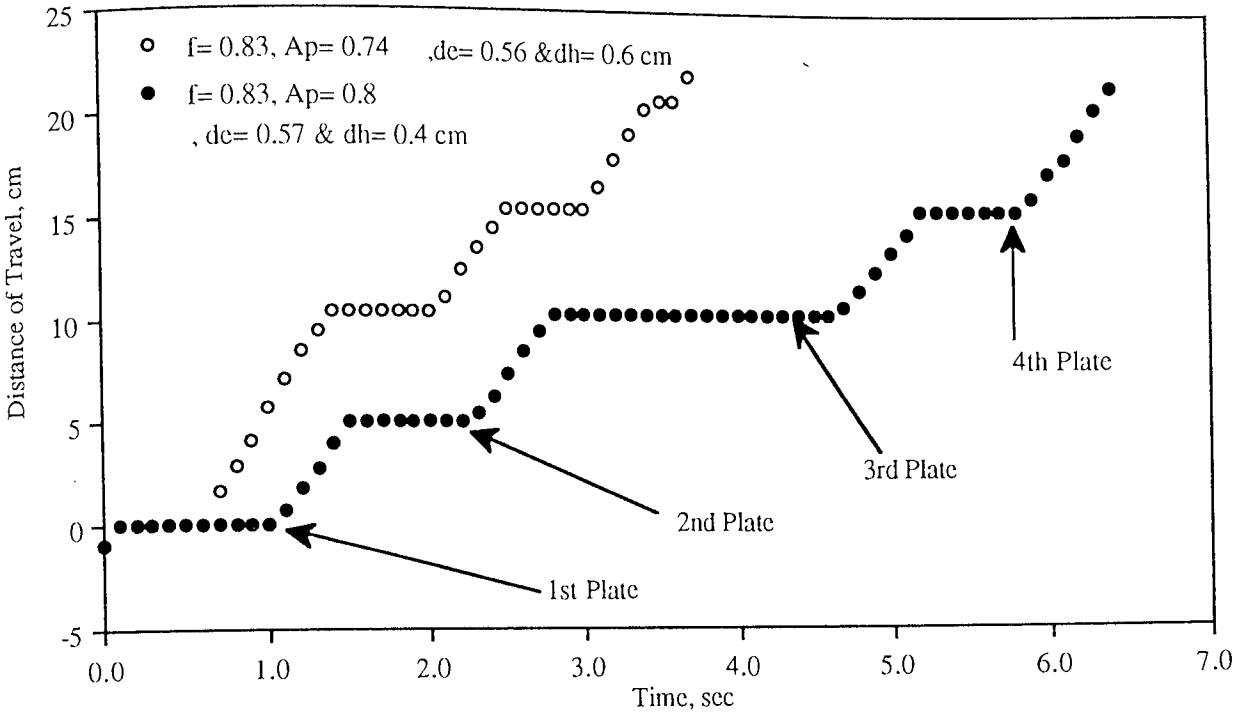

Figure 7.23 Effect of Sieve-Plate on Droplet Movement for, h_c = 5.0 cm

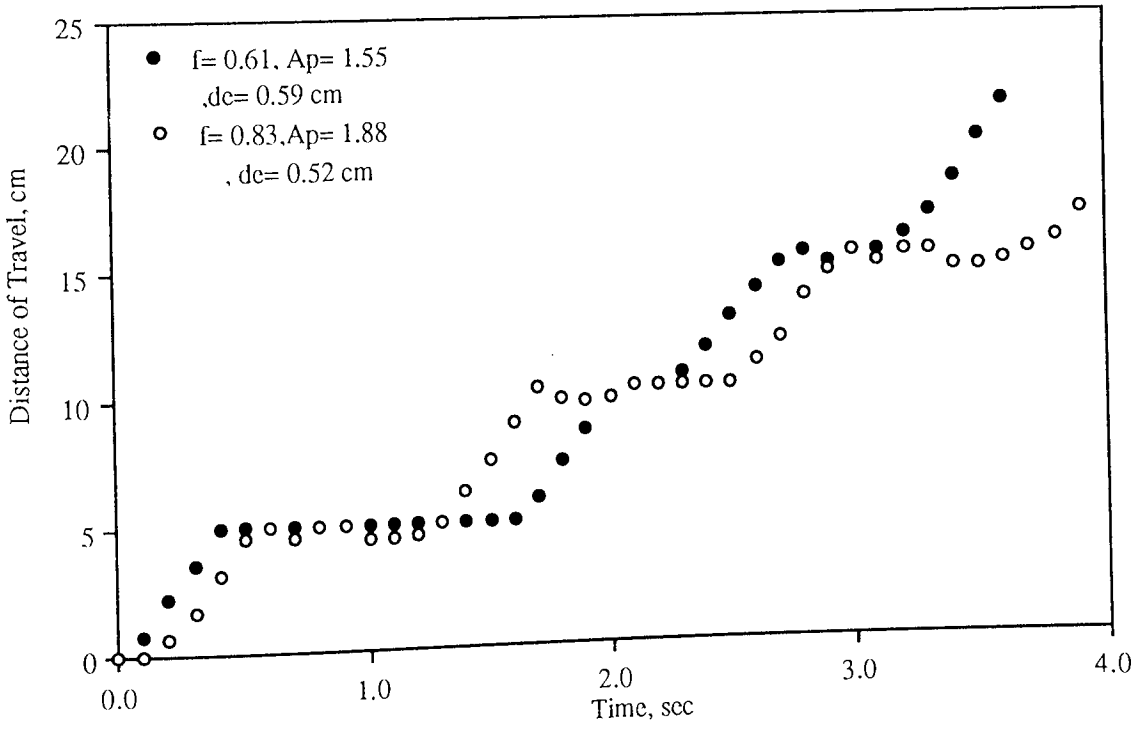

Figure 7.24 Effect of Sieve-Plate on Droplet Movement for, h_c = 5.0 cm & d_h = 0.6 cm

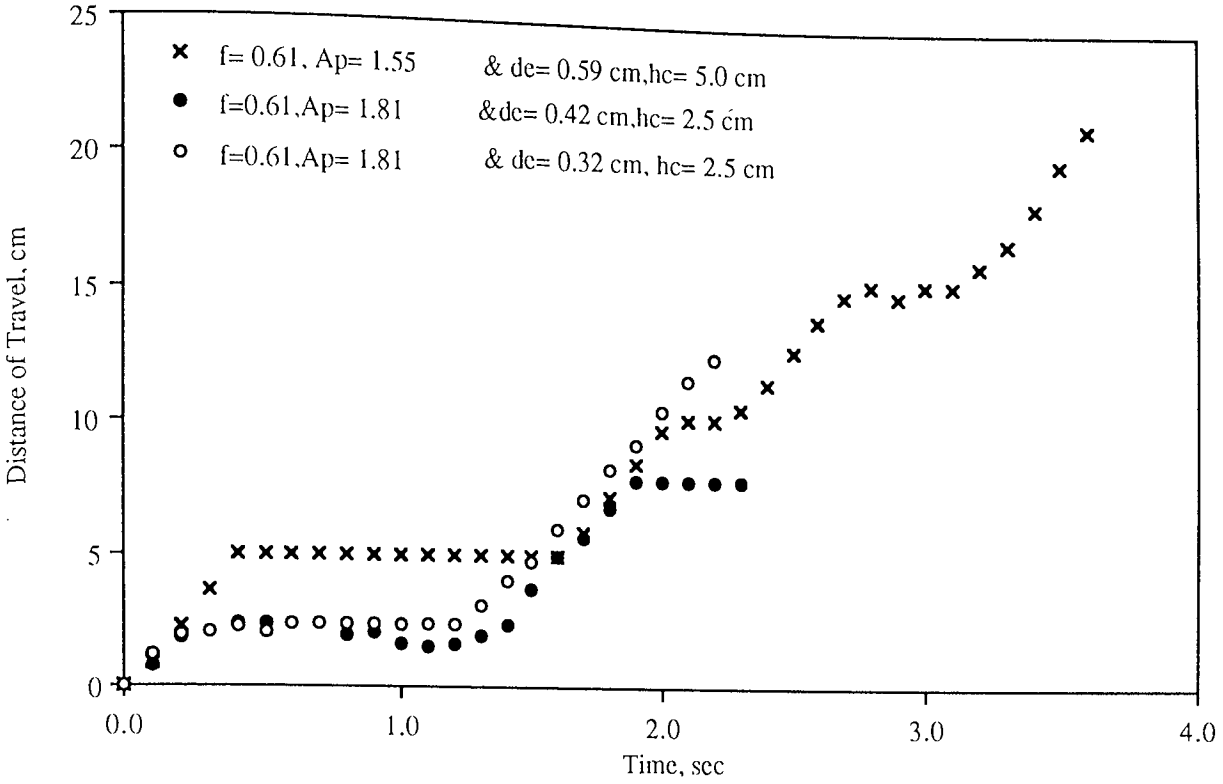

Figure 7.25 Effect of Sieve-Plate on Droplet Movement for, $d_h = 0.4$ cm

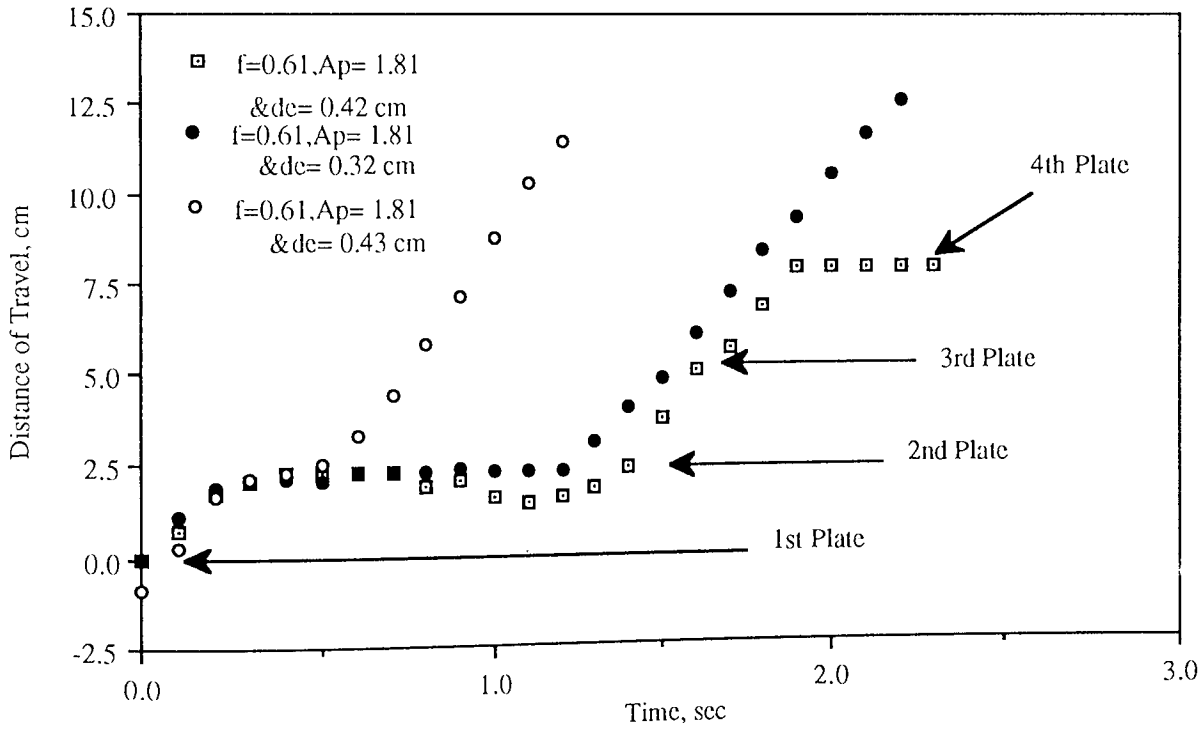

Figure 7.26 Effect of Sieve-Plate on Droplet Movement for, $h_c = 2.5$ cm & $d_h = 0.4$ cm

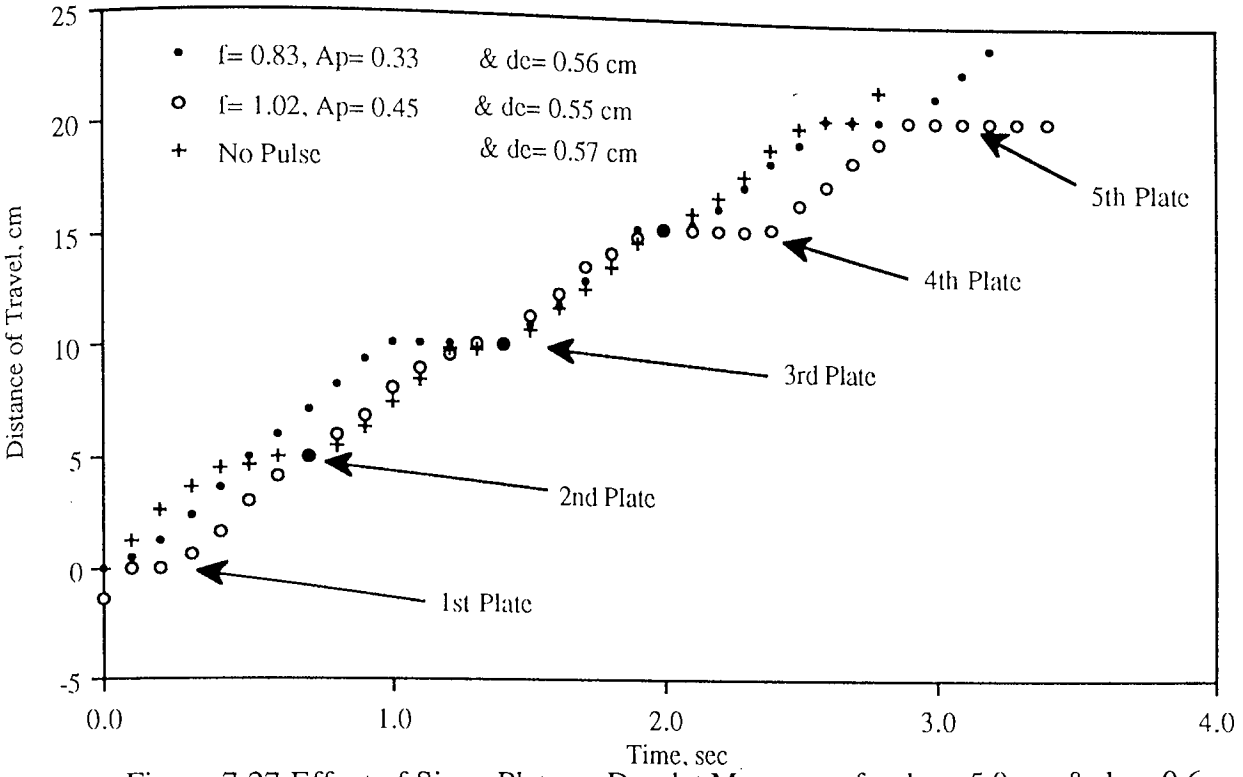

Figure 7.27 Effect of Sieve-Plate on Droplet Movement for, h_c = 5.0 cm & d_h = 0.6 cm

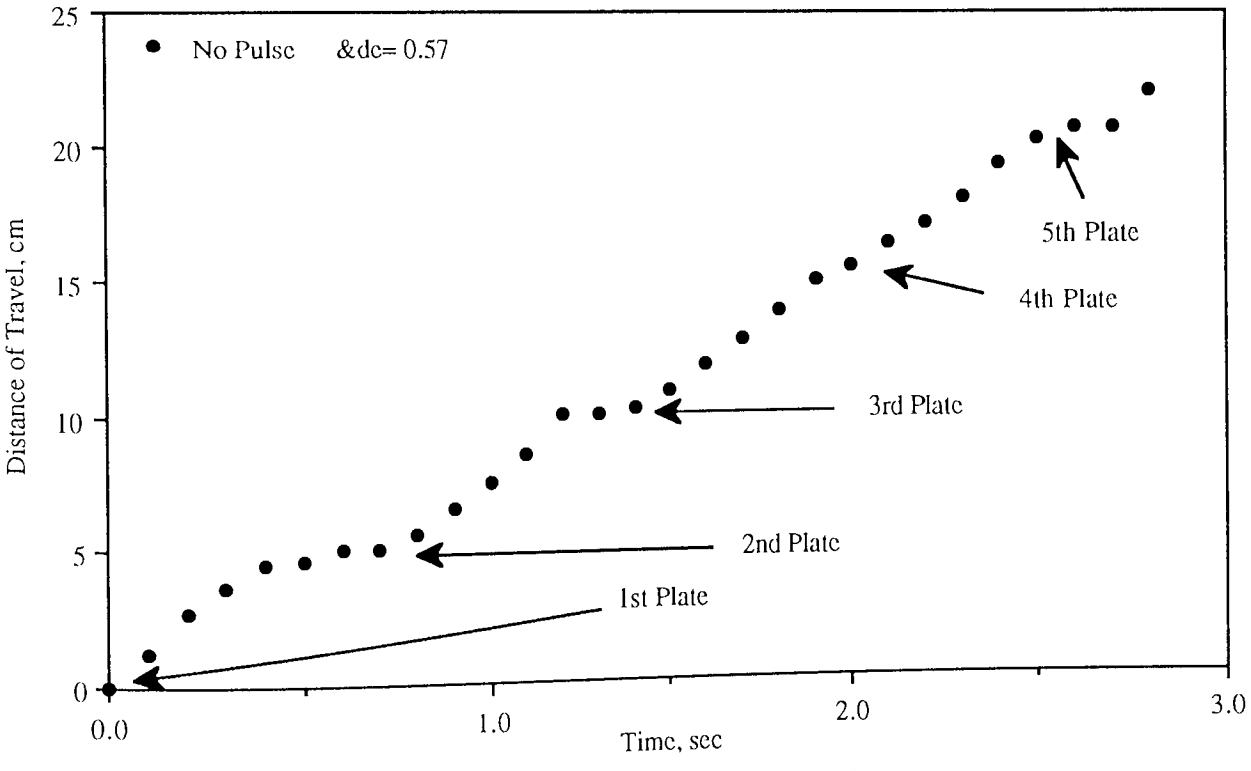

Figure 7.28 Effect of Sieve-Plate on Droplet Movement for, h_c = 5.0 cm & d_h = 0.6 cm

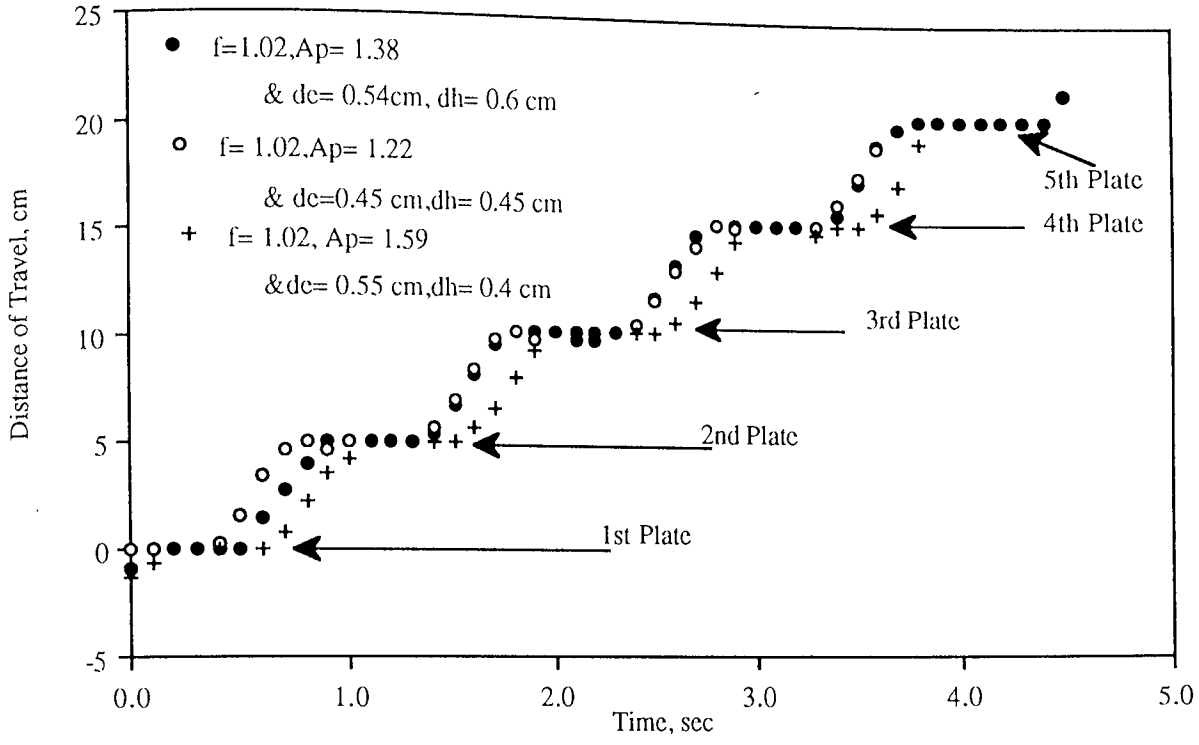

Figure 7.29 Effect of Sieve-Plate on Droplet Movement for, h_c = 5.0 cm

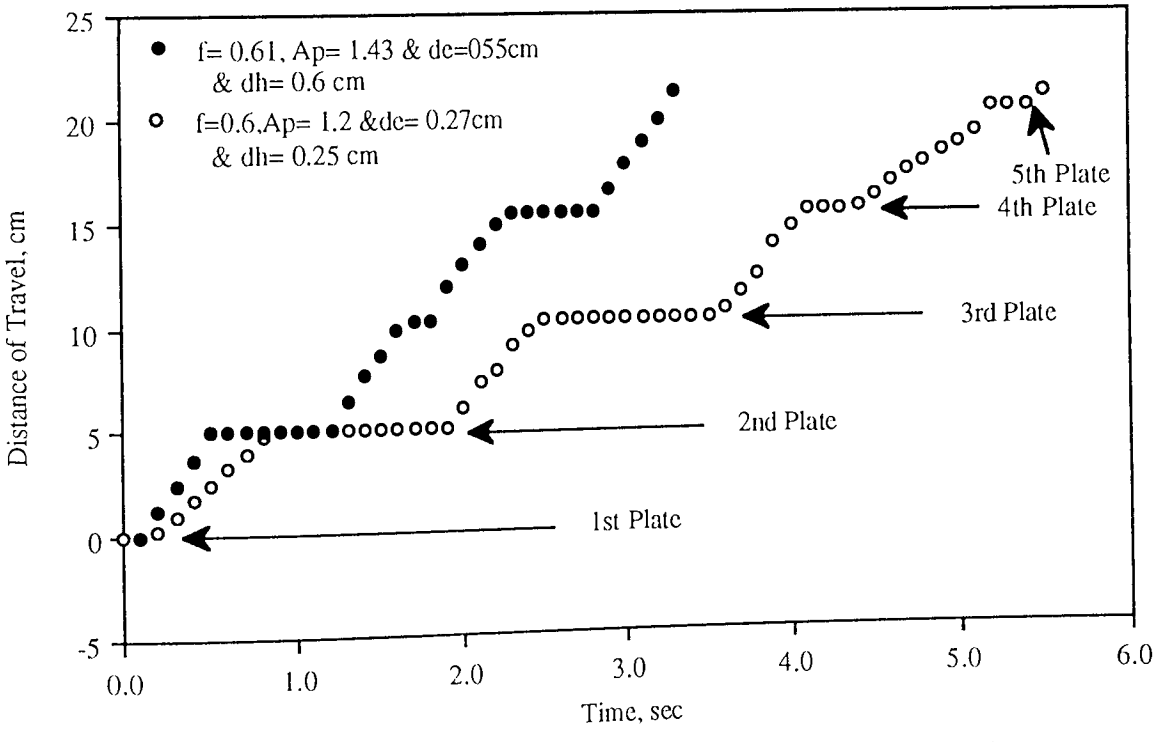

Figure 7.30 Effect of Sieve-Plate on Droplet Movement for, h_c = 5.0 cm

after some modification. The modified correlation is as follows:-

$$d_{32} = 1.592 \left(\frac{\sigma}{\Delta \rho g} \right)^{0.5} \left(\frac{2 g d_h}{\left(\frac{A_p f}{\phi} \right)^2} \right)^{0.0665} \qquad 7.1$$

Kumar and Hartland (95) proposed another correlation for droplet formation resulting from jet breakup. This correlation is modified for the pulsed sieve-plate column as follows :-

$$d_{32} = 1.591 \left(\frac{\sigma}{\Delta \rho g d_h^2} \right)^{0.278} \left(\frac{\sigma}{\Delta \rho d_\eta \left(\frac{A_p f}{\phi} \right)^2} \right)^{0.068} d_h \qquad 7.2$$

Kumar and Hartland (95) proposed a correlation for non-jetting droplet formation in spray columns. By modifying this correlation, for the pulsed sieve plate column, we get the following correlation :-

$$d_{32} = 1.546 \left(\frac{\sigma}{\Delta \rho g d_h^2} \right)^{0.214} \left(\frac{\sigma}{\Delta \rho d_h \left(\frac{A_p f}{\phi} \right)^2} \right)^{0.021} d_h \qquad 7.3$$

Figures 7.31 & 7.32 show a comparison between the theoretical data based on the first droplet breakup mechanism and the experimental data.

7.1.3.2 Isotropic Turbulence Breakup Mechanism

The isotropic turbulence theory was introduced by Kolmogoroff (82, 83); it illustrates droplet formation in a turbulent field. As is discussed in Chapter 3, most of the correlations which are suggested to calculate droplet diameter in a pulsed sieve plate column are based on this theory. Figures 7 .33 & 7.34 & 7.35 show a comparison between experimental and theoretical data from equations 3.20-3.31. The usage of the isotropic turbulence theory is discussed in more detail in section 7.1.4.

7.1.3.3 Impact Breakup Mechanism

Thornton (163) explained the observed change in droplet diameter in a packed column by introducing an impact-break up mechanism. He (163) studied the impact of single droplets travelling at their terminal velocity on a fixed baffle representing the packing elements. It was found that for each system there is a critical droplet diameter below which impact-break up does not occur. Assuming thermal effects to be negligible, in an energy balance before and after impact with the packing element the following equation was derived by which the critical droplet diameter could be calculated.

$$1.79\, d_{crit}^2\, \Delta\rho\, g + d_{crit}\, V_t^2\, \rho_d = 3.12\, \sigma \qquad 7.4$$

where V_t is the terminal velocity of the droplet on impact with the baffle.

From the experimental observations in the present study, it was found that the breakup of a droplet occurred when it hit the rim of the orifice in the sieve plate. Thus droplet breakup in a pulsed sieve-plate column may be explained by the impact-break up mechanism proposed by Thornton (163).

Equation 7.4 is modified for pulsed sieve- plate column conditions. Let us consider that, in a pulsed sieve-plate column, for any droplet diameter there is a critical velocity at which the droplet will breakup when it hits the rim of the orifice. Equation 7.4 can be rearranged and modified to give the following equation:-

$$V_{crit} = \sqrt{3.12 \frac{\sigma}{d'_{crit}\,\rho_d} - 1.79 \frac{d'_{crit}\, g\, \Delta\rho}{\rho_d}} \qquad 7.5$$

where:-

V_{crit} is the droplet critical velocity under pulsed conditions, below which the impact-breakup of the droplet for the critical droplet diameter (d'_{crit}) does not occur.

For a pulsed sieve plate column, let

$$V_{crit} = V_t + \frac{(A_p * f)_{crit}}{\phi} \qquad 7.6$$

where:-

V_t is the terminal velocity of the droplet.

and

$(A_p * f)_{crit}$ is the critical pulse intensity below which droplet impact-breakup does not occur.

The terminal velocity data is measured experimentally, or it can be calculated using equations 2.11- 2.15. The critical pulse intensity for each droplet can be calculated using equations 7.5 and 7.6.

Figure 7.36 shows the relationship between the critical pulse intensity $(Apf)_{crit}$ and the critical diameter of the droplet (d_{crit}). Figure 7.36 exhibits four regions as follows:-

Region I The droplet breaks up because its diameter is greater than the critical diameter (d_{crit}) and the pulse intensity is greater than critical pulsing intensity.

Region II The droplet breaks up because the pulse intensity is greater than the critical pulsing intensity .

Region III The droplet does not breakup as its diameter is below the droplet critical diameter and the pulse intensity is less than the critical pulsing intensity.

Region IV The droplet does not breakup as the pulse intensity is less than the critical pulsing intensity.

The negative value of pulsing intensity in Figure 7.36 represents the down-stroke in the pulse cycle.

Under non-pulsing conditions the droplet in region II should not breakup whereas droplets in region IV should breakup because the diameter is greater than the critical diameter of the droplet. Figure 7.37 presents the comparison between the experimental data and theoretical data from equations 7.5 &7.6.

Equation 7.5 may be more useful if it is presented as a dimensionless equation. By the rearrangement of equation 7.5, the following equation may be achieved.

$$\frac{d_{crit} V_{crit}^2 \rho_d}{\sigma} + 1.79 \frac{d_{crit}^2 g \Delta\rho}{\sigma} = 3.12 \qquad 7.7$$

The first term on the left hand side of the above equation represents droplet Weber number and the second term on the left hand side represents the Eotvos number. Equation 7.7 may be rewritten as follows:-

$$(We)_{crit} = 3.12 - 1.79 (Eo)_{crit} \qquad 7.8$$

Equation 7.8 is valid only for the following condition.

$$0 \leq Eo \leq 1.743$$

Figure 7.38 presents equation 7.8, which covers two regions, as shown in Figure 7.38, the breakup region and non-breakup region. A comparison between the experimental data and the theoretical data from equation 7.8 is presented in Figures 7.39 & 7.40.

From the experimental observation in the present study, the droplet behaviour in the pulsed sieve plate column differs in a number of respects from the droplet behaviour in the spray column in that the droplet may experience one or more of the following situations:-

1. The droplets may move freely through the hole of the sieve plate without any change in its shape or size.

2. The droplet may be distorted during its passage through the hole and it oscillates with a rotational motion after leaving the hole of the sieve-plate. This phenomenon occurs when the droplet diameter is

equal or greater than the hole diameter of the sieve-plate, and the droplet reaches the sieve-plate at the down stroke of the pulse cycle.

3. The droplet may breakup into two or more smaller droplets as a result of hitting the rim of the hole. The breakup occurs when the droplet reaches the rim of the hole at the up stroke of the pulse.

4. The droplet may be arrested beneath the sieve plate because the interfacial tension forces are more significant than the forces due to the pulsing intensity. The droplet may pass through the hole if the pulsing intensity overcomes the interfacial tension or a sufficiently large head is built-up. The previous mechanisms are represented in Figure 7.41.

7.1.4 Droplet Diameter

As is mentioned in the introduction to this chapter, video recording provides a permanent record of experimental data of the droplet behaviour in the test section. The droplet diameter is one of the most important parameters which this study has been concerned with. In most experiments the measurement of the three axes of each droplet was taken from video recording via a TV screen. The equivalent droplet diameter is calculated as follows:-

Since the shape of the droplet in most of the experiments was of the ellipsoidal "oblate shape", the volume (V_1) of the droplet is calculated as follows :-

$$V_1 = \frac{4}{3}\pi a * b * c \qquad 7.9$$

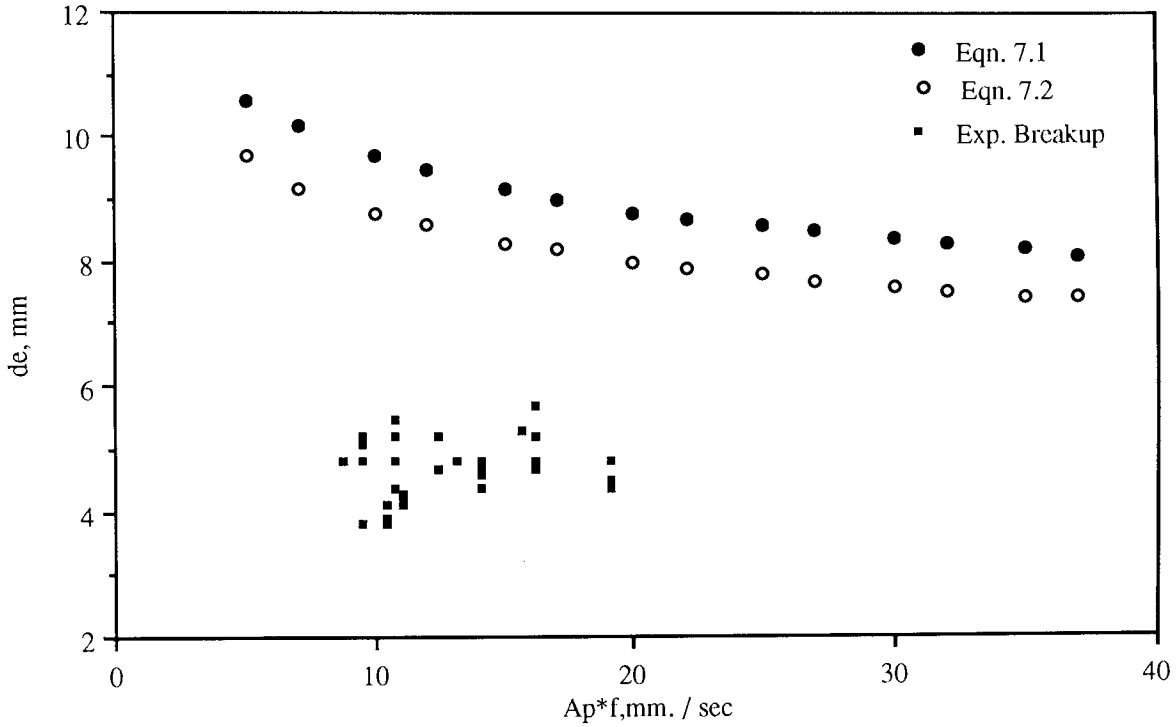

Figure 7.31 Comparison between Experimental Data and Theoretical Data based on Jetting Mechanism

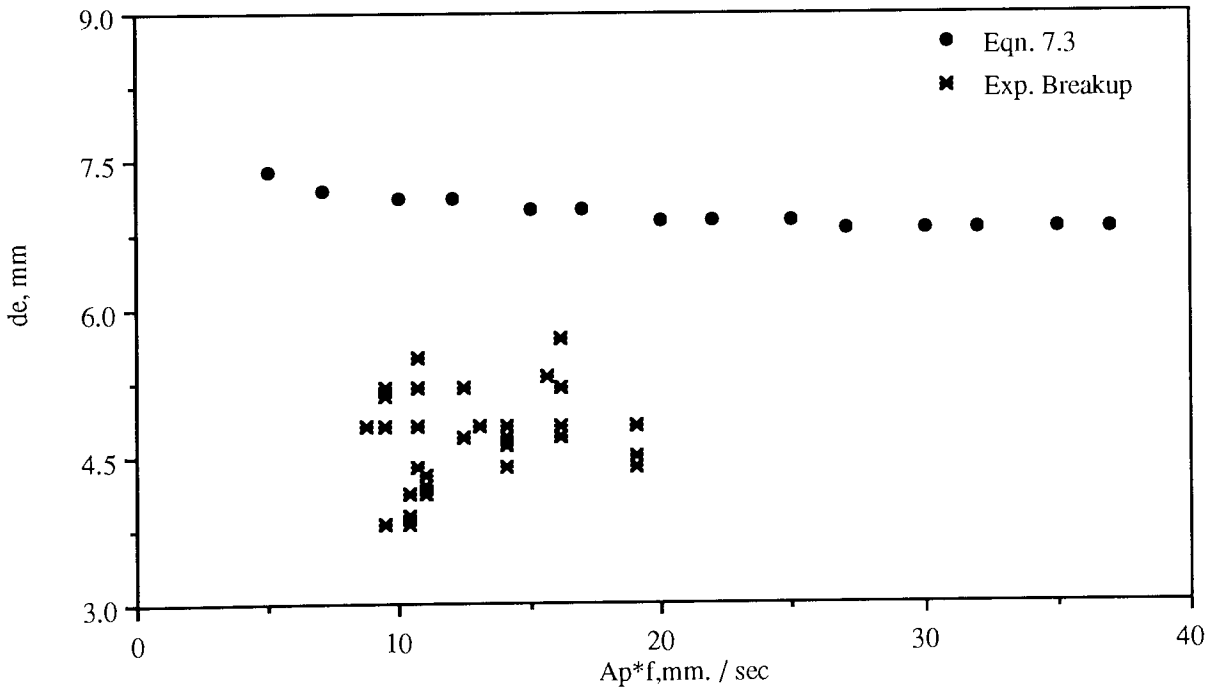

Figure 7.32 Comparison between Experimental Data and Theoretical Data based on Non-Jetting Mechanism

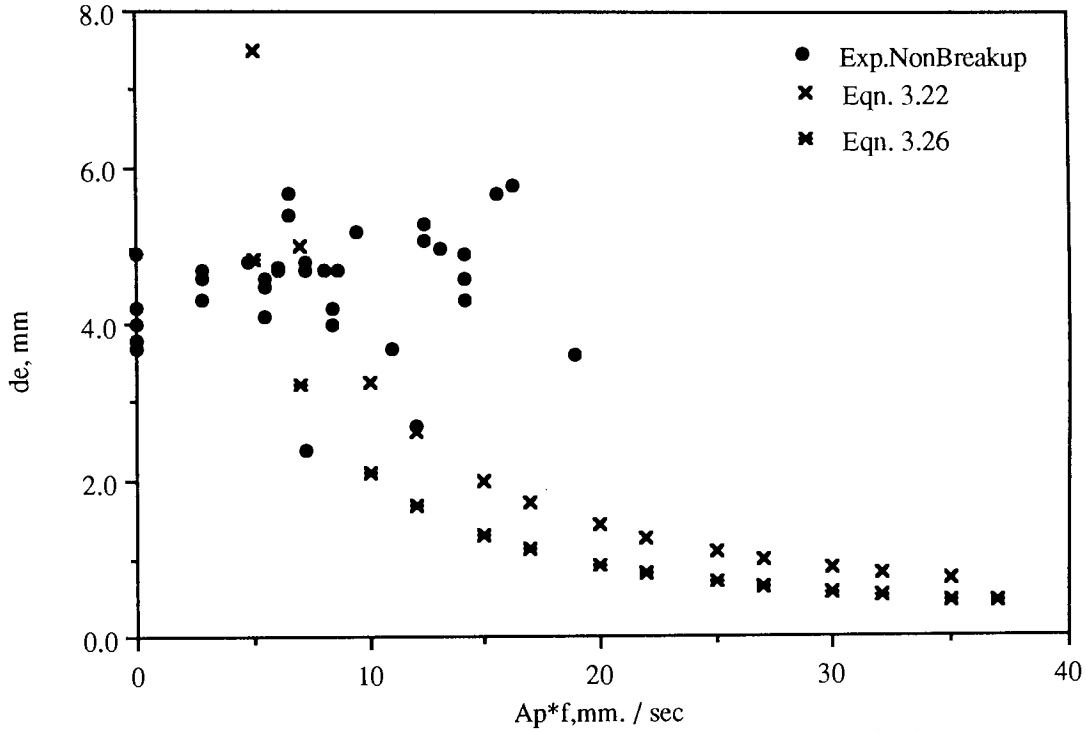

Figure 7.33 Comparison between Experimental & Theoretical Data based on 2nd Mechanism

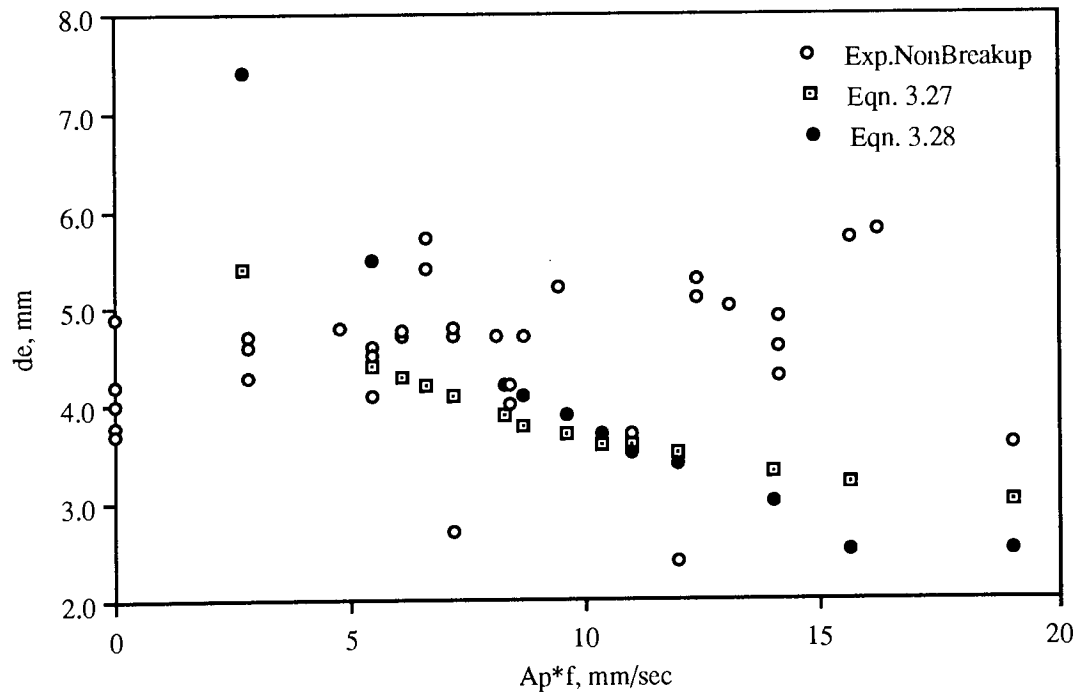

Figure 7.34 Comparison between Experimental & Theoretical Data based on 2nd Mechanism

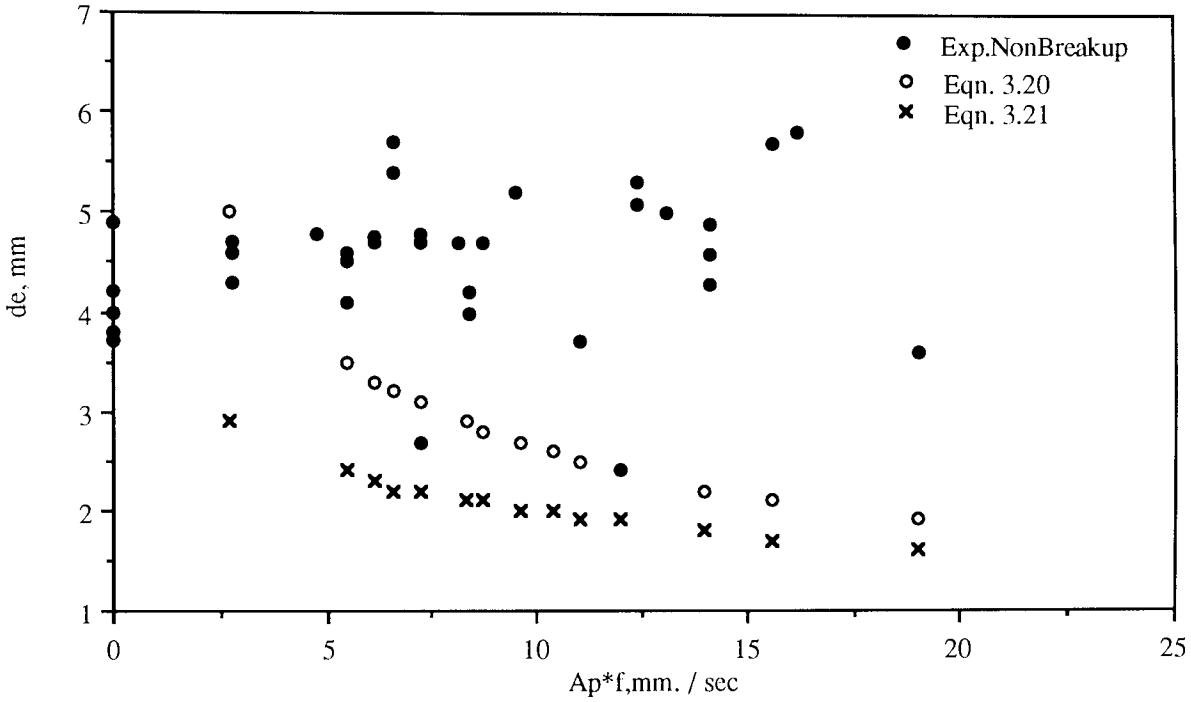

Figure 7.35 Comparison between Experimental & Theoretical Data based on 2nd Mechanism

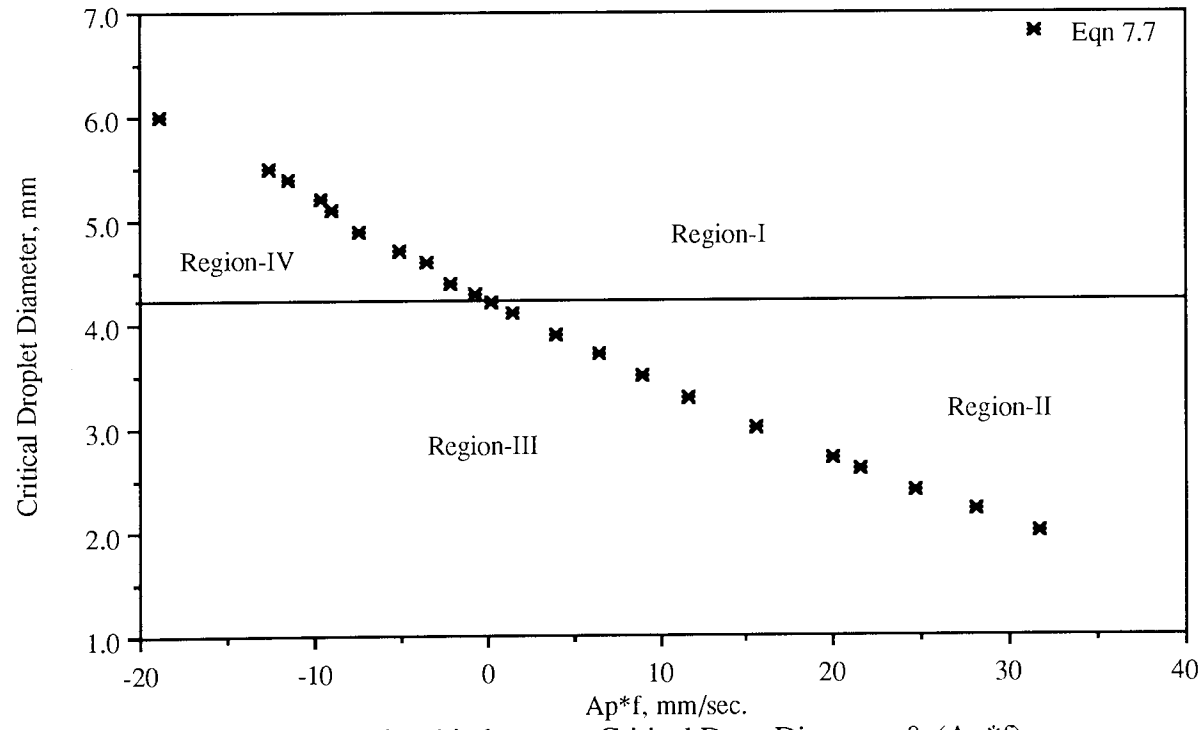

Figure 7.36 Relationship between Critical Drop Diameter & (Ap*f) in Pulsed Sieve Plate Column

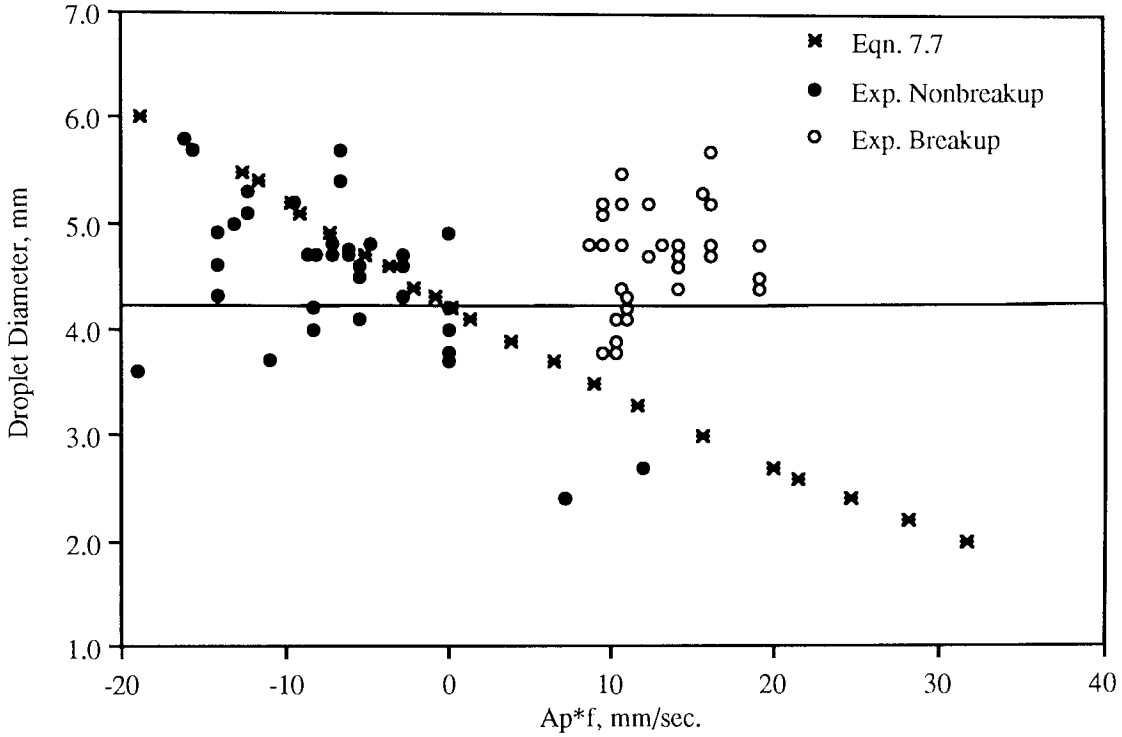

Figure 7.37 Comparison between Predicted & Experimental Data based on 3rd Mechanism

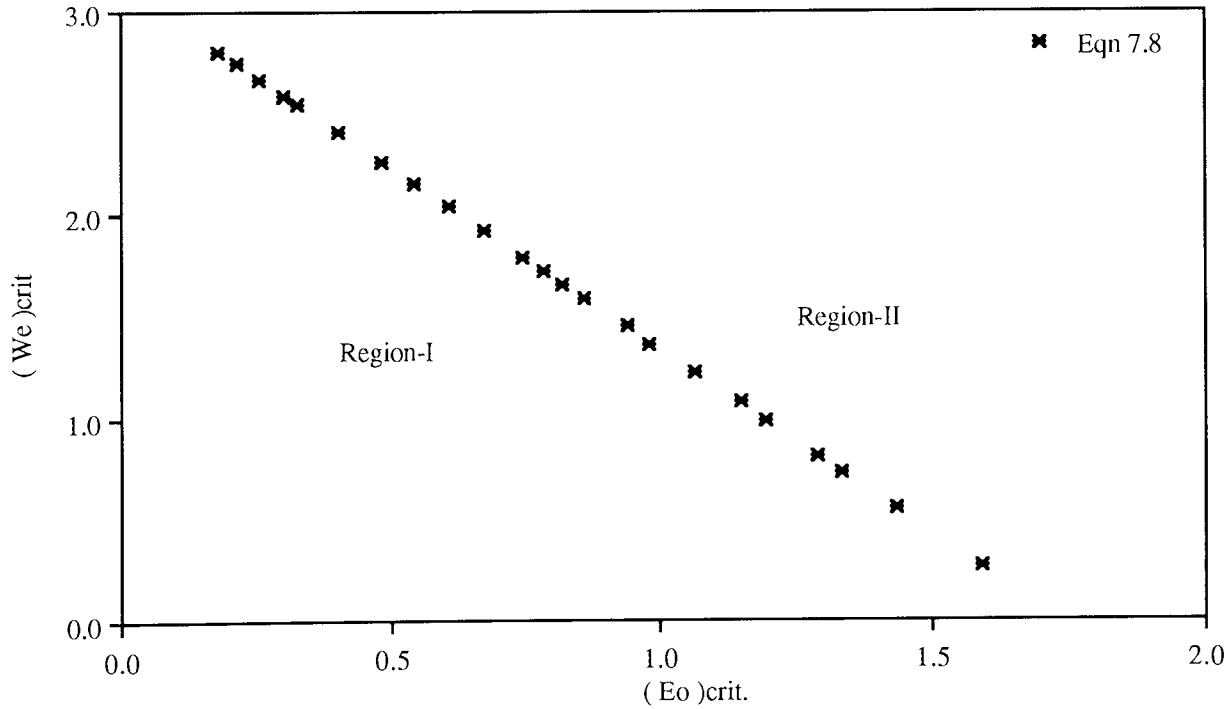

Figure 7.38 Relationship between (We)crit & (Eo)crit in Pulsed Sieve Plate Column

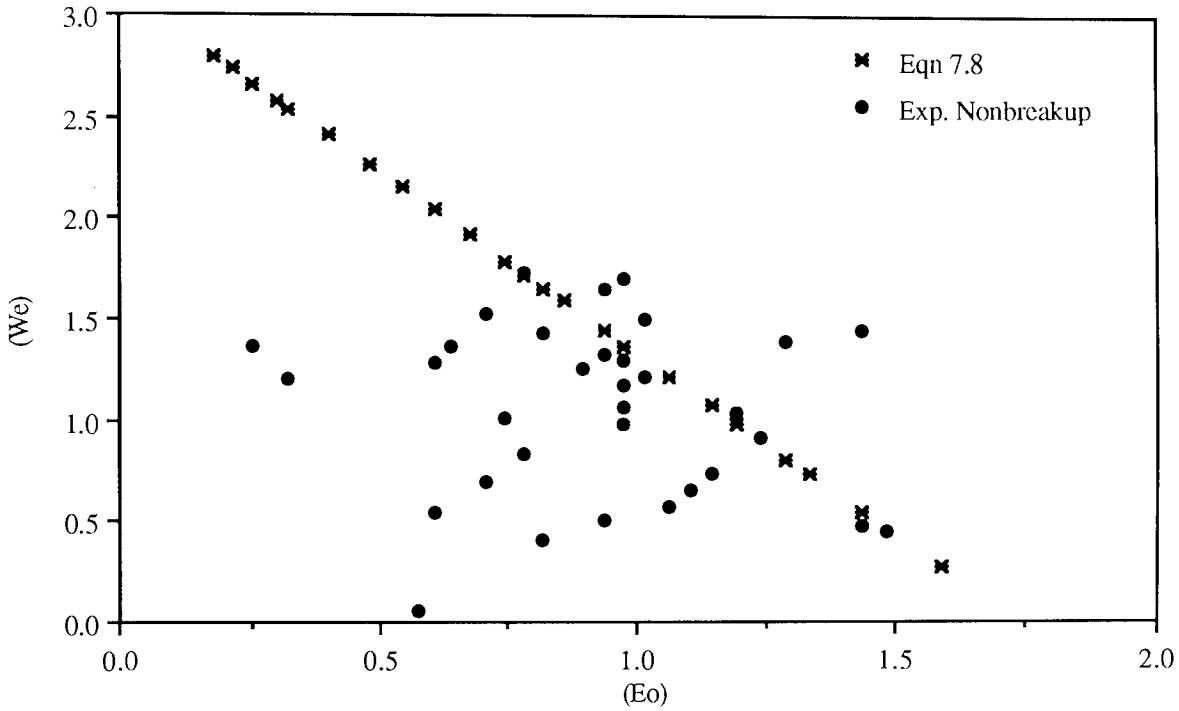

Figure 7.39 Comparison between Predicted Data and Experimental Non-Breakup Data

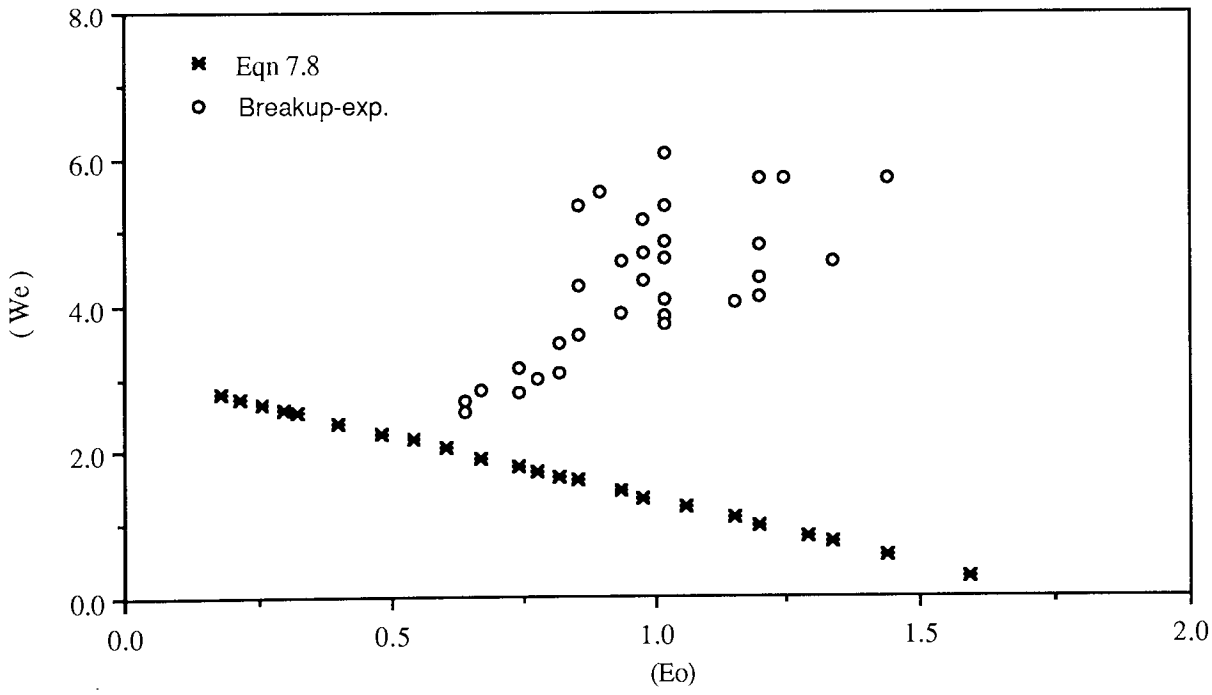

Figure 7.40 Comparison between Predicted Data and Experimental Breakup Data

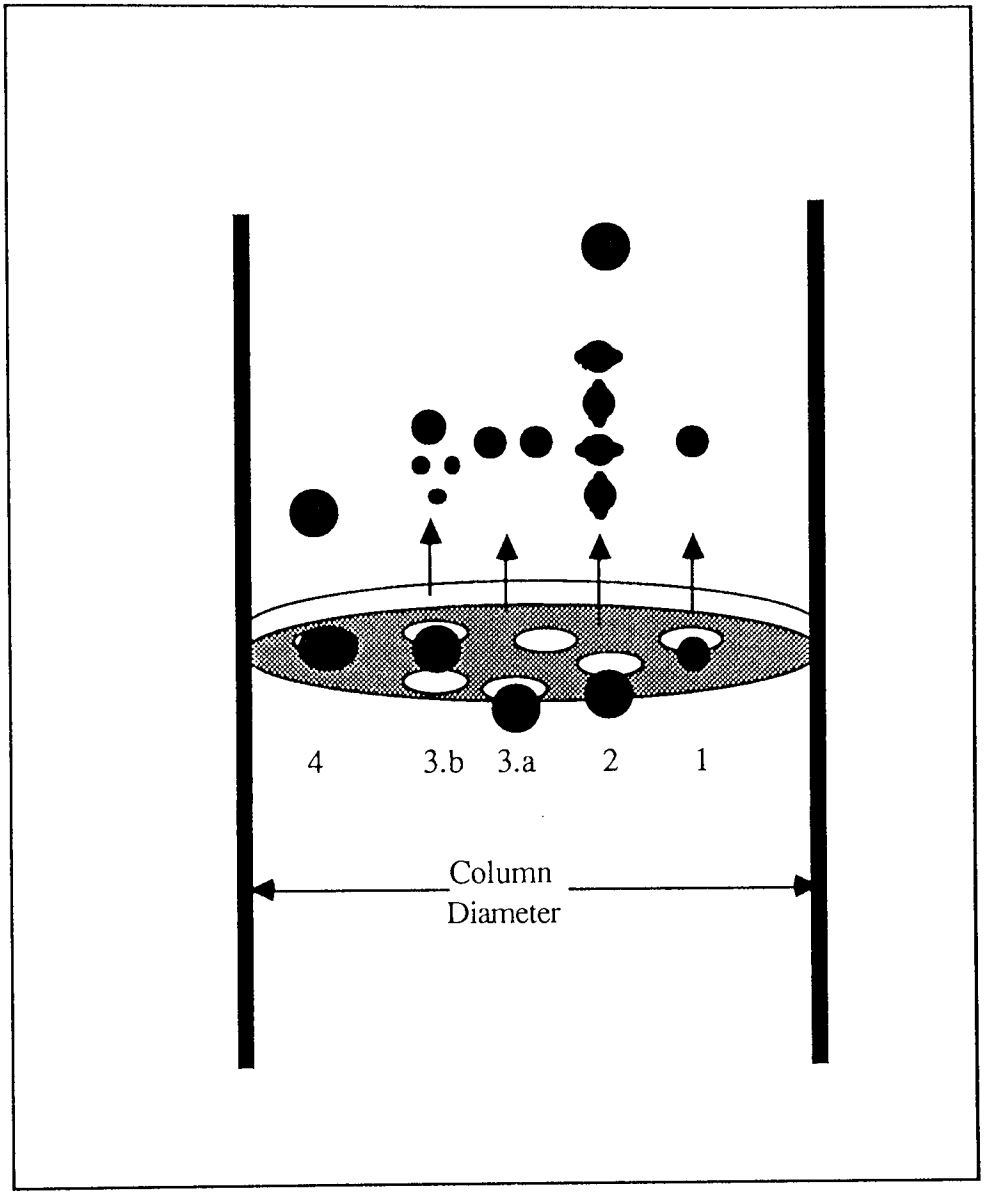

Figure 7.41 Droplet Situations in Pulsed Sieve Plate Column

where a, b, and c are the semi-axes of the droplet in x, y, and z direction respectively. The volume of spherical droplet (V_2) is as follows :-

$$V_2 = \frac{4}{3} \pi r^3 \qquad 7.10$$

By equating the two volumes; V_1 & V_2 one can get

$$r = \sqrt[3]{a * b * c} \qquad 7.11$$

or

$$d_e = \sqrt[3]{8 * a * b * c} \qquad 7.11\ a$$

Some of the droplet diameter data is presented in Table 7.1. Comparison between the experimental data and the theoretical data obtained using equations 3.21-3.30 are presented in Figures 7.33-7.35.

As is mentioned in Chapter 3, most of the equations for the calculation of the droplet diameter in mechanically agitated columns are based on the energy dissipation concept. Unfortunately there was no agreement about a general formula for energy dissipation. In this study an effort has been made to introduce a new correlation for energy dissipation.

Determination of the rate of energy dissipation in a pulsed sieve plate column is made using mass and mechanical energy balances at a single sieve plate. Assuming that the density of the continuous phase is constant and there is no change in the cross sectional area of the column "S" before and after the sieve plate.

Mass balance

$$V_1 \rho_c S = V_2 \rho_c S \qquad 7.12$$

and

$$V_1 = V_2 = V_p \qquad 7.13$$

For constant density and no potentional energy change the *mechanical energy balance* may be presented as follows :-

$$\frac{1}{2}\left\{ V_2^2 - V_1^2 \right\} + \frac{1}{\rho_c}\left\{ P_2 - P_1 \right\} + E_v = 0 \qquad 7.14$$

where "E_v" is the friction loss

since; $V_1 = V_2 = V_p$ " equation 7.13 "

Therefore;

$$\frac{1}{2}\left\{ V_2^2 - V_1^2 \right\} = 0 \qquad 7.15$$

and

$$E_v = \frac{1}{2}\, e_v\, V_p^2 \qquad 7.16$$

where e_v is the friction loss factor.

For turbulent flow through an orifice with a sharp edge the friction loss factor (15) is as follows:-

$$e_v = 2.7\, \frac{\left(1 - \phi\right)\left(1 - \phi^2\right)}{\phi^2} \qquad 7.17$$

From equations 7.15, 7.16 , and 7.17 , one can get the following equation

$$\frac{1}{2}\ 2.7\ V_p^2\ \frac{(1-\phi)(1-\phi^2)}{\phi^2}+\frac{1}{\rho_c}\{P_2-P_1\}=0 \qquad 7.18$$

By rearrangement of equation 7.18, we get the following equation.

$$\Delta P=\frac{1}{2}\frac{2.7\ V_p^2\rho_c}{\phi^2}(1-\phi)(1-\phi^2) \qquad 7.19$$

For practical use , the above equation is divided by (C_o^2) and becomes:-

$$\Delta P=\frac{1}{2}\frac{2.7\ V_p^2\rho_c}{\phi^2\ C_o^2}(1-\phi)(1-\phi^2) \qquad 7.20$$

Equation 7.20 is valid only for one sieve plate, so for a number of plates "N" with cross sectional area "S" , the rate of dissipation is given by the following equation;

$$=\left\{\frac{1}{2}\frac{2.7\ V_p^2\rho_c}{\phi^2\ C_o^2}(1-\phi)(1-\phi^2)\right\}N\ S\ V_p \qquad 7.21$$

Hence for the energy dissipation per unit mass of fluid in a column with "H" height, the above equation is divided by " $\rho_c H\ S$ " and becomes:-

$$\psi=\left\{\frac{2.7}{2\phi^2\ C_o^2}(1-\phi)(1-\phi^2)\right\}\frac{N}{H}V_p^3 \qquad 7.22$$

For a pulsed column, $V_p = f\ A_p$

and since $h_c=\frac{H}{N}$,equation 7.22 becomes;

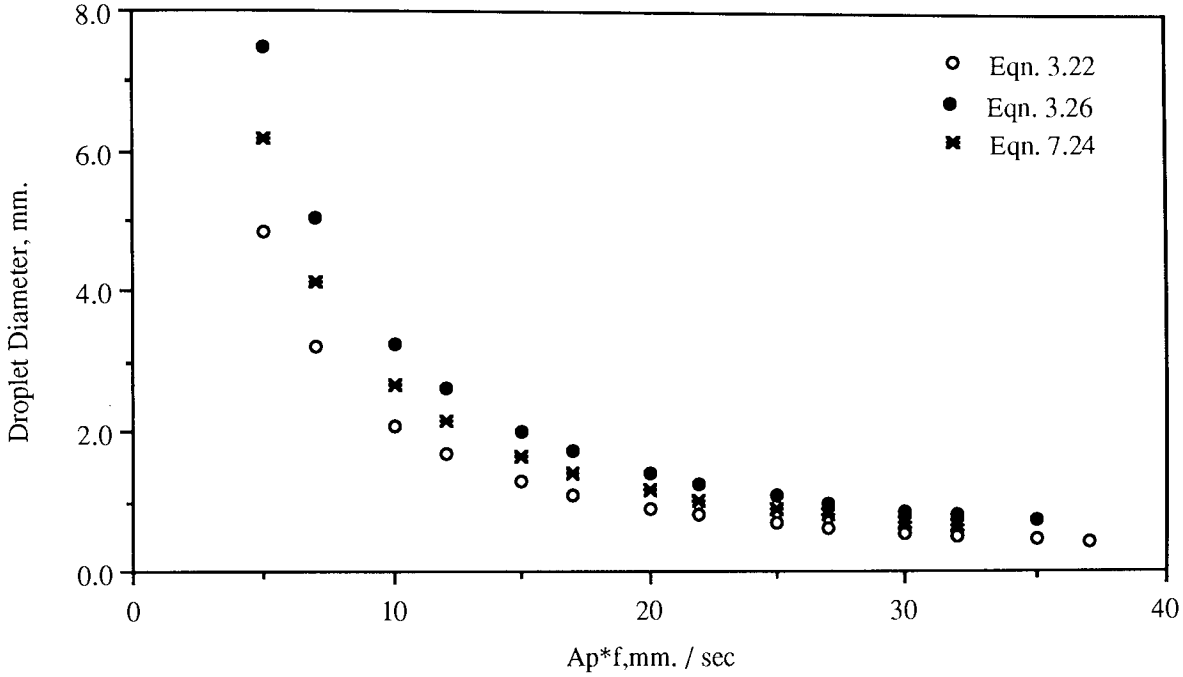

Figure 7.42 Comparison between Equations for Prediction of Droplet Diameter in Pulsed Sieve Plate Column

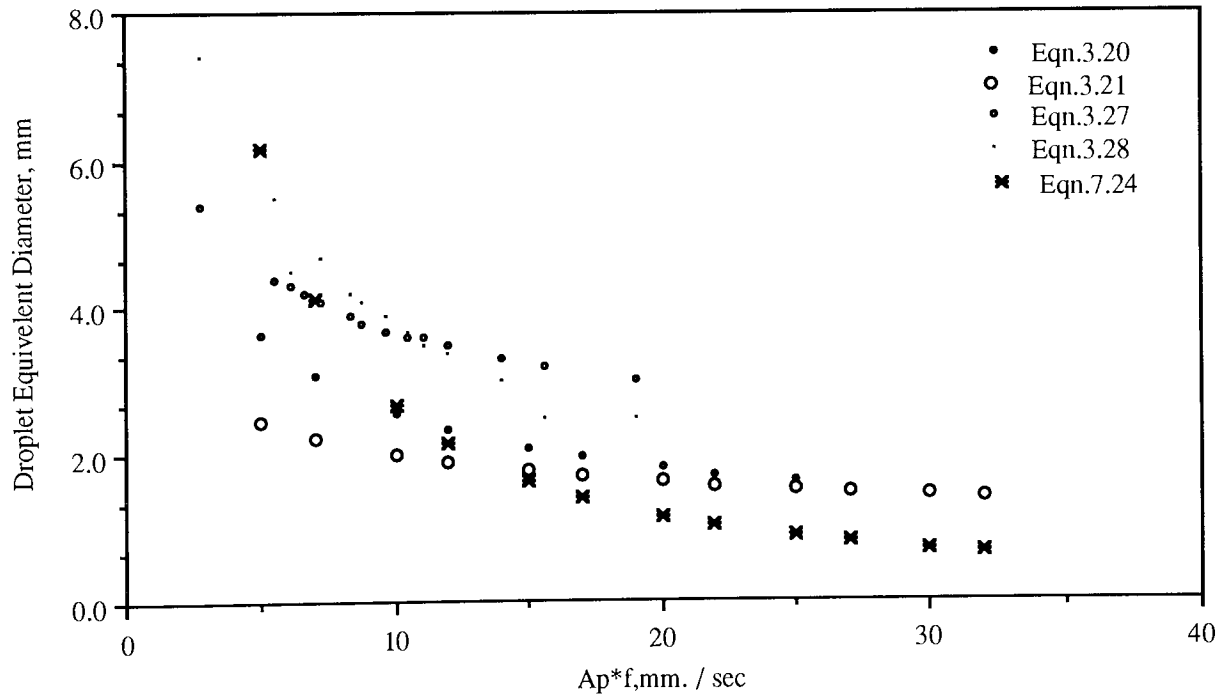

Figure 7.43 Comparison between Equations for Prediction of Droplet Diameter in Pulsed Sieve Plate Column

Table 7.2 Predicted Droplet Diameter under Pulsing Conditions

Ap * f mm/sec	Predicted Droplet Diameter, mm					
	Eq.3.20	Eq-3.21	Eq-3.22	Eq-7.1	Eq-7.2	Eq-7.3
5.0	3.64	2.46	7.50	10.60	9.70	7.40
7.0	3.08	2.22	5.03	10.20	9.20	7.20
10.0	2.57	2.00	3.28	9.70	8.80	7.10
12.0	2.35	1.89	6.63	9.50	8.60	7.10
15.0	2.10	1.77	2.00	9.20	8.30	7.00
17.0	1.97	1.70	1.73	9.00	8.20	7.00
20.0	1.82	1.62	1.43	8.80	8.00	6.90
22.0	1.73	1.58	1.27	8.70	7.90	6.90
25.0	1.63	1.52	1.10	8.60	7.80	6.80
27.0	—	1.48	0.99	8.50	7,70	6.80
30.0	1.49	1.44	0.88	8.40	7.60	6.80
32.0	1.44	1.41	0.81	8.30	7.50	6.80
35.0	—	—	0.73	8.20	7.40	6.80
37.0	—	—	—	8.11	7.40	6.80

$$\psi = \left\{ \frac{2.7}{2\phi^2 C_o^2 h_c} \left(1-\phi\right)\left(1-\phi^2\right) \right\} \left(A_p * f\right)^3 \qquad 7.23$$

The above equation is considered a new correlation for calculating the energy dissipation in a pulsed sieve plate column.

From equation 3.1 and equation 7.23, a new correlation to calculate the droplet diameter in a turbulent field can be achieved as follows: -

$$d_{32} = K_8 \left(\frac{\sigma}{\rho_c}\right)^{0.6} \psi^{-0.4} \qquad 7.24$$

where ψ is defined in equation 7.23, and K_8 is a constant and equal to $9.03 * 10^{-2}$

Comparison between equation 7.21 and the other correlations proposed to calculate droplet diameter under similar circumstances is presented in Figures 7.42 & 7.43; some of the results are listed in Table 7.2.

7.2 Mass Transfer Rate Calculation

Part of this study was to evaluate experimentally the rate of mass transfer from a single droplet moving through a column under three different operating conditions. These operating conditions were; spray column, pulsed spray column, and pulsed sieve plate column conditions. In this section the mass transfer results are treated and the effect of pulsing and the presence of a sieve plate on the mass transfer rate is evaluated.

The application of the different empirical correlations and equations, mentioned in Chapter 4, for prediction of overall mass transfer coefficients for a range of droplet

sizes studied experimentally, are presented in this section.

The mass transfer rate and the overall mass transfer coefficient from the droplet during:-

a. Droplet formation period.

b. Droplet ascent period.

were calculated by determining the acetone concentration in the droplets after detachment, or after detachment and travel through the continuous phase for a given distance countercurrent to the continuous phase.

7.2.1 Mass Transfer During Droplet Formation.

The overall mass transfer coefficient during droplet formation was determined experimentally, or predicted using the correlations mentioned in Chapter 4 as follows:-

7.2.1.1 Based on Experimental Data.

The mass transfer coefficient of the dispersed phase during droplet formation is calculated from experimental data using equation 1.1

$$N_f = K_{df} A_{mf} (C_1 - C^*) \qquad 1.1$$

where A_{mf} is the average mean area of droplet during formation. Al-Hassan (4) proposed an equation to calculate "A_{mf}" as follows:-

$$A_{mf} = \frac{3}{5} \pi^{\frac{1}{3}} \left\{ 6\, t_t\, f_d \right\}^{\frac{2}{3}} \qquad 7.25$$

Since the volumetric flow rate of the continuous phase was in all cases approximately 45-50 times greater than that of the dispersed phase, the value of the C^* in the above equation was taken as zero. A sample calculation is presented in Appendix C.2. The results of experimental overall dispersed phase mass transfer coefficient during formation period are listed in Tables 7.3 & 7.4.

7.2.1.2 Predictions from Theory

Johnson and Hamielec (79) proposed equation 4.12 to calculate the efficiency of extraction, from which the value of C_2 could be calculated theoretically and by using equation 1.1, the overall mass transfer coefficient of the dispersed phase was calculated.

A sample calculation of these theoretical values of overall mass transfer coefficient during formation is presented in Appendix C.2. Table 7.5 contains the results of predicted data. Figure 7.44 shows a comparison between experimental and theoretical values of the overall mass transfer coefficient of the dispersed phase during droplet formation. Figure 7.45 illustrate the effect of pulsing on the overall mass transfer coefficient during the formation period.

7.2.2 Mass Transfer During Droplet Travel

The overall mass transfer coefficient of the dispersed phase during droplet ascent may be estimated experimentally and theoretically as follows:-

7.2.2.1 Based on Experimental Data

From the fundamental equation the overall mass transfer coefficient during ascent may be estimated.

$$N_t = (K_d)_{exp} A (C_2 - C^*) \qquad 1.1$$

where A is the mean surface area of droplet during ascent. The surface area of non-oscillating oblate droplet ellipsoidal droplet may be estimated using the following equation (192) :-

$$A = \frac{\pi}{2}\left\{ \frac{d_H^2}{4} + \frac{d_V^2}{2E} \ln\left\{ \frac{1+E}{1-E} \right\} \right\} \qquad 7.26$$

The eccentricity " E " is difined as follows:-

$$E = \frac{\sqrt{\frac{d_H^2}{4} - \frac{d_V^2}{4}}}{\frac{d_H}{2}}$$

Table 7.6 shows the experimental overall mass transfer coefficient during the travel period. Figures 7.46, 7.47 & 7.48 illustrate the effect of pulsing and the presence of a sieve plate on the overall mass transfer coefficient.

Experimental work was carried out to ensure that the droplets do not reach the equilibrium state and to see the effect of travelled distance on the dispersed phase mass transfer rate during the travelling period. The results are listed in Table 7.7. The relationship between travelling distance and concentrations and overall mass transfer coefficient of the dispersed phase is shown in Figure 7.49 & 7.50 respectively.

7.2.2.2 Predictions from Theory

In assessing the theoretical overall mass transfer coefficient during ascent, three different situations need to be considered. The droplet may be stagnant, or the

circulation of the solute inside the droplet might be laminar or turbulent, depending upon the Reynolds number and the physical properties of the phases.

For a stagnant droplet, the value of K_d may be evaluated using equation 4.12 proposed by Newman (121). The results are listed in Table 7.8.

For a droplet with laminar circulation, the value of the overall mass transfer coefficient of the dispersed phase (K_d) may be evaluated using equation 4.16 for the range $1.0 < Re < 10.0$. The limiting assumptions are that the time of circulation is small compared with the time of solute transfer or diffusion, that the solute transfer is in a direction perpendicular to the internal stream lines, and that the continuous phase resistance is negligible. The results are listed in Table 7.8.

For a droplet with turbulent circulation of solute inside it, the value of the overall mass transfer coefficient of the dispersed phase (K_d) was evaluated using equation 4.20, where k_c and k_d can be predicted using Higbie's theory and the Handlos correlation respectively. The results are listed in Table 7.8.

Equations 4.10-4.22 and equations 4.31-4.42 were used to evaluate the individual mass transfer coefficients of dispersed phase and continuous phase (k_d & k_c) respectively. The data are substituted in equation 1.2 to predict the overall phase mass transfer coefficient; all the data are presented in Appendix B.2.1. A comparison between the experimental and predicted data for the overall dispersed phase mass transfer coefficient is presented in Figures 7.51 & 7.52.

All the mass transfer experiments were carried out for the $d_e/d_h < 1$ condition only. An effort was made to study the effect of pulsing parameters on mass transfer rate for $d_e/d_h \geq 1$. Unfortunately, because of the reduction in the interfacial and surface

Table 7.3 Experimental Mass Transfer Data of Single Droplets in Pulsed and Non-pulsed Conditions

Run No.	t_f sec	f 1/ sec	A_p cm	$A_p * f$ cm/ sec	$f_d * 10^2$ cm^3 /sec	f_c cm^3/sec
1Po	1.14	-----	-----	------	1.74	2.86
2Po	1.26	0.82	0.87	0.71	1.49	2.86
3Po	1.27	0.82	1.42	1.16	1.35	2.86
4Po	1.26	0.82	0.62	0.51	1.20	2.86
1P	1.05	1.03	0.95	0.98	4.74	2.87
2P	1.33	0.83	1.78	1.48	3.35	3.16
3P	1.01	1.00	1.24	1.24	4.92	4.07
4P	1.00	1.03	0.89	0.92	1.41	2.94
5P	0.98	1.03	1.44	1.48	1.26	2.94
6P	1.19	0.84	1.33	1.72	2.05	—
7P	1.18	0.84	0.87	0.73	2.00	—
8P	1.20	0.84	1.53	1.28	2.37	—
9P	1.18	0.61	1.37	0.83	1.69	—
10P	1.19	0.61	1.94	1.19	1.40	—
11P	1.10	0.61	1.14	0.69	1.75	—

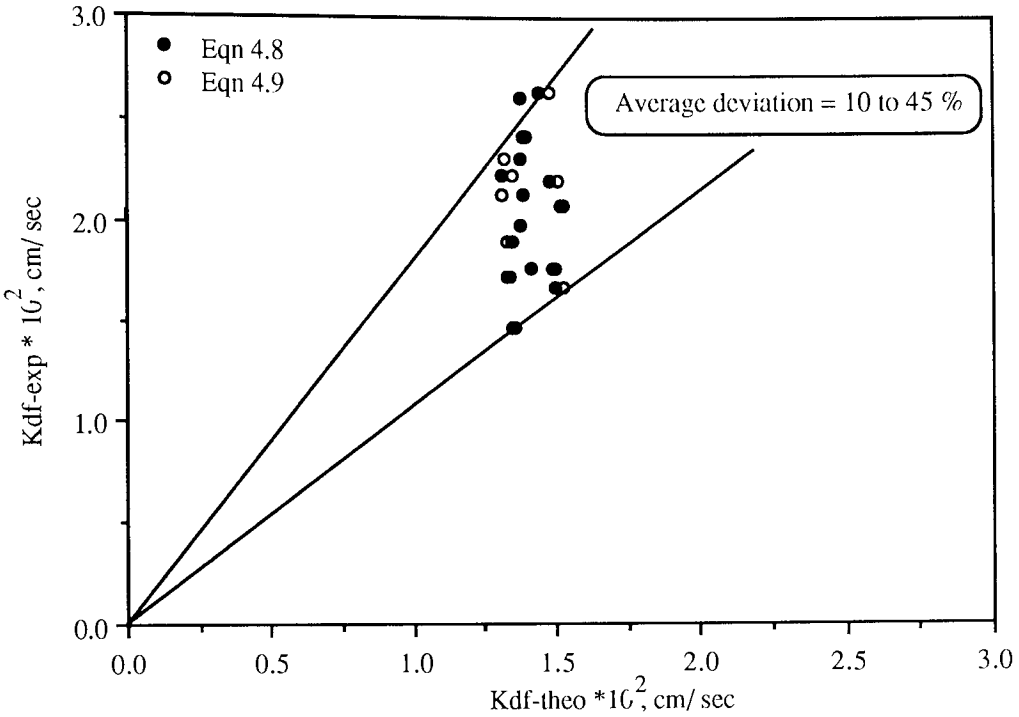

Figure 7.44 Comparison between Experimental & Predicted Overall Mass Transfer Coefficient during Droplet Formation

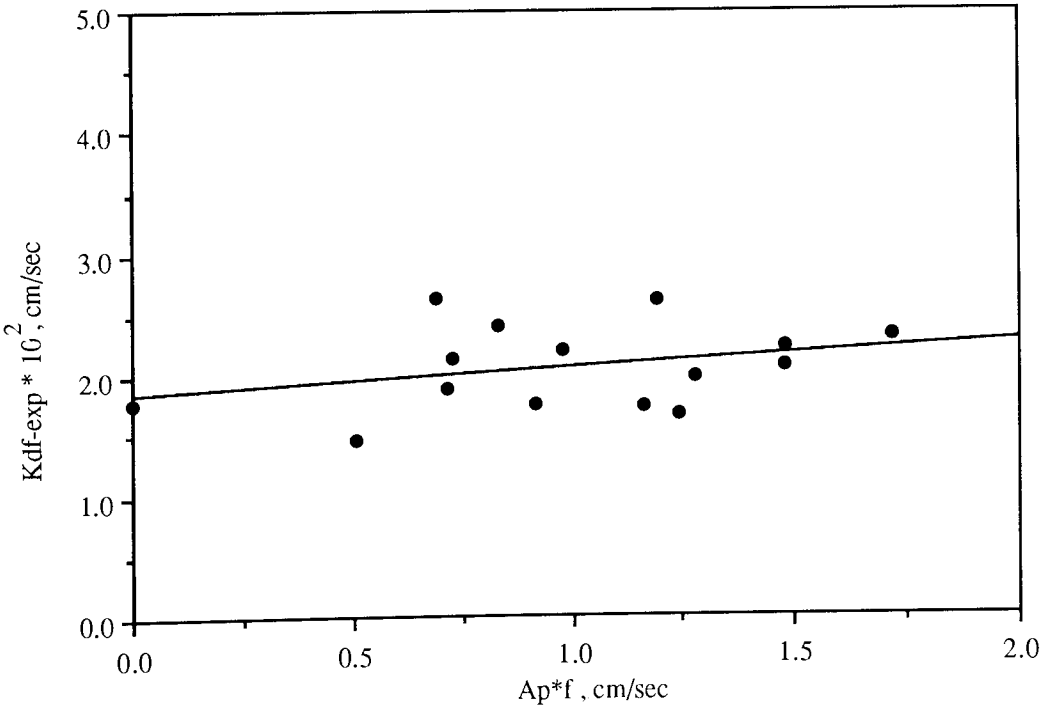

Figure 7.45 Effect of Pulsing on Overall Mass Transfer Coefficient During Droplet Formation

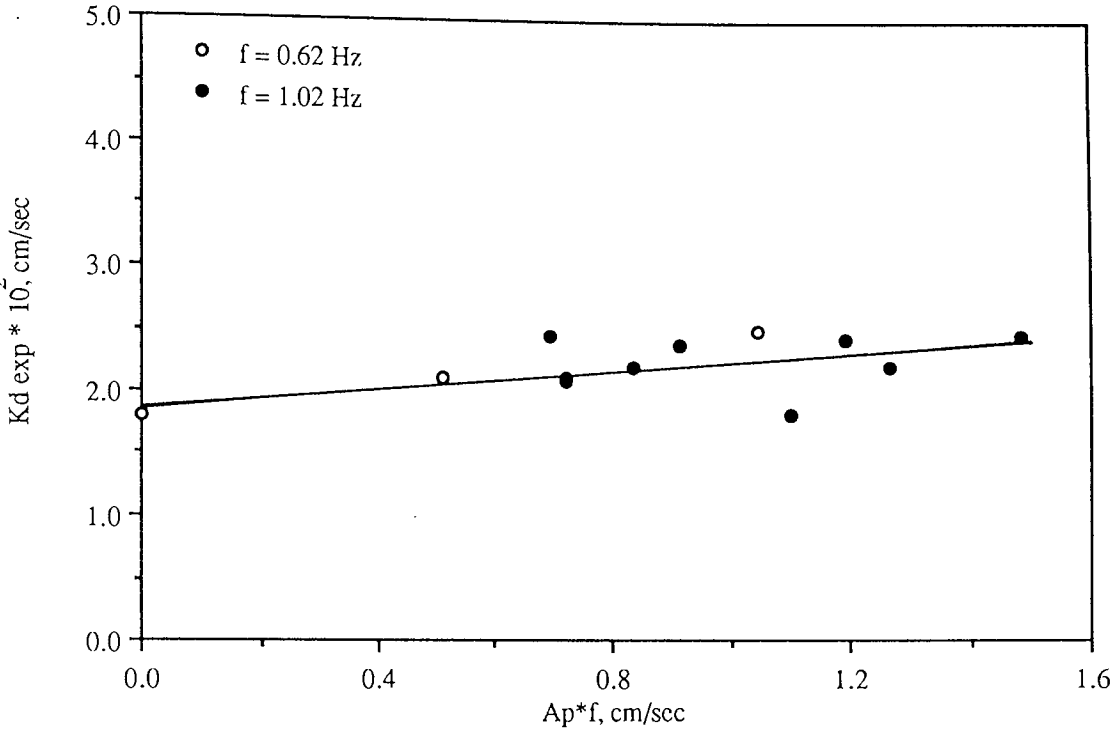

Figure 7.46 Effect of Pulsing on Overall Mass Transfer Coefficient

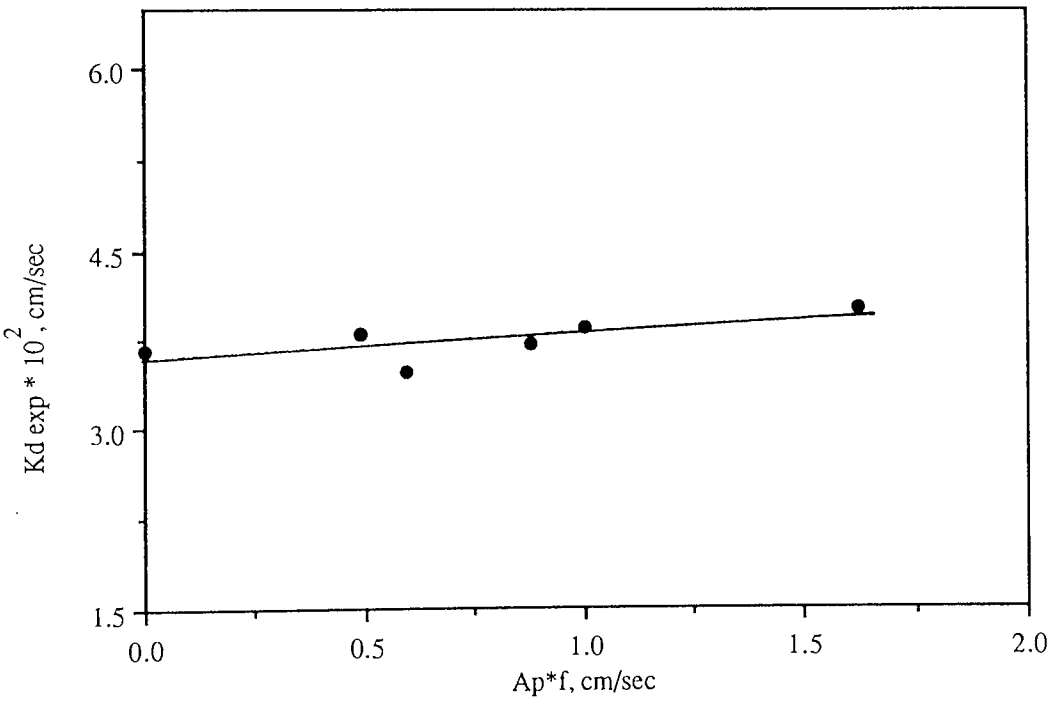

Figure 7.47 Effect of Pulsing on Overall Mass Transfer Coefficient

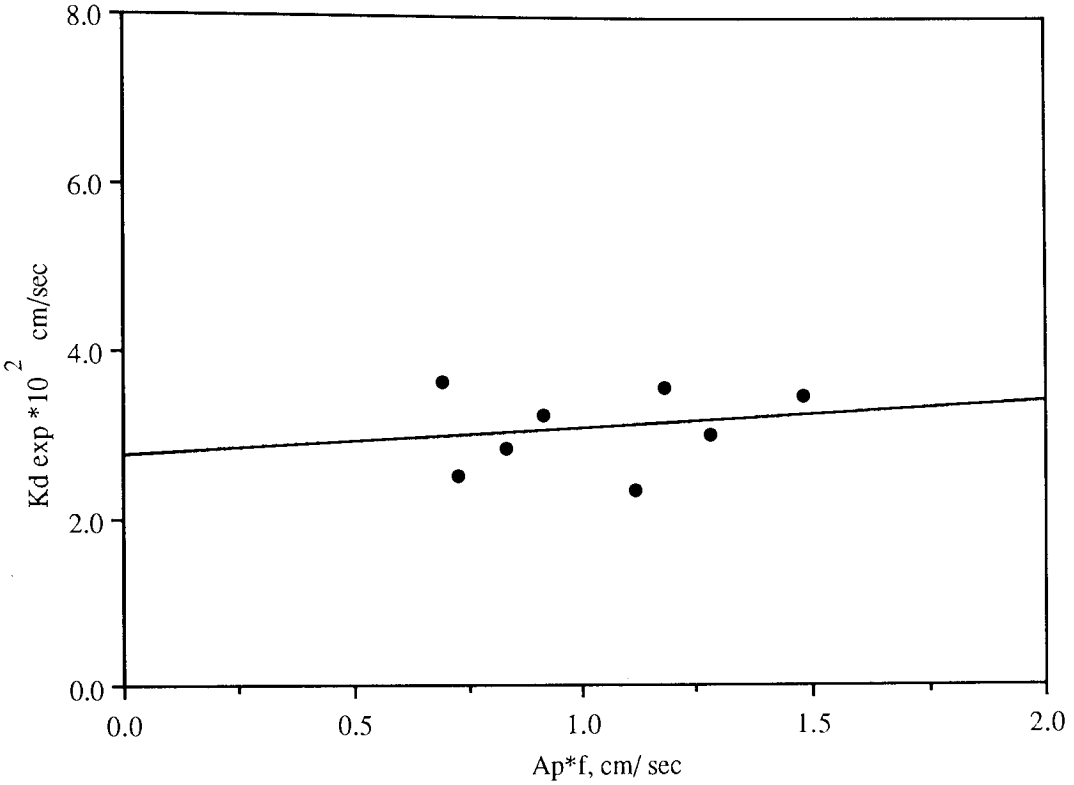

Figure 7.48 Effect of Pulsing on Overall Mass Transfer Coefficient

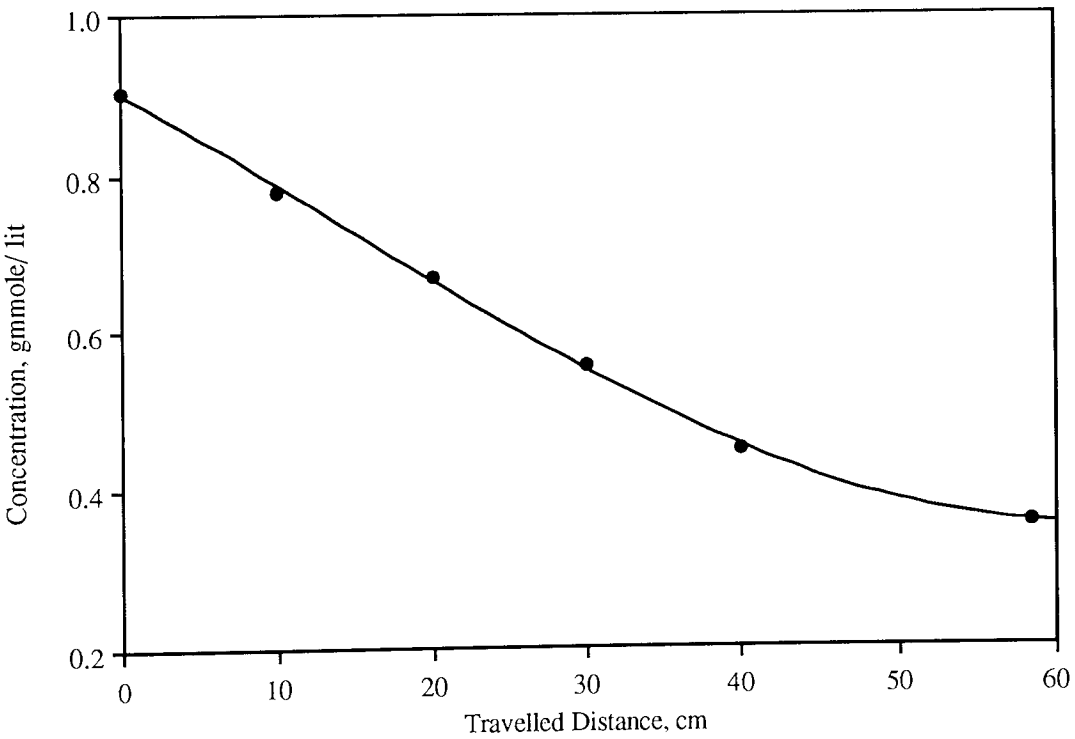

Figure 7.49 Relationship between Travelled Distance and Dispersed Phase Concentration

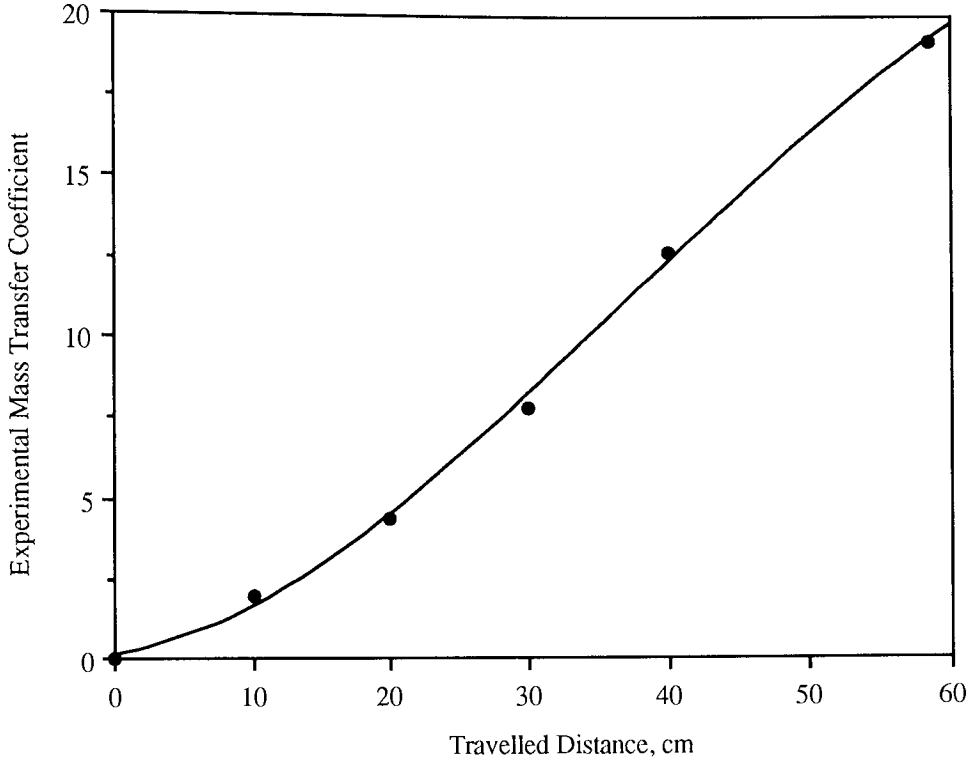

Figure 7.50 Relationship between Travelled Distance and Overall Mass Transfer Coefficient

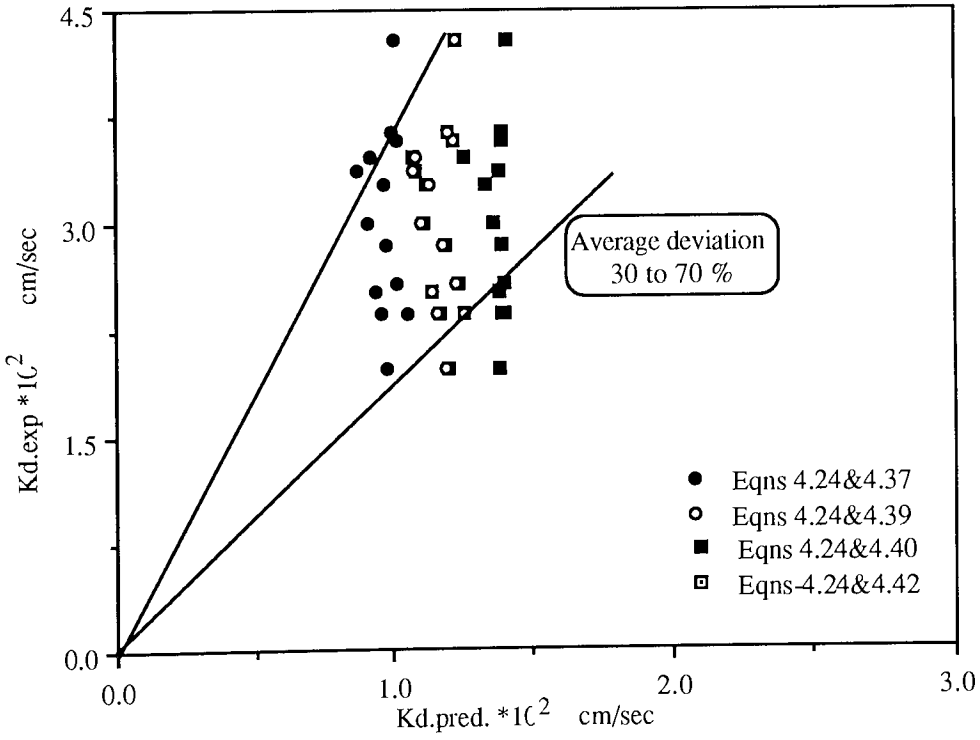

Figure 7.51 Comparison between Experimental & Predicted Overall Dispersed phase Mass Transfer Coefficient

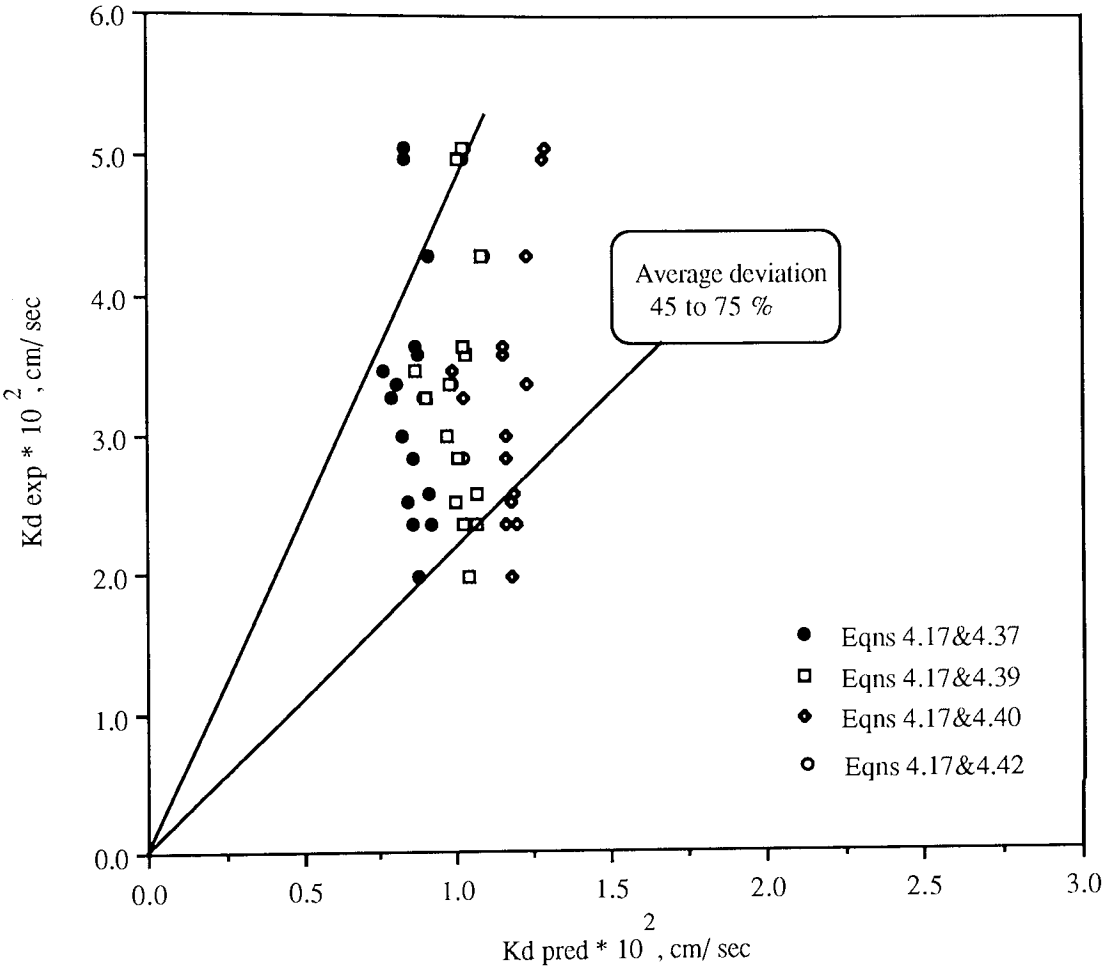

Figure 7.52 Comparison between Experimental and Predicted Overall Dispersed phase Mass Transfer Coefficient

Table 7.4 Experimnetal Overall Mass Transfer Coefficient during Formation of Single Droplets in Pulsed and Non-Pulsed Conditions

Run No.	A_{mf} cm^2	C_1 gmole/lit	C_2 gmole/lit	$N_{f.exp} * 10^6$ gmole/sec	$K_{df-exp} * 10^2$ cm/sec
1Po	0.21	1.15	0.90	4.35	1.77
2Po	0.21	1.15	0.85	4.47	1.90
3Po	0.23	1.15	0.89	3.55	1.73
4Po	0.18	1.15	0.90	3.00	1.47
1P	0.39	1.04	0.85	9.01	2.20
2P	0.37	0.95	0.72	7.71	2.22
3P	0.39	0.90	0.78	5.90	1.67
4P	0.17	0.90	0.71	2.68	1.76
5P	0.16	0.90	0.67	2.90	2.08
6P	0.24	1.02	0.74	5.74	2.31
7P	0.24	1.02	0.76	5.20	2.13
8P	0.27	1.02	0.79	5.45	1.98
9P	0.21	1.02	0.71	5.24	2.41
10P	0.19	1.02	0.66	5.04	2.61
11P	0.21	1.02	0.70	4.60	2.64

Table 7.5 Theoretical Overall Mass Transfer Coefficient during formation of single droplets

Run No.	d_e cm	C_1 gmole/lit	C_2 gmole/lit	$N_{f.theo} * 10^6$ gmole/sec	$K_{d.f.theo} * 10^2$ cm/sec	
					Eqn 4.8	Eqn 2.9
1Po	0.34	1.15	0.95	3.48	1.42	1.42
2Po	0.33	1.15	0.94	3.13	1.35	1.33
3Po	0.35	1.15	0.95	3.50	1.34	1.33
4Po	0.31	1.15	0.92	2.76	1.35	1.36
1P	0.46	1.04	0.91	6.16	1.48	1.51
2P	0.44	0.95	0.81	4.69	1.31	1.35
3P	0.46	0.90	0.79	5.41	1.50	1.53
4P	0.30	0.90	0.74	2.26	1.50	1.49
5P	0.29	0.90	0.74	2.14	1.52	1.53
6P	0.37	1.02	0.85	3.28	1.38	1.32
7P	0.37	1.02	0.85	3.20	1.39	1.31
8P	0.38	1.02	0.85	3.79	1.38	1.38
9P	0.34	1.02	0.83	3.04	1.39	1.40
10P	0.32	1.02	0.83	2.66	1.38	1.38
11P	0.33	1.02	0.84	3.15	1.44	1.48

Table 7.6 Experimental Overall Mass Transfer Coefficient of single droplets during ascent

Run No.	D_H cm	D_V cm	A cm^2	C_2 g mole/lit	C_3 g mole/lit	$N_{t.exp} * 10^6$ g mole/sec	$K_d * 10^2$ cm/sec
$1P_0$	0.35	0.31	0.36	0.90	0.53	6.44	1.99
$2P_0$	0.34	0.31	0.34	0.85	0.35	7.45	2.58
$3P_0$	0.37	0.31	0.38	0.89	0.28	10.68	4.29
$4P_0$	0.31	0.30	0.30	0.90	0.37	6.36	2.36
1P	0.47	0.43	0.65	0.85	0.27	27.49	4.98
2P	0.45	0.42	0.61	0.72	0.28	14.74	3.36
3P	0.47	0.43	0.65	0.78	0.26	25.58	5.05
4P	0.31	0.28	0.28	0.71	0.25	6.49	3.26
5P	0.29	0.28	0.26	0.67	0.19	6.05	3.47
6P	0.38	0.34	0.42	0.74	0.38	7.38	2.37
7P	0.39	0.33	0.43	0.76	0.35	8.20	2.51
8P	0.40	0.34	0.44	0.79	0.35	10.43	3.00
9P	0.35	0.31	0.36	0.71	0.28	7.27	2.84
10P	0.32	0.31	0.32	0.66	0.12	7.56	3.58
11P	0.35	0.30	0.35	0.70	0.19	8.93	3.64

Table 7.7 Relationship between Travelled Distance & Experimental Mass Transfer Coefficient

Travelling Distance cm	Residence Time sec	Droplet Concentration g mole / lit	$N_t * 10^3$ g mole / sec	$K_{d\text{-}exp} * 10^2$ cm / sec
0.00	0.00	0.902	0.000	0.000
10.0	0.87	0.780	9.39	1.95
20.0	1.78	0.670	17.86	4.33
30.0	2.69	0.555	26.72	7.82
40.0	3.61	0.449	34.88	12.61
58.5	5.28	0.355	42.12	19.26

$f_d = 7.7 * 10^{-2}$ cm^3/sec $t_f = 0.80$ sec

$f_c = 2.167$ cm^3/sec $C_i = 1.04$ gmole / lit

$A = 6.16 * 10$ cm^2

Table 7.8 Predicted Overall Mass Transfer Coefficient of Single Droplets During Travelling Period in Pulsed and Non-pulsed Conditions.

Run No.	t_c sec	A cm^2	Predicted Overall Mass Transfer Coefficient (K_d)				$K_{d\,exp}$ **
			Eqn 4.12 *	Eqn 4.16 *	4.17&4.37 **	4.17&4.39 **	
$1P_0$	6.00	0.54	0.800	1.179	0.880	1.040	1.99
$2P_0$	5.86	0.50	0.695	1.043	0.910	1.070	2.58
$3P_0$	5.70	0.54	0.707	1.036	0.940	1.080	4.29
$4P_0$	5.90	0.24	0.659	1.011	0.920	1.070	2.36
1P	5.81	0.21	1.076	1.615	0.830	1.010	4.98
2P	6.24	0.35	0.810	1.356	0.810	0.980	3.36
3P	5.70	0.36	1.040	1.582	0.830	1.020	5.05
4P	7.53	0.38	0.946	1.455	0.790	0.900	3.26
5P	7.17	0.30	0.987	1.443	0.760	0.870	3.47
6P	6.16	0.26	0.817	1.225	0.860	1.020	2.37
7P	6.24	0.29	1.130	1.690	0.840	1.000	2.51
8P	6.37	0.30	0.821	1.199	0.820	0.970	3.00
9P	5.27	0.28	0.698	1.076	0.860	1.010	2.84
10P	6.29	0.32	0.745	1.152	0.880	1.030	3.58
11P	6.31	0.24	0.825	1.238	0.870	1.020	3.64

* cm / sec $*_{10^{-5}}$ ** cm / sec $*_{10^{-2}}$

Table 7.8 *continued*

Run No.	Predicted Overall Mass Transfer Coefficient (K_d)						$K_{d\,exp}$ **
	4.17&4.40 **	4.17&4.42 **	4.24&4.37 **	4.24&4.39 **	4.24&4.40 **	4.24&4.42 **	
$1P_0$	1.180	1.040	0.980	1.190	1.380	1.180	1.99
$2P_0$	1.190	1.070	1.020	1.230	1.400	1.180	2.58
$3P_0$	1.230	1.080	1.010	1.230	1.410	1.230	4.29
$4P_0$	1.160	1.070	1.050	1.260	1.390	1.160	2.36
1P	1.280	1.010	0.870	1.080	1.380	1.280	4.98
2P	1.230	0.980	0.870	1.070	1.380	1.230	3.36
3P	1.290	1.020	0.870	1.080	1.390	1.290	5.05
4P	1.020	0.900	0.970	1.130	1.340	1.020	3.26
5P	0.990	0.870	0.920	1.080	1.260	0.990	3.47
6P	1.200	1.020	0.960	1.160	1.400	1.200	2.37
7P	1.180	1.000	0.940	1.140	1.380	1.180	2.51
8P	1.160	0.970	0.910	1.100	1.360	1.160	3.00
9P	1.160	1.101	0.980	1.180	1.390	1.160	2.84
10P	1.150	1.030	1.020	1.220	1.390	1.150	3.58
11P	1.150	1.020	1.000	1.200	1.390	1.150	3.64

** cm / sec $*_{10^{-2}}$

tensions, most of the droplets broke up when they hit the rim of the hole and therefore it was difficult to achieve mass transfer experiments in a pulsed sieve plate column, for the toluene-acetone-distilled water system, without droplet breakage. A better opportunity may exist for a successful study of the mass transfer rate of single droplets without droplet breakage in pulsed sieve plate column if higher interfacial and surface tensions systems are used. This point is discussed in more detail in Chapter 8.

CHAPTER EIGHT

DISCUSSION OF RESULTS

8.1 HYDRODYNAMICS

8.1.1 Terminal Velocity

For single droplet terminal velocity, the relationship between the travelled distance and the measured time is linear. In the present study, the experimental technique for measuring droplet terminal velocity provided reasonably accurate data as shown in Figures 7.1, 7.2, 7.3 and 7.4 where the relationship between the two variables is almost linear. Figure 7.6 shows a comparison between the experimental and predicted terminal velocity using equations 2.11, 2.12, 2.15 and 2.16.

Figure 7.6 shows that there is no agreement between experimental and predicted data using equation 2.11. This is not surprising as, unusually, equation 2.11 suggests an inverse relationship between the terminal velocity and droplet diameter where other relationships suggest direct proportionality. Figure 7.6 shows that equation 2.12 is valid only for small droplet diameter ($d_e < 0.30$ cm) and low Reynolds number.

Figure 7.6 shows that there is a good agreement between experimental and predicted data using equation 2.15, when the criteria which the data have to meet ($d_e/D < 0.12$ and for $Re > 100$) are satisfied. In the present study the column diameter is 5.0 cm, so the droplet diameter should not be larger than 0.6 cm which means that the wall effects are negligible. Figure 7.6 shows also that there is agreement between experimental and predicted data using equation 2.16.

It may be proposed therefore that when experimental data is not available then equations

It may be proposed therefore that when experimental data is not available then equations 2.15 and 2.16 may be used for the prediction of droplet terminal velocity with reasonable success.

One reason for interest in the droplet terminal velocity is to allow study of the effect of continuous phase pulsing on the velocity of a single droplet by comparing its terminal velocity both with pulsing with that without pulsing. The results of this study are discussed in the next subsection.

8.1.2 Characteristic Velocity

As mentioned in Chapters 6 and 7, experiments were carried out to study the effect of pulsing on the velocity of a single droplet in an oscillating continuous phase (water). The experimental data show that the velocity of a single droplet under pulsing conditions is lower than its terminal velocity in a stagnant continuous phase and it further reduces as frequency and amplitude of the pulse increase.

In order to study the characteristic velocity for different droplet diameters, or even for the same droplet diameter but for different systems, the use of the dimensionless ratio (V_k/V_t) is useful. This ratio was adopted because it was found practically impossible to achieve constant droplet diameter between experimental runs thus making direct comparison of the data very difficult. Using the ratio (V_k/ V_t) eliminates the droplet size effect and the data can be compared.

As shown in Figure 8.1, the reduction in the ratio (V_k/ V_t) is between 1% and 11% depending on; pulsing frequency, pulsing amplitude and droplet diameter. The scatter of data of Figure 8.1 suggests that a simple relationship between the ratio (V_k / V_t) and (f*Ap) does not exist and a more complex relationship is required.

In Chapter 7, the theoretical equations 3.36-3.38 were considered to evaluate the experimental data in the absence of a sieve-plate. In this paragraph, the validity of these equations for the pulsed spray column is discussed. Equation 3.32 was not helpful because of the limiting assumptions of high frequency (5-50 Hz) and low amplitude (0.0-1.0 cm). Equation 3.36 shows a little reduction in (V_k/V_t) ratio and the key parameter is the density ratio. Equation 3.38 predicts a larger reduction than is in fact observed and is thought not useful because it considers the effect of frequency only.

8.1.2.1 Effect of Pulsing Parameters

When a single droplet is subjected to pulsing its instantaneous velocity will decrease or increase as a result of the pulsing depending upon the stage in the pulsing cycle; e g. it will decrease during the upstroke of the pulse or it will increase during the downstroke of the pulse. The effect of frequency and amplitude of pulsing and droplet size on droplet motion is discussed in more detail in the next paragraphs.

a. Effect of Amplitude

Figures 7.7, 7.8, 7.9, 7.10 show, in general, the effect of amplitude of pulsing on droplet movement. Figure 7.7 shows that at a constant frequency of f=0.54 Hz the slope of the distance of travel of the droplet / time graph (i.e. the velocity) during the downstroke of pulsing is lower than the droplet terminal velocity. During the upstroke of pulsing the slope becomes higher than the droplet terminal velocity. The effect of amplitude increases as the amplitude increases. For example, in each of Figures 7.7-7.10 a comparison between two droplets has been made. It is clear from these Figures that during the downstroke of pulsing the droplet velocity decreases and this effect increases as the amplitude increases and the velocity may be momentarily reduced to zero as shown in Figures 7.6 and 7.7 for f = 0.54 Hz and A_p = 7.09 cm. In this case the droplet suffered reduced velocity and then stopped for about 0.5 seconds then

Figures 7.8 & 7.9 show unique behaviour for the droplet during the downstroke of pulsing, where for f = 0.54 Hz & A_p= 9.61 cm and f = 0.62 Hz & A_p = 8.67 cm, the droplet velocity has not only reduced to zero for about 0.4 second but it moved backwards for about 0.3 seconds.

b. Effect of Frequency

Figures 7.11, 7.12, 7.13 & 7.14 show the effect of frequency of pulsing on droplet movement for amplitudes held in the narrow range of about 0.09 - 0.20 cm with frequencies of 0.62, 0.71, 0.85 & 1.04 Hz. From these Figures, the effect of frequency on droplet velocity may be examined. The fluctuations in the droplet velocity increases as the pulse frequency increases as shown in Figures 7.11, 7.12, 7.13 & 7.14. This is due to the increase in liquid displacement in the same interval of time at almost constant amplitude as the frequency increases.

8.1.2.2 Effect of Droplet Diameter

Figures 7.15, 7.16, 7.17, 7.18 & 7.19 show the effect of droplet diameter on droplet movement in pulsing conditions for a constant frequency and a narrow range of amplitude of about 0.0 - 0.51 cm. From these Figures, the effect of the change in the droplet diameter on droplet velocity may be examined. Figures 7.15 & 7.18 show that, for a constant frequency and amplitude (f=0.71 Hz & A_p=5.14 cm) and (f=0.85 Hz & A_p=4.8 cm) respectively, the droplet velocity increases as the droplet size increases.

From the above observations, it is clear that the droplet under the effect of pulsing will move with an average velocity different from and usually lower than its velocity in an unpulsed continuous phase (terminal velocity). This different velocity is called, in this study, the characteristic velocity.

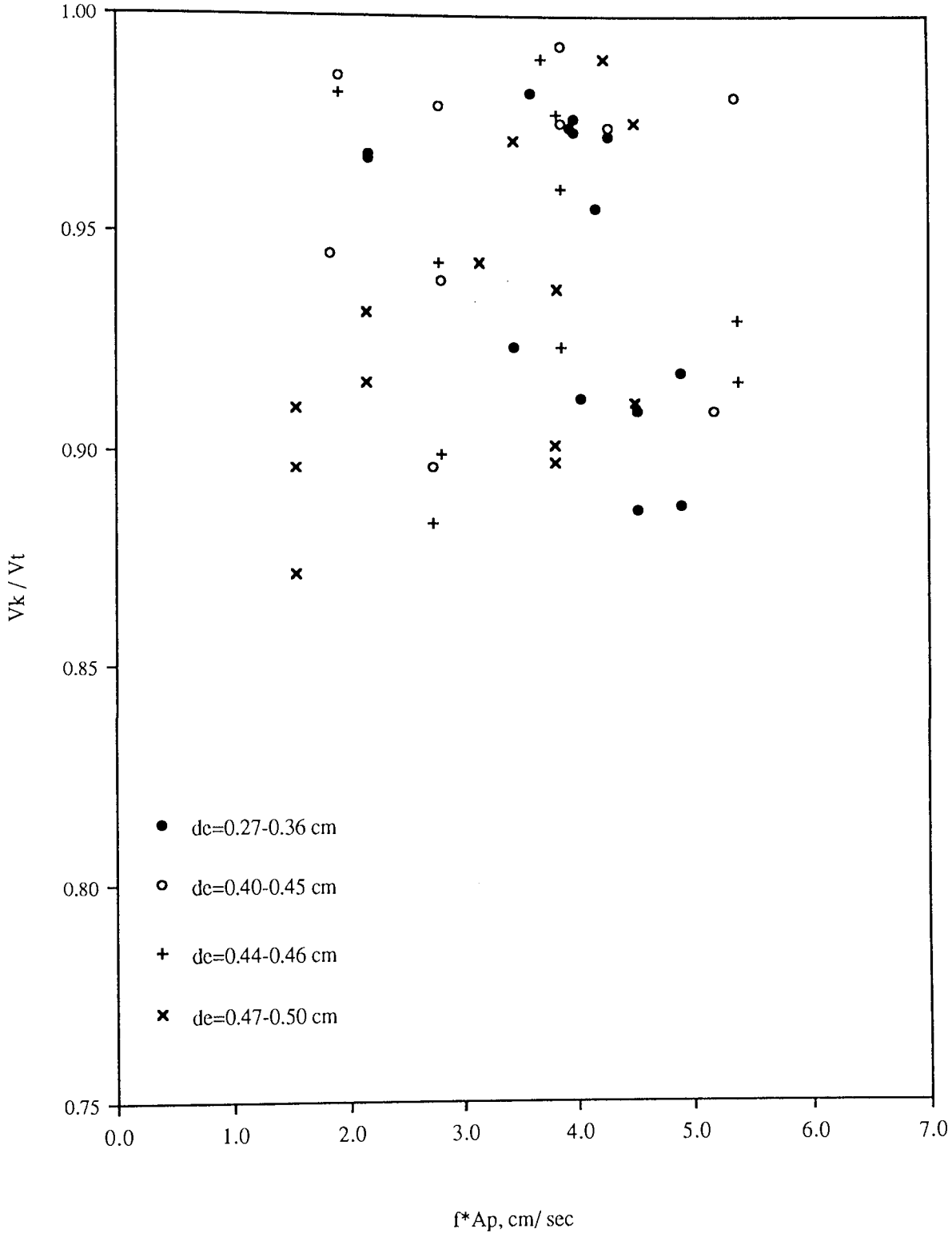

Figure 8.1 Effect of Pulsing on Experimental (Vk/Vt) ratio

Table 8.1. Effect of Sieve-plate on the droplet behaviour without pulsing

Plate spacing cm	Plate hole cm	Droplet diameter cm	de / dh	Terminal velocity cm / sec	Average velocity cm / sec	Average time delay sec
5.0	0.6	0.57	0.950	12.15	9.11	0.15
5.0	0.4	0.45	1.125	12.05	9.89	0.23
5.0	0.4	0.45	1.125	12.05	10.26	0.30
5.0	0.4	0.46	1.150	12.20	9.54	0.18
2.5	0.4	0.45	1.125	12.05	9.95	0.13
2.5	0.4	0.45	1.125	12.05	9.68	0.23
2.5	0.4	0.47	1.175	12.30	9.65	0.18

study, the characteristic velocity.

8.1.2.3 Effect of a Sieve Plate

Figures 7.20-7.30 show the effect of the presence of a sieve-plate on droplet movement in both pulsed and unpulsed conditions. Figures 7.27 & 7.28 show that the droplet in an unpulsed sieve-plate column moves between the sieve-plates with an average velocity less than its terminal velocity. When the droplet reaches a sieve-plate it stops for an average time of 0.1 - 0.5 second depending upon the (d_e/d_h) ratio as shown in Table 8.1. The characterisation of droplet velocity between the sieve-plates can be illustrated by recognising that a droplet leaving the sieve-plate from rest is undergoing the same process as a droplet undergoing formation or reformation at a nozzle. Various workers have reported that the droplet moves with its acceleration velocity after leaving the sieve-plate and attains its terminal velocity only after a rise of about 5.0-15.0 cm above the sieve-plate. This confirmed the previous observation in this study that in unpulsed conditions the droplet moves between the sieve-plates with its acceleration velocity which is usually less than its terminal velocity. The effect of the sieve-plate on droplet movement in pulsed conditions is discussed in the next subsection.

8.1.2.4 Combined Effect of the Pulsing Parameters and Plate Characteristics

Figures 7.20 - 7.30, except Figure 7.28, show the effect of sieve-plate characteristics on droplet behaviour in pulsed conditions. The sieve plate characteristics were as follows; h_c = 2.5 & 5.0 cm, d_h = 0.25, 0.40 & 0.6 cm; plate free area was constant and equal to 23%. The pulsing parameters were as follows; frequencies equal to:- 0.61, 0.71, 0.83 & 1.02 Hz and amplitudes in the range of 0.33 - 5.58 cm.

Figure 7.38 shows the results of the various interactions between a single droplet and

the sieve-plate under pulsed conditions. Droplets that do not breakup are discussed in the next paragraph of this subsection, and the other droplets are discussed in section 8.1.3.

The first case represented in Figure 7.38, (no. 1) exists when the ratio $(d_e/d_h) < 1.0$. The droplet may pass through the sieve-plate without stopping during the major part of the upstroke of pulsing i.e. for the period which starts shortly after the upstroke begins until shortly before it ends. Figures 7.21, 7.22 & 7.26 illustrates this situation for different operating conditions; f=0.83 Hz & A_p = 0.33 & 0.74 cm, f=1.02 Hz & A_p = 0.47 cm, f =0.61 Hz & A_p =1.81 cm.

If the droplet reaches the sieve-plate during any other part of the pulsing cycle, it stops for a period of time below the sieve-plate. This period of time depends on the droplet's location relative to the nearest sieve-plate hole i.e. if the droplet is exactly beneath one of the holes it will pass through the hole shortly after the beginning of the next upstroke of the pulsing cycle. Otherwise the droplet will migrate during the upstroke of the pulsing cycle, searching for a hole to pass through. As shown in Figure 7.20 this migration may take more than one cycle of pulsing. The period of migration depends on the following main factors; the droplet's location relative to the nearest hole, the point of the pulse cycle at which the droplet reaches the sieve-plate and the ratio (d_e / d_h).

The second case represented in Figure 7.38 (no. 2), exists when the ratio $(d_e/d_h) \geq 1.0$. The droplet may pass through the sieve-plate without stopping during the major part of the upstroke of the pulse i.e. for the period which starts shortly after the upstroke begins until shortly before it ends. Figures 7.23, 7.24, 7.26 & 7.29 illustrate this situation for different operating conditions. In most cases, as described for the first case, the droplet will search for a hole to pass through, but there are two exceptions: where the migration period is longer than in the first case, as shown in Figure 7.30,

and when a droplet leaves the sieve-plate and then oscillates and deforms with rotational movement, as illustrated in Figure 7.38. In the two above cases, the minimum migration period is about 40-50% of the pulsing cycle. The migration period increases as the ratio (d_e / d_h) increases and/or the droplet's location relative to the nearest sieve-plate hole increases and/or the point of pulse cycle at which the droplet reaches the sieve-plate as discussed before.

The droplet moves, between the sieve-plates, with higher or lower velocity than its terminal velocity depending on whether it is subjected to an upstroke or a downstroke, and the change in velocity increases as amplitude increases at constant frequency, and as frequency increases at constant amplitude. The droplet may be forced not only to stop between the plates but also to move backwards for about 0.3-0.5 seconds at the downstroke of the pulse cycle as shown Figures 7.20, 7.25 & 7.26. But as discussed above, in most of the cases the droplet leaves the sieve-plate shortly after the beginning of the upstroke of the pulse and reaches the next sieve-plate shortly before the end of the upstroke and the beginning of the downstroke i.e. in general for each droplet moving between the sieve-plate, its velocity is not constant. The highest velocity will be seen after it leaves the sieve-plate and the lowest velocity will be before it reaches the next sieve-plate where the droplet velocity approaches zero.

8.1.3 Droplet Breakup

In this study, three different mechanisms are considered to illustrate droplet breakup in the pulsed sieve-plate column under mixer-settler and transitional regimes. In this section the three different mechanisms are discussed and they are evaluated according to the experimental results given in Chapter 7.

The first mechanism is based on droplet formation at a nozzle, for either jetting or non-jetting droplet formation. This mechanism is represented by equations 7.1 & 7.2

for jetting and by equation 7.3 for non-jetting droplet formation. Figures 7.31 & 7.32 show a comparison between the experimental data and the theoretical data based on jetting and non-jetting mechanisms respectively. In these Figures each predicted point, using equations 7.1, 7.2 & 7.3, represents a critical droplet diameter, above this value the droplet should breakup and below this value the droplet should not breakup. As shown in these Figures there is no agreement between the experimental data and the predicted data based on the first mechanism, i.e.the experimental droplets which breakup are below the predicted data and not above them as expected. This lack of agreement may be because of the fact that the droplet under the effect of a pulse leaves the sieve-plate with a velocity greater than the velocity with which the droplet leaves the sieve-plate under non-pulsed conditions, which means in pulsed conditions smaller droplets are produced. In equations 7.1, 7.2 & 7.3, a good agreement is expected if the velocity of droplet leaving the sieve plate is combined with the ($f * A_p / \phi$) parameter.

The second mechanism is based on the isotropic turbulence theory introduced by Kolmogoroff and represented by equations 3.20-3.28. Figures 7.33, 7.34 & 7.35 show comparisons between the experimental and theoretical data using equations 3.20-3.28. Figures 7.34 & 7.35 show that there is poor agreement between the experimental and theoretical data using equations 3.20, 3.21, 3.27 & 3.28 respectively.

From Figure 7.33, predicted data using equations 3.22 & 3.26 show a better agreement, with experimental data, than the predicted data shown in Figures 7.34 & 7.35. From the previous comparison, it is clear that the isotropic mechanism is not valid for the operating conditions of the mixer-settler and transitional regimes, however, it is worth considering the validity of this mechanism for the emulsion regime where the degree of turbulence is higher.

The third breakup mechanism to be discussed in this section is the impact breakup mechanism. Based on the experimental observations in the present study, (see Chapter

7), as well as the previous experimental observations, (see Chapter 3) mentioned by several workers (118, 150, 31), it is clear that the breakup of a droplet occurred when it hit the rim of the orifice in the sieve-plate. New correlations 7.7 & 7.8 are introduced in Chapter 7 to illustrate the impact breakup mechanism in a pulsed sieve-plate column for the mixer-settler and transitional regimes. Equations 7.7 & 7.8 are presented in Figures 7.36 & 7.39 respectively.

Figure 7.36 exhibits four regions; two regions (I & II) are where droplets breakup after hitting the rim of the orifice and the other two regions (III & IV) are where droplets do not breakup because of a number of different reasons. Under nonpulsed conditions a droplet existing in region II does not breakup even after hitting the rim of the orifice at its terminal velocity because its diameter is less than the critical diameter. On the other side and under pulsed conditions, a droplet existing in region II breaks up because of the pulsing effect even if its diameter is less than the critical diameter of the droplet. Under nonpulsed conditions a droplet existing in region IV should breakup because its diameter is greater than the critical diameter. But under pulsing conditions, a droplet existing in region IV does not breakup even if its diameter is greater than the critical diameter because of the pulsing effect, particularly during the down stroke of the pulse cycle where the velocity of the droplet becomes not only less than its terminal velocity but it may approach zero value as discussed in section 8.1.2. Figure 7.37 shows a good agreement between the predicted data using equation 7.7 and the experimental data.

Figures 8.2, 8.3, 8.4 & 8.5 show a comparison between predicted data based on the three different breakup mechanisms mentioned in Chapters 3 & 7 to illustrate the breakup of a droplet in a pulsed sieve-plate column. From Figures 7.31-7.35, 7.37 & 8.2-8.5; it is clear that correlation 7.7, which is based on the impact breakup mechanism, is the most useful correlation to illustrate the droplet breakup process in pulsed sieve-plate columns for the mixer-settler and transitional regimes.

Equation 7.7 becomes more useful when its parameters are converted to dimensionless groups as represented by equation 7.8. Figure 7.39 presents equation 7.8 and exhibits two regions; the breakup region (region I) and the nonbreak up region (region II). Figures 7.40 & 7.41 show a good agreement between the predicted data using equation 7.8 and the experimental data for nonbreak up and breakup droplets respectively. The only disadvantage of equation 7.8 is the relatively small range of its valid operating conditions ; i.e. $0 \leq Eo \leq 1.743$.

8.1.4 Droplet Diameter

As shown in subsection 3.2.3, most of the correlations which have been developed to predict the droplet size in pulsed sieve-plate columns are based on the isotropic theory and particularly on the energy dissipation concept which was mentioned in subsection 3.2.2. These correlations are evaluated and discussed in subsection 8.1.3. From the previous discussion, it is clear that the correlations based on the isotropic theory to predict droplet diameter indicate a generally unsatisfactory state of affairs for the operating conditions of mixer-settler & transitional regimes. However, it is worth evaluating the validity of this mechanism for the emulsion regime where the degree of turbulence is higher.

As mentioned in subsection 3.2.1, the calculation of the energy dissipation in the presence of a sieve plate in a pulsed column has been carried out in various ways. From the previous equations, 3.2-3.18, it is clear that there has been no agreement about a general formula for energy dissipation. As shown in subsection 7.1.4 an effort has been made to introduce a new correlation, 7.23, for the calculation of the energy dissipation. A general formula may be achieved by making a comparison between the correlations and evaluating the different ways by which these correlations have been carried out. By assuming a pressure recovery after the plate, a general formula may be proposed as follows:-

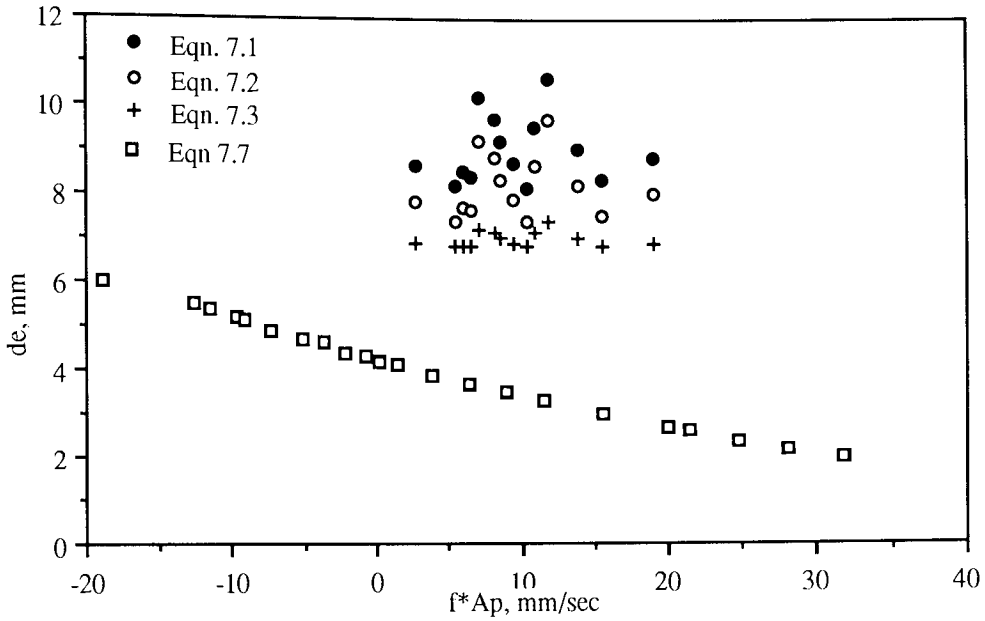

Figure 8.2 Comparison between Predicted data based on 1st & 3rd mechanisms

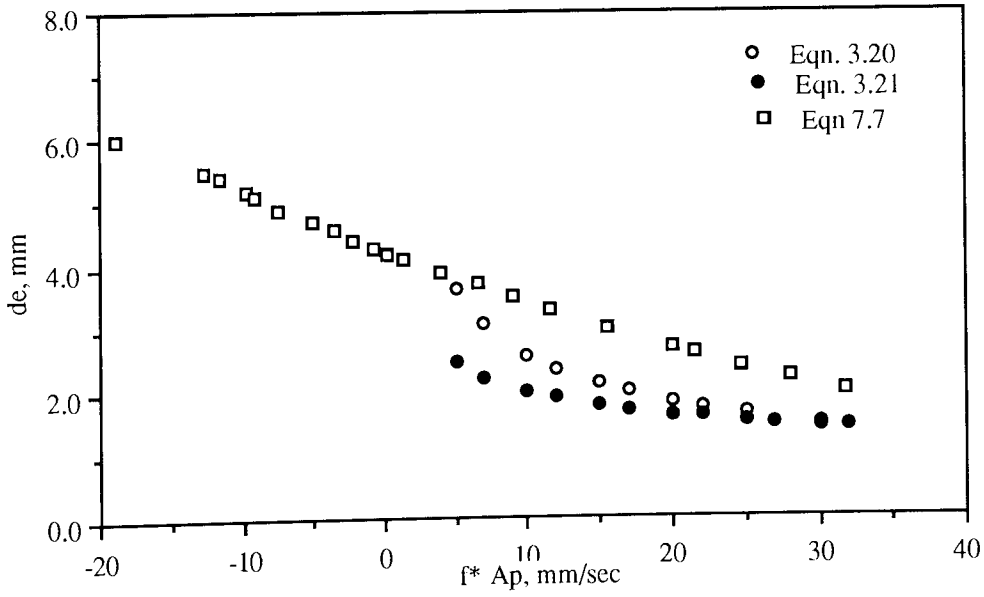

Figure 8.3 Comparison between Prediced data based on 2nd & 3rd mechanisms

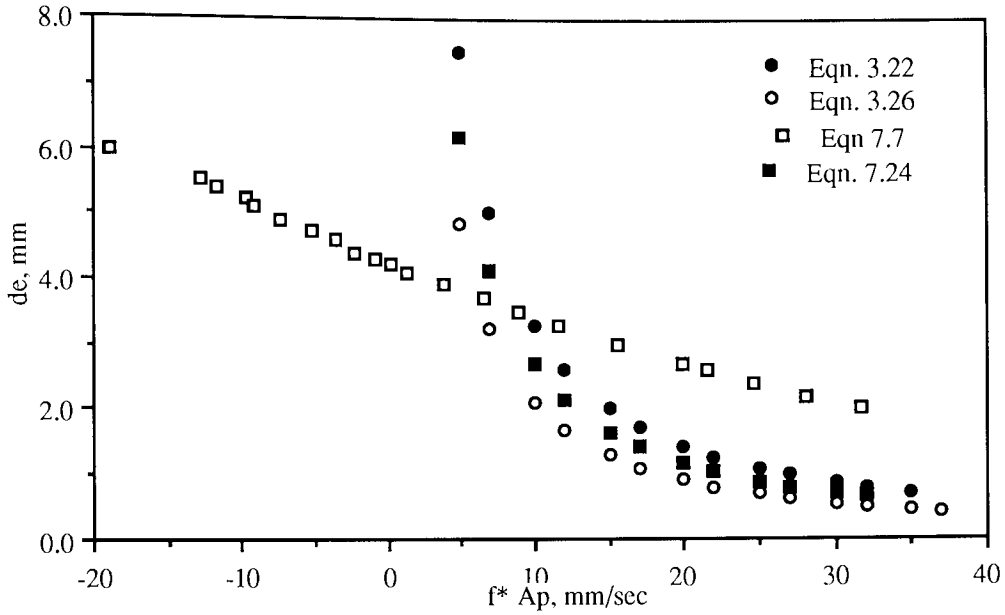

Figure 8.4 Comparison between Predicted Data based on 2nd & 3rd Mechanisms

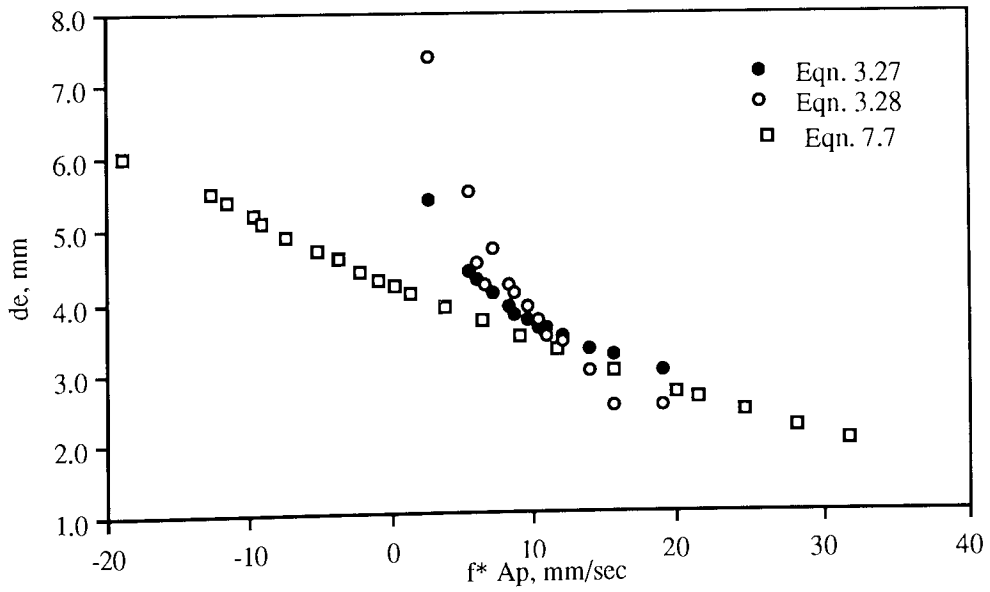

Figure 8.5 Comparison between Predicted Data based on 2nd & 3rd Mechanisms

$$\psi = \frac{Ç}{2\phi^{2} C_o^2 h_c} (1-\phi)\left(1-\phi^{2}\right)\left(A_p * f\right)^3 \qquad 8.1$$

where Ç is a constant with an average value equal to 5.98 ± 2.28

Figure 8.6 shows a comparison between the general formula and the correlations proposed to calculate the energy dissipation.

In this study, a new correlation 7.24 based on isotropic turbulence is introduced to predict the droplet size in a pulsed column for the emulsion regime. A comparison between the new correlation and equations 3.22 & 3.26 and the experimental data is represented in Figures 7.42. As shown in this Figure a good agreement between this equation and equations 3.22 & 3.26 is achieved. However, equation 7.24 should be verified experimentally for the case of a high degree of turbulence, which is unfortunately outside the experimental range of this study.

As discussed in subsection 8.1.3, for the mixer-settler and transitional regimes, the correlation 7.7, which is based on the impact breakup mechanism, is the most accurate correlation in predicting the droplet diameter in these operating conditions. As shown in subsection 8.1.3, droplet formation at a sieve plate as well as droplet breakup may be illustrated using this equation.

8.2 MASS TRANSFER IN PULSED COLUMNS

As indicated in Chapter 4, mass transfer studies reported in the literature have either concentrated on the single drop in non agitated systems or upon mass transfer from swarms of drops in agitated systems. The study of mass transfer for single drops in agitated systems has been largely neglected.

In Chapter 7, of the present investigation, the mass transfer coefficients of single droplets, during their formation and travelling periods, under pulsed and nonpulsed conditions were evaluated experimentally. In this section the effect of pulsing parameters on the mass transfer rate of a single droplet during its formation and travelling periods is discussed.

An improved sampling technique developed by Jeffreys and Bonnet (77) was used to withdraw the dispersed phase droplet after its formation and/or from different positions within the column.

8.2.1 Mass Transfer During Droplet Formation

Figure 7.44 shows a comparison between experimental and predicted data of the overall mass transfer coefficient during the droplet formation period, while Figure 7.45 shows the effect of pulsing on the experimental overall mass transfer coefficient during this period.

The correlations proposed to evaluate the dispersed phase mass transfer rate of the droplet during formation, section 4.1, were examined; the agreement between the theoretical and experimental data was generally found to be not good , but it was better for the predicted data using equations 4.8 and 4.9. These equations gave the best agreement with the experimental data at pulsed conditions with an average deviation from the experimental values ranging from 10 to 45 %, as shown in Figure 7.44.

Equation 4.8 was proposed by Sawistowski and Goltz (134) to calculate the overall dispersed phase mass transfer coefficient during droplet formation as follows:-

$$k_{df} = \frac{40}{7}\sqrt{\frac{D_d}{\pi\, t_f}} \qquad 4.8$$

The results are shown in Table 7.5.

Figure 7.45 shows the pulsing effect on the overall mass transfer coefficient of single droplet during formation. From this Figure, it is clear that in the mixer-settler and transitional regimes; pulsation has very little effect on the overall dispersed phase mass transfer coefficient during droplet formation.

8.2.2 Mass Transfer During Droplet Travel

The correlations proposed to evaluate the dispersed phase mass transfer rate for the droplet during its travelling period, sections 4.2 & 4.3, were examined; disagreement between the theoretical and experimental data was generally found (Tables B.2.1 & B.2.2), but it was better for the predicted data using combined equations groups; 4.24 & 4.35, 4.24 & 4.37, 4.24 & 4.38, 4.24 & 4.40, 4.17 & 4.35, 4.17 & 4.37, 4.17 & 4.40, 4.17&4.38. These combined equation groups gave the best agreement with the experimental data at pulsed conditions with an average deviation from the experimental values ranging from 30 to 75 %. Figures 7.51 & 7.52 show a comparison between the experimental and predicted data using these groups.

Figures 7.46, 7.47 & 7.48 show the effect of pulsing parameters on the mass transfer rate of single droplets with and without the presence of a sieve plate. From these Figures, it is clear that in the mixer-settler and transitional regimes and for non-break droplets pulsation has a small effect on the overall dispersed phase mass transfer coefficient during the travelling period. This small increase in the overall mass transfer coefficient may be due to the increase in the time of contact between the single droplets and the continuous phase because of reduction in the droplet velocity as a result of operating conditions in the pulsed sieve plate column. As shown in Figures 4.1-4.4, there is a good agreement between the observation of the present study and the observations of the previous studies (31, 41, 73, 82, 152), presented in Chapter 4, about the effect of pulsing upon the mass transfer rate of droplets that do not break up.

As mentioned in Chapter 7, in the present study all the mass transfer experiments were

carried out for the $d_e/d_h < 1$ condition only. An effort was made to study the effect of pulsing parameters on mass transfer rate for $d_e/d_h \geq 1$. Unfortunately, because of the reduction in the interfacial and surface tensions as a result of the addition of the acetone to the dispersed phase, most of the droplets broke up when they hit the rim of the hole and therefore it was difficult to achieve mass transfer experiments in a pulsed sieve plate column, for toluene-acetone-distilled water system, without droplet breakage.

From experimental observations of the hydrodynamics in the present study, as shown in Chapter 7, it is clear that droplets oscillate and deform with a rotating motion during their passage through the sieve plate. Observations recorded by several workers (1, 2, 31, 36, 37, 76) using a range of equipment types, e.g. RDC, mixer-settler and sieve plate columns, suggest that small droplets which are not observed to deform and oscillate in the absence of agitation will deform and oscillate when mechanical agitation is applied and an enhancement of the mass transfer rate of such droplets may be anticipated.

From the above, it is clear that the induced oscillation caused by the agitation of the droplets as they hit and pass through the sieve plate under the influence of a pulse may be expected to be a factor which will affect the droplet mass transfer rate in a pulsed sieve plate column. There would, however, be a better opportunity for studying the mass transfer rate of single droplets in a pulsed sieve plate column in such a way that the droplets do not break up , if the study is carried out on systems of higher interfacial and surface tension than have been studied here.

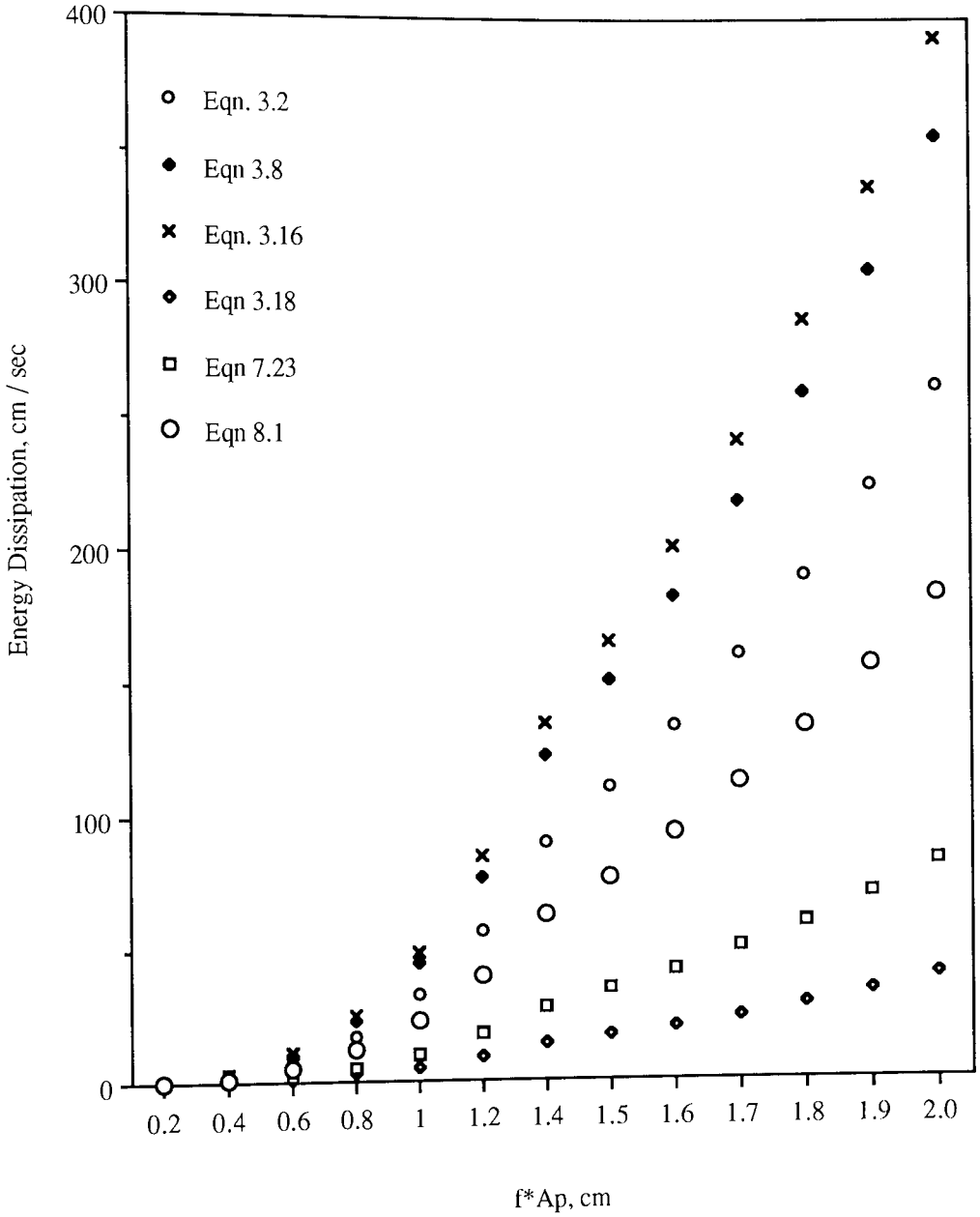

Figure 8.6 Relationship between Pulsing Intensity and Energy Dissipation

CHAPTER NINE

CONCLUSIONS AND RECOMMENDATIONS FOR FURTHER WORK

The hydrodynamics behaviour and the mass transfer characteristics of large single droplets ($0.25 \leq d_e \leq 0.6$ cm) in a pulsed spray column and a pulsed sieve plate column for mixer-settler and transitional regimes, under a constant operating temperature of 22°C, were studied. The dispersed phase flowed countercurrently to the continuous phase with flow rates of 0.015 & 60.0 cm^3/ sec respectively. Toluene was the dispersed phase and water was the continuous phase. The phases were mutually saturated, and acetone, present in the dispersed phase with concentrations of up to 10% wt/wt, constituted the solute.

An important component of the present study was the improvement of the photographic techniques for following and recording the droplet behaviour, measuring the pulse parameters and checking the pulse shape. The improved techniques proved to be successful. A unique illumination technique was developed in this work by which a moving droplet could be photographed using a cine or video camera with good contrast without using any dye.

A sampling technique was developed for withdrawing the dispersed phase droplet after formation and/or from different positions in the column. This technique ensured more accurate results than the sampling technique used previously. Ultra-violet spectrophotometry was used to measure the acetone concentration in both phases.

9.1 CONCLUSIONS

The main conclusions arising from this study are as follows:-

1. Good agreement was found between experimental and predicted terminal velocity data (V_t) using equation 2.15, when the criteria ($d_e/D \leq 0.12$ and for Re >100) are satisfied. Good agreement between experimental and predicted terminal velocity are also achieved using equation 2.16.

2. In an oscillating continuous phase, the experimental terminal velocity of a droplet is reduced as a result of the pulsation. In this study, the reduced velocity is called the characteristic velocity (V_k).This reduction is between 1% and 11% depending on ; the pulse amplitude, the pulse frequency and the droplet size.

3. At constant pulse frequency, droplet velocity during the downstroke of pulsing is lower than its terminal velocity, while during the upstroke of pulsing droplet velocity becomes higher than its terminal velocity. The effect of pulse amplitude on droplet velocity is that it increases as the amplitude increases.

4. At a narrow range of pulse amplitude, the fluctuations in the droplet movement increase as the pulse frequency increases.

5. At constant pulse frequency and a narrow range of pulse amplitude, droplet velocity increases as the the droplet size increases.

6. In an unpulsed sieve-plate column, a single droplet moves between the sieve-plate with an average velocity less than its terminal velocity and when it reaches a sieve-plate it stops for an average time of 0.1-0.5 second depending upon the (d_e/d_h) ratio.

7. In a pulsed sieve-plate column, a single droplet shows various interactions with the sieve-plate as follows:-

a. The droplet does not breakup and it moves between the sieve-plates with velocity higher or lower than its terminal velocity depending on whether it is subjected to an upstroke or a downstroke. The change in the droplet velocity increases as the frequency and amplitude of pulsation increase. The droplet, with (d_e/d_h) ratio more than one, leaves the sieve-plate with deformation, oscillation and a rotational movement.

b. The droplet breaks up into two or three smaller droplets when it hits the rim of the orifice in the sieve-plate. This type of breakup is called impact breakup mechanism.

8. Two other droplet breakup mechanisms were examined. The first one is based on the droplet formation at a nozzle and the second one is based on the isotropic turbulence theory. Both mechanisms were not valid for the operating conditions of mixer-settler and transitional regimes.

9. The proposed correlations based on the impact breakup mechanism (7.7 & 7.8) for predicting the droplet diameter in a pulsed sieve plate column, mixer-settler and transitional regimes, gave better agreement than those

mentioned previously. The proposed correlations are as follows:-

$$\frac{d_{crit} V_{crit}^2 \rho_d}{\sigma} + 1.79 \frac{d_{crit}^2 g \Delta\rho}{\sigma} = 3.12$$

or in dimensionless groups as follows:-

$$(We)_{crit} = 3.12 - 1.79 (Eo)_{crit}$$

10. A correlation based on the isotropic turbulence theory, 7.24, for prediction of droplet diameter is proposed.

$$d_{32} = 9.03 * 10^{-2} \left(\frac{\sigma}{\rho_c}\right)^{0.6} \psi^{-0.4}$$

11. A general formula, 8.1, for calculating the energy dissipation is proposed.

$$\psi = \frac{Ç}{2 \phi^2 C_0^2 h_c} (1 - \phi)\left(1 - \phi^2\right)(A_p * f)^3$$

12. There was very poor agreement, average deviation ranging from 10 to 45 %, between experimental and predicted overall dispersed phase mass transfer coefficient during droplet formation period.

13. For mixer-settler and transitional regimes, pulsation has little effect on the overall dispersed phase mass transfer coefficient during the droplet formation period.

14. There was a poor agreement, average deviation from 30 to 75 %, between experimental and predicted overall dispersed phase mass transfer coefficient

during the droplet travel period.

15. For mixer-settler and transitional regimes, pulsation has little effect on the overall dispersed phase mass transfer coefficient during the droplet travel period. The increase in overall mass transfer coefficient in the two regimes may be due to the increase in the time of contact between the two phases.

9.2 RECOMMENDATIONS FOR FURTHER WORK

The following projects could usefully be studied:-

1. The effect of pulsing parameters and sieve-plate characteristics on droplet characteristic velocity and axial mixing for $(d_e/d_h) \geq 1.0$ & $d_e/d_h \leq 1.0$ and for different liquid-liquid systems.
2. The effect of pulsing parameters, sieve-plate characteristics and physical properties of the system on the droplet breakup process and mass transfer rate from and/or to single droplet for different operating conditions, i.e. mixer-settler, transitional and emulsion regimes.
3. Effect of pulsing parameters on droplet formation characteristics with and without mass transfer for different liquid-liquid systems.
4. Effect of pulsing parameters upon wake characteristics.
5. Effect of different operating temperatures on mass transfer rate from and/or to single droplet under different pulsing conditions.
6. Effect of pulsing parameters on the hydrodynamics and mass transfer rate for single droplets in high interfacial tension systems.
7. Exam and evaluate the present mass transfer correlations and their applications for single droplets in pulsing conditions.

PART IV

APPENDICES AND REFERENCES

APPENDIX A

A.1 SPECIFICATION OF MATERIALS USED

A.1.1 Toluene " Analar "

Wt. per ml at 20° C	0.863 - 0.866 gm
Refractive Index at 20° C	1.494 - 1.497

Not less than 92% distils within 0.4° C in the range 110.0°-111.0° C

Impurities	Maximum Limit Percent
Acidity	0.012
Alkalinity	0.012
Non-Volatile Matter	0.002
Benzene	0.5
Organic Impurities	Passes Acid-Wash Test
Sulphur Compounds	0.0003
Thiophen Homologues	0.0002
Water	0.03

A.1.2 Acetone " Analar "

Wt. per ml at 20° C	0.789 - 0.791 gm
Boiling Range (95 %)	56.0 - 56.5° C
Refractive Index	1.3580 - 1.3600

Impurities	Maximum Limit percent
Water	0.2
Acidity (CH_3COOH)	0.02
Alkalinity	0.03 ml N/l
Non-Volatile Matter	0.0005
Aldehyde (HCHO)	0.002
Methanol (CH_3OH)	0.05

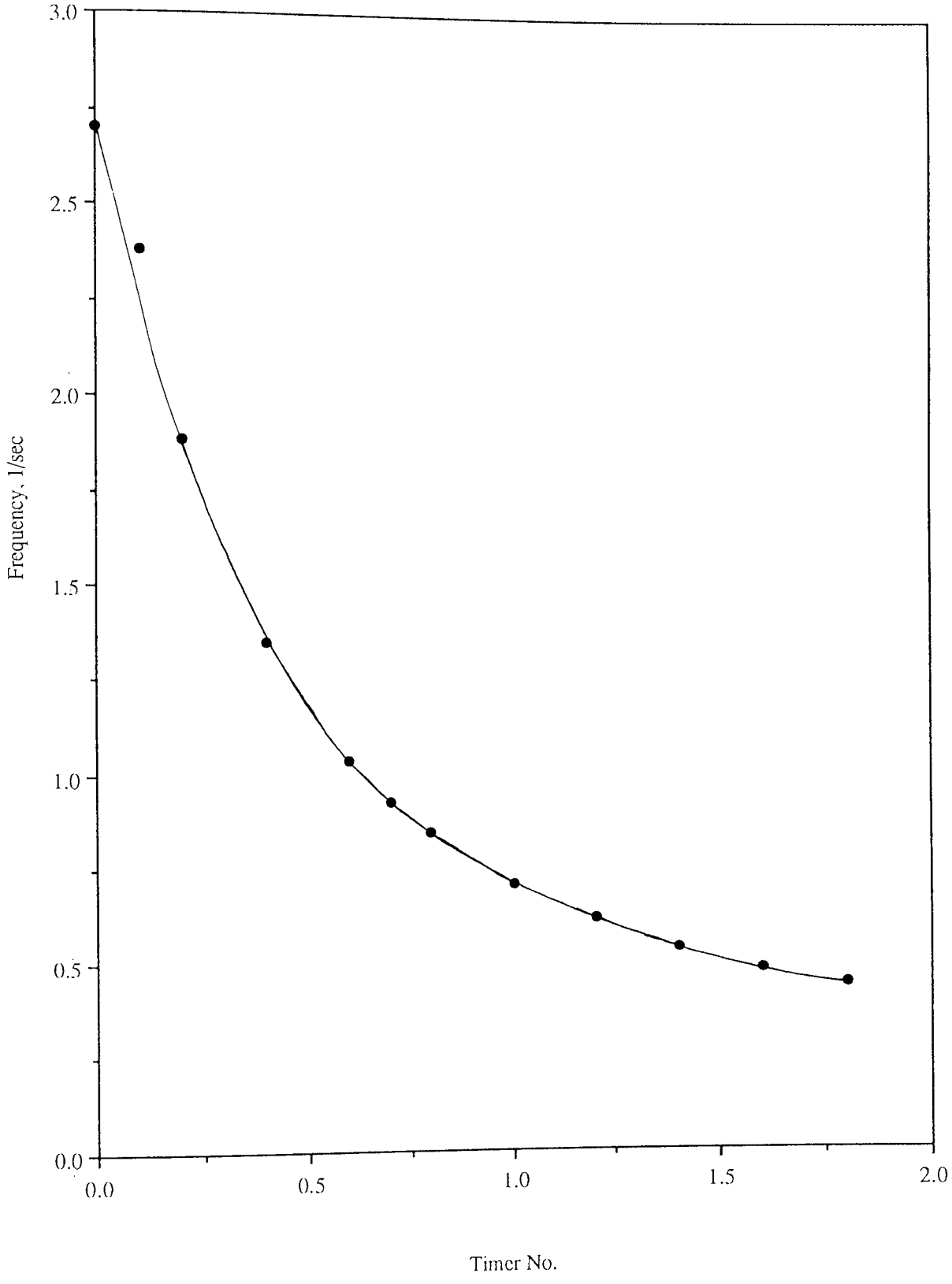

Figure A.1 Calibration Curve of Timer Number vs. Pulse Frequency

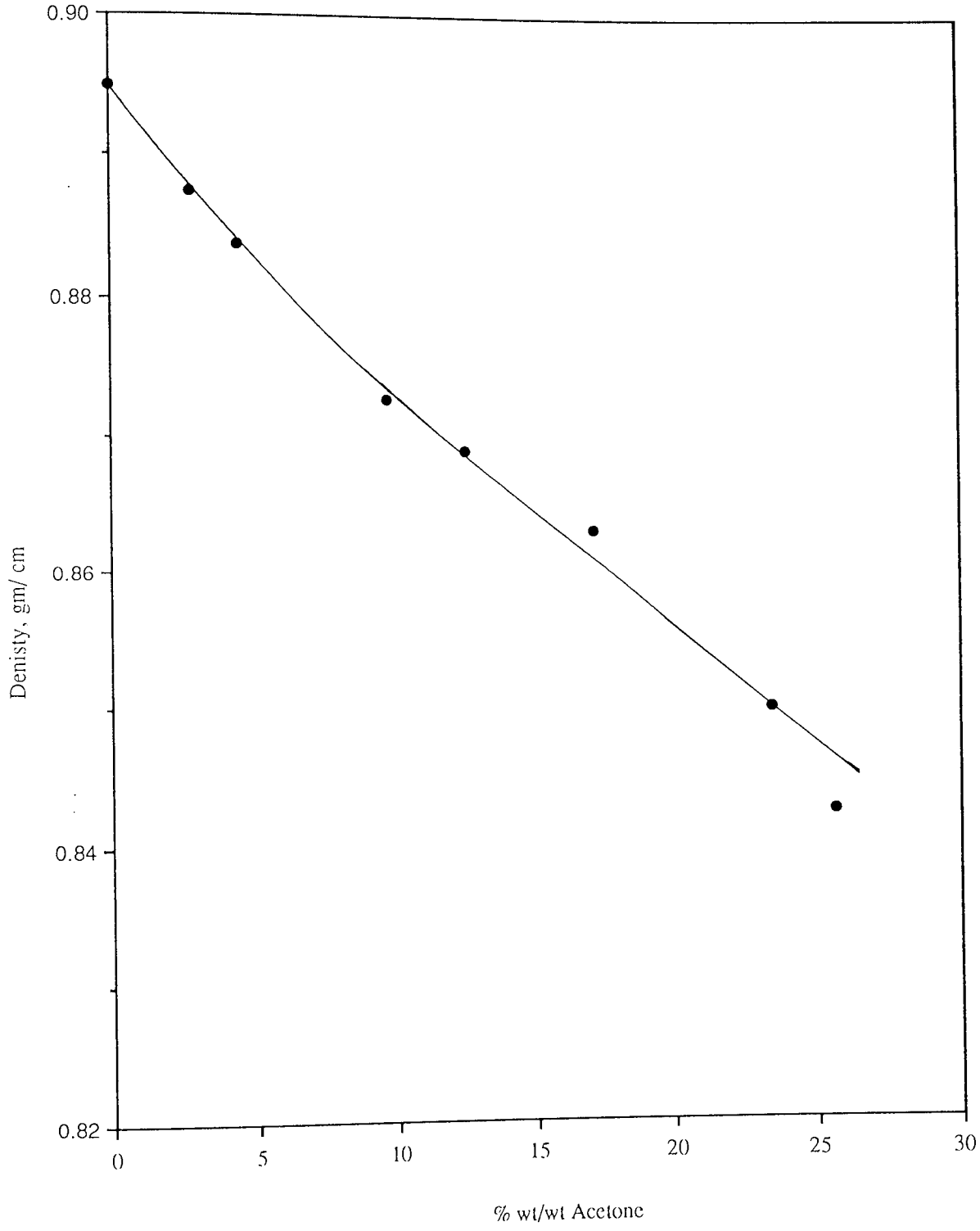

Figure A.2 Density vs. % Acetone Concentration in Dispersed Phase

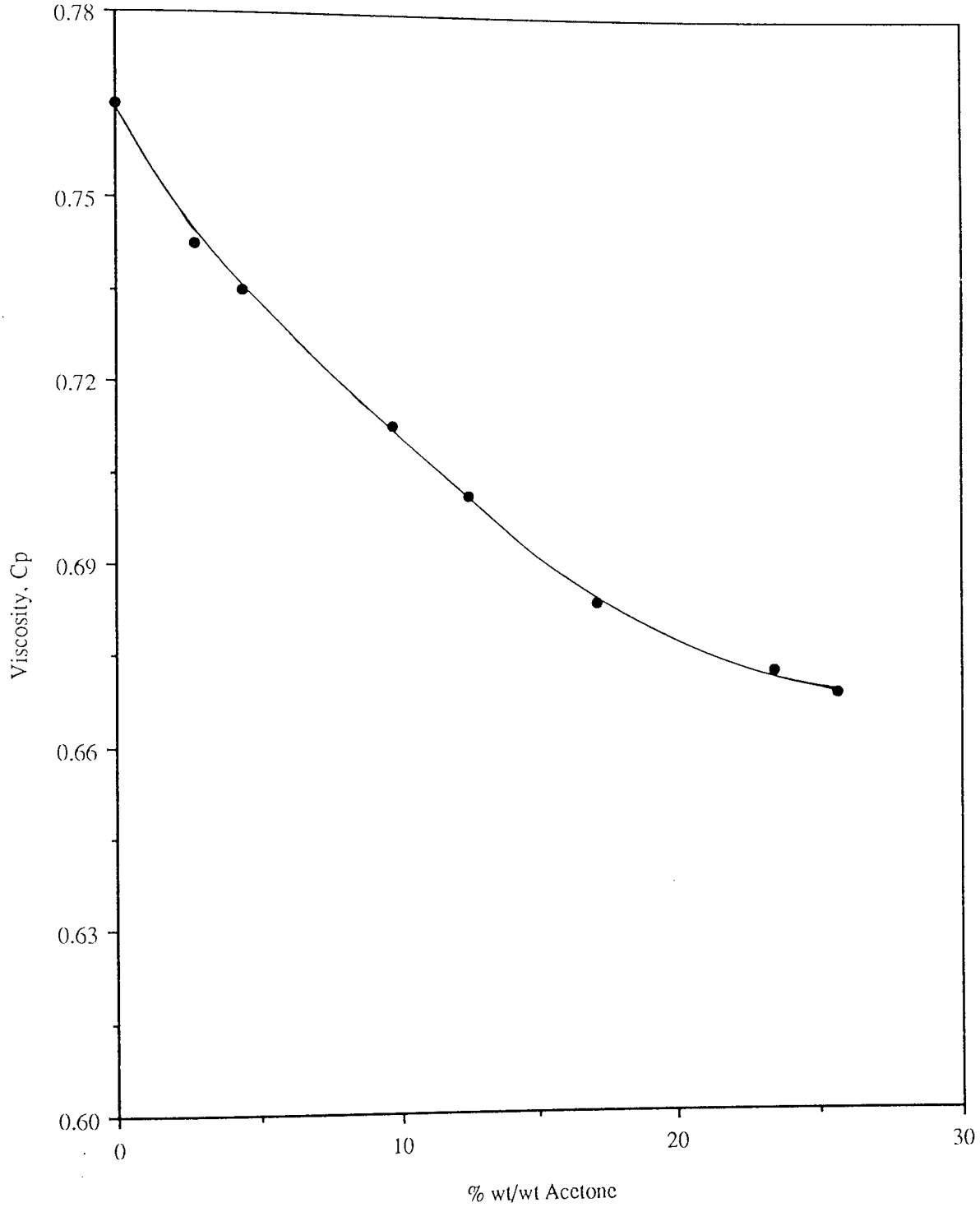

Figure A.3 Viscosity vs. % Acetone Concentration in Dispersed Phase

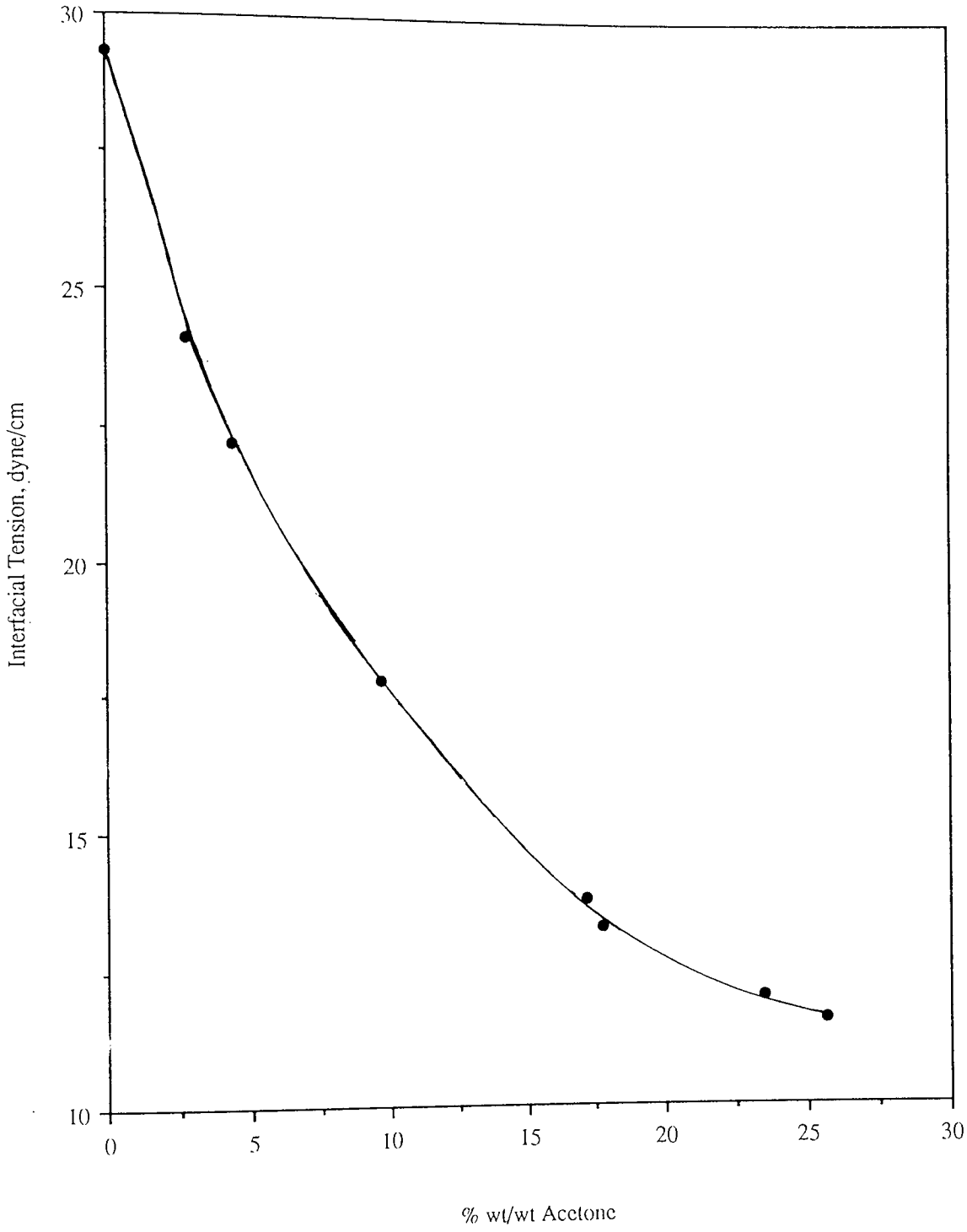

Figure A.4 Interfacial Tension vs. Acetone Percentage Concentration in Dispersed Phase.

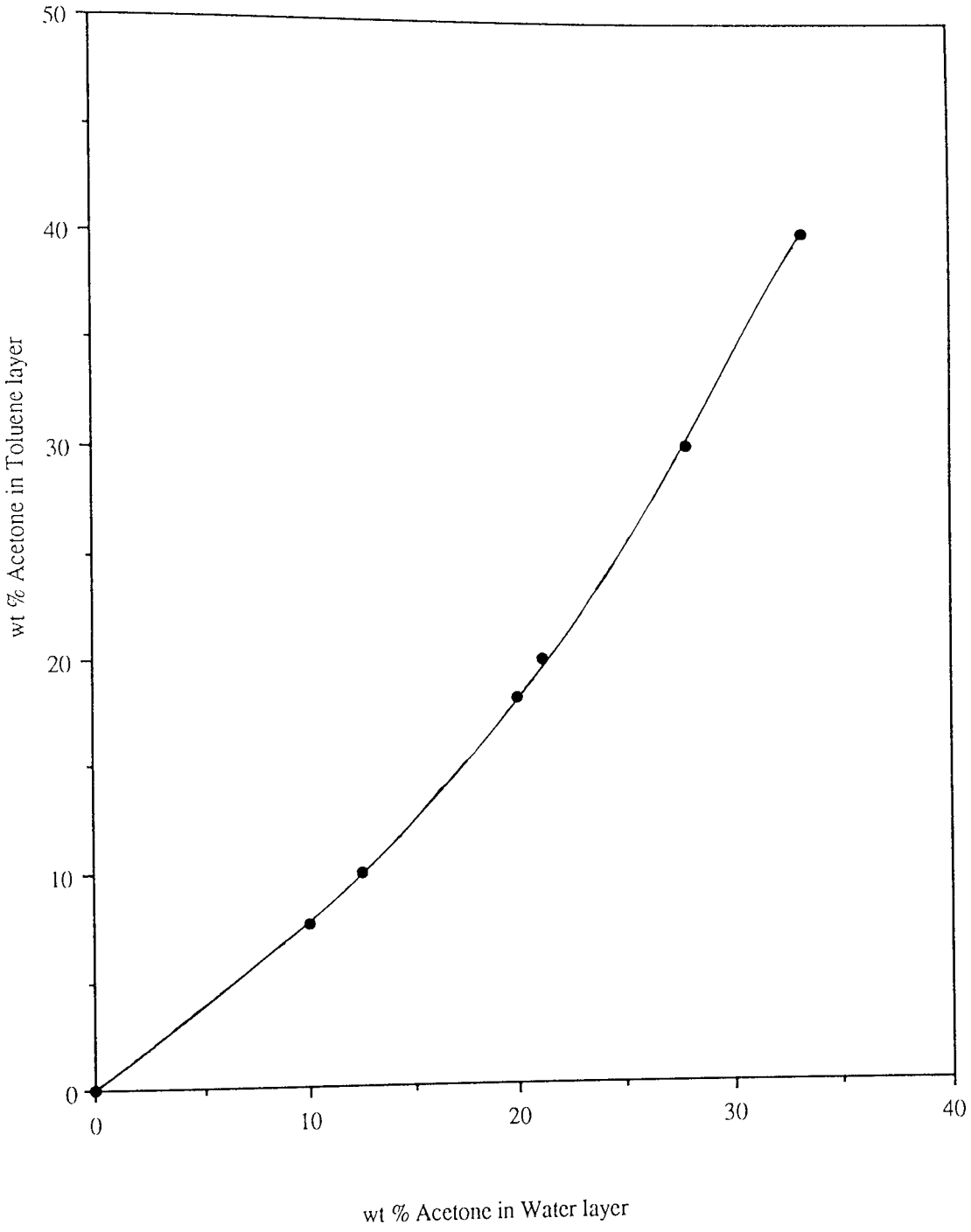

Figure A.5 Distribution of Acetone between Water & Toluene at 25 - 26 ^{o} C (3)

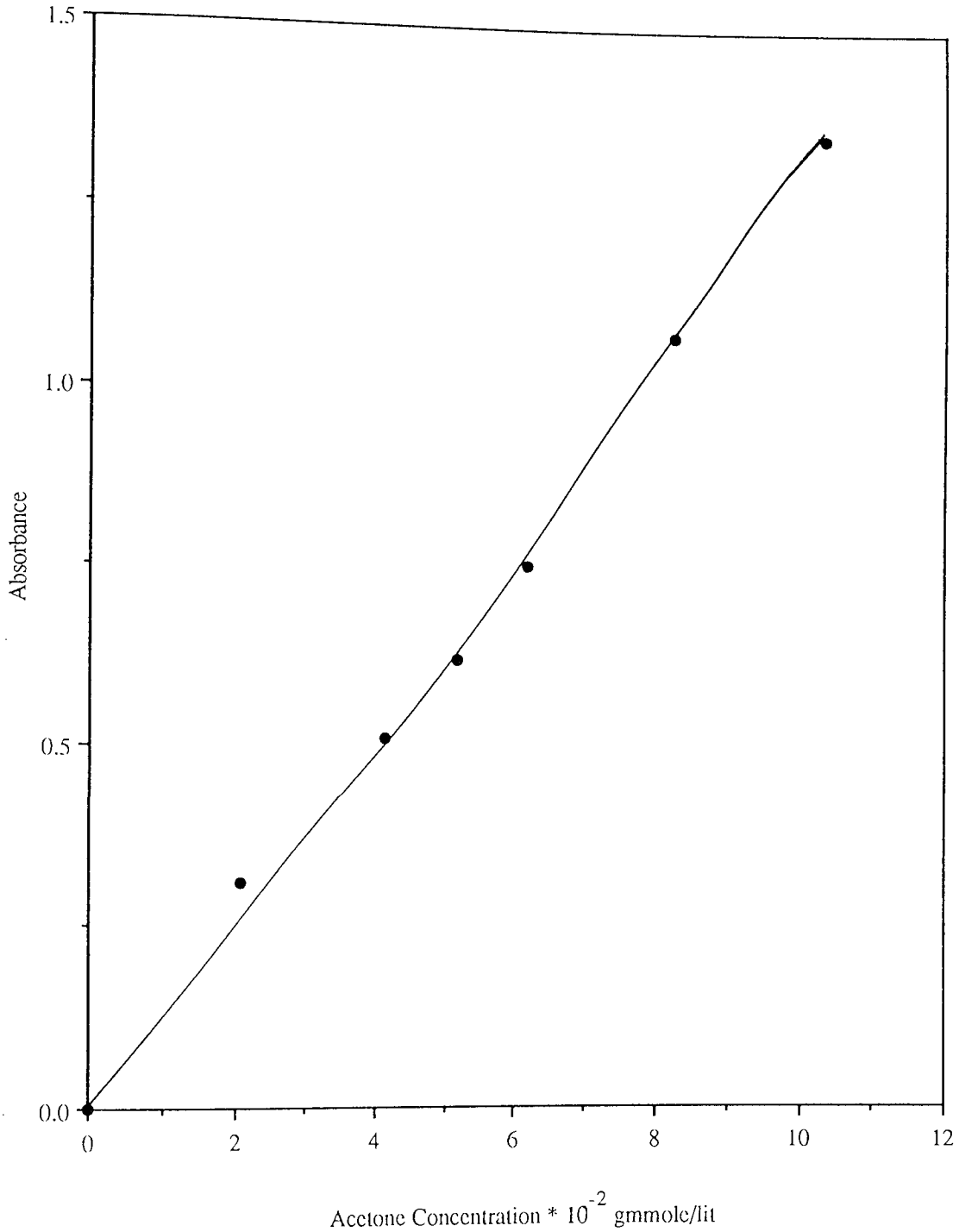

Figure A.6 Ultra-violet Spectrophotometry Calibration Curve for

Toluene layer at max. λ = 286 nm with 10 mm cell

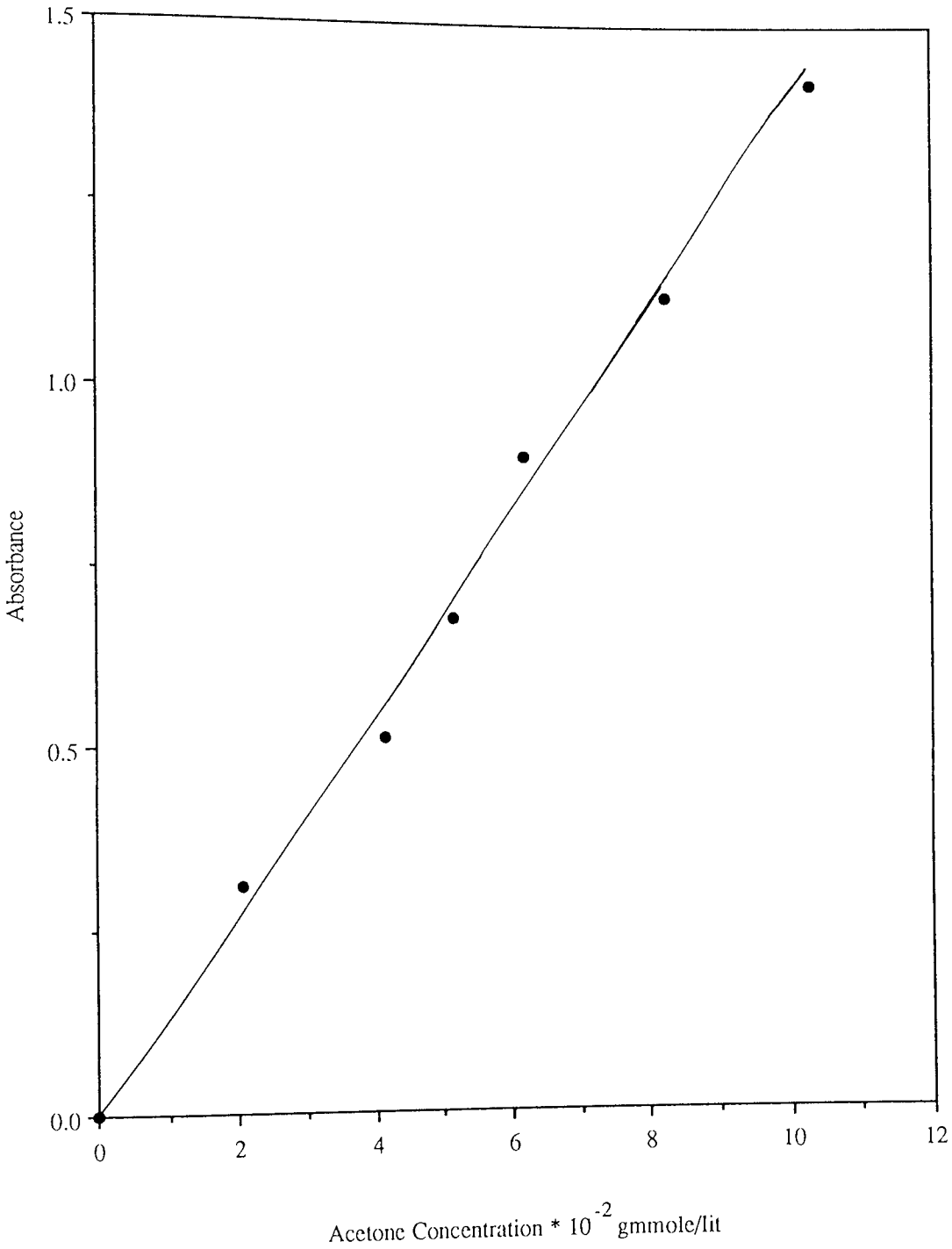

Figure A.7 Ultra-violet Spectrophotometry Calibration Curve for Water layer at max. $\lambda = 276$ nm with 10 mm cell

Appendix B.1.1 Data for pulse frequency = 0.54 Hz & no sieve plate

Time sec	Droplet Position in Column, cm			
	de = 0.46*	de = 0.39#	de = 0.42#	de = 0.62**
0.0	0.5	1.0	0.5	0.25
0.1	3.0	2.8	2.5	1.25
0.2	4.5	5.0	4.5	2.50
0.3	6.5	6.5	6.5	3.25
0.4	8.0	8.0	7.5	4.50
0.5	9.0	9.0	8.5	5.25
0.6	10.0	9.5	8.5	6.50
0.7	10.5	9.5	8.5	7.00
0.8	10.8	9.5	8.5	8.00
0.9	11.0	9.5	8.3	8.75
1.0	11.3	9.3	8.3	9.75
1.1	11.5	9.2	8.0	10.75
1.2	11.5	9.3	8.0	12.25
1.3	12.3	9.5	----	13.50
1.4	13.8	10.8	----	15.50
1.5	15.0	12.0	11.5	17.00
1.6	16.5	14.8	13.5	19.00
1.7	18.0	16.5	16.5	20.50
1.8	20.6	19.5	18.5	22.50
1.9	23.5	------	21.0	23.75
2.0	25.0	24.0	23.0	25.00
2.1	27.0	25.5	25.0	26.25
2.2	28.0	27.5	26.5	27.50
2.3	30.0	29.0	27.5	28.50
2.4	30.6	29.5	28.0	29.75
2.5	31.5	29.5	28.5	30.50
2.6	32.0	29.5	28.5	31.50
2.7	32.3	29.0	28.3	32.75
2.8	32.5	29.0	28.0	33.50
2.9	32.5	29.0	27.8	34.50
3.0	23.5	29.3	27.5	35.75
3.1	33.0	30.0	27.8	37.00
3.2	33.3	31.0	28.5	39.00
3.3	34.5	33.0	30.5	40.50
3.4	36.0	35.0	31.5	42.50
3.5	38.0	38.0	33.3	44.00
3.6	40.0	39.0	36.0	46.00
3.7	42.5	42.3	38.0	47.25
3.8	44.3	45.0	40.0	49.00
3.9	-----	47.0	43.5	50.00
4.0	-----	48.0	44.8	
4.1	46.5	49.5	46.5	
4.2	46.8	50.0	47.0	
4.3	47.0	50.0	47.8	
4.4		50.5	48.0	
4.5				

Amplitude * = 7.1 cm, # = 9.61 cm, ** = 3.25 cm

Appendix B.1.2 Data for pulse frequency = 0.62 Hz & no sieve plate

Time sec	Droplet Position in Column, cm					
	de = 0.5*	de = 0.44*	de = 0.46#	de = 0.50**	de = 0.62 ##	de = 0.60##
0.0	------	1.0	0.0	0.5	0.0	0.3
0.1	0.2	3.0	3.0	2.5	1.0	1.0
0.2	1.0	4.0	5.5	5.5	1.8	2.0
0.3	2.5	5.0	6.5	8.0	2.5	2.5
0.4	4.0	5.5	7.5	9.5	3.3	3.5
0.5	5.0	6.0	8.5	10.0	4.0	4.3
0.6	6.0	6.3	8.5	10.5	5.0	5.5
0.7	6.5	6.3	8.5	10.5	5.8	6.8
0.8	6.5	6.5	8.5	10.5	7.5	8.5
0.9	7.0	7.0	7.7	10.5	8.5	10.0
1.0	-----	7.5	8.3	10.5	10.5	12.0
1.1	------	9.0	8.8	10.5	12.0	13.3
1.2	------	10.5	9.5	11.5	14.0	15.0
1.3	------	12.5	11.5	13.5	15.5	16.3
1.4	10.0	14.5	13.0	15.5	17.5	17.8
1.5	11.5	16.5	16.0	18.5	18.5	18.5
1.6	14.0	18.5	18.0	20.5	20.0	20.0
1.7	15.5	20.5	21.0	22.5	21.3	20.8
1.8	18.0	21.5	23.5	25.5	22.5	21.5
1.9	20.0	22.5	25.0	27.5	23.5	22.3
2.0	21.5	23.5	26.0	-----	24.5	23.3
2.1	23.0	24.0	27.0	30.5	25.3	24.0
2.2	23.5	24.0	27.0	31.5	26.0	25.5
2.3	24.3	24.3	27.5	31.5	26.8	26.8
2.4	24.6	24.3	27.5	31.5	28.0	28.8
2.5	25.0	24.5	-----	31.5	29.0	30.0
2.6	25.3	-----	-----	31.5	31.0	32.3
2.7	25.6	26.0	-----	-----	32.3	33.8
2.8	------	27.5	-----	-----	34.5	35.5
2.9	-----	29.5	-----	33.5	36.0	37.0
3.0	27.6	31.5	-----	35.0	38.0	38.5
3.1	29.0	33.5	33.5	37.5	39.5	39.5
3.2	31.5	35.5	35.5	39.5	41.3	41.0
3.3	33.0	37.5	38.0	41.8	42.3	41.8
3.4	35.5	38.5	40.0	44.8	44.0	42.8
3.5	37.0	40.0	42.5	46.5	44.5	43.5
3.6	39.0	41.0	44.0		45.8	44.3
3.7	40.3	41.5	45.0		46.5	45.0
3.8	41.5	41.6	46.0		47.3	46.3
3.9	42.0	42.0	46.0		48.0	47.5
4.0	42.5	42.0	46.0		49.0	49.3
4.1	43.0	42.0	46.0		50.0	50.5
4.2	43.0	42.5	46.5			
4.3	43.0	44.0	46.5			
4.4	-----	-----	47.0			
4.5	43.5	46.5	48.0			

Amplitude * = 6.14 cm, # = 8.45 cm, ** = 8.67 cm, ## = 3.10 cm

Appendix B.1.3 Data for pulse frequency = 0.85 Hz & no sieve plate

Time sec	Droplet Position in Column, cm				
	de=0.53*	de =0.61*	de =0.59#	de =0.45#	de =0.53**
0.0	0.0	0.0	----	1.0	1.0
0.1	----	1.3	1.0	2.0	2.5
0.2	1.5	2.5	2.5	3.5	3.75
0.3	2.5	3.0	3.0	3.8	4.5
0.4	4.3	3.6	3.5	4.0	4.5
0.5	5.5	4.0	3.5	4.0	4.5
0.6	8.0	5.0	3.8	4.5	4.5
0.7	9.0	5.6	4.5	5.5	5.0
0.8	11.0	7.5	6.0	7.0	6.5
0.9	11.6	8.6	8.0	8.5	8.0
1.0	12.5	11.0	9.5	11.0	11.0
1.1	------	12.3	12.5	13.0	12.5
1.2	14.0	14.3	14.5	15.0	15.5
1.3	14.5	15.3	16.5	16.5	17.0
1.4	15.5	16.3	17.5	17.5	18.5
1.5	16.5	------	18.0	18.0	19.0
1.6	18.0	16.6	18.5	18.5	19.0
1.7	19.5	17.0	18.8	18.5	19.0
1.8	------	19.0	19.0	19.0	19.0
1.9	23.0	20.0	20.0	19.5	19.75
2.0	24.5	22.0	20.5	21.5	21.25
2.1	25.5	23.5	22.5	22.5	22.50
2.2	27.0	25.5	24.5	25.0	25.00
2.3	27.3	27.0	27.0	27.0	27.00
2.4	27.6	29.0	28.5	29.0	29.50
2.5	28.5	30.0	30.5	30.5	31.00
2.6	29.5	31.3	31.5	31.5	32.00
2.7	31.5	------	32.5	32.5	32.50
2.8	32.5	32.5	32.8	33.0	32.75
2.9	34.6	32.6	33.0	33.0	32.75
3.0	36.0	33.6	33.0	33.5	32.75
3.1	37.6	34.5	34.0	34.0	33.25
3.2	38.5	-----	35.0	35.0	34.50
3.3	39.5	37.5	37.0	36.0	36.00
3.4	-----	40.0	38.5	39.5	38.50
3.5	-----	41.5	41.0	41.0	40.50
3.6	40.5	43.5	43.0	43.5	43.50
3.7	-----	44.3	45.0	44.0	44.75
3.8	42.0	45.5	46.0	46.0	46.25
3.9	43.0	46.0	47.0	47.0	46.50
4.0	46.0	46.5	47.5	47.0	47.00
4.1	48.5	47.0	47.5	47.0	47.00
4.2	49.5	47.6	47.5	47.5	47.00
4.3	51.0	48.6	48.0	48.0	47.50
4.4		50.3	49.0		49.00
4.5			51.0		50.25

Amplitude * = 2.18 cm, # = 4.46 cm, ** = 4.9 cm

Appendix B.1.4 Data for pulse frequency = 1.04 Hz & no sieve plate

Time sec	Droplet Position in Column, cm					
	de = 0.46*	de = 0.58#	de = 0.59**	de = 0.41##	de = 0.45*#	de = 043#*
0.0	0.0	0.0	0.5	-----	0.0	1.75
0.1	2.5	2.0	1.8	1.5	1.3	2.75
0.2	3.5	3.5	2.5	2.5	1.8	3.75
0.3	4.5	5.0	4.0	3.5	2.3	4.25
0.4	5.0	6.0	5.3	3.8	3.0	4.5
0.5	5.5	6.5	6.8	4.0	4.8	4.75
0.6	6.0	6.5	9.5	4.3	5.8	5.5
0.7	7.5	7.0	10.5	4.8	8.3	7.0
0.8	8.5	8.0	11.5	5.8	10.0	10.0
0.9	10.5	9.5	12.5	7.5	12.0	------
1.0	12.0	11.0	13.8	9.3	12.8	13.0
1.1	13.0	15.5	14.5	11.3	14.0	14.0
1.2	14.0	15.0	16.3	12.3	14.3	15.75
1.3	15.5	16.5	17.5	13.5	14.8	15.0
1.4	16.0	17.0	19.0	13.8	15.3	15.25
1.5	16.5	18.0	20.0	14.0	16.8	15.75
1.6	17.5	------	21.8	14.0	18.3	17.0
1.7	19.0	19.0	22.8	14.8	20.3	18.25
1.8	20.5	20.0	24.0	15.8	21.8	20.5
1.9	22.5	21.5	25.0	17.5	-----	21.75
2.0	23.5	23.0	26.3	19.0	-----	23.5
2.1	24.0	25.5	27.3	20.8	25.3	24.5
2.2	25.0	27.0	29.0	21.8	25.8	25.25
2.3	25.5	28.5	30.0	22.8	26.8	25.5
2.4	26.3	29.0	31.5	23.0	27.3	25.75
2.5	26.6	29.5	33.0	23.5	28.8	26.25
2.6	27.5	29.5	34.5	24.5	30.0	-------
2.7	28.5	30.3	35.5	25.5	32.3	28.5
2.8	30.5	31.3	36.5	27.5	33.8	31.0
2.9	32.0	32.3	37.5	28.8	35.3	32.5
3.0	34.0	35.0	39.0	30.5	36.3	34.25
3.1	35.0	37.0	40.5	31.5	36.8	35.0
3.2	36.5	38.5	41.8	32.0	37.3	36.0
3.3	37.0	40.0	43.0	32.5	37.5	36.25
3.4	37.5	40.5	46.5	32.5	37.8	36.5
3.5	38.0	41.0	-----	32.8	39.8	37.0
3.6	39.5	41.3	-----	34.0	40.8	------
3.7	40.5	42.0	48.5	35.0	43.3	39.5
3.8	43.0	43.0	49.5	-----	44.8	42.0
3.9	45.0	44.0	51.0	-----	46.3	43.5
4.0	46.0	47.0		40.3	47.0	------
4.1	46.5	49.0		41.0		46.0
4.2	47.5	50.0		41.8		46.75
4.3	48.0	51.5		42.0		46.75
4.4	48.5			42.3		47.25
4.5	49.5			42.5		47.75

Amplitude * = 2.10 cm, # = 3.21 cm, ** = 0.71 cm, ## = 2.70 cm, *# = 2.57 cm, #* = 2.74 cm

Appendix B.1.5 Experimental velocities ratio $\frac{V_k}{V_t}$, with pulsation & no sieve plate

No.	Droplet diameter cm	Frequency sec^{-1}	Amplitude cm	$\frac{V_k}{V_t}$
1	0.27	0.83	4.86	0.912
2	0.29	0.62	6.71	0.955
3	0.30	0.62	6.90	0.972
4	0.31	0.70	6.46	0.909
5	0.32	0.83	4.80	0.976
6	0.32	0.70	7.00	0.918
7	0.32	0.70	5.14	0.982
8	0.33	0.83	4.80	0.973
9	0.33	0.70	6.46	0.886
10	0.34	0.70	7.00	0.887
11	0.34	0.70	4.94	0.924
12	0.34	0.70	4.94	0.964
13	0.35	1.03	2.11	0.968
14	0.35	0.83	4.74	0.974
15	0.36	1.03	2.11	0.967
16	0.39	1.03	2.74	0.992
17	0.40	0.62	6.91	0.974
18	0.40	0.62	6.91	0.954
19	0.40	0.54	9.61	0.911
20	0.41	1.03	2.74	0.939
21	0.41	0.62	8.67	0.981
22	0.41	0.54	9.61	0.909
23	0.42	0.83	3.37	0.979
24	0.42	0.62	6.23	0.993
25	0.43	1.03	1.78	0.971
26	0.43	1.03	1.86	0.945
27	0.43	0.83	3.29	0.986
28	0.43	0.62	6.23	0.896
28	0.44	1.03	1.86	0.982
30	0.44	1.03	2.74	0.899
31	0.44	0.83	3.29	0.883
32	0.44	0.62	6.23	0.960
33	0.45	0.83	3.37	0.943
34	0.45	0.83	4.46	0.990
35	0.45	0.70	7.70	0.916
36	0.45	0.70	7.70	0.930
37	0.45	0.54	7.09	0.977
38	0.46	0.62	6.23	0.924
39	0.47	1.03	1.50	0.871
40	0.47	0.62	6.14	0.901

Appendix B.1.5 continued

No.	Droplet diameter cm	Frequency sec^{-1}	Amplitude cm	$\frac{V_k}{V_t}$
41	0.48	1.03	1.50	0.910
42	0.48	1.03	1.50	0.896
43	0.48	0.70	4.51	0.943
44	0.48	0.70	4.94	0.971
45	0.49	1.03	2.10	0.932
46	0.49	1.03	2.10	0.916
47	0.49	0.70	6.43	0.911
48	0.49	0.62	6.14	0.897
49	0.49	0.62	6.84	0.990
50	0.49	0.54	7.09	0.937
51	0.495	0.70	6.43	0.975
52	0.50	1.03	2.10	0.932
53	0.51	0.83	2.18	0.931
54	0.51	0.62	6.14	0.904
55	0.51	0.62	6.14	0.861
56	0.52	0.70	3.45	0.942
57	0.53	0.83	4.90	0.977
58	0.53	0.70	3.45	0.969
59	0.53	0.70	3.45	0.939
60	0.575	1.03	3.21	0.984
61	0.58	1.03	3.21	0.969

Appendix B.2.1 . Dispersed phase mass transfer coefficient (kd)

Run No.	de cm	t_c sec.	Diffusivity $cm^2/sec * 10^5$	Dispersed phase mass transfer coefficient				
				Eq.4.13$_{* 10^4}$	Eq. 4.19 $* 10^2$	Eq. 4. $* 10^3$	Eq 4.17 $* 10^2$	Eq. 4. $* 10^3$
1P	0.33	6.00	2.18	4.347	2.864	1.182	2.078	1.138
2P	0.32	5.86	2.18	4.482	2.943	1.219	2.128	1.165
3P	0.32	5.70	2.18	4.482	2.984	1.219	2.187	1.198
4P	0.30	5.90	2.18	4.781	4.781	1.301	2.113	1.158
1P1	0.45	5.81	2.18	3.187	2.492	0.867	2.146	1.176
2P1	0.44	6.24	2.16	3.230	2.421	0.879	1.986	1.087
3P1	0.44	5.70	2.17	3.245	2.539	0.883	2.184	1.193
4P1	0.31	7.53	2.16	4.584	2.625	1.247	1.651	0.903
5P1	0.30	7.17	2.16	4.737	2.735	1.289	1.739	0.948
6P1	0.36	6.16	2.17	3.966	2. 700	1.079	2.018	1.102
7P1	0.36	6.24	2.17	3.966	2.682	1.079	1.995	1.090
8P1	0.36	6.37	2.17	3.966	2.655	1.079	1.954	1.069
9P1	0.32	6.27	2.16	4.441	2.832	1.208	2.359	1.287
10P1	0.32	6.29	2.16	4.431	2.824	1.205	1.976	1.077
11P1	0.32	6.31	2.16	4.441	2.823	1.208	1.970	1.075

Appendix B.2.2. Continuous phase mass transfer coefficient (kc)

Run No.	de cm	$(Re)_c$	Continuous phase mass transfer coefficient			
			Eq.4. $*10^3$	Eq. 4.29 $*10^4$	Eq. 4.30 $*10^3$	Eq 4.32 $*10^3$
1P	0.33	335	0.360	0.760	1.093	1.098
2P	0.32	332	0.370	0.780	1.093	1.127
3P	0.32	342	0.375	0.792	1.108	1.143
4P	0.30	309	0.380	0.794	1.127	1.127
1P1	0.45	471	0.313	0.661	0.915	0.945
2P1	0.44	429	0.305	0.645	0.861	0.925
3P1	0.44	470	0.320	0.675	0.935	0.965
4P1	0.31	251	0.331	0.700	0.991	1.022
5P1	0.30	255	0.345	0.729	1.031	1.064
6P1	0.36	355	0.340	0.717	1.002	1.034
7P1	0.36	351	0.338	0.713	0.997	1.029
8P1	0.36	344	0.334	0.706	0.987	1.019
9P1	0.32	370	0.357	0.824	1.149	1.186
10P1	0.32	310	0.357	0.754	1.058	1.092
11P1	0.32	309	0.375	0.753	1.057	1.090

$(Sc)_c$ is equal to 812

Appendix B.2.2. (continued)

Run No.	de cm	$(Re)_c$	Continuous phase mass transfer coefficient				
			Eq.4.33 $*10^3$	Eq. 4.35 $*10^2$	Eq. 4.37 $*10^2$	Eq 4.38 $*10^2$	Eq 4.40 $*10^2$
1P	0.33	335	2.109	1.120	1.515	1.940	1.526
2P	0.32	332	2.165	1.150	1.553	1.990	1.563
3P	0.32	342	2.197	1.167	1.583	1.990	1.597
4P	0.30	309	2.228	1.183	1.581	1.929	1.584
1P1	0.45	471	1.834	0.974	1.379	2.334	1.413
2P1	0.44	429	1.790	0.950	1.330	2.309	1.358
3P1	0.44	470	1.873	0.995	1.408	2.309	1.443
4P1	0.31	251	1.943	1.032	1.332	1.959	1.315
5P1	0.30	255	2.024	1.075	1.391	1.929	1.375
6P1	0.36	355	1.990	1.057	1.442	2.101	1.457
7P1	0.36	351	1.979	1.051	1.431	2.101	1.445
8P1	0.36	344	1.959	1.040	1.413	2.101	1.425
9P1	0.32	370	2.286	1.214	1.666	1.990	1.687
10P1	0.32	310	2.092	1.111	1.485	1.990	1.489
11P1	0.32	309	2.089	1.109	1.482	1.990	1.485

$(Sc)_c$ is equal to 812

APPENDIX C

SAMPLE OF CALCULATIONS

C.1 Derivation of the Maximum Local Kinetic Energy Dissipation

C.2 Overall Mass Transfer Coefficient During Droplet Formation

a. Experimental Values

b. Predicted Values

C.3 Overall Mass Transfer Coefficient During Droplet Ascent

a. Experimental Values

b. Predicted Values

b.1 Stagnant Droplet

b.2 Circulating Droplet

i. Laminar Circulation

ii. Turbulent Circulation

C.1 Derivation of the Maximum Local Kinetic Energy Dissipation and Droplet Diameter Correlation Based on this Concept

According to the theory of the local structure of turbulent pulsation the breakup process may be governed by several mechanisms, depending on the type of forces which control this process (195, 196, 197). For sufficiently high turbulence intensity, assuming that the mechanism based on capillary and the dynamic forces acting on a single droplet controlled the dispersion process in liquid-liquid system (191, 193).

Based on the above mechanism, the maximum stable droplet diameter is given by the following equation;

$$d_{max} = k_1 \left(\frac{\sigma}{\rho_c}\right)^{0.6} \left(\frac{l}{U^3}\right)^{0.4} \qquad C.1$$

where:-

l	equivalent radius of the plate hole
U	maximal flow velocity

Equation C.1 has been presented(65) in another form as follows:-

$$d_{max} = k'_1 \left(\frac{\sigma}{\rho_c}\right)^{0.6} \left(\frac{l}{\psi}\right)^{0.4} \qquad C.2$$

Let:-

$$l = \frac{d_h}{2}$$

and

$$U = \frac{A_p * f}{\phi}$$

By combining equations C.2 & C.3, one gets the following equation;

$$\psi = k_2 \frac{\left(\frac{A_p * f}{\phi} \right)^3}{\frac{d_h}{2}} \qquad \text{C.3}$$

substitute equation C.3 into equation C.2, one obtains the follows:-

$$d_{max} = k_3 \left(\frac{\sigma}{\rho_c} \right)^{0.6} \left\{ d_h \left(\frac{\phi}{A_p * f} \right)^3 \right\}^{0.4} \qquad \text{C.4}$$

From a practical point view, the mean volume-surface (Sauter) diameter d_{32} is more important than the maximum diameter d_{max}. Unfortunately, the information about the relation between d_{32} and d_{max} is very little. According to certain experimental results of droplet formation in agitated vessel the ratio (d_{32}/d_{max}) varies between 0.38 and 0.67 (193, 194).

Therefore, d_{32} may be calculated using the following equation;

$$d_{32} = k_4 \left(\frac{\sigma}{\rho_c} \right)^{0.6} \left\{ d_h \left(\frac{\phi}{A_p * f} \right)^3 \right\}^{0.4} \qquad \text{C.5}$$

and

$$e_m = \left(\frac{\{A_p * f\}^3}{d_h \phi^3} \right) \qquad \text{C.6}$$

C.2 Overall Mass Transfer Coefficient During Droplet Formation

All the calculations are, for example, based upon the data relevant to Run 7P

a. Experimental

$$N_f = K_{df} A_{mf} \Delta C \qquad 1.1$$

where:-

$N_f = f_d (C_o - C_1) = 2.07 * 10^{-2} (1.02 - 0.76) = 5.382 * 10^{-3}$ gmole/ sec

and

$$A_{mf} \frac{3}{5} \pi^{\frac{1}{3}} \left\{ 6 t_f f_d \right\}^{\frac{2}{3}}$$

$$A_{mf} \frac{3}{5} \pi^{\frac{1}{3}} \left\{ 6 * 1.18 * 2.07 * 10^{-2} \right\}^{\frac{2}{3}} = 0.24 \text{ cm}^2$$

$\Delta C = (1.02 - 0.00)$

By substituting the above values into equation 1.1, the value of K_{df} may be obtained

$K_{df} = 2.20 * 10^{-2}$ cm /sec

b. Predicted

i. Johnson and Hamielec's (79) correlation (4.9) to calculate the efficiency during droplet formation:-

$$E_m = \frac{C_o - C_1}{C_o - C^*} = \frac{20.6}{d_e} \left\{ \frac{D_d t_f}{\pi} \right\}^{0.5}$$

$$E_m = \frac{20.6}{0.36}\left\{\frac{2.19*10^{-5}\ 1.18}{\pi}\right\}^{0.5} = 0.164$$

where C_1 may be calculated as follows;

since

$$0.164 = \frac{1.02 - C_1}{1.02 - 0.00}$$

then

$C_1 = 0.853$ gmole/ lit

By substituting C_1 into equation 1.1, the value of K_{df} may be obtained as follows:-

$$N_f = K_{df}\ A_{mf}\ \Delta C$$

where:-

$$N_f = \frac{\pi\ d^3}{6\ t_f}\left\{\ 1.02 - 0.853\ \right\}$$

$$= \frac{\pi\ 0.36^3}{6 * 1.18} * 0.167$$

$$= 0.346 \text{ gmole/ sec}$$

and

$$o.346 = K_{df} * 0.24\ (\ 1.02 - 0.00\ )$$

$K_{df} = 1.41$ cm /sec

C.3 Overall Mass Transfer Coefficient During Droplet Ascent

a. Experimental

$$N_t = K_{exp}\, A\, \Delta C$$

1.1

where:-

$N_t = f_d\,(C_2 - C_3) = 2.07 * 10^{-2}\,(0.76 - 0.35) = 8.487 * 10^{-4}$ gmole/ sec

and

$$A = \frac{\pi}{2}\left\{\frac{d_H^2}{4} + \frac{d_V^2}{2E}\ln\left\{\frac{1+E}{1-E}\right\}\right\} \qquad 7.26$$

$$A = \frac{\pi}{2}\left\{\frac{0.39^2}{4} + \frac{0.33^2}{2 * 0.533}\ln\left\{\frac{1+0.533}{1-0.533}\right\}\right\} = 0.429\ cm^2$$

$\Delta C = (0.76 - 0.00)$

By substituting the above values into equation 1.1, the value of K_{dexp} may be obtained

$K_{dexp} = 3.00 * 10^{-2}$ cm /sec

b. Predicted

b.1 Stagnant Droplet

The efficiency of mass transfer was calculated using Newman's (121) correlation (4.12)

$$E_m = \frac{C_1 - C_2}{C_1 - C^*} = \pi \left\{ \frac{D_d t_e}{r^2} \right\}^{0.5}$$

where:-

$$t_e = \frac{d_e}{U_t}$$

therefore

$$E_m = 1.59 * 10^{-2}$$

$$1.59 * 10^{-2} = \frac{0.76 - C_2}{0.76 - 0.00}$$

$$C_2 = 0.748 \text{ gmole / lit}$$

$$2.07 * 10^{-2} (0.76 - 0.748) = K_d \, 0.29 (0.76 - 0.00)$$

$$K_d = 1.13 * 10^{-3} \text{ cm/ sec}$$

b.2 Laminar Circulation

$$E_m = \frac{C_1 - C_2}{C_1 - C^*} = \pi \left\{ \frac{R D_d t_e}{r^2} \right\}^{0.5}$$

$$E_m = \pi \left\{ \frac{2.25 * 2.17 * 10^{-5} t_e}{0.18^2} \right\}^{0.5} = 2.385 * 10^{-2}$$

$$2.385 * 10^{-2} = \frac{0.76 - C_2}{0.76 - 0.00}$$

$C_2 = 0.742$ gmole/ lit

$2.07 * 10^{-2} (0.76 - 0.742) = K_d \, 0.29 \, (0.76 - 0.00)$

$K_d = 1.69 * 10^{-5}$ cm /sec

By using equations 4.37, 4.39, 4. 40 & 4.42 to calculate k_c and equations 4.17 & 4.24 to calculate k_d

where:-

$$Re_c = \frac{d_e U_t \rho_c}{\mu_c} = 351$$

$$Sc_c = \frac{\mu_c}{\rho_c D_c} = 816$$

$$Ga = \frac{d_e^3 g \rho_c^2}{\mu_c^2} = 49.6 * 10^4$$

$$k_c = \frac{D_c}{d_e} \left\{ 0.6 \, Re^{0.5} \, Sc^{0.5} \right\}$$

$$k_c = \frac{1.178 * 10^{-5}}{0.36} \left\{ 0.6 * 351^{0.5} * 816^{0.5} \right\} = 1.051 * 10^{-2} \text{ cm/sec}$$

$$k_c = \frac{D_c}{d_e}\left\{ -126 + 1.8\, Re^{0.5} Sc^{0.42}\right\}$$

$$k_c = \frac{1.178*10^{-5}}{0.36}\left\{ -126 + 1.8 * 351^{0.5} * 816^{0.42}\right\} = 1.431 * 10^{-2} \text{ cm/sec}$$

$$k_c = \frac{D_c}{d_e}\left\{ 1.04\ Ga^{0.49}\right\}$$

$$k_c = \frac{1.178*10^{-5}}{0.36}\left\{ 1.04 * \left(49.6 * 10^{4}\right)^{0.49}\right\} = 2.1 * 10^{-2} \text{ cm/sec}$$

$$k_c = \frac{D_c}{d_e}\left\{ -178 + 3.62\, Re^{0.5} Sc^{0.33}\right\}$$

$$k_c = \frac{1.178*10^{-5}}{0.36}\left\{ -178 + 3.62 * 351^{0.5} * 816^{0.33}\right\} = 1.445 * 10^{-2} \text{ cm/sec}$$

$$k_d = 3.75 * 10^{-3} U_t \left\{ \frac{\mu_c}{\mu_c + \mu_d}\right\}$$

$$k_d = 3.75 * 10^{-3} \frac{58.5}{6.24}\left\{ \frac{9.58*10^{-3}}{9.58*10^{-3} + 7.30*10^{-3}}\right\} = 1.995*10^{-2}$$

The overall mass transfer coefficient of dispersed phase may be calculated by substituting the values of k_d & k_c into equation 1.2.

NOMENCLATURE

A	Surface area of droplet, cm^2 (7.26)
A_p	Amplitude of pulse (full travel), cm
A	Constant = $\frac{3 \mu \pi d}{(1 + 1/N)}$
A_{mf}	Average mean surface area during formation, cm^2 (7.25)
a	Constant = $\frac{3 \rho_c \lvert \rho_p - \rho_c \rvert C_D}{\left[2 \left(\rho_p + 0.5 \rho_c \right)^2 R \omega^2\right]}$
a	Semi-axes of spheroid in x direction, cm
b	Semi-axes of spheroid in y direction, cm
b	Constant = $\frac{V_k^2}{\sqrt{0.905 \frac{d_h}{\phi}}}$
C	Concentration, gmmole/ lit. & gm/ cm^3
C_o	Orifice discharge coefficient
C_i	Initial concentration
C*	Equilibrium concentration
Ç	Constant = 4.98 ± 2.28, equation 8.1
C_D	Drag coefficient
C'_D	Drag coefficient in equation 3.30
ΔC	Concentration different
c	Semi-axes of spheroid in z direction, cm
D	Diffusivity, cm^2/ sec
D_c	Diffusivity of continuous phase
D_d	Diffusivity of dispersed phase

D_E	Effective diffusivity
DR	Diameter ratio, equations 2.16-2.18
d	Diameter of droplet , cm
d_e	Equivalent diameter of droplet, cm
d_{crit}	Critical droplet diameter, cm
d_H	Horizontal droplet diameter, cm
d_h	Diameter of hole plate
d_T	Diameter of column, cm
d_V	Vertical droplet diameter, cm
d_{32}	Sauter-mean diameter of droplet
E	Eccentricity of droplet
E_m	Extraction efficiency
E_v	Friction loss, equation 7.22
e_m	Maximum local kinetic energy dissipation, equations 3.19 & 3.25
e_v	Friction loss factor, equation 7.23
F	Drag force
F_p	Form drag (2.1)
F_T	Total drag (2.3)
F_μ	Viscous drag (2.2)
f	Frequency of pulse, 1/sec
$f*A_p$	Intensity of pulse, cm/sec
$(f*A_p)_{crit}$	Critical intensity of pulse, cm/sec
f_c	Correlation factor, equation 4.36

f_c	Flow rate of continuous phase
f_d	Flow rate of dispersed phase
g	Acceleration of gravity, cm/sec
H	Constant
H	Column hieght, cm
h_c	Plate spacing
J	Constant
K	Overall mass transfer coefficient, cm/sec
K_{df}	Overall mass transfer coefficient of droplet during formation
k	Individual mass transfer coefficient, cm/sec
k_1&k_2	Constant, equation 3.51
k_4	Constant, equation 3.24
k_8	Constant, equation 7.30
M	Molecular wieght
M'	$\text{Constant} = 0.084 \left\{ \frac{\mu_c}{\mu_d} \right\}^{0.26} P^{0.17}$
m&m	Distribution coefficient
m	Constant, equation 4.30
m'	Constant, equation 3.44
N, N_t, N_f	Mass transfer rates, gmole/sec
N_A	Interfacial flux in solute,gmoles/sec
N	Number of plates
n	Constant, equation 4.30
P	Physical property group
P	Pressure

q $$\text{Constant} = \frac{3\rho_c \left| \rho_p - \rho_c \right| C_D A_p}{\left[4 \left(\rho_p + 0.5\ \rho_c \right)^2 R \right]}$$

R Constant effective diffusivity, equation 4.15

R&r Radius of droplet, cm

S Total area of sieve plate, cm^2

T Temperature, ^oK

t Time, sec

t_e Time of contact during travel, sec

t_f Time of formation, sec

V Molal Volume of solute, equation 5.1

V Volume of droplet, cm^3

V Volume of Extractor

V Velocity of droplet, cm/sec

V_k Characteristic velocity, cm/sec

V_{crit} Critical velocity of droplet

V_p Volume of particle

V_p Superficial velocity

V_{pl} Velocity due to pulsation

V_s Slip velocity

V_{stokes} Velocity of droplet, equation 2.6

V_t Terminal velocity

U_o Pulse velocity, cm/sec, equation 3.6

U_o Orifice velocity, cm/sec, equation 3.9

x Hold-up

x Virtual mass coefficient, for spheres = 0.5

Dimensionless Groups

$\ddot{Eo}$ Eotvos number = $\frac{g \Delta\rho d^2}{\sigma}$

$(\ddot{Eo})_{crit}$ Critical Eotvos number = $\frac{g \Delta\rho d_{crit}^2}{\sigma}$

Ga Galileo number = $\frac{d^3 \rho^2 g}{\mu^2}$

M Morton number = $\frac{g \mu^4 \Delta\rho}{\rho^2 \sigma^3}$

P Physical property group = $\frac{\sigma^3 \rho_c^2}{g \Delta\rho \mu_c^4}$

Pe Peclet number = $\frac{d_e V}{D}$

Re Reynolds number = $\frac{d_e V \rho}{\mu}$

$\dot{Re}$ modified Reynolds number = $\frac{d_e^2 \omega \rho_c}{\mu_c}$

Sc Schmidt number = $\frac{\mu}{\rho D}$

Sh Sherwood number = $\frac{k d_e}{D}$

We Weber number = $\frac{d_e V^2 \rho}{\sigma}$

$(We)_{crit}$ Critical Weber number = $\frac{d_{crit} V_{crit}^2 \rho}{\sigma}$

Functions

A_n Function of k_c

h Function of $\left\{ \frac{\mu_c}{\mu_c + \mu_d} \right\}$, equation 4.38

λ_n Function of k_c

Greek Letters

ρ Density, gm/cm^3

μ Viscosity, C_p

$\Delta\rho$ $= (\rho_c - \rho_d)$, gm/cm^3

σ Interfacial tension, dyne / cm

ω Angular velocity = $2\pi f$

ω Frequency of oscillation, rad/sec or sec^{-1}

ψ Energy dissipation, cm^2/sec^3

ϕ Free area of sieve plate

ξ $= \rho_d / \rho_c$

β_c $$\text{Constant} = \frac{\phi^2}{\{1-\phi\}\{1-\phi^2\}}$$

γ_c $$\text{Constant} = \frac{5\pi^2}{6\sqrt{2}} \frac{1+\frac{h_c}{H}}{C_o}$$

Subscript

A	Component A
a	Average
c	Continuous phase
cal.	Calculated value
corr.	Correlated value
D,d	Dispersed phase
df	During droplet formation
E	Extract phase
e	Equivalent
f	Final, formation
h	Horizontal
HB	Handlos & Baron
max	Maximum
min	Minimum
obs.	Observed value
i	Initial
R	Raffinate phase
s	Sphere

t	During droplet travel
T	Column
theo	Theoretical value
-	Average
*	Equilibrium

REFERENCES

1. Al-Aswad, K.K.M.
"Liquid Liquid Extraction in a Pilot Scale Rotating Disc Contactor"
Ph.D. Thesis, University of Aston in Birmingham, UK (1982).

2. Al-Aswad,K.K.M., Mumford, C.J. and Jeffreys, G.V.
A.I.Ch.E.J. 9, 1488 (1985).

3. Al-Faize, M.M.
"Mass Transfer Characteristics of Large Oscillating Drops"
Ph.D. Thesis, University of Aston in Birmingham, UK (1986).

4. Al-Hassan, T.S.
"Mass Transfer from Large Oscillating Drops"
Ph.D. Thesis, University of Aston in Birmingham, UK (1979).

5. Al-Hemiri, A.A.
"The Effect of Surface Renewal on Mass Transfer in Agitated Contactor "
Ph.D. Thesis, University of Aston in Birmingham, UK (1973).

6. Amundson, N.R.
" The Mathematical Understanding of Chemical Engineering System "
Aris, R. and Varma, A., Eds, Pergamon Press, UK (1980).

7. Angelo, J.B., Lightfoot, E.N. and Howard, D.W.
A.I.Ch.E.J. 12, 751 (1966).

8. Assenov, A., Penchev, I.
I. Compte rendu de 1' Academie Bulgare des Science
vol. 24, No. 10, 1381 (1971).

9. Bailes, P.J. and Thornton, J.D.
Proc. I.S.E.C. 71, Vol.2, 1431, London (1971).

10. Baird, M.H., Senior, M.G. and Thompson, R.T.
Ch. Eng. Sci. 22, 551 (1967).

11. Baird, M.H. and Ritcey, G.M.
Proc. I.S.E.C. 74, Vol.2, 1571 (1974).

12. Batey, W., Arthur, T., Thompson, P.J. and Thornton, J.D.
Proc. I.S.E.C. 83, 2, 166 (1983).

13. Batey, W., Thompson, P.J. and Thornton, J.D.
I. Ch. E. Symp. 103, 133 (1987).

14. Billerbeck, C.J., Farquhar III, J., Reid, R.C., Bresee, J.C. and Hoffman, A.S.
Ind. Eng. Chem. 48, 2, 183 (1956).

15. Bird, R.B., Stewart, W.E. and Lightfoot,E.N.
" Transport Phenomena " Wiley, NY (1960).

16. Blass, E.
Int. Ch. Eng. 30, 2, 206 (1990).

17. Bond, W.N. and Newton, D.A.
Phil. Mag. 5, 69 (1962).

18. Bonnet, J.C. and Jeffreys, G.V.
A.I.Ch.E.J. vol.31, No. 5, 778 (1985).

19. Bonnet, J.C. and Jeffreys, G.V.
A.I.Ch.E.J. vol.31, No. 5, 795 (1985).

20. Boussinesq, J.
C.R. Acad. Sci., 156, 1124, 1130 (1913).
"Bubbles, Drops and Particles"
Clift, R. et al , Eds, Pub. Academic Press, London (1978).

21. Boyadziev, L. and Spassov, M.
Ch. Eng. Sci. 37, 2 , 337 (1982).

22. Bronswerk, P.C.E.
"The Bronswerk Technical Bulletin on Pulsed Packed Column"
In Sec. 1.10 "Handbook of Separation Techniques for Chemical Engineers" by Schweitzer, P.A., Ed, McGraw-Hill 2nd edn. (1988).

23. Brounshtein, B.I. and Simakova, I.V.
Ch. Abs. 87, 7988 (1977).

24. Brunson, R.J. and Wellek, R.M.
Can. Ch. Eng. J. 48, 266 (1970).

25. Brush, L.M., Ho, H. and Singamsetti, S.R.
Iowa A.S.H. Commission on Land Erosion, 59, 293 (1963).

26. Calderbank, P.H. and Korchinski, I.J.O.
Ch. Eng. Sci. 6, 65 (1956).

27. Caly, P.H., from, Collins, S.B. and Knudsen, J.G."
A.I.Ch.E.J. 16, 6, 1072 (1970).

28. Chang, L.S. and Berg, J.C.
Proc. I.S.E.C. 83, Vol.1, 50, (1983).

29. Carra, S. and Morbidelli, M.
In"Handbook of Heat and Mass Transfer" Chapter 4
Cheremishisionoff, N.P. Ed., Gulf Pub. (1986).

30. Chonowski, A. and Anglino, H.
Can. J. Ch. Eng. 50, 23 (1972).

31. Clark, M.M.
Ch. Eng. Sci. vol. 43, No. 3, 681 (1988).

32. Clift, R., Grace, J.R. and Weber, M.E.
"Bubbles, Drops and Particles"
Pub. Academic Press, London (1978).

33. Coggan, G.
Inst. Ch. Eng. Symp. Ser. 26,138 (1967).

34. Coulson, J.H. and Skinner, S.J.
Ch. Eng. Sci. 1, 197 (1957).

35. Davies, J.T.
"Mass Transfer and Interfacial Phenomena"
Adv. in Ch. Eng. vol. 4, Acad. Press (1963).

36. Dawodu, F.A
"Mechanisms of Liquid Extraction in Pilot Plant Sieve Plate Column"
Ph.D. Thesis, University of Aston in Birmingham, UK (1983).

37. Dawodu, F.A, Mumford, C.J. and Jeffreys, G.V.
I.Ch. Symp. Ser. 88, Dounreay (1984).

38. Eid, K., Gourdon, C. and Casamatta, G.
Ch. Eng. Sci. 46, 7, 1608 (1991).

39. Elizinga, E.R. and Banchero, J.T.
Ch. Eng. Prog. Symp. Ser. 55, 29, 149 (1959).

40. Elizinga, E.R. and Banchero, J.T.
A.I.Ch.E.J. 7,394 (1961).

41. Feick, G. and Anderson, H.M.
Ind. Eng. Chem. 44, 404 (1952).

42. Fogler, H.S.
Ch. Eng. Prog. Symp. Ser. 109,1 (1971).

43. Forsyth, J.S., Fish, L.W. and Cavers, S.D.
Proc.I.S.E.C. 74, vol. 1, 417 (1974).

44. Garner, F.H. and Hale, A.R.
Ch. Eng. Sci. 2, 157 (1953).

45. Garner, F.H. and Skelland, A.H.P.
Ch. Eng. Sci. 4, 149 (1955).

46. Garner, F.H. and Suckling, R.D.
A.I.Ch.E.J. 4, 114 (1958).

47. Garner, F.H., Foord, A. and Tayeban, T.
Appl. Ch. 9, 315 (1959).

48. Garner, F.H., Jenson, V.C. and Keey, R.T.I.
Trans. Inst. Ch. Engrs. 37, 191 (1959).

49. Garner, F.H. and Tayeban, M.
An. Roy. Soc. Esp. Fis. Quim. B56, 479 (1960).

50. Gayler, R., Roberts, N.W. and Pratt, H.R.C.
Trans. Inst. Ch. Engrs. 31, 57 (1953).

51. Godfrey, J.C., Houlton, D.A., Marley, S.T., Marrocchelli, A. and Slater, M.J.
Ch. Eng. Res. Des. 66, 445 (1988).

52. Grace, J.R., Wairegi, T. and Nguyen, T.H.
Tran. Inst. Ch. Engrs., 54, 167 (1976).

53. Groothuis, H. and Kramers, H.
Ch. Eng. Sci. 4, 17 (1955).

54. Grothius, H. and Zuiderweg, F.J.
Ch. Eng. Sci. 7, 288 (1960).

55. Goltz, G.E. and Glew, D.N.
Analg. Chem. 29, 816 (1957).

56. Gunn, R.
J. Geophys. Res. 54, 383 (1949).

57. Hadamard, J.S.
C R Acad. Sci. Paris, 152, 1735 (1911).

58. Handlos, A.E. and Baron, T.
A.I.Ch.E.J. 3, 127 (1957).

59. Heertjes, O.M., Holve, W.A. and Talsma, H.
Ch. Eng. Sci. 3, 122 (1954).

60. Heertjes, P.M.and De Nie, L.H.
Ch. Eng. Sci. 21, 755 (1966).

61. Hendrix, C.D., Dave, S.B. and Johnson, H.F.
A.I.Ch.E.J. 13, 1072 (1967)

62. Hesketh, T.W., Russell, T.W. and Etchells, A.W.
A.I.Ch.E.J. 33, 4, 663 (1987).

63. Hesketh, R.P., Etchells, A.W. and Russell, T.W.
Ch. Eng. Sci. 46, 1, 1 (1991).

64. Higbie, R.
Trans. Am. Inst. Ch. Engrs. 31, 365 (1935).

65. Hinze, J.O.
A.I.Ch.E.J. 1, 3, 289 (1955).

66. Holm, A. and Terjesen, S.G.
Ch. Eng. Sci. 4, 265 (1955).

67. Holmes, J.H. and Schafar, A.C.
Ch. Eng. Prog., 52, 5, 201 (1956).

68. Houghton, G.
Proc. R. Soc. 272. A, 33 (1963).

69. Hughes, R.R. and Gilliland, E.R.
Ch. Eng. Prog. 48, 497 (1952).

70. Hughmark, G.A.
Ind. Eng. Ch. Funds. 6, 408 (1967).

71. Hu, S. and Kintner, R.C.
A.I.Ch.E.J. 1, 42 (1955).

72. Hussain, A.A., Liang, T.B. and Slater, M.J.
Ch. Eng. Res. Des. 66, 541 (1988).

73. Hussain, A.A., Slater, M.J. and Marrocchelli, A.
Proc. I.S.E.C. 86, 3, 149 (1986).

74. Ilkovic, D.
Colln. Czech. Ch. Commun. 6, 498 (1934).

75. Jealous, A.C. and Johnson, H.F.
Ind. Eng. Ch. 47, 1160 (1955).

76. Jeffreys, G.V.
Chem. Ind. ,181, 16 March (1987).

77. Jeffreys, G.V.and Bonnet, J.C.
J. Ch. Tech. Biotechnol. 33A, 176 (1983).

78. Johnson, A.I. and Braida, C.
Can. J. Ch. Eng. 35, 165 (1957).

79. Johnson, A.I. and Hamielec, A.E.
A.I.Ch.E.J. 7, 145 (1960).

80. Kagan, S.Z., Aerov, M.E., Lonic, V., Volvoka, T.S.
Int. Ch. Eng. 5, 4, 656 (1965).

81. Khandelwal, A.N.
Ph. D. Thesis, University of Aston in Birminghan, UK (1978).

82. Khemangkorn, V., Molinier, J. and Angelino, H.
Ch. Eng. Sci. 33, 501 (1978).

83. Khemangkorn, V., Muratet, G. and Angelino, H.
Proc. I.S.E.C. 71, 429 (1979).

84. Kiating, W., Chunyao, S. and Chenfuan, W.
Huagong Xuebao, 4, 211 (1965).

85. Kinard, G.E., Manning, F.S. and Manning W.P.
Brit. Ch. Eng. 8, 326 (1963).

86. Kintner, R.C.
In " Advance in Chemical Engineering" Vol.4
Academic Press, NY (1963).

87. Kintner, R.C., Horton, T.J., Graumann, R.E. and Amberkar,S.
Can. J. of Ch. Eng. 39, 235 (1961).

88. Klee, A.J. and Treybal, R.E.
A.I.Ch.E.J. 2, 444 (1956).

89. Koshy, A., Das, T.R. and Kumar, R.
Ch. Eng. Sci. vol. 43, No. 3, 649 (1988).

90. Kronig, R. and Brink, J.C.
Appl. Sci. Res., A.2, 142 (1950).

91. Kubica, J. and Zdunkiewicz, K.
Int. Ch. 7, 903 (1977).

92. Kuipers, J.A.M., Prins, W. and VanSwaaij, W.P.M.
Ch. Eng. Sci. 46, 11, 2881 (1991).

93. Kumar, A. and Hartland, S.
Can. J. Ch. Eng. 67, 17 (1989).

94. Kumar, S., Kumar, R. and Gandhi, K.S.
Ch. Eng. Sci. vol.46, No. 10, 2483 (1991).

95. Kumar, A. and Hartland, S.
Trans. I. Ch. Eng. 60, 35 (1982).

96. Laddha, G.S. and Degaleesan, T.E.
"Transport Phenomena in Liquid Extraction"
Tata McGraw-Hill, New Delhi (1976).

97. Lamb, H.
In "Hydrodynamics" 6th Ed.
Cambridge University Press, London & NY (1948).

98. Levich, V.G.
"Physicochemical Hyrodynamics" , Prentice Hall, NY (1962).

99. Licht, W. and Conway, J.B.
Ind. Eng. Ch. 42, 115 (1950).

100. Licht, W and Narasimhamurty, G.S.R.
A.I.Ch.E.J. 1, 366 (1955).

101. Licht, W. and Pensing, W.F.
Ind. Eng. Ch. 45, 1885 (1953).

102. Linton, M. and Sutherland, K.L.
Proc. Internat. Congr. Surface Activity, 2nd. London (1957)

103. Linton, M. and Sutherland, K.L.
Ch. Eng. Sci. 12, 214 (1960).

104. Li, W.H and Newton, W.M.
A.I.Ch.E.J. 3, 56 (1957)

105. Lochiel, A.C.
Can. J. Ch. Eng. 43, 40 (1965).

106. Logsdail, D.H. and Slater, M.
In"Handbook of Solvent Extraction" Chapter11.2
Lo,T.C.,Baird,M.H. and Hanson Eds.
Wiley-Interscience (1983).

107. Logsdail,J.S., Das, P.K. and Kumar, R.
Ch. Eng. Sci. 41, 65, (1988).

108. Lurie, R.M. and Shaver, R.G.
"Effect of Vibration on Liquid-Liquid Extraction"
M.I.T. Practice School. Carbide & Carbon Chemicals Co.,
Memo. E.P.S-K-184, Oak Ridge, K-25 (1952).

109. Magarvey, R.H. and Bishop, R.L.
Can. J. Phys. 39, 1418 (1961).

110. Magnusson, K.
Ch. Proc. Eng. 35,276 (1954).

111. Mar, B.W. and Babb, A.L.
Ind. Eng. Chem. 51, 101 (1959)

112. Maxworth, T.J.
Fluid Mech. 27, 367, 9 (1967).

113. McManamey, W.J.
Ch. Eng. Sci. 34, 432 (1979).

114. Mekasut, L., Molinie, J. and Angelino, H.
Ch. Eng. Sci. 33, 821 (1978).

115. Misek, T.
Coll. Cezch. Chem. Commun. 28, 570 (1963).

116. Misek, T.
Coll. Czech. Ch. Comm. 28, 1631 (1963).

117. Misek, T.
Coll. Cezch. Chem. Commun. 29, 1755 (1964).

118. Miyanami, K., Tojo, K., Yano, T., Miyaji, K. and Minami, I.
Ch. Eng. Sci. 30, 1415, (1975).

119. Miyauchi, T. and Oya, H.
A.I.Ch.E.J. 11, 395 (1965).

120. Mukundan, R.
"Studies in Pulsed Spray Column"
M. Tech. Thiese, University of Madras (1971).

121. Newman, A.B.
Trans. Am. Inst. Ch. Eng. 27, 203 (1931).

122. O'Brien, D.C.
"Orifice Plate Pulse Column for Liquid-Liquid Extraction"
M.Sc. Thesis, M.I.T., Cambridge, Massachusetts (1954).

123. Olander, D.R.
A.I.Ch.E.J. 12, 1018 (1966).

124. Pietzsch, W. and Pilhofer, Th.
Ch. Eng. Sci. 39, 6, 961 (1984).

125. Raymond, D.R. and Zieminski, S.A.
A.I.Ch.E.J. 17, 57 (1971).

126. Rodger, W.A., Trice, V.G. and Rushton, J.H.
Ch. Eng. Prog. 52, 515 (1956).

127. Rose, R.M. and Kintner, R.C.
A.I.Ch.E.J. 12, 530 (1966).

128. Rouyer,H., Lebouhellec, J., Henry, E. and Michel, P.
Proc. I.S.E.C. 74, Vol. 2, 2339 (1974).

129. Rowe, P.N., Claxton, K.T. and Lewis, J.B.
Trans. Inst. Ch. Engrs. 43, 14 (1965).

130. Ruckenstein, E.
Ch. Eng. Sci. 23, 363 (1951).

131. Rybezynski, W.
Bull. Acad. Sci. Cracovie, Ser. A, 40 (1911).

132. Sarkar, S.
"Liquid Liquid Extraction With Chemical Reaction in Agitated Columns"
Ph.D. Thesis, University of Aston in Birmingham, UK (1976).

133. Sawistowski, H.
In "Recent Advances in Liquid-Liquid Extraction" page 293-366
Hanson, C. Ed., Pergamon, Oxford (1959).

134. Sawistowski, H.and Goltz, G.E.
Trans.Inst. Ch. Eng. 41, 174 (1963).

135. Scheele, G.F. and Meister, B.T.
A.I.Ch.E.J. 14, 9 (1968).

136. Shenlin, Z., Boaqing, Z., Zhongyao, S. and Jiading, W.
J. Ch. Ind. Eng. (Chaina) 1, 1 (1982).

137. Schmidt, H.
Proc. I.S.E.C. 83, 164 (1983).

138. Scriven, L.E. and Sternling, C.V.
Nature, 187, 186 (1960).

139. Sege, G. and Woodfield, F.M.
Ch. Eng. Prog. no.8, 50, 396 (1954)

140. Seidell, A.
"Solubilities of Inorganic and Organic Compounds"
American Chemical Society (1965).

141. Sherwood, T.K., Evans, J.E. and Longcar, J.V.A.
Ind. Eng. Ch. 31, 1146 (1939).

142. Shinner, R. and Church, J.M.
Ind. Eng. Chem. Vol. 52, No. 3, 253 (1960).

143. Shou, C. and Zheng, F.
Proc. I.S.E.C. 86, Vol.3, 437, (1986).

144. Skelland, A.H.P. and Cornish, A.R.H.
A.I.Ch.E.J. 9, 73 (1963).

145. Skelland, A.H.P. and Minhans, S.S.
A.I.Ch.E.J. 17, 1316 (1971).

146. Skelland, A.H.P. and Wellek, R.M.
A.I.Ch.E.J. 10, 491 (1964).

147. Sleicher, C.A.
A.I.Ch.E.J. 8,471 (1962).

148. Smith, A.R., Caswell, J.E. and Larson, P.P.
Can. J. Ch. Eng. 41, 150 (1963).

149. Smoot, L.D. and Babb, A.L.
Ind. Eng. Ch. Fund. 1, 93 (1962).

150. Sovova, H., Prochazka, J.
Proc. I.S.E.C. 86, Vol.3, 231, (1986).

151. Stapathy, R. and Smith, W.
Fluid Mech. J. 10, 56 (1961).

152. Steiner, L., Bensalem, A.K. and Hartland, S.
Proc. I.S.E.C. 86, 3, 191 (1986).

152a. Steiner, L., Oezdemir, G. and Hartland, S.
Ind. Eng. Ch. Res. 29, 1313 (1990).

153. Stewart, G. and Thornton, J.D.
Inst. Ch. Eng. Symp. Ser. 26, 29 (1967).

154. Stewart, G. and Thornton, J.D.
Inst. Ch. Eng. Symp. Ser. 26, 37 (1967).

155. Streeter, V.L.
" Fluid Dynamics " McGraw-Hill, NY (1948).

156. Strom, J.R. and Kintner, R.C.
A.I.Ch.E.J. 4, 153 (1958).

157. Takamatsu, T., Yamagushi, M. and Katayamu, T.
J. Ch. Eng. Japan, Vol. 16, No. 4, 267 (1983).

158. Tamano, K.
Inter. Ch. Eng. Vol. 26, No. 4, 698 (1986).

159. Thompson, P.J.
Chem. Eng. Res. Des. vol. 65, sep. (1987).

160. Thornton,J.D.
Ch. Eng. Prog. Symp. Ser. 13 (1954).

161. Thornton, J.D.
Trans. Inst. Ch. Engrs. 35, 316 (1957).

162. Thornton, J.D.
Trans. Inst. Ch. Eng. 35, 316 (1975).

163. Thornton,J.D.
Ind. Chemist, 632 (1963).

164. Thornton, J.D. and Pratt, H.R.
Trans. Inst. Ch. Engrs. 31, 289 (1953)

165. Thorsen, G. and Terjesen, S.G.
Ch. Eng. Sci. 17, 137 (1962).

166. Thorsen, G., Strodalen, R.M. and Terjesen, S.G.
Ch. Eng. Sci. 23, 413 (1968).

167. Torobin, L.B. and Gauvin, W.H.
Can. J. Ch. Eng. 37, 167 (1959).

168. Treybal, R.E.
"Liquid-Liquid Extraction" , 2nd ed., McGraw-Hill, NY (1963).

169. Tunstall, E.B. and Houghton, G.
Ch. Eng. Sci. 23, 1067 (1968).

170. Van Dijck, W.J.D.
U.S.Patent 2, 11, 186, (1935).
Sec. 1.10 "Handbook of Separation Techniques for Chemical Engineers" by Schweitzer, P.A., Ed, McGraw-Hill 2nd edn. (1988).

171. Vassallo, G., Thornton, J.D. and Dowrschak, H.
Proc. I.S.E.C. 83, 2, 168 (1983).

172. Vedaiyan, S., Degallesan, T.E. and Laddah, G.S.
Indian J.I. Tech. 12, 4, 135 (1974).

173. Vermeulen, T.
Ind. Eng. Ch. 45, 1664 (1953).

174. Vermeulen, Th., Williams, G.M. and Langlois, G.E.
Ch. Eng. Prog. 51, 85F (1955).

175. Vignes, A.
Genie Chimique, 93, 173 (1965).

176. Vohradsky, J. and Sovova, H.
Ch. Eng. Sci. 45, 12, 3563 (1990).

177. Wallis, G.B.
"One-Dimensional Two Phase Flow" , page-220.
McGraw-Hill Press, NY (1969).

178. Wegener, P.P. and Parlange, J.Y.
Annu. Rev. Fluid Mech. 5, 79 (1973).

179. Wellek, R.M. and Skelland, A.H.P.
A.I.Ch.E.J. 11, 557 (1965).

180. West, F.B., Robinson, A., Morgenthalor, A.C., Beck, T.R. and McGregor, D.K.
Ind. Eng. Ch. 43, 234 (1951).

181. West, R.C.
"Handbook of Chemistry and Physics" , 53rd Ed.
The Chemical Rubber Co. (1972-1973).

182. Wiezhi, D., Derong, T., Xien, H., Chunrong, W., Lichun, Y., Shihao, D. and Shuru, F.
Proc.I.S.E.C. 83, 1, 141 (1983).

183. Wilke, C.R. and Chang, P.
A.I.Ch.E.J. 1, 264 (1955).

184. Wilson, M.P.
"Characteristics of theVortex and Wake at the Rear of a moving Droplet"
Ph.D. Thesis, University of Aston in Birmingham, UK (1971).

185. Winnikow, S. and Chao, B.T.
Phys. Fluids, 9, 1, 50 (1966).

186. Yamaguchi, M., Fujamato, T. and Katayama, T.
J. Ch. Eng. Japan, 8, 361 (1975).

187. Yamaguchi, M., Watanabe, T. and Katayama, T.
J. Ch. Eng. Japan, 8, 4151 (1975).

188. Yamaguchi, M., Takamatsu, T., Yashida, F. and Katayamu, T.
J. Ch. Eng. Japan, Vol. 18, No. 4, 325 (1985).

189. Yeheskel, J. and Kehat, E.
Ch. Eng. Sci. 26, 223 (1971).

190. Yeheskel, J. and Kehat, E.
Ch. Eng. Sci. 26, 2037 (1971).

191. Boyadzhiev, L. and Elenkov, D.
Coll. Czech. Ch Commum. 31, 1072 (1966).

192. Rektorys, K.
"Survey of Applicable Mathematics" page 148
Pub. Illiffe Books Ltd, London (1969).

193. Sprow, F.B.
Ch. Eng. Sci. 22, 435 (1967).

194. McManamey, W.J.
Ch. Eng. Sci. 34, 432 (1979).

195. Baranaev, M.K., Kaverovsky, E.N. and Tergubova, E.L.
C.R. Acad. Sci. USSR, 66, 821 (1949).

196. Shinnar, R.J.J.
J. Fluid. Mech., 10, 259 (1961).

197. Kolmogorov, A.N.
C.R. Acad. Sci. USSR, 65, 743 (1949).